University of Liège - Faculty of Applied Science

Experimental study of the hydraulic behaviour of Piano Key Weirs

Olivier MACHIELS
Ingénieur Civil des Constructions (ULg) - FRIA research fellow

Dissertation submitted in fulfillment of the requirements for the degree of « Docteur en Sciences de l 'Ingénieur »

June 2012

Hydraulics in Environmental and Civil Engineering

Acknowledgments

At the end of this PhD research, I want to give particular thanks to all the people that help, support and encourage me all along these four years.

First of all, I want to thank the University of Liège and the Belgian Fund for education to Industrial and Agricultural Research (FRIA) that provide me the resources necessary to my work.

I also want to acknowledge Pr. Michel Pirotton and Dr. Sébastien Erpicum for their enthusiastic reception in the HECE unit and their pertinent advices provided all along the present research.

The member of the jury: the president Pr. Jean-Pierre Jaspart, Pr. Jorge Matos, Ir. Frédéric Laugier and Ir. Christophe Daux are acknowledged here for their expert advice given on this work.

I also have to thank some people for their scientific collaboration and the exchange of experimental results essential to the validation of the methods and models developed in this work. Particular thanks to Dr. Marcelo Leite Ribeiro (EPFL – Stucky) and to Francois Lempérière and Jean-Pierre Vigny (Hydrocoop) to have supplied their experimental measurements. Thanks to Ir. Frédéric Laugier (EDF) and Ir. Christophe Daux (Coyne et Bellier) to authorize the publication of the results obtained during prototype studies ordered to the laboratory. Thanks to Ir. Marie Colombié (EDF) for his welcome and his help to the study of the Escouloubre Piano Key Weir.

Acknowledgments should also be given to all my colleagues for all the scientific as well as the human exchanges that made the benefits of a team work.

Finally, special thanks have to be given to my family: my girlfriend Géraldine, my parents, my grandparents and my sisters for their support and their encouragements all along these years.

Table of content

I. Introduction

I.1. Dams and spillways

"*The water control is an ambition as old as the world. In the history, great civilizations flourished thanks to the water control … In the twentieth century, the water control is exercised on a large scale. Dams, canals, dikes have enabled the incredible development of our societies. But are we immunized from the disasters of the past?*" [8]

37641 large dams, of minimum 15 m height, have been identified all around the world [2]. Almost two thirds of these dams play role in irrigation. The other main roles of dams are hydropower, water supply and flood mitigation. Each of these roles is played by about one quarter of the existing dams. Considering only the reservoirs with a storage capacity of more than 0.1 km³, 6862 dams, with a cumulative storage capacity of 6197 km³, have been stored in the Global Reservoir and Dams database (GRanD) [3]. The Figure I-1 shows the geographic repartition of these dams around the world.

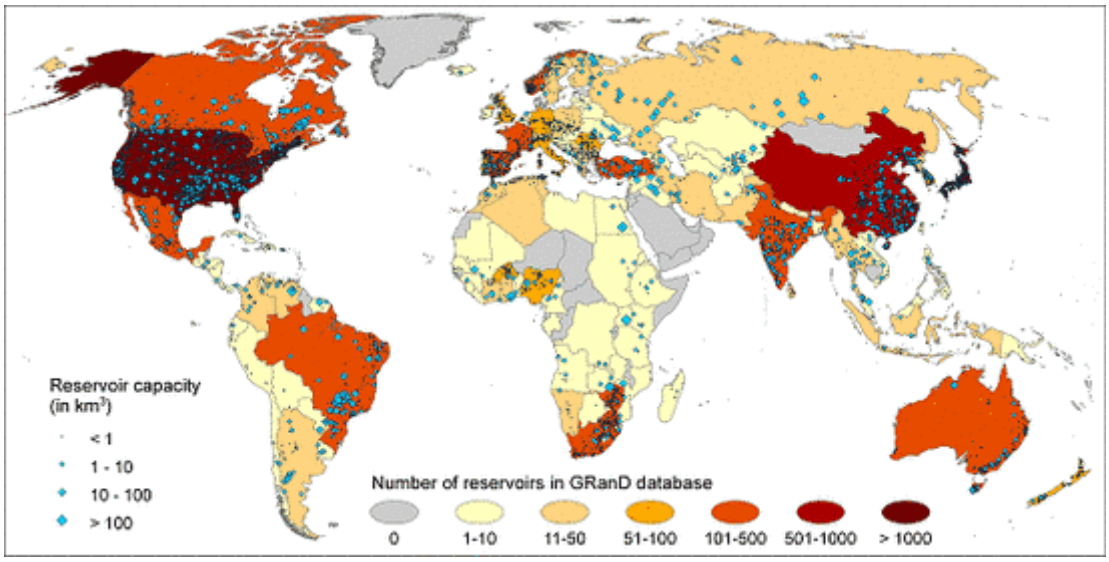

Figure I-1 Geographic repartition of dams took into account in the GRanD database [3]

As dams contain important volumes of water, their safety is a main issue. The two most famous dam failures in Europe are the ones of the Malpasset and the Vajont dams. In 1959, the failure of the Malpasset dam, in France, killed 421 persons [45]. Four years later, the Vajont dam failure killed 1910 persons in Italy [4]. The overall failure rate of dams through the world is around 1% [2]. Reports on incidents of dam failure have shown that almost a third of accidents is related to insufficient capacity of the spillway. Therefore, the ICOLD has recommended the rehabilitation of a large number of them to ensure dam safety [93].

The spillway, also called weir, is the safety component of the dam regarding flood release. It consists in a structural breach created in the dam body or in the

reservoir bank to allow the evacuation of extreme floods, acting like an overflow. The geometry of the breach crest and the difference between the breach crest and the maximal reservoir elevations determine the maximal discharge which can be released over the weir. As long as this discharge capacity stays over the maximal flood discharge, the dam safety is ensured.

Two types of weir are generally distinguished:

- The gated weir, which is controlled by mechanical structures limiting the discharge passing through the breach;
- The free weir, which is only managed by the reservoir level.

The main advantage of the gated weir is to provide a better reservoir management. However, the use of mechanical structures requests an attentive operating system and a regular maintenance. Failure in one of that way could create quick dam deterioration during floods. The main advantage of the free weir is that it works by itself, assuring the release of exceeding water whatever the incoming discharge. This is also its inconvenient. As the free weir releases water as soon as the reservoir level rises over its crest, the crest elevation determines the normal reservoir level and limits thus the storage capacity of the reservoir.

The design of the spillway is thus a main issue, aiming at the definition of the safety level as well as the storage capacity of the dam.

I.2. Spillway enhancements

I.2.1. Increase of the design discharge

Today, more than 50 % of all existing dams are over 50 years old [11]. Taking into account the actual knowledge on climate changes, as well as the increase in available data for statistics, a re-evaluation of the safety criteria of hydraulic works should be done [87]. The results of these studies globally show an increase in the frequency and the intensity of the maximal flood discharges. The question of the safety of the structures is therefore a priority for managers, owners and engineers. The re-evaluation of the maximal flood discharges thus leads to the rehabilitation of a large number of existing dams, as well as to the research of new solutions to upgrade the spillways release capacity.

In this framework, a labyrinth shape, multiplying the effective weir length, offers an interesting solution to increase discharges by maintaining the width of conventional weirs (ogee-crested type). However, the cost of such structures limits their application and encourages studying other weir shapes.

I.2.2. Increase of the storage capacity

The free weirs are generally preferred as they are simpler and safer than gated ones. However, they induce generally important losses in storage capacity due to the larger tranche of the reservoir needed to allow discharging the floods. 100 10^9 m³ of water are lost every year around the world [67]. Furthermore, sedimentation of the reservoir limits more and more the resources. This is a main issue as the need in water could affect almost 2 billion people around the world in 2025 [7].

I.3. Piano Key Weir

In this context, the company Hydrocoop-France, in collaboration with the University of Biskra in Algeria, has developed a new geometry of weir enabling to evacuate, for a same water head, a more important discharge than traditional weirs [5]. While using the discharge capacity increase obtained from the use of a labyrinth shape, their research aimed to develop a spillway multiplying the crest length while maintaining the basis length of the conventional weirs.

That is the way the Piano Key Weirs (PKW) were born, drawing their name from their geometry in alternating cell. These weirs offer the advantages of the traditional labyrinth weirs: multiplication up to 4 of the specific standard weirs discharges, maintenance and easy use, evacuation of specific discharges up to 100 m³/s/m and gain on the reservoir level for a same level of safety [94]. In addition, they have the advantage of their lower cost. Indeed, the presence of cantilevers, decreasing the volume of concrete, and a simple geometry, allowing the use of prefabricated components, significantly decrease the costs of these structures [94].

As it allows a significant increase of the release capacity compared with traditional weirs capacity and as its geometry allows an easy use on dam crest, the PKW is a relevant tool to increase the safety level of an existing dam.

Another opportunity for the application of the PKW is their advantage to require a small reservoir tranche to evacuate important discharges. Their use allows thus to increase the reservoir level, keeping constant the hydraulic safety level and increasing significantly the volumes stored [9]. For example, the use of PKW on the Algerian dams could enable to increase their total storage capacity of 250 10^6 m³ [93]. This offers thus interesting prospects for the mitigation of the increasingly marked limitation of the available water resources [1].

The PKW are thus of main interest both for the rehabilitation of existing structures, and for the development of new equipments. It stays, however, of main importance to understand their hydraulic and structural working, and to optimize their design.

I.4. Goals and strategy of the study

Before the present study was initiated, the design of the first PKW was essentially based on the experimental knowledge [57]. Using existing experimental results from idealized scale models, a first geometry was designed by extrapolation of the main geometric parameters. This geometry was then tested on a scale model to confirm its efficiency. The initial geometry was modified step by step following the ideas of the project engineers until the final design was reached. There was thus a strong need in fundamental and applied studies on PKW enabling to improve the understanding of the flow and to set up efficient design rules.

The aim of this research is thus to help in the development of methods of effective pre-design taking into account the physics of the flows over the structure and the influence of its main geometric parameters.

In a first step, the study aims at improving the understanding of the flow behaviour on PKW to define clearly its interests but also its limitations. To achieve this goal, a large scale model has firstly been widely exploited in the laboratory, enabling to visualize the flow along the structure and to characterize it in terms of discharge capacity, streamlines, velocity, pressure and free surface profiles (see IV). This model allows confirming the interest of PKW in terms of conveyance while highlighting some limitations compared with the expected results of the first studies. The study results also highlight the relative importance of the influence of the various geometrical parameters.

In a second step, the influence of the main geometrical parameters has been extensively studied on physical models with variable geometry (see VII, VIII and IX). These have been pre-designed based on a first assessment of the influence of each parameter on the overall release capacity using a simplified numerical model.

This model, called Wolf1D-PKW, is based on a one-dimensional representation of the keys composing the PKW taking into account the exchanges of mass and momentum in-between them (see XIV.2). It has been developed from the experimental results obtained on the large scale model. It has then been validated and enhanced on the basis of the experimental results of the parametric study.

The experimental results have also been exploited to evaluate the relative influence on the release capacity of the various hydraulic phenomena observed along the PKW (see V).

Keeping these influences in mind, the experimental results have been at the root of the setting up of an analytical formulation of the release capacity (see XI.4). This is a valuable tool to improve the efficiency of PKW design.

Finally, design advices are given assembling the observations and the conclusions from all the tests realized along the study (see XI).

The Figure I-2 summarizes the goals and the strategy of the study.

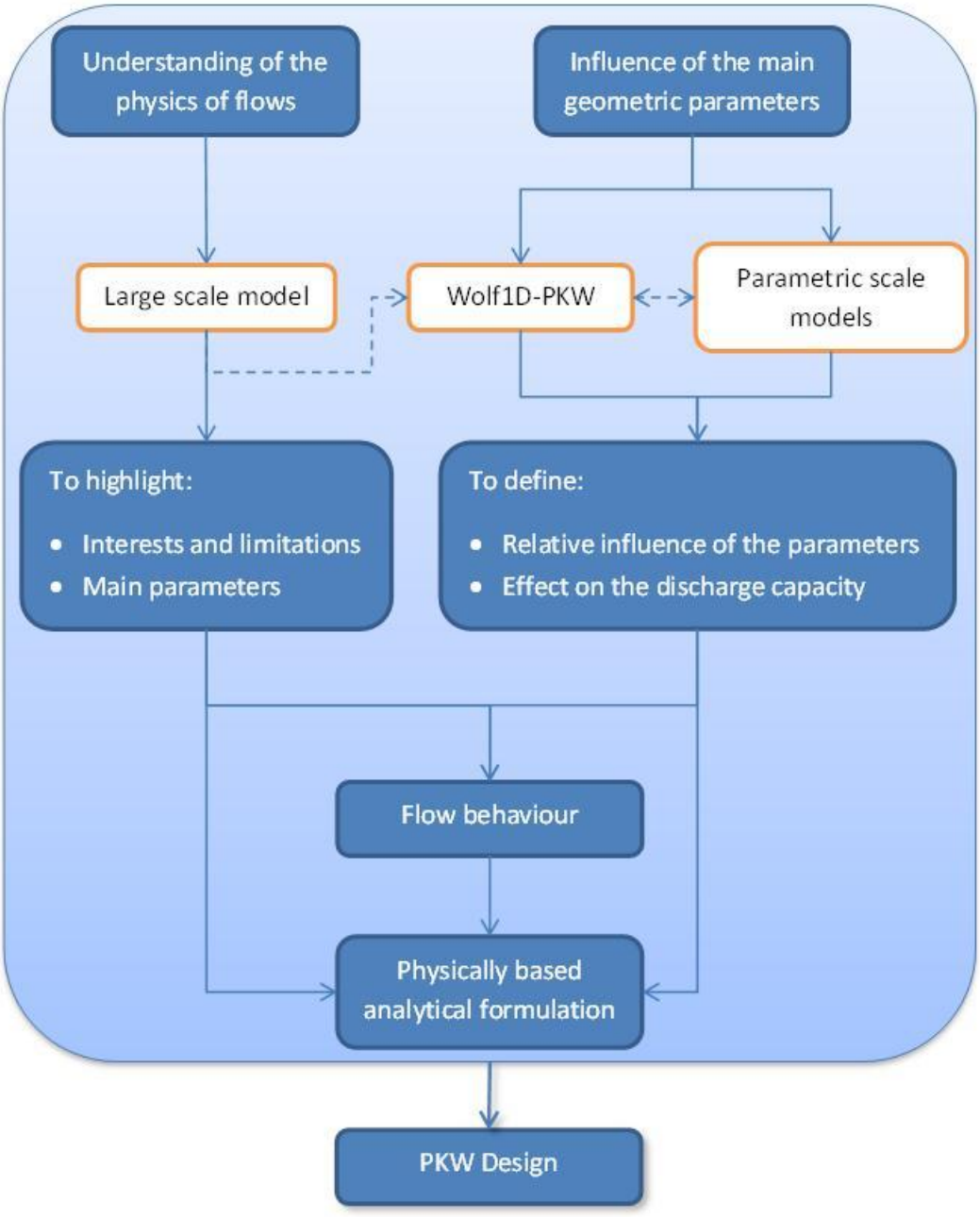

Figure I-2 Goals and strategy of the research

II. Weirs and spillways

II.1. Various weir types

Weirs or spillways are structures allowing the passage of surplus water from a dam. They are an essential element for dam safety. The weir efficiency is traduced by its capacity to delivery discharge downstream for a given upstream head. It is mainly dependent of the weir crest length and shape. Several shapes of weir have been developed until the Piano Key Weir. In this section we will interest in the main of them and the ones that help to the Piano Key Weir flow understanding.

II.1.1. Sharp-crested weir

The basic shape of weir is the so called sharp-crested weir. It consists in a thin vertical wall placed transversally to the main flow (Figure II-1).

Figure II-1 Flow over a sharp-crested weir

Its discharge capacity can be calculated from the traditional Poleni equation:

$$Q = C_{dL} L \sqrt{2gH^3} \qquad \text{II-1}$$

where Q is the discharge passing over the structure, L is the crest length, H is the water head upstream the weir calculated as the sum of the water depth over the crest and the kinetic energy component, and C_{dL} is a discharge coefficient approximately equal to 0.429 for sharp-crested weirs [17, 51].

The discharge coefficient value is slightly dependent of the weir thickness and height. A sharp-crested weir is theoretically a weir without thickness. However, a thick-crested weir works as a sharp-crested one as long as the ratio between the upstream head and the weir thickness H/T is larger than 1.8 [51]. For lower values of this ratio, the discharge coefficient decreases to tend to the one of a broad-crested weir for H/T lower than 0.5 [51].

The influence of the weir height, traduced in the ratio H/P between upstream head and weir height, has been largely studied and many authors proposed empirical relations of the discharge coefficient depending on this ratio [18]. From these, the one

of the Swiss Society of Engineers and Architects (SIA) [107] is presented here as it is used to characterize sharp-crested weir flows hereafter:

$$C_{dL} = 0.41\left(1+\frac{1}{1000H+1.6}\right)\left(1+0.5\left(\frac{H}{H+P}\right)^2\right) \qquad \text{II-2}$$

II.1.2. Broad-crested weir

A thick-crested weir is called broad-crested one as long as its thickness is sufficient to enable the development of a critical water depth h_c over the crest (Figure II-2). This is the case if the H/T ratio is lower than 0.5 [51]. The discharge coefficient C_{dL} for broad-crested weirs is equal to 0.385.

Figure II-2 Flow over a broad-crested weir

II.1.3. Ogee-crested weir

The ogee-crested weir is actually the most used weir. Its shape follows the trajectory of the free nappe observed on a sharp-crested weir for the design head (Figure II-3). The discharge coefficient for the design head is equal to 0.494.

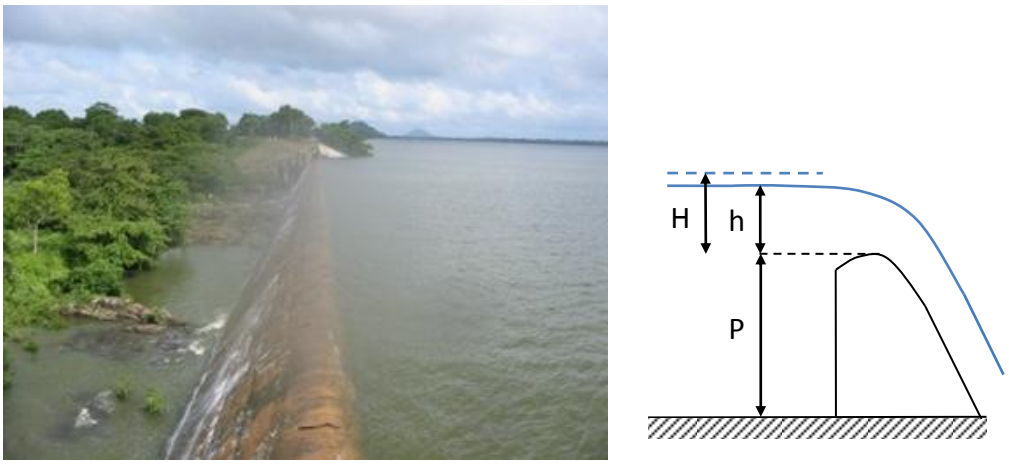

Figure II-3 Flow over an ogee-crested weir

As this weir seems to be the optimal design for linear free weir, it will be used hereafter as a reference to compare the various weir geometry efficiencies.

II.1.4. Side weir

The side weir is a linear weir placed parallel to the main flow direction (Figure II-4). Its discharge capacity is thus affected by the variation of flow depth along the weir, the flow velocity and the outflow angle [44].

Figure II-4 Flow over a side weir

Hager [44] proposed to correct the discharge coefficient of the traditional linear weir C_{dL} by coefficients taking into account the influence of the three parameters listed here above. The general formulation of the discharge coefficient for side weir C_{dLs} is:

$$C_{dLs} = C_{dL}\left(\frac{h}{H}\right)^{3/2}\left(\frac{H}{3H-2h}\right)^{1/2} \qquad \text{II-3}$$

where h is the water depth over the side crest.

II.1.5. Labyrinth weir

The labyrinth weir is a multi linear thick crested weir (Figure II-5). Using trapezoidal horizontal scheme, it enables to increase the crest length L for a given weir width W.

Figure II-5 Flow over a labyrinth weir

As the discharge capacity is directly proportional to the weir crest length, the ratio between labyrinth and sharp-crested weirs efficiencies should reach the value of the L/W ratio. This is true for low upstream heads. This advantage made of the

labyrinth weir a strong solution for dam projects needing a high specific discharge capacity or with low reservoir section allocated to the flood discharge.

However for increasing heads, the discharge capacity of the labyrinth weir decreases due to nappe interactions [109]. Furthermore, as parts of the crest are not perpendicular to the main flow direction, the crest efficiency decreases with the inclination of the side walls α. Tullis et al. [109] give formulations to compute C_{dL} in terms of H/P ratio and α.

II.2. Piano Key Weir

II.2.1. Definition

The Piano Key Weir (PKW) is a particular shape of labyrinth weir, using up- and/or downstream overhangs (Figure II-6). The horizontal rectangular labyrinth shape allows to multiply the crest length for a given weir width. As the labyrinth weir, the PKW is so a strong solution for dam projects needing a high specific discharge capacity or with low reservoir section allocated to the flood discharge. Furthermore, the use of overhangs limits the footprint of the structure. The PKW could thus be placed directly on dam crest, what makes it a useful tool for dam rehabilitation.

(a)

(b)

Figure II-6 Piano Key Weirs of (a) L'Etroit and (b) St Marc dams

The PKW was firstly designed in 2001 by Lempérière [13], from the non-governmental organisation "*Hydrocoop*", who was searching for a weir shape efficient and easy to build for development projects all over the world. He looked for a shape allowing a large specific discharge capacity, for the use of precast elements and for a design based on a single parameter. This goal was finally achieved and developed in [68]. The first PKW has been built in 2006 for the Goulours dam rehabilitation by "*Electricité de France* (EDF)" [57]. Since this time, EDF developed several projects of PKW for dam rehabilitation in France [12, 20, 30, 38, 39, 58, 60, 63, 64, 96]. Since 2010, PKW is also studied for new dam projects in Asia [22, 48, 49, 103] and in Africa [35, 37, 39, 40, 60].

II.2.2. Nomenclature [98]

The PKW geometry involves a large set of parameters. In order to ensure a unicity in terminology, a naming convention has been developed by a workgroup gathering *"EDF-Hydro Engineering Center"*, *"Ecole Polytechnique Fédérale de Lausanne - Laboratory of Hydraulic Constructions"* and *"University of Liège - Laboratory of Hydraulics in Environmental and Civil Engineering (HECE)"* [98].

The structure of the PKW can be described as the gathering of different elements: the basic structure, the parapet walls and the noses. The inlet key is the alveoli opened on the upstream part and is delimited by two side walls and the downstream crest. The outlet key is the alveoli opened on the downstream part and is delimited by two side walls and the upstream crest. The basic structure is composed of "PKW units". The parameters relying to the basic structure are the total width of the PKW W, the total developed crest length L and the number of PKW units constituting the structure N_u.

The unit represents the smallest extent of a complete structure, composed of an entire inlet key with two side walls and half an outlet on both sides. The parameters dedicated to the PKW unit are defined with an index u, when the ones dedicated to the inlet key, the outlet key and the side wall are respectively defined with indexes i, o and s. The main parameters defining the geometry of the PKW unit are the unit width W_u, the inlet and outlet keys widths W_i and W_o, the inlet and outlet keys heights P_i and P_o, the slopes of the inlet and outlet keys S_i and S_o, the up- and downstream overhangs lengths B_o and B_i, the upstream-downstream PKW length B, the base length B_b, and the crest thickness T_x with x index equal to i for the crest downstream of the inlet key, o for the upstream crest of the outlet key and s for the crest on the side wall (Figure II-7).

The parapet wall is a vertical extension that can be placed over a part or the entire PKW crest. The geometry of the parapet wall is mainly defined by its height P_{px} and thickness T_{px} with x index equal to i for the crest downstream of the inlet key, o for the upstream crest of the outlet key and s for the crest on the side wall. The inlet and

outlet keys heights P_i and P_o, considered from the PKW crest, include thus the possible parapet wall height (Figure II-7).

The nose is a feature placed under the upstream overhang to enhance the flow pattern at inlet key entrance. Its shape can vary from triangular profile to rounded one. The geometry of the nose is mainly defined by its horizontal length B_n.

As the PKW is mainly used on dam crest, the dam height under the weir P_d has to be characterized.

The global cross section layout enables to distinguish several categories of PKW. A basic classification has been proposed by Lempérière a few years ago according to the arrangement of the upstream and downstream overhangs. PKW with symmetrical upstream and downstream overhangs is classified as Type A, one with only upstream overhangs as Type B, one with only downstream overhangs as Type C, and one without overhangs as Type D.

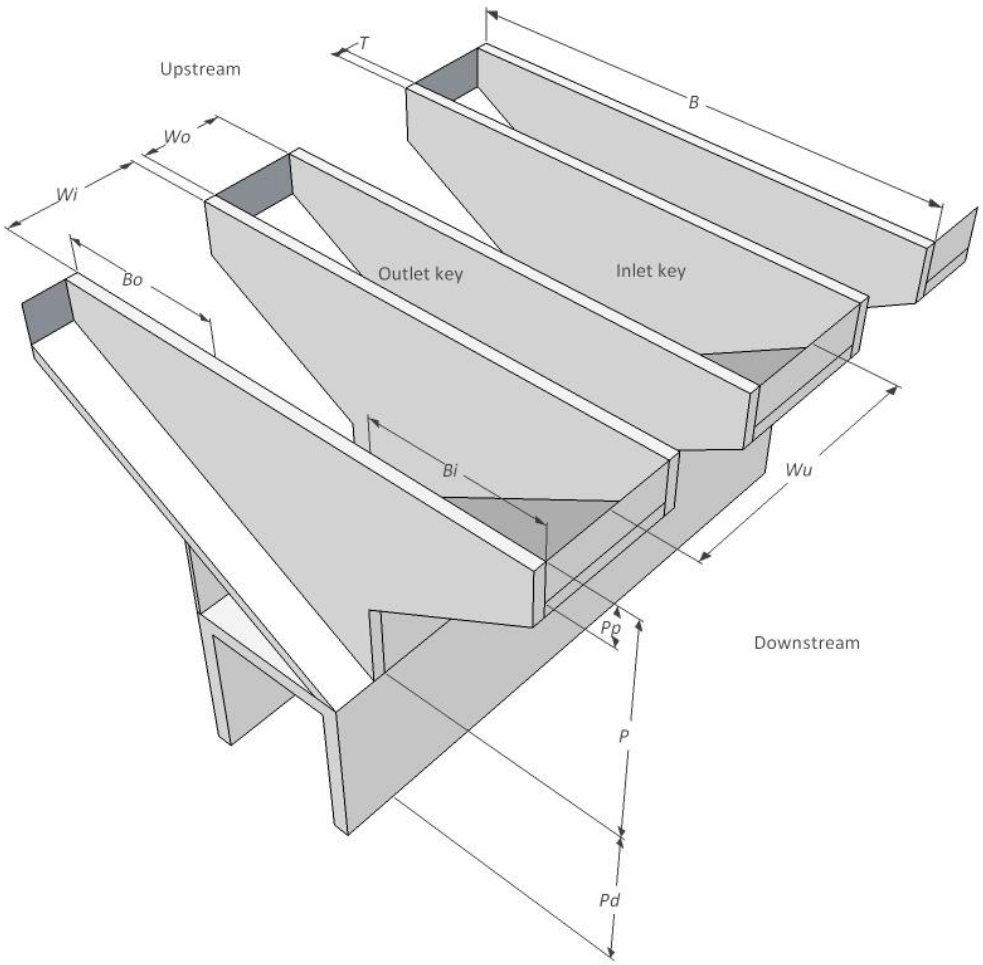

Figure II-7 3D sketch of the basic structure of a PKW and its main geometrical parameters

III. Experimental set-up

III.1. Flume of experimentation

A specific experimental facility has been built to perform all the scale model tests depicted hereafter. The flume, 7.2 m long, 1.2 m wide and 1.2 m high is fed up by two pumps delivering up to 300 l/s in an upstream stilling basin (Figure III-1). The upstream entry of the flume is equipped with a metal grid and a synthetic membrane ensuring uniform alimentation conditions. Two Plexiglas plates on both flume sides allow to observe the flow patterns on the whole flume height at the location of the PKW model. Specific convergent structures allow reducing the flume width to the variable width of the tested models. Downstream of the tested models, optional dividing walls allow the separation of the flows coming out from the different keys. These dividing channels are closed downstream by triangular sharp-crested weirs for which the stage-discharge curve was previously established.

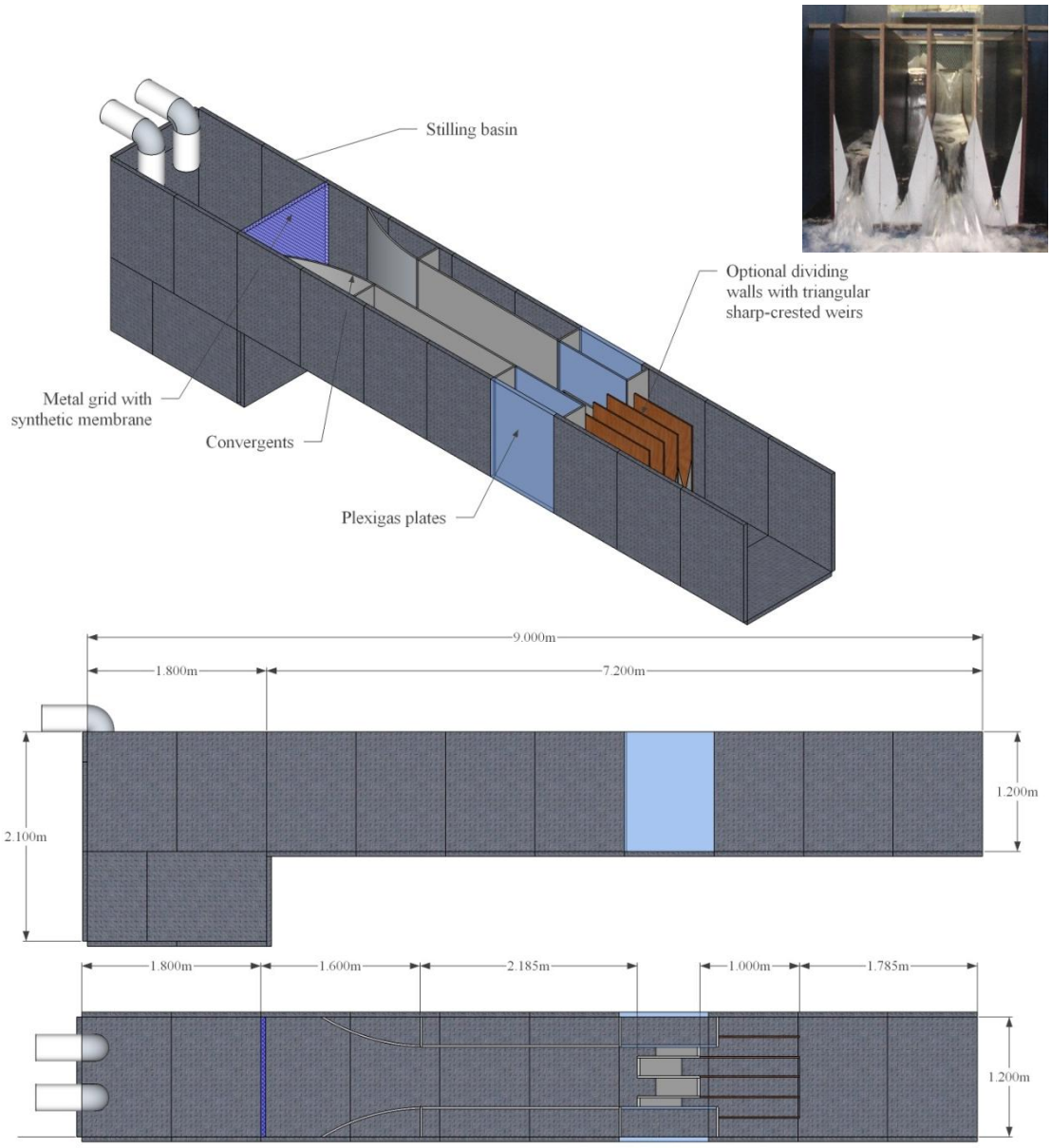

Figure III-1 Experimental flume layout

Figure III-2 View of the experimental flume

III.2. PKW models

During the study, 39 models of PKW (1 large scale model, 3 prototypes and 35 parametric models) and 6 of sharp-crested weir (5 inclined weirs and 1 vertical weir) have been tested. All PKWs have been made in PVC and sharp-crested weirs in plywood to minimize the effects of friction. The various thicknesses of the PVC plates have been chosen in agreement with the structural considerations of concrete prototypes. All PKWs have been placed on a support representing the dam crest height below the structure.

In order to enhance the understanding of the physics of the flows on a PKW, a 1:10 scale model of a basic geometry (W_i/W_o = 1, B_o/B_i = 1, L/W = 4.15, P_i/W_u = 1.31, P_i/P_o = 1) has firstly been exploited in a wide range of discharges. The model has been used to investigate flow types on the weir crests and to characterize these flow types in terms of discharge, velocity, pressure and flow patterns. To achieve this goal, 1.5 inlets and 1.5 outlets have been modelled (Figure III-3). The halves outlet and inlet, along the Plexiglas walls, allow the observation of the flow. The full ones, at the centre of the flume, enable measurements without side effects. Table III-1 and Figure III-4 give the value of the geometrical parameters of the model.

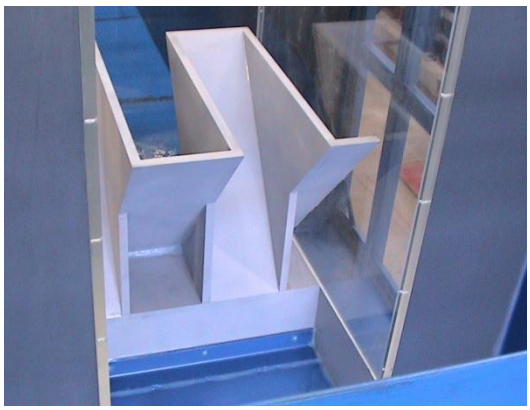

Figure III-3 View of the 1:10 scale model

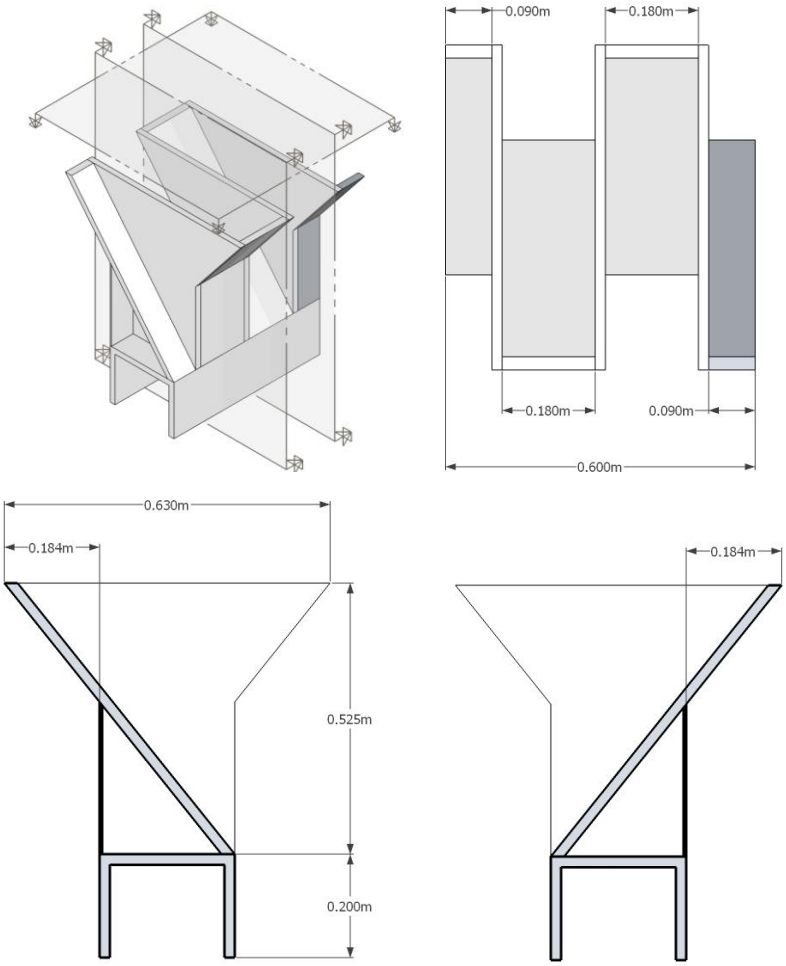

Figure III-4 Experimental 1:10 scale model layout

Table III-1 – 1:10 scale model dimensions

W	0.6 m
L	2.49 m
$P_i = P_o$	0.525 m
P_d	0.2 m
W_u	0.4 m
$W_i = W_o$	0.18 m
T_s	0.02 m
$T_i = T_o$	0.024 m
B	0.63 m
$B_i = B_o$	0.184 m

Then, the study aims at determining the influence of the different geometrical parameters of the PKW on its discharge capacity. To achieve this goal, several scale models with variable geometries have been tested. The description of these models is done at the beginning of the sections concerning the different tested parameters. In parallel to these experimental tests, numerical modelling has been performed to improve existing flow solvers at University of Liège and to help in defining the most

important geometrical parameters of the weir. The tested geometries are also depicted at the beginning of the related sections.

III.3. Measurement tools

During the various experimental tests, discharges, water free surface levels, streamlines trajectories, flow velocities and pressures have been measured.

The upstream discharges have been measured using an electromagnetic flowmeter with a precision of ± 0.001 m³/s. Measurements of partial discharges have been realized, on the 1:10 scale model, separately downstream of the inlet, the outlet and both the half-inlet and –outlet keys. The discharges *Q* in the four channels have been calculated based on tables giving the discharge/head relation for triangular sharp-crested weirs [19]. Water depth *h* measurements have been performed in the four channels using limnimeters with a precision of ± 0.5 mm. The discharge has then been calculated iteratively, calculating the head *H* by:

$$H = h + \frac{Q^2}{2gW_c^2h^2} \qquad \text{III-1}$$

where W_c is the channel width, and searching the corresponding discharge value in the discharge/head tables. By comparing the sum of the calculated partial discharges with the global discharge measurement obtained from the electromagnetic flowmeter, the accuracy of the method has been estimated at 5.5 % of the calculated discharges.

The free surface level measurements have been performed using electronic limnimeters with a precision of ± 0.5 mm. Two of them have been placed 2.5 m upstream of the tested models to measure the upstream head. The others have been put along both inlet and outlet keys to measure the free surface elevations.

Streamline measurements upstream of the weir and in the inlet keys have been done using systematically colouring agent (fluoresceine) injection upstream of the 1:10 scale model for particular discharges (Figure III-5).

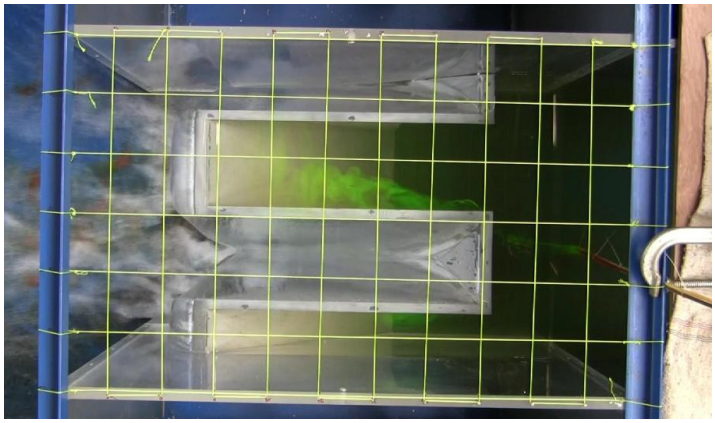

Figure III-5 Colouring agent injection

The fluoresceine was introduced 0.38 m upstream of the weir basis, at five different heights above the bottom of the flume and at five points on the flume width (Figure III-6).

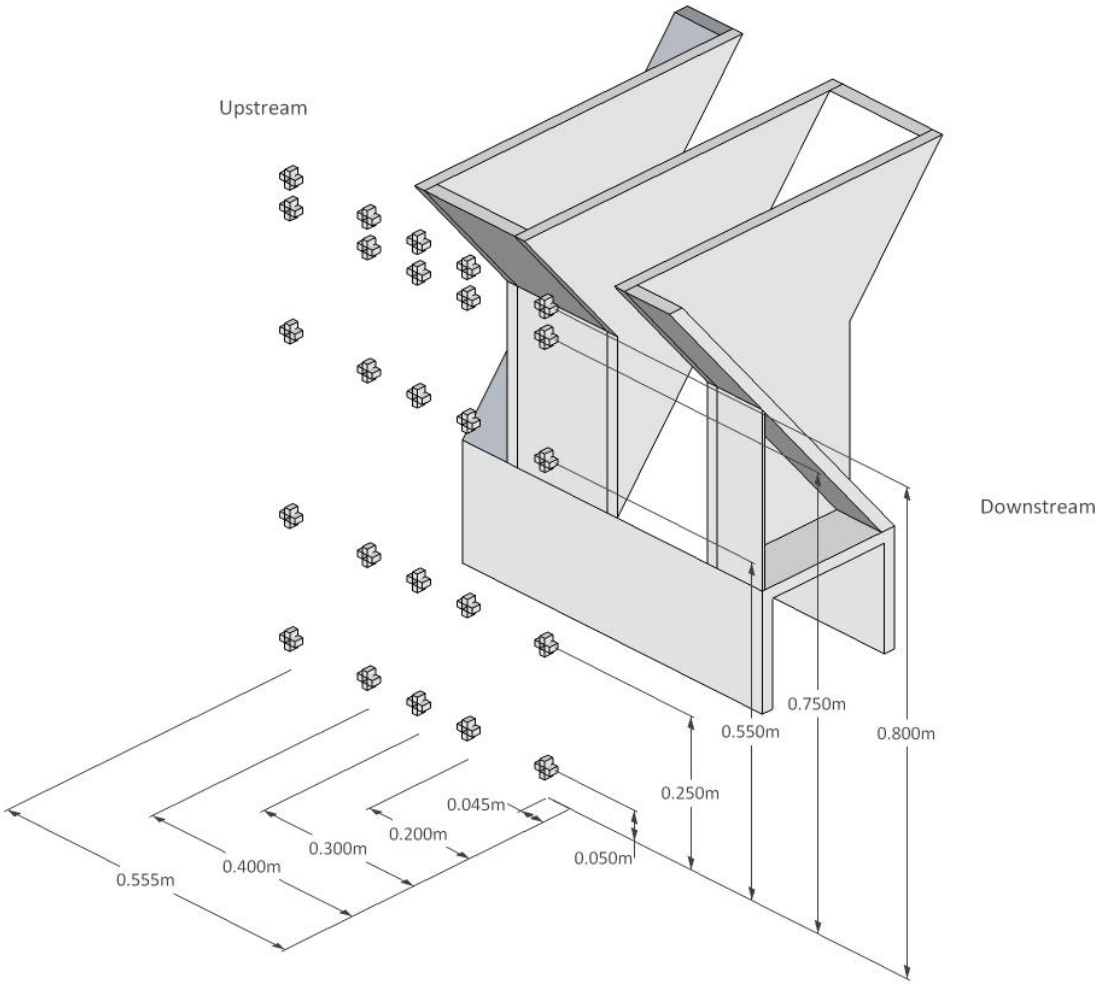

Figure III-6 Location of colouring agent injections

Six Pitot tubes [55] have been placed on the flume cross section to measure the flow velocity and the pressure at different heights and at different points upstream the weir and along the inlet key (Figure III-7). The accuracy of these measurements is ± 1 mm. That corresponds to a precision of ± 0.15 m/s on velocity measurements. The measurements have been performed at four cross sections upstream of the downstream crest of the PKW. Measurement points have been defined over the whole width of the flume with a step of 3.3 cm and at four elevations from the bottom of the flume. There are thus in total 117 measurement points (Figure III-8).

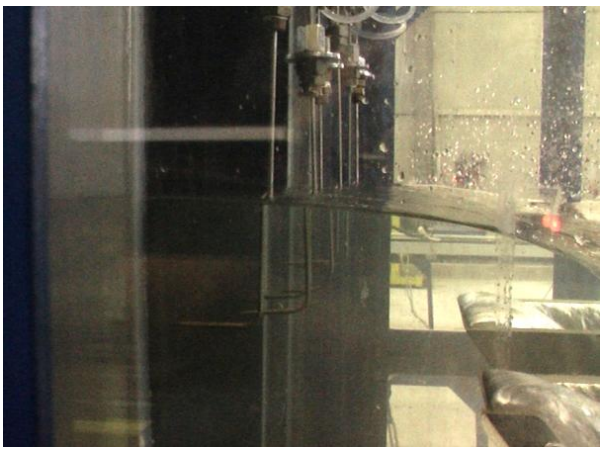

Figure III-7 Pitot tubes

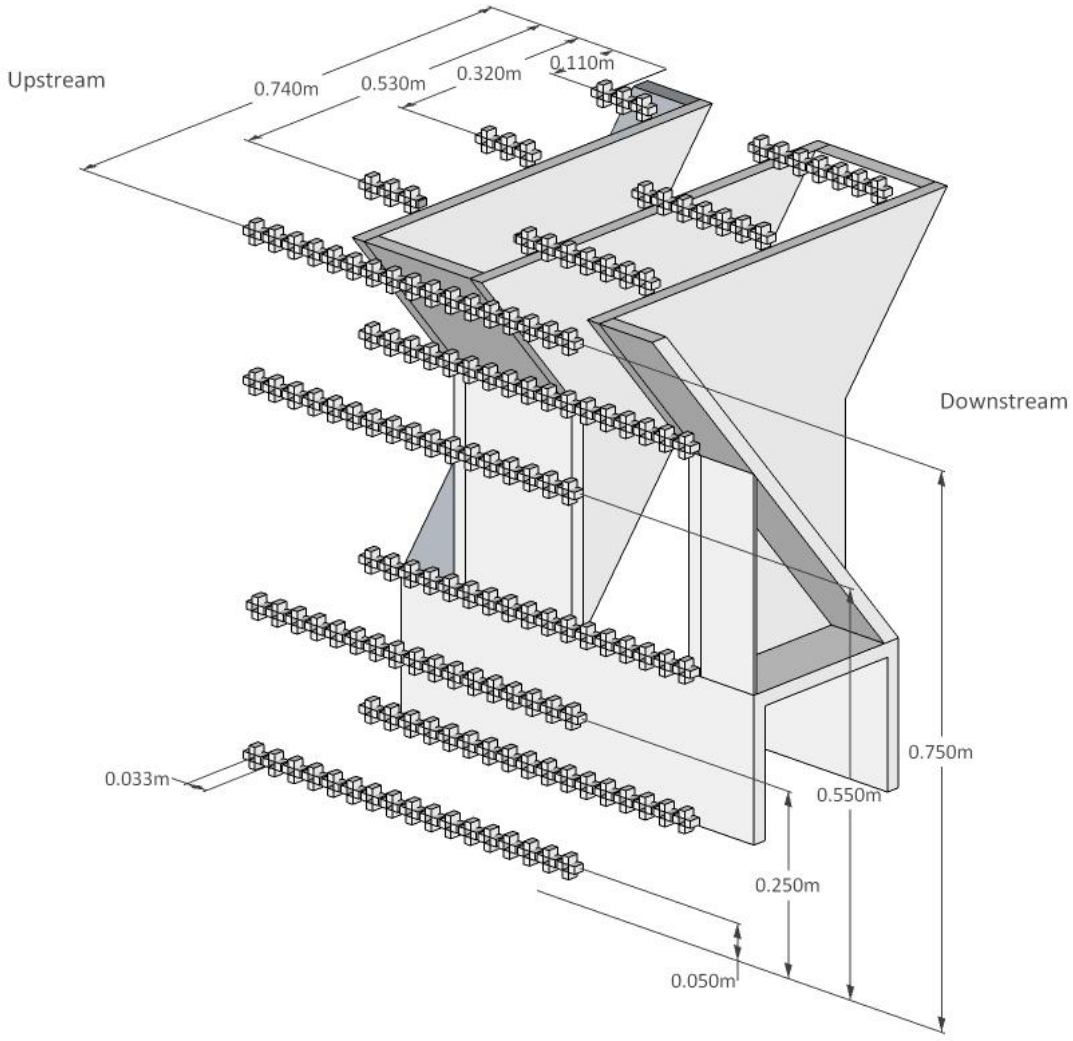

Figure III-8 Location of Pitot tube measurements

IV. Flow characteristics over PKW [81, 85]

IV.1. Objectives

The 1:10 scale model has been exploited in order to enhance the understanding of the physics of the flows on a PKW. To achieve this goal, the head-discharge curve of the model as well as the streamlines, the free surface, the pressure and the velocity profiles, measured on it, are analysed hereafter.

IV.2. Head-discharge curve [71, 74-76]

The tests on the 1:10 scale model aim at characterizing the global flow pattern on the PKW model depending on the upstream head. Because of the complexity of the PKW geometry, the discharge capacity is a function of many geometric parameters. It is of a common use to express, as in Eq. IV-1, the discharge Q on a PKW under an energy head H as a function of the weir length W on the dam crest:

$$Q = C_{dw} W \sqrt{2gH^3} \qquad \text{IV-1}$$

For the scale model of Figure III-4:

$$W = 1.5\ W_i + W_o + 2T_s \qquad \text{IV-2}$$

The influence of all the weir geometric specificities is thus lumped into the discharge coefficient C_{dw} [94].

The non-dimensional head/discharge curve of the 1:10 scale model has been carefully measured in a wide range of discharges (Figure IV-1).

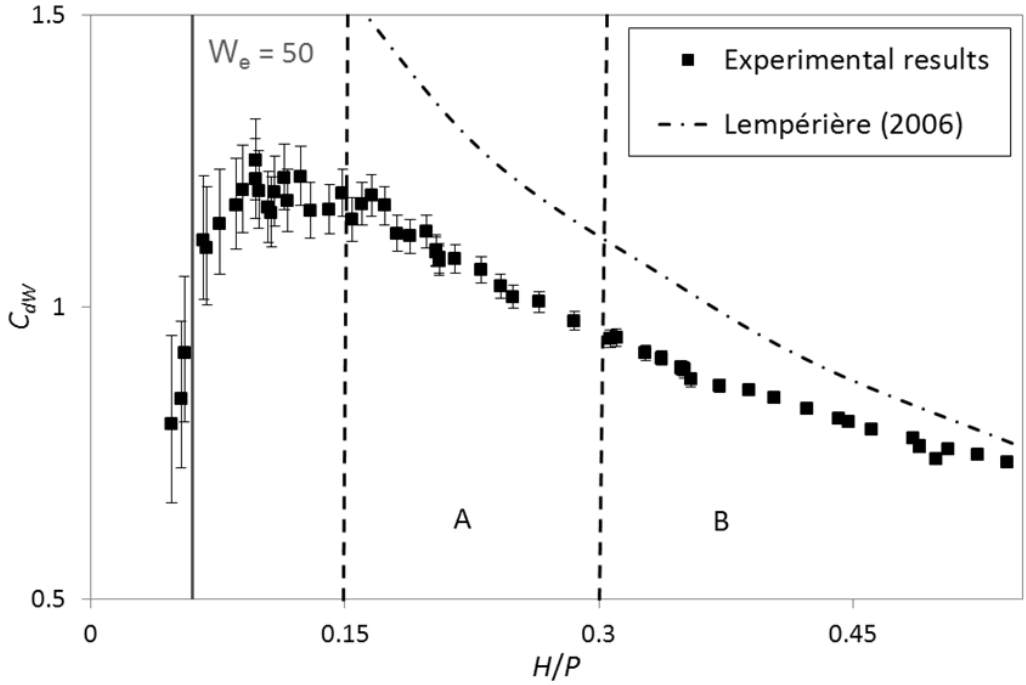

Figure IV-1 Non-dimensional head/discharge coefficient relation measured on the physical model

The error bars show the influence of the discharge measurement accuracy on the C_{dw} values. The comparison to the Lempérière results as well as the interpretation of the different zones depicted on the Figure IV-1 is realized hereafter.

IV.2.1. Side wall effects

The measure of discharges, downstream of the different parts of the model, shows the influence of the side walls of the experimental flume on the discharge capacity. The influence on the downstream crest is directly highlighted by measuring the discharges downstream of the full and half inlet keys. To isolate the influence on the side and upstream crests, measurements of the full and half outlet keys discharges have been performed with or without the upstream crest closed, using a PVC plate to raise the upstream crest level over the free surface (Figure IV-2). This closure involves variations of less than 1% of the discharge curve downstream of the inlet key, what is ensuring a similar flux repartition with or without the PVC plate.

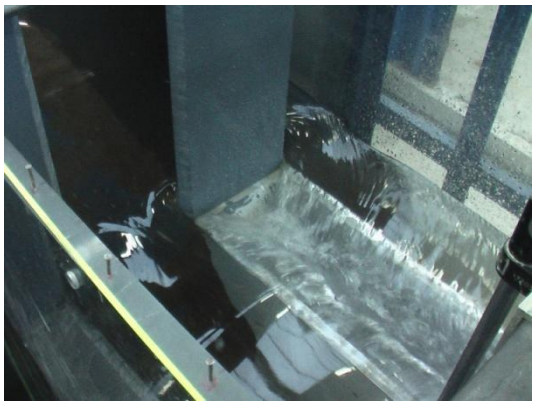

Figure IV-2 Isolation of the side crest discharge by closing of the upstream crest

The discharge on the downstream crest of the inlet key increases up to 15% with the side wall presence (Figure IV-3). Considering the outlet keys without the upstream crests, the discharge is almost not influenced by side wall effects compared with the measurements accuracy. Less than 5% difference between half and full outlet keys is observed (Figure IV-4 – (b)). The discharge capacity of the side crest is thus similar considering the complete or the half-outlet key and the wall, confirming the symmetry of the flow characteristics along the outlet axis. The discharge in the half-outlet key, considering the whole crest, decreases down to 15% compared with the full key (Figure IV-4 – (a)). This decrease can thus be linked to a decrease of the upstream crest discharge.

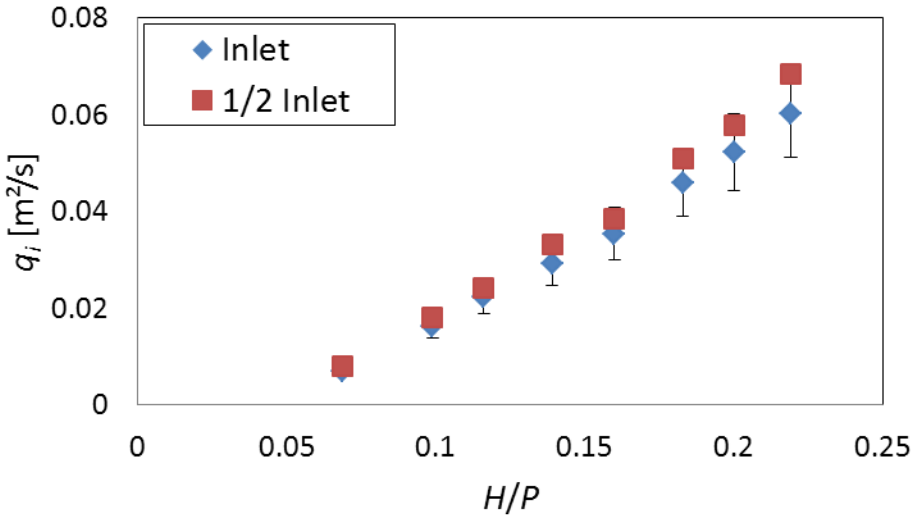

Figure IV-3 Comparison between discharges downstream of the inlet and the half-inlet keys (error bars = 15 %)

(a)

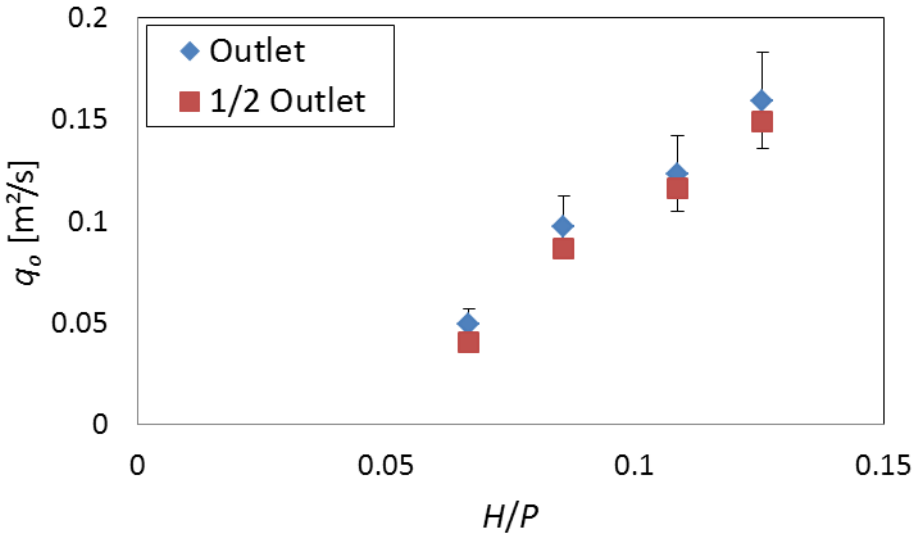

(b)

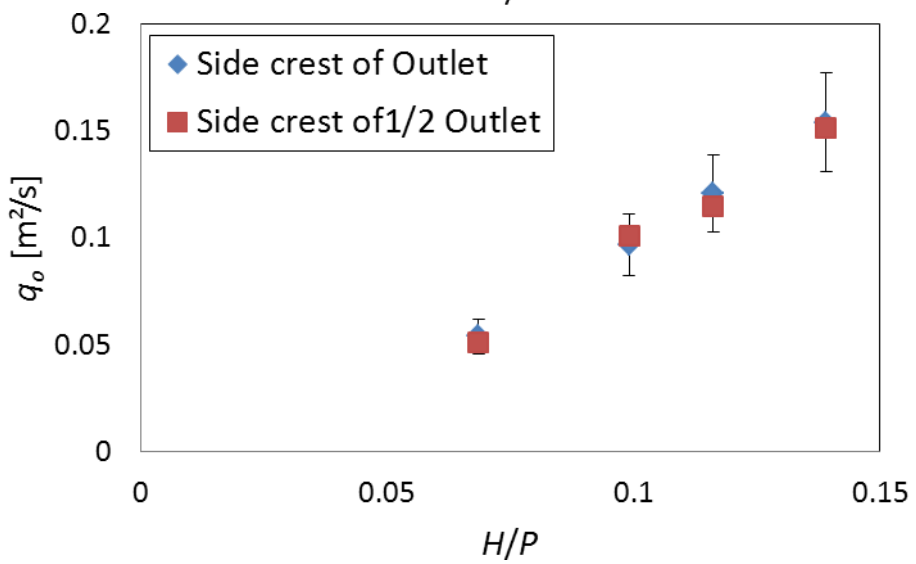

Figure IV-4 Comparison between discharges downstream of the outlet and the half-outlet keys (error bars = 15 %): (a) – with upstream crest; (b) – without upstream crest

The comparison between combined discharges of the full-inlet and -outlet keys with the combined discharges of the two half-inlet and -outlet keys shows differences close to 0.001 m³/s, which corresponds to the flowmeter accuracy. The increase of the discharge in the half-inlet key is thus counterbalanced by the decrease in the half-outlet one. The head/discharge curve of Figure IV-1, established considering one and half PKW-units, enables thus to represent the flow over a similar PKW geometry whatever the number of units. This justifies the study of a limited number of PKW-units on this model.

These results match with the conclusions drown by previous authors concerning the influence of the number of units on the discharge capacity of the weir whatever the W_i/W_o ratio [61, 70].

IV.2.2. Low heads behaviour

The non-dimensional head/discharge curve of the model (Figure IV-1) is relatively close to the curves presented by Ouamane and Lempérière [94] for non-optimal characteristics of PKW. Indeed, the geometry of the model has been defined to emphasize the differences between various flow types on the weir by increasing the slopes of both inlet and outlet keys, thus globally decreasing the PKW efficiency.

However, for low water heads ($H/P < 0.15$), there is an important decrease in the discharge coefficient compared with Ouamane and Lempérière's results. The explanation of this phenomenon lies on the influence of the crest thickness and shape. Ouamane and Lempérière's models used thin steel plates, whereas the present model used 2 cm thick PVC plates.

Moreover, for $H/P < 0.06$, the Weber number W_e, defined in Eq. IV-3 (where ρ is the water density, σ is the surface tension and U is the velocity), is lower than 50 and surface tension effects may thus become significant [89].

$$W_e = \frac{\rho U^2 H}{\sigma} \qquad \text{IV-3}$$

For low heads, the transition from a partially clinging nappe to a leaping nappe and then to a springing nappe [51] can be observed on the different parts of the PKW crest. These transitions occur for different heads depending on the crest thickness T and shape. Using 2 cm thick PVC plates, the side crest thickness is 2 cm, while the upstream and downstream crests thickness is 2.4 cm because of the slope of the plates.

On the side crests, for the smallest head ratio ($H/P = 0.05$), the leaping nappe remains in contact with the crest. For H/P ratios between 0.09 and 0.1, which corresponds to H/T_s ratios of 2.35 to 2.6, the nappe becomes springing and is detached

from the crest on the most downstream 3/4 of the crest length (Figure IV-5). This situation persists for higher water heads.

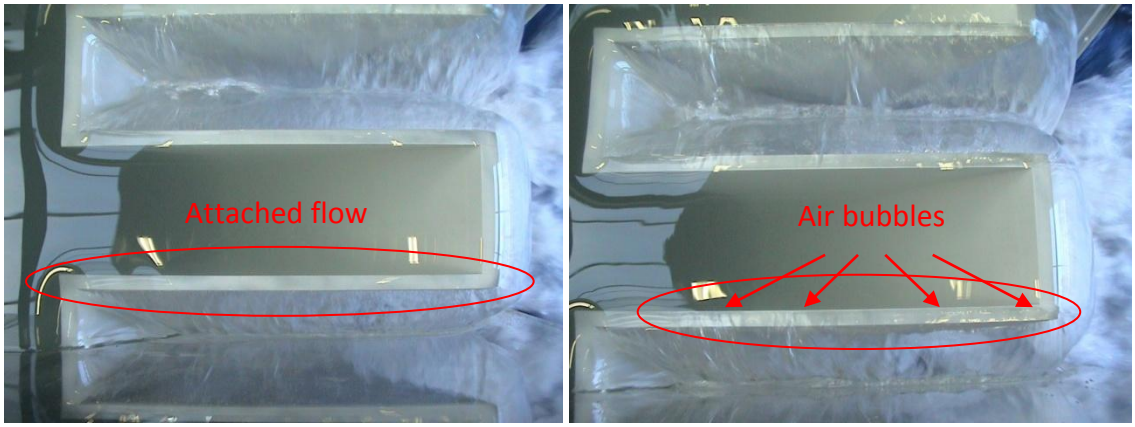

Figure IV-5 Transition from a leaping to a springing nappe on the side crest

The same behaviour is observed on the downstream crest of the inlet key (Figure IV-6). The transition from a leaping to a springing nappe is observed for H/P ratios between 0.11 and 0.12, which corresponds to H/T_i ratios between 2.4 and 2.6. As the same transitions are observed for the same H/T ratios on side and downstream crests, the inlet key slope seems to have no effect on the nappe shape for low heads.

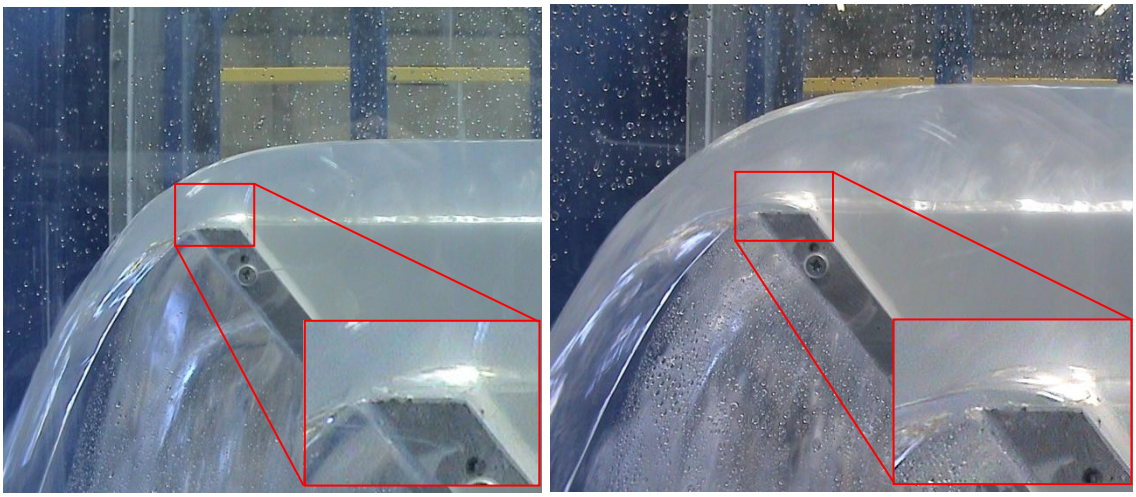

Figure IV-6 Transition from a leaping to a springing nappe on the downstream crest

The flow behaviour on the upstream crest is different. Indeed, for the lowest head ratios, the nappe is completely attached to the walls. Then for H/P ratios between 0.16 and 0.17, i.e. H/T_o ratios between 3.48 and 3.64, the nappe is directly fully aerated (Figure IV-7). The downstream slope of the outlet key has thus an important effect on the nappe shape, delaying the transition to a springing nappe for higher H/T_o ratios.

Figure IV-7 Transition from a clinging to a springing nappe on the upstream crest

Johnson [51] has shown that the transition from a leaping nappe to a springing nappe occurs for H/T values between 1.8 and 3 depending on the weir dimensions. The smaller are the weir dimensions, the more important is the H/T value at the transition. Considering the weir efficiency, this transition corresponds to a variation in the slope of the non-dimensional discharge/head curve.

In order to evaluate the evolution of the PKW crest efficiency with head, a comparison with the efficiency of traditional thick-crested weir has been realized. Swamee [106] proposed a formulation of the discharge coefficient C_{dL}* for linear weirs with a finite thickness crest (Eq. IV-4). He considers the influence of the weir thickness for low heads and of the weir height for higher ones. This formulation is in agreement with the observation of a transition from an important positive slope of the C_{dL} curve for heads corresponding with a leaping nappe to a low slope for heads corresponding with springing ones.

$$C_{dL}^{*} = 0.707\left\{\left(\frac{14.14P}{8.15P+h}\right)^{10} + \left(\frac{h}{h+P}\right)^{15} + 1.834\left[1+0.2\left(\frac{\left(\frac{h}{T}\right)^{5}+1.5\left(\frac{h}{T}\right)^{13}}{1+\left(\frac{h}{T}\right)^{3}}\right)^{0.1}\right]^{-10}\right\}^{-0.1} \qquad \text{IV-4}$$

$$Q = C_{dL}^{*} L\sqrt{2gh^{3}} \qquad \text{IV-5}$$

However, the discharge coefficient C_{dL}* proposed by Swamee is associated to a Poleni equation IV-5 based on the water depth h instead of the traditional discharge coefficients for linear weir C_{dL} calculated based on the water head H. To compare values obtained on the PKW scale model, C_{dL} is calculated based on the Swamee

formulation IV-4, considering the definition of the water head as the sum of the water depth and the kinetic energy component, by:

$$C_{dL} = C_{dL}^{*} \left(1 + \frac{C_{dL}^{*2}}{\left(1 + \frac{P}{h}\right)^2} \right)^{-1.5} \qquad \text{IV-6}$$

The comparison of the curve of Eq. IV-6 with the non-dimensional head/discharge curve calculated considering the developed crest length *L*, highlights a decrease of the crest efficiency, characterized by C_{dL} becoming smaller with increasing heads, while the efficiency of a linear weir is always increasing (Figure IV-8).

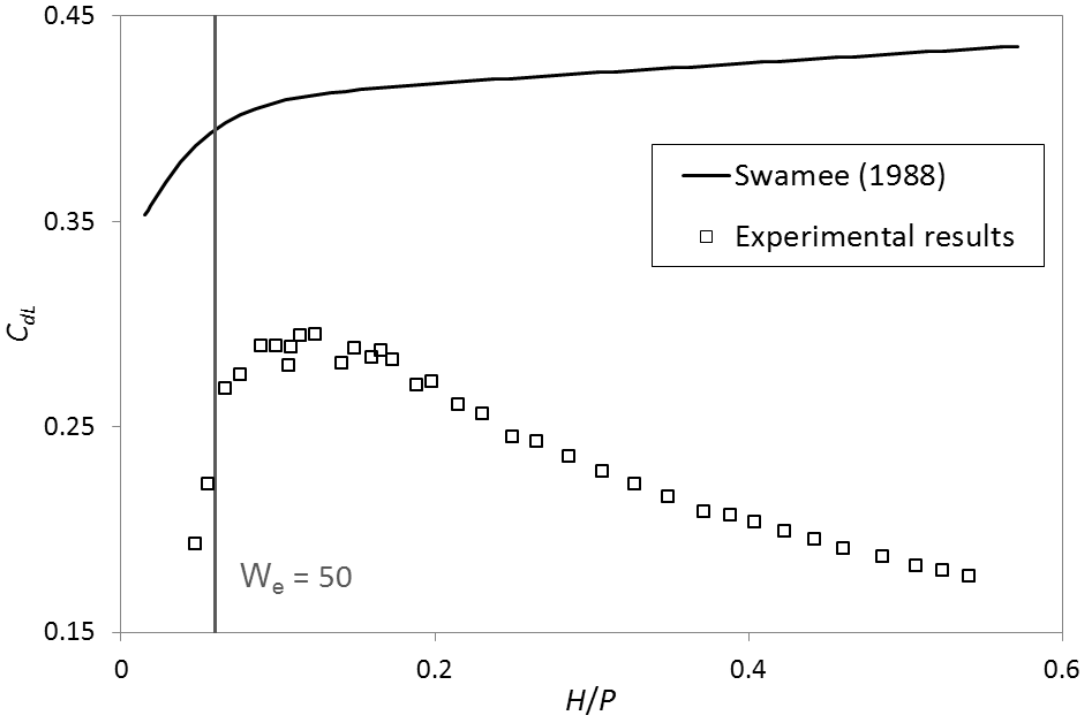

Figure IV-8 Comparison between crest efficiencies of the tested model and of a linear weir

This phenomenon has been observed on trapezoidal labyrinth weirs with an influence of the angle α between the side crest and the main stream direction [109]. For PKW, α is 0. The smaller is α, the more important is the decrease of C_{dL} with head. However, small α values enable to increase the L/W ratio. The global weir efficiency, characterized by the C_{dw} value, increases thus with decrease of α [21].

Schoder and Turner (1929), cited by Lakshmana Rao [56], studied the variations of the discharge coefficient with the nappe shapes at very low heads on sharp crested weirs, i.e. the same case as in the scale model. Their results are summarized in Figure IV-9, where (a) and (b) denote springing nappes, (c) denotes leaping nappes, and (d) and (e) denote respectively partially and fully clinging nappes.

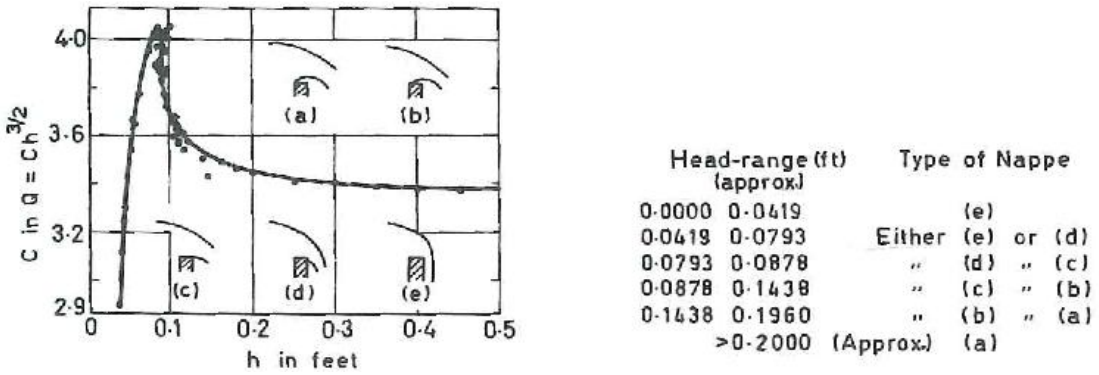

Figure IV-9 Variation of discharge coefficient at low heads (sharp crested weirs) [56]

The same correlation has been found on the PKW scale model (Figure IV-10). For very low heads (H/P < 0.06), surface tension effects unable concluding on the discharge capacity of the model. Until the transition from a leaping nappe to a springing one, the discharge coefficient increases with the head as the crest efficiency increases (Figure IV-10 – A'). For head ratios H/P over 0.1, a springing nappe appears on the 3/4 of the side crest length, the discharge coefficient stabilizes with increasing heads (Figure IV-10 – B'). That can be explained by the combined effects of the decrease of the side crest efficiency due to its orientation (α = 0), and the increase of efficiency due to the leaping nappe on the downstream crest and the clinging nappe on the upstream crest. When the downstream nappe becomes springing (Figure IV-10 – C'), the discharge coefficient begins to decrease continuously with increasing heads because of a less important increase of efficiency only due to clinging nappe on the upstream crest. Finally, the discharge coefficient decreases more importantly when the upstream nappe is free (Figure IV-10 – D').

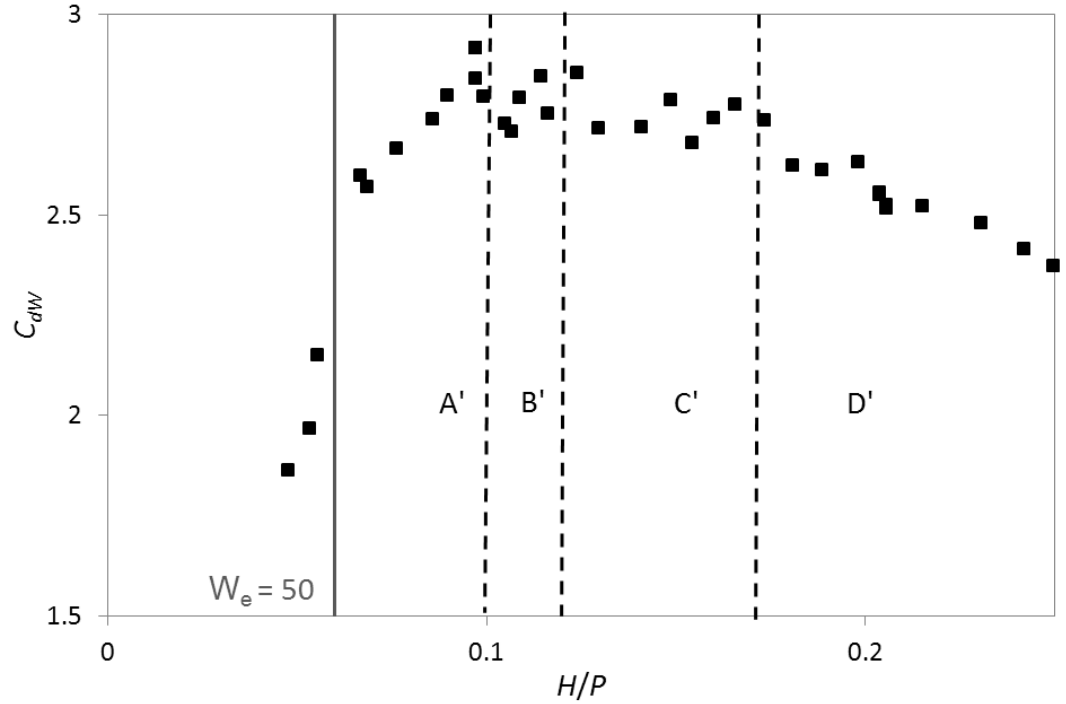

Figure IV-10 Non-dimensional head/discharge coefficient relation for low heads

IV.3. Streamlines [74]

The streamlines on the PKW have been determined for 12 different heads, from H/P = 0.05 to 0.45. For low heads (H/P < 0.2), the streamlines are rather homogeneously distributed along the whole weir crest. The downstream crest of the inlet key is mainly supplied by the bottom stream. The upstream crest of the outlet key is mainly supplied by the surface stream. Finally, the side crest is supplied in its downstream part by streams coming in front of the inlet keys and on its upstream part by streams coming in front of the outlet keys, under the crest level (Figure IV-11).

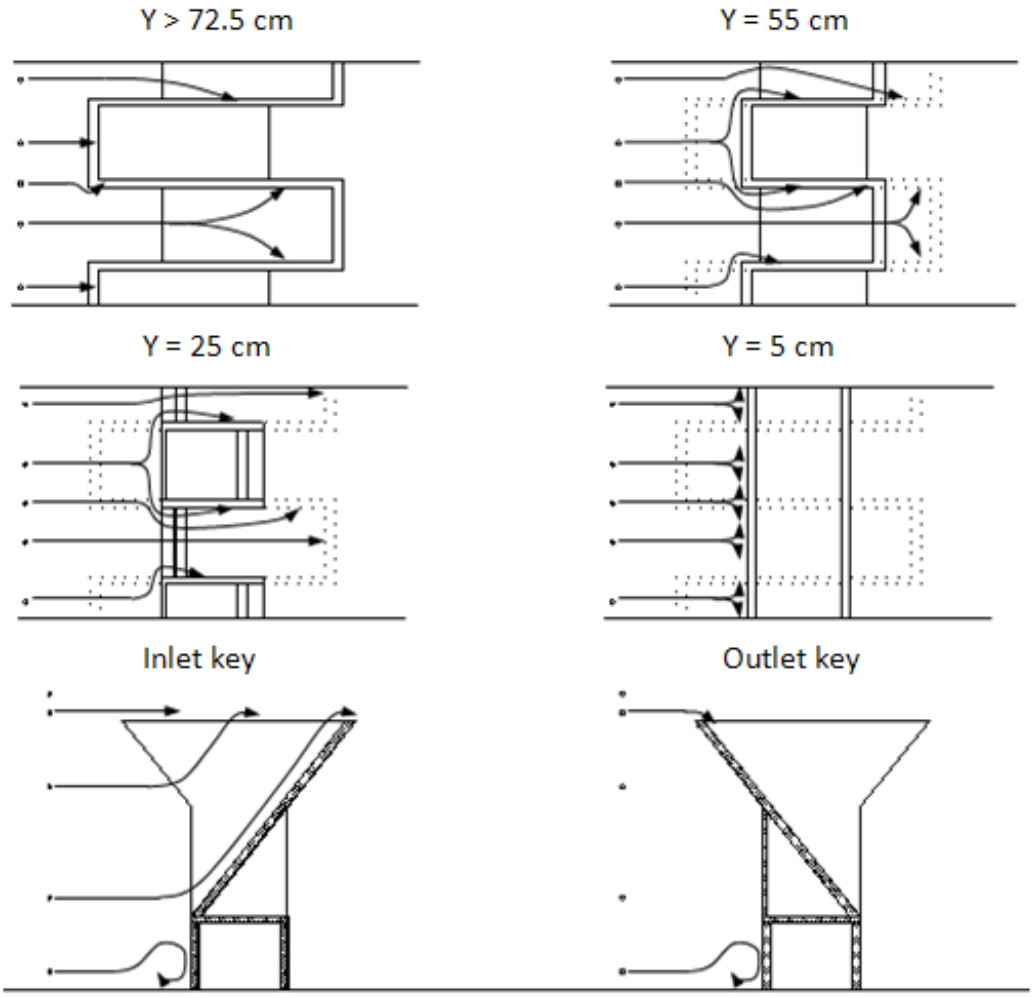

Figure IV-11 Streamlines for low heads (H/P < 0.2)

For H/P > 0.2, the stream lines distribution appears less optimal. Indeed, the downstream crest of the inlet key is importantly supplied, still by the bottom stream but also by streams coming in front of the inlet key with high velocity. The upstream crest of the outlet key is still supplied by the surface stream. Finally, the side crest is poorly supplied by streams coming in front of the outlet keys, under the crest level (Figure IV-12).

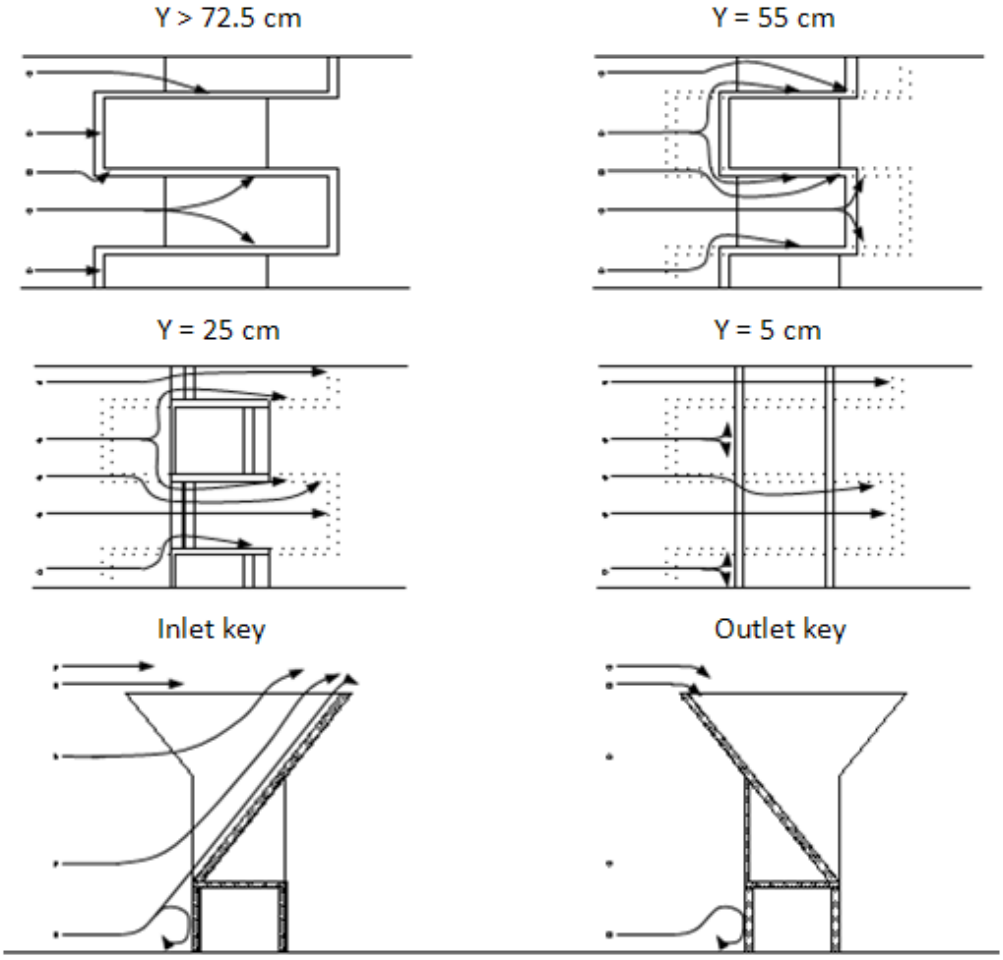

Figure IV-12 Streamlines for high heads (H/P > 0.2)

The transition between these main streamlines sketch corresponds to the transition from a flat to a rippled free surface line along the inlet key (Figure IV-13). That traduces a non-homogeneous alimentation of the side crest.

Figure IV-13 Surface line profiles for low and high heads (H/P = 0.15 and 0.35)

The continuous decrease in efficiency, observed in Figure IV-1, can be explained by the analysis of the streamlines distribution for high heads. For these heads, the downstream crest of the inlet key is over supplied because of the flow inertia in the downstream direction. More streamlines than for low heads reach this section of the PKW. The side crest is poorly supplied because of the same longitudinal flow inertia. The streamlines along this crest are less dense. The upstream crest of the outlet key is supplied equally for high heads and for low heads (same streamlines).

Because of the inlet slope and the corresponding water depths variations, a critical section may appear from the downstream crest and moves upstream, along the inlet key, for increasing heads. This phenomenon is directly observed on the model by the apparition of a rippled free surface, corresponding to the position of the critical section. The displacement of the critical section along the inlet key decreases progressively the effective crest length and so the global discharge coefficient of the PKW.

IV.4. Free surface profile [75]

Free surface, velocity and pressure profiles have been measured upstream of the weir and along the inlet key. The turbulent flow behaviour and air entrainment don't enable these measurements along the outlet key.

Four head ratios have been studied: low head (H/P = 0.1), high heads (H/P = 0.35 and 0.5) and the transition zone highlighted by the streamlines study (H/P = 0.2). The free surface measurements confirm the transition between a flat free surface along the inlet key for low head (H/P = 0.1) to a rippled one for high head (H/P = 0.35) (Figure IV-14). For the highest head (H/P = 0.5), an important water depth decrease is observed at the inlet key entrance.

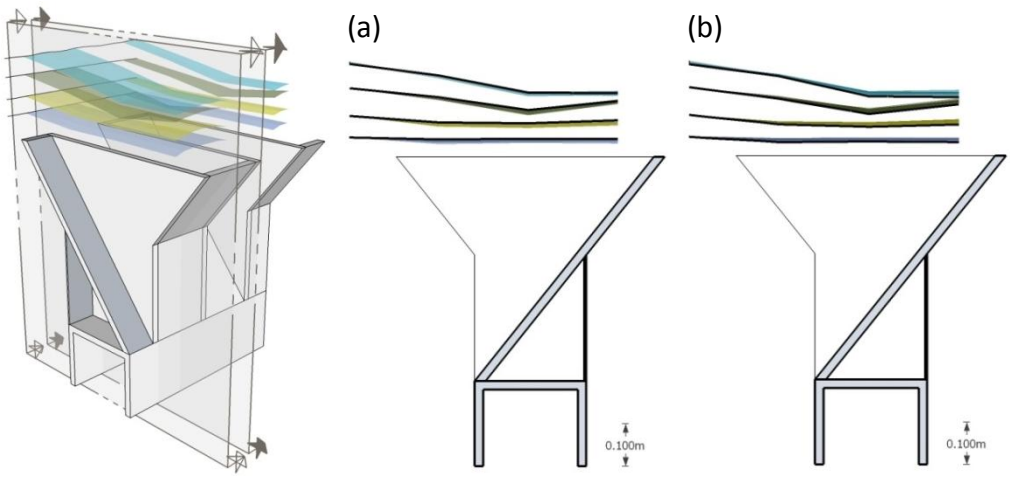

Figure IV-14 Free surface profiles along the inlet keys (clear blue - H/P = 0.5; green - H/P = 0.35; yellow - H/P = 0.2; dark blue - H/P = 0.1): (a) – cut in the middle of the key; (b) – cut along the side wall

The Figure IV-15 shows the variation of the free surface along the inlet key with the upstream head, confirming the measured flow characteristics. The transition from a flat free surface to a rippled one for the transition head (H/P = 0.2) and a more important decrease of free surface level at inlet entrance as the head is more important are observed.

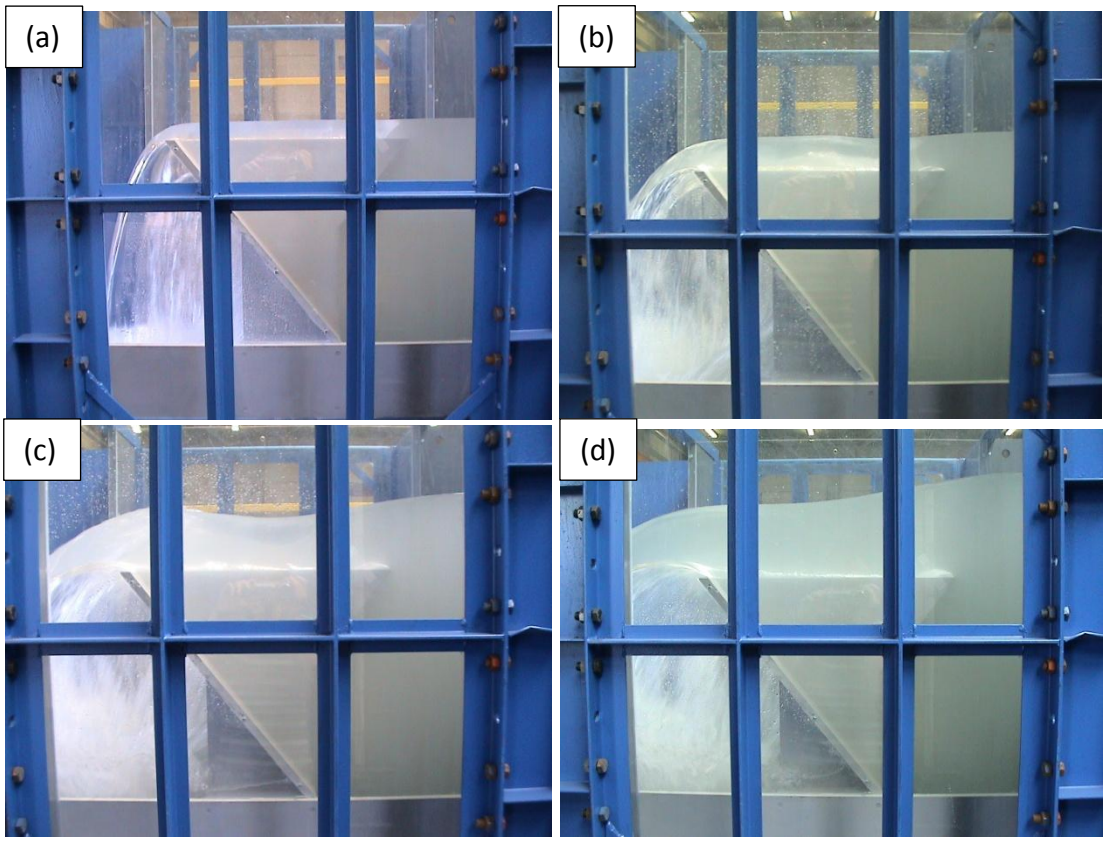

Figure IV-15 View of the inlet free surface variation with head: H/P = (a) – 0.1; (b) – 0.2; (c) – 0.35; (d) – 0.5

The Figure IV-16 shows the variation of the free surface along the outlet key. As the free surface couldn't be measured along these keys, due to the lateral nappe interference, these observations are of prime importance. On the 1:10 scale model, even if the outlet key seems submerged for highest heads, the flow is still largely aerated under the lateral nappes. The outlet key flow seems so to stay supercritical whatever the upstream head and to have no influence on the release capacity of the weir. The feeling of submergence is given by the lateral nappes interference zone situated over the main outlet flow.

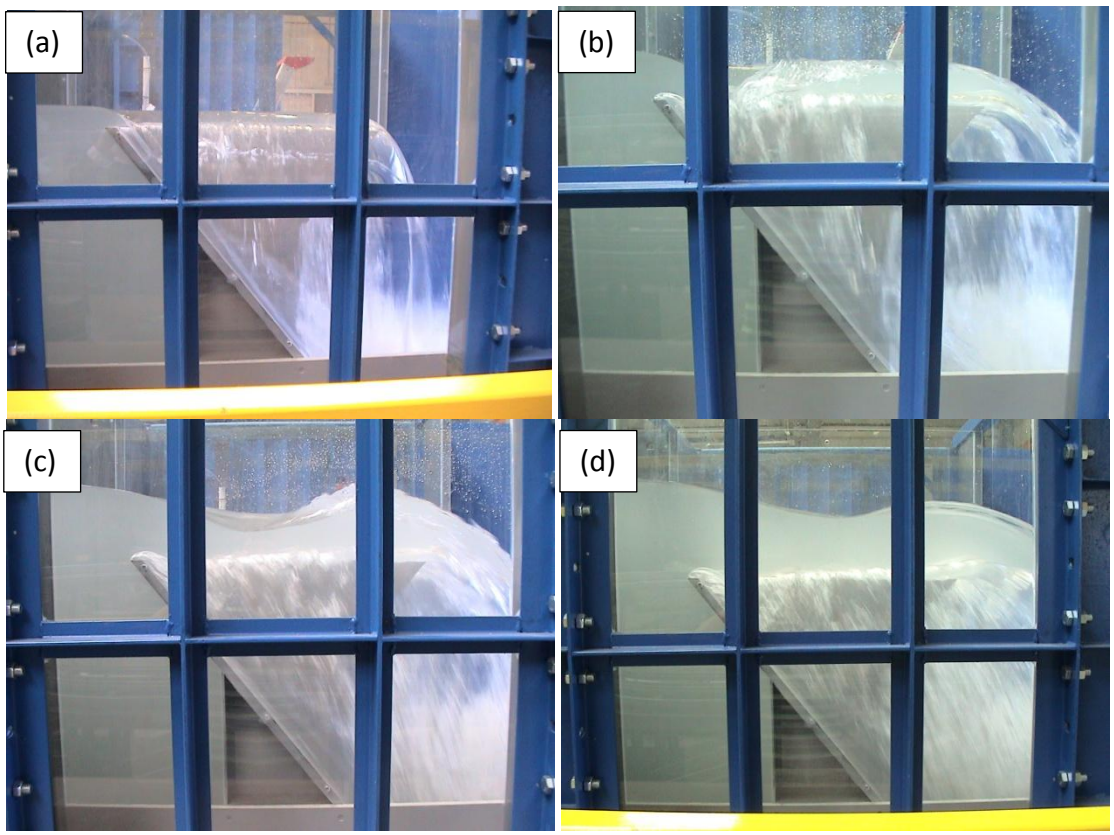

Figure IV-16 View of the outlet free surface variation with head: H/P = (a) – 0.1; (b) – 0.2; (c) – 0.35; (d) – 0.5

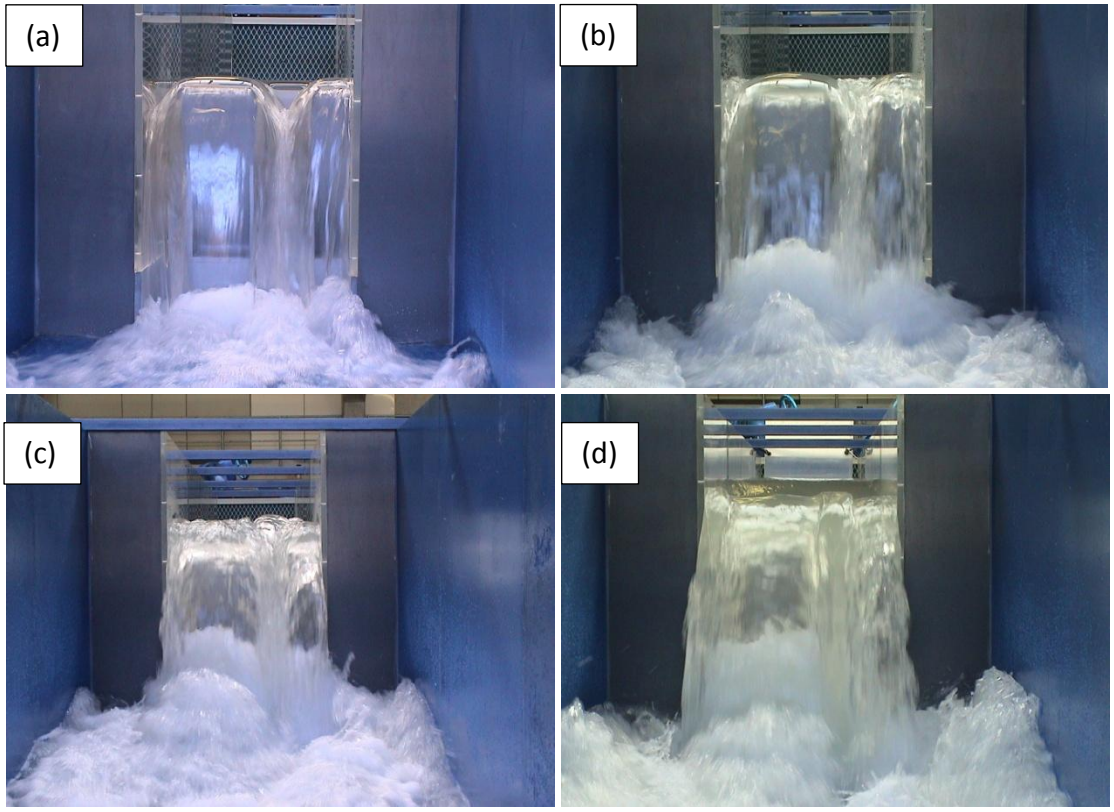

Figure IV-17 View of the transverse free surface variation with head: H/P = (a) – 0.1; (b) – 0.2; (c) – 0.35; (d) – 0.5

Regarding the transverse free surface profile (Figure IV-17), the lateral nappe interference zone is still under the crest elevation for low heads (H/P = 0.1 and 0.2). For higher heads (H/P = 0.35), as this zone moves over the crest elevation, it modifies the free surface profiles over the side crests and so the release capacity of the weir. Finally, for H/P = 0.5, the transverse free surface profile becomes close to the horizontal, traducing negligible discharges on the side crests.

IV.5. Pressure distribution [75, 76]

The measured pressure profiles are close to hydrostatic along the side wall as well as in the middle of the inlet key except in particular points (Figure IV-18 and Table IV-1). An over-pressure zone can be observed compared with the hydrostatic profile where the streamlines are denser (Figure IV-11 and Figure IV-12). It is the case in the part of the flow in front of the angles near the entrance (Table IV-1 - bold). This over-pressure increases when the upstream head rises.

Table IV-1 – Difference between measured pressures and hydrostaticity (%) (in the centre / along the side wall of the inlet key), (+ under-pressure, - over-pressure), (X horizontal distance from the downstream crest, Z vertical elevation)

H/P	0.1				0.2			
Z (m)\X (m)	0.74	0.53	0.32	0.11	0.74	0.53	0.32	0.11
0.75	0.2 / -0.1	-0.1 / -0.6	0.0 / 0.1	0.1 / -0.2	0.3 / 0.4	-0.3 / 0.1	-0.1 / 0.6	0.2 / 1.2
0.55	0.4 / 0.3	-0.4 / -0.8	0.3 / -0.3		0.0 / -0.3	**-1.7 / -2.3**	0.0 / -0.8	
0.25	0.3 / -0.1	-0.5 / **-1.3**			-0.7 / -0.3	**-2.8 / -3.0**		
0.05	0.3 / 0.0	-0.8 / **-1.2**			-0.5 / -0.4	**-3.0 / -3.4**		
H/P	0.35				0.5			
Z (m)\X (m)	0.74	0.53	0.32	0.11	0.74	0.53	0.32	0.11
0.75	-0.3 / -0.4	0.5 / 0.3	-0.3 / 0.3	2.5 / 5.0	-0.4 / -0.8	1.5 / 3.1	-1.5 / 0.1	1.9 / 4.4
0.55	-0.6 / -0.8	**-2.2 / -2.8**	-0.2 / -1.1		**-1.7 / -2.1**	0.6 / **-3.1**	-1.1 / 0.9	
0.25	**-1.3 / -1.4**	**-3.7 / -3.5**			**-2.2 / -2.7**	**-3.0 / -5.5**		
0.05	**-1.4 / -1.7**	**-4.3 / -4.8**			**-2.5 / -2.5**	**-5.3 / -6.0**		

(a)

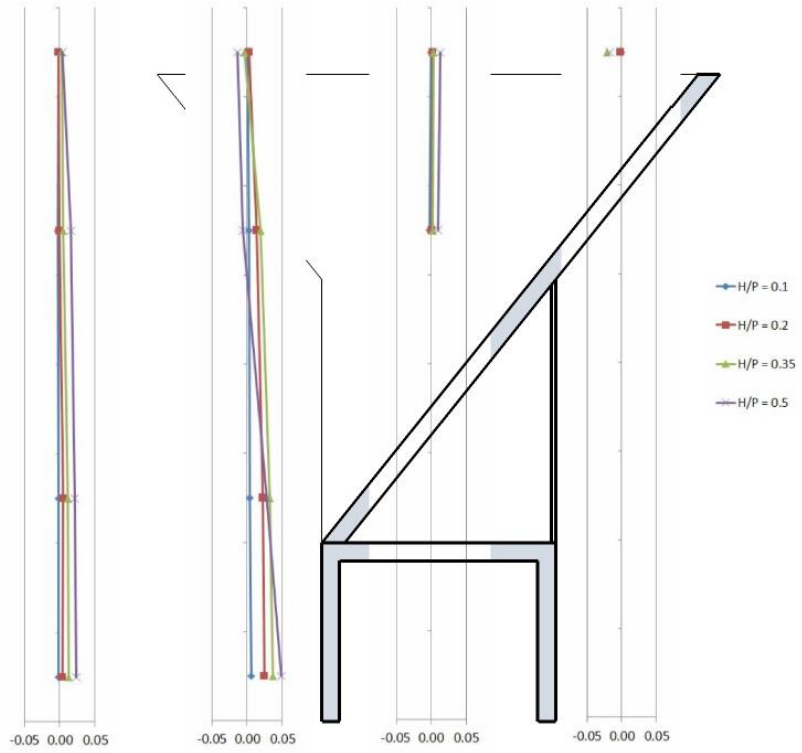

(b)

Figure IV-18 $\frac{p - p_{hydrostatic}}{\rho g}$ ***profiles (m): (a) in the middle of the inlet key; (b) along the side wall***

IV.6. Velocity distribution [75]

The velocity profiles for low heads (H/P = 0.1 and 0.2) are relatively uniform along the side wall as well as in the middle of the inlet key (Figure IV-19 and Figure IV-20). This illustrates the homogeneity of streamlines distribution. For higher heads (H/P = 0.35 and 0.5), the velocity increases in the middle of the inlet key (Figure IV-19 and Figure IV-20). The closer the measurement point from the downstream crest, the higher the velocity. This illustrates the streamlines concentration in this zone. For H/P = 0.5, negative velocities are observed near the side walls at the inlet entrance (recirculation zones, Figure IV-19 – (b) and Figure IV-20 – (b)).

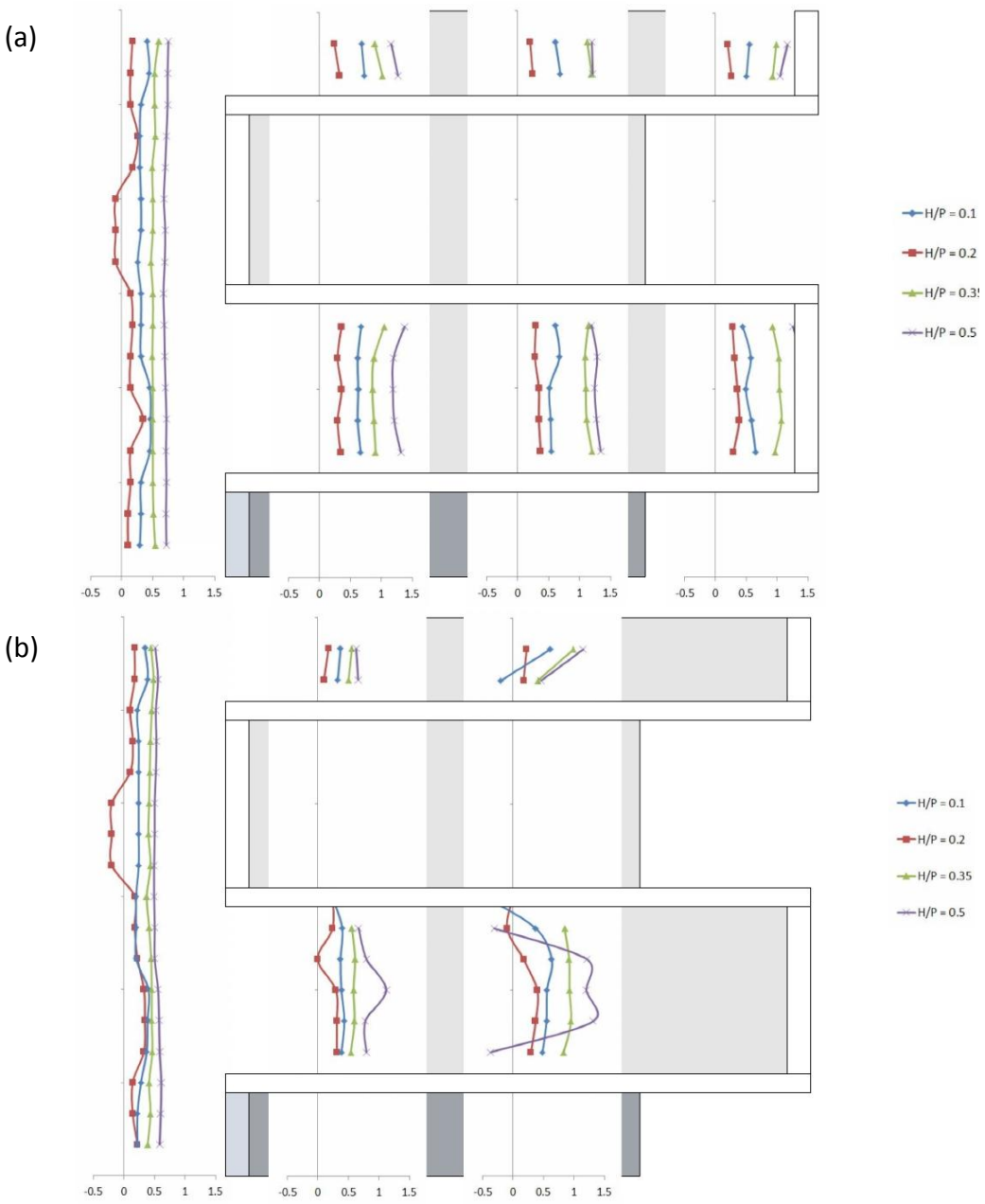

Figure IV-19 Horizontal velocity profiles (m/s): (a) over the weir Z = 0.75 m; (b) in the weir Z = 0.55 m

(a)

(b)

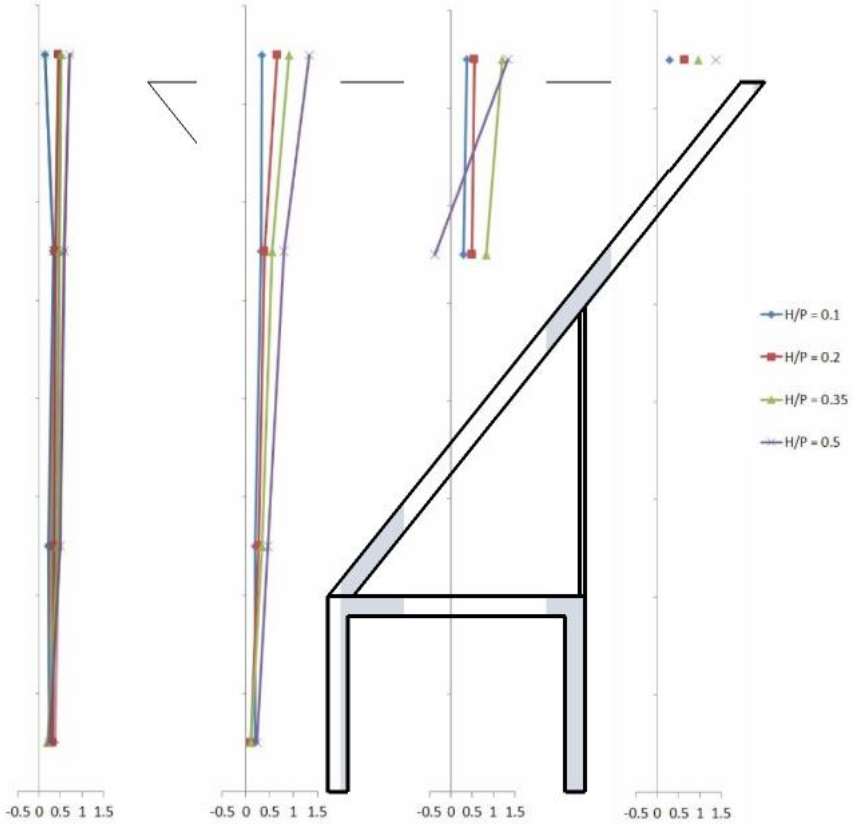

Figure IV-20 Horizontal velocity profiles (m/s): (a) in the middle of the inlet key; (b) along the side wall

Because of the inlet slope and the corresponding water depth variations, the streamlines density increases along the inlet key. The recirculation zones observed along the side walls increase this phenomenon. The size of these recirculation zones increases with the upstream head, reducing the effective section of the inlet key. This reduction of section causes an important concentration of the streamlines and so increases velocities in the middle of the inlet key entrance (Figure IV-19).

Considering that the flow velocity *U* is horizontal at the free surface and parallel to the bottom along it, as the pressure profile is close to hydrostatic, the Froude number can be calculated at each measurement point by:

$$F_r = \frac{U}{\sqrt{gh}} = \frac{U_x\left(\frac{z}{h} + \frac{1}{\cos\theta_i}\left(1 - \frac{z}{h}\right)\right)}{\sqrt{gh}} \qquad \text{IV-7}$$

where, U_x is the horizontal component of flow velocity, z is the vertical coordinate of the measurement point considered from the bottom and θ_i is the inlet inclination. Froude values over 1 traduce flow influenced by the upstream of the streamline, when values under 1 traduce influence of the downstream part of the streamline.

Regarding Froude profiles over the weir (Figure IV-21), a control section (F_r = 1) appears where the velocities become too important. This control section moves upstream with the rising head, where the water height is more important. The efficient length of the weir, and thus the global discharge coefficient of the PKW, decreases more and more importantly (Figure IV-1 – A). Finally, for higher heads the control section should be located directly at the entrance of the inlet key. The discharge capacity decreases asymptotically (Figure IV-1 – B) and seems to tend to a limit value.

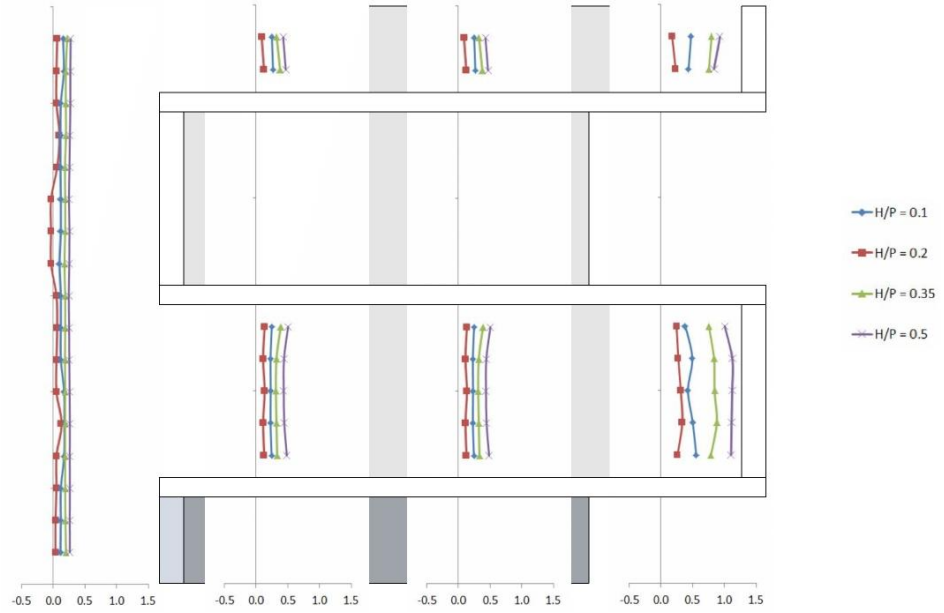

Figure IV-21 Froude profiles over the weir Z = 0.75 m

These observations enable to explain the interest of increasing the inlet width [72, 94], slope or height (using crest extension by example) [93, 94] to increase the inlet cross section. This would limit the occurrence of control section, improving thus the discharge capacity of the weir. It also explains the hydraulic interest of using only upstream overhangs [94], which reduce the inlet key length and increase its slope, so the influence of the control section is limited. Finally, the use of a non-rectangular shape of the front part of the upstream overhangs [93] decreases the recirculation zones size and therefore increases the discharge capacity.

IV.7. Validation of the experimental approach

According to the results obtained from the 1:10 scale model, the experimental approach aims at defining the main hydraulic characteristics of the flows over PKW. As these characteristics enable to explain the head/discharge curve of the PKW and the influence of geometric parameters on it, the prime importance of experimental approach seems clearly highlighted.

Furthermore, at this point of the study, the numerical solvers for PKW were at the beginning of their developments and had a strong need of validation data. The flow understanding was still also essential for solver enhancements.

These assumptions confirm the interest of the experimental study on the 1:10 scale model, and validate the experimental approach of the parametric studies developed hereafter. However, parallel to these experimental studies, 1D numerical model and analytical developments have been realized as they are less time consuming than experimental or 3D numerical models.

V. On the hydraulic behaviour of PKW [82]

V.1. Introduction

As shown before, PKW are interesting structures for dam rehabilitation as they allow discharges until four times more important than ogee-crested weirs for the same water head [13]. This discharge increase is mainly due to the crest length increase created by the labyrinth geometry. However, if we focus on the discharge coefficient calculated based on the developed crest length (Eq. V-1), a quick decrease on crest efficiency can be observed compared with sharp (Figure IV-8) or ogee-crested weirs [6, 81].

$$C_{dL} = \frac{Q}{L\sqrt{2gH^3}} \qquad \text{V-1}$$

In the scope of the enhancement of the PKW geometry, it is of prime importance to clearly depict the reasons of this crest efficiency decrease. In this part, the various theories proposed in literature are analysed and their contributions are combined to develop a general description of the PKW behaviour.

Several authors have been interested in the PKW efficiency decrease for increasing heads and three different approaches have been proposed: the first one developed from parametric as well as prototype experiments carried out at the "*Ecole Polytechnique Fédérale de Lausanne*", the second one based on the experimental results obtained at the "*University of Liège*" and presented here before, and the third one issued from experimental comparison of PKW and labyrinth weirs performed at the "*Utah State University*".

The first proposed approach is the one of the "*Ecole Polytechnique Fédérale de Lausanne*" described by Leite Ribeiro et al. [63]. It explains the crest efficiency decrease as a reduction of the effective length of the crest for increasing head, due to the submersion of the frontal weirs, as well up- or downstream, and to the overcrossing jets. The effective length L_{eff} is defined as a function of the upstream head H, the developed crest length L and the weir width W:

$$L_{eff} = W + \frac{1}{\left(kH + \frac{1}{\sqrt[n]{L-W}}\right)^n} \qquad \text{V-2}$$

where k and n are coefficients including effects of other geometrical parameters. These two coefficients have to be fit to correspond with experimental measurements. The global discharge of the PKW is then calculated considering the Poleni equation for the developed length:

$$Q = C_{dL} L_{eff} \sqrt{2gH^3} \qquad \text{V-3}$$

where the discharge coefficient C_{dL} is calculated by the equation of SIA [107] for sharp-crested weirs considering the height of vertical walls equal to its mean value $P/2$:

$$C_{dL} = 0.41\left(1 + \frac{1}{1000H + 1.6}\right)\left[1 + 0.5\left(\frac{H}{H + P/2}\right)^2\right] \qquad \text{V-4}$$

This approach is correlated to the experimental observation of the flow surface shape variation with head. With increasing heads, a progressive submersion of the upstream part of the outlet can be observed combined with an overcrossing of the nappes coming from the side crests, limiting the effective crest length [63]. This explains the interest of keeping the outlet sufficiently large and of providing a sufficient outlet slope to avoid outlet submersion. Indeed, it has been shown that a PKW with a too small outlet width or slope is less efficient (see VII, VIII and IX), and that increasing P_o, keeping P_i constant, increases the discharge efficiency [62]. However, this approach doesn't explain the interest in increasing the inlet key height [62] (see VII). Moreover, this approach is in contradiction with the experimental results showing the interest of increasing the ratio between inlet and outlet key widths [62, 94] (see VIII).

This approach doesn't make any difference between side or transversal crests and doesn't take into account the approach conditions (approaching slope, flow direction, velocities). These approximations may be the causes of the contradictions presented before.

The Liège approach [81] completes the Lausanne one's by explaining the reduction of the effective crest length in the downstream part of the inlet key. Indeed, apparition of a control section in the downstream part of the inlet key has been observed on the 1:10 scale model (see IV). For increasing heads, this control section moves upstream along the key, limiting the effective crest length.

Even if these observations enhance the Lausanne approach, explaining the interest in increasing the inlet cross section by increasing inlet height [62] (see VII) or/and width [62, 94] (see VIII), to avoid the critical section apparition or limit its progression along the inlet key, no direct relation between the critical section position and the upstream head has been established. It is thus very difficult to quantify the real impact of this phenomenon on the global PKW discharge capacity.

In a third approach, Anderson [6] explains the decrease in global PKW efficiency with increasing heads as a cause of an increase of the head loss at the inlet entrance. Indeed, the inlet entrance can be seen as a progressive flow contraction along the upstream overhang before a sudden vertical contraction at inlet entrance. This double

contraction may involve a head loss depending on the section variation and the flow velocity.

This theory explains well the interest in increasing the W_i/W_o ratio [62, 94] to limit the contraction as well as the flow velocity, even if it doesn't explain the decrease in PKW efficiency for highest values of this ratio (see VIII). It also explains the interest in increasing the inlet height to decrease the flow velocity and thus the head loss [62] (see VII). Furthermore, it confirmed that the use of noses under the upstream overhangs, providing a smoothly flow contraction, helps to enhance PKW performance by decreasing the local head loss [6, 110].

In its experiments, Anderson [6] compared PKW with similar geometries of rectangular labyrinth weirs with or without sloped floors in both inlet and outlet keys. He found a higher efficiency for PKW compared with rectangular labyrinth weirs as the upstream overhangs provide a more progressive variation of the flow section limiting the head loss at inlet entrance. However, he also highlights small differences in efficiency between the various rectangular labyrinth weirs considering or not sloped floors in the inlet and/or the outlet keys. This last behaviour can't be explained by the presence of a head loss at the inlet entrance.

All the physical processes at the basis of the three approaches presented here before have been observed on the experimental models tested in this study. They all have an influence on the global discharge capacity. However, other phenomena may play a role in the decrease of efficiency with increasing heads. The careful observation of the flow over varied geometries of PKW enables to show the influence on the global discharge capacity of:

- The crest shape and thickness [59, 63] ;
- The submersion of the upstream part of the outlet key [63] ;
- The nappe interferences [63] ;
- The approach flow conditions (slope, flow direction, velocity) of the crests ;
- The critical section apparition along the inlet key ;
- The head losses at the inlet entrance [6].

V.2. Crest shape

As for thick-crested weirs, the crest thickness and the crest shape may influence the discharge capacity of PKW.

V.2.1. Crest geometry

The influence of the crest shape on the discharge capacity of thick-crested weirs has been studied by several authors [44, 51, 52, 101]. In a general way, Hager [44] proposed to correct the C_{dL} coefficient of Eq. V-1, equal to 0.429 for sharp-crested

weirs, by a coefficient *c* depending on the upstream head and the crest shape. For flat topped crests, *c* is calculated by:

$$c = 1 - \frac{2}{9\left(1 + \left(\frac{H}{T}\right)^4\right)} \qquad \text{V-5}$$

where *H* is the upstream head and *T* the crest thickness. For upstream rounded crests, *c* is calculated by:

$$c = 0.866\left(1 + \frac{0.272\left(\frac{H}{r}\right)^2}{1 + 0.5\left(\frac{H}{r}\right)^2}\right) \qquad \text{V-6}$$

where *r* is the radius of the crest curvature. The Figure V-1 shows the variation of the discharge coefficient proposed by Hager for finite thick weirs depending on the crest shape. As observed on the model of PKW tested in Liège (see IV.1), the flat topped crest works as a sharp crest for *H*/*T* values over 2.6. This is in agreement with the experimental results of Johnson [51], who observed variations of C_{dL} between 0.33 and 0.429 for *H*/*T* between 0.45 and 1.8. The use of a rounded crest enables to increase the discharge capacity of the sharp-crested weir up to 30%.

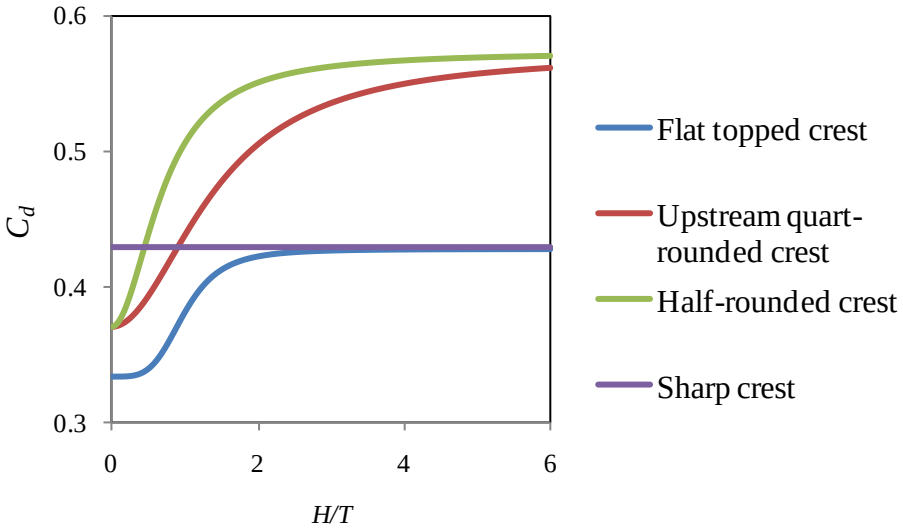

Figure V-1 Variation of the discharge coefficient of a thick-crested weir depending on the crest shape

On labyrinth weirs, rounded crests are generally preferred to sharp and flat crests because their discharge coefficient is higher [109]. Tests performed on labyrinth weirs with quarter-rounded, half-rounded and ogee type crests highlighted the influence of the crest shape for low heads [108]. For low heads, the half-rounded and

the ogee type crests provide discharges up to 11% and 28% higher than the quart-rounded crest. However, for high heads, no more difference is observed between the three variants.

The design of the crest shape for the first PKW, built on Goulours dam, has been performed based on general knowledge of the behaviour of thick-crested weirs. A triangular shape, providing a sharp crest profile, is supposed to have a correct discharge capacity, a long term durability and an easy building on site [57]. For the St-Marc PKW, three geometries of crest have been tested: a flat topped crest and two quart-rounded crests with the round face on the upstream or on the downstream direction [63]. The main observed differences concern the nappe detachment. Indeed, the downstream quart-rounded crest provides leaping nappe for all tested discharges when the nappe is detached for heads over 0.55m (H/T = 2.2) and 0.35m (H/T = 1.4) respectively with a flat topped and an upstream quart-rounded crests. These observations agree with the Hager formulations which provides equivalence with the sharp crest configuration respectively for H/T = 2.6 and 0.9 for flat topped and quart-rounded crests (Figure V-1). The upstream quart-rounded shape seems thus to be the best in terms of nappe aeration and energy dissipation. However, the discharge capacity of the PKW for the design head of 1.35m (H/T = 5.4) is identical for all of the three considered configurations. Anderson [6] compared the discharge efficiency of PKW with half-rounded and flat topped crests. One more time, the interest of the rounded shape in terms of discharge capacity is well demonstrated for low heads, associated to the nappe aeration. The gain in efficiency then gradually decreases for higher heads. Quart-rounded, half-rounded, chamfered and triangular shapes have been placed on the already built PKW. From the experience of these first buildings, the quart-rounded or chamfered shapes are preferred for efficiency and lifetime considerations [110].

Regarding the link observed on the 1:10 scale model with the flat topped crests tested at Liège (cf. IV.1) between the nappe aeration and the discharge capacity, the main difference between the discharges for varied crest shapes should be, one more time, essentially observed for low heads. It is thus natural that there is no difference related to the crest type for the design head on the St-Marc PKW, or for highest heads studied by Anderson.

From the formulations proposed by Hager [44] for the discharge coefficients of thick-crested weirs, an increase of the thickness of the crest reduces the discharge capacity of the weir. However, a decrease of the crest thickness under 0.4H, 0.25H and 0.2H, respectively for a flat topped, a half-rounded and a quart-rounded crests, does not change the discharge coefficient of more than 0.5%.

V.2.2. Crest thickness

On PKW side walls, the crest thickness also influences the effective section of the inlet and outlet keys. Indeed, considering a constant unit width, an increase of the side wall thickness corresponds to an equivalent decrease of the inlet key width, of the outlet key one or of both of them.

An investigation of the influence of an increase of the side crest thickness, considering an equivalent decrease of both inlet and outlet key widths, has been performed by Laugier et al. [59]. Based on the type A PKW with a flat topped crest along the side wall and a sharp crest along both the upstream and downstream apexes, a 3D numerical model, validated by Pralong et al. [97], has been used. The results highlight a large decrease of efficiency for low heads up to 22% for a crest thickness equal to 10% of W_u compared with a thin crest configuration (T_s/W_u = 0.4%). For increasing heads, the loss in efficiency decreases, first quickly, then with a smoother trend.

Laugier et al. explain the observed decrease in efficiency by a diminution of the effective crest length due to the side wall thickness. Indeed, the side crest length does not change from a model to another, but it is not the case for the up- and downstream crests. The effective downstream crest length is reduced by the side wall thickness. The upstream crest length is reduced by the side wall thickness when the nappe is leaping on the side crest and kept constant when the nappe is springing on the side crest. As shown by Laugier et al., the losses in effective width are in the same range than the observed losses in efficiency.

However, as it is the developed crest length that contributes to the total discharge capacity, the effective geometrical loss observed is equal to $2T_s/L_u$. This relation reaches a maximal value of 3.5% only on the tested configurations. Furthermore, the first quick decrease in efficiency observed by Laugier et al. may be attributed to the transition from a leaping to a springing nappe over the flat topped crest. Indeed this decrease is observed for H/T values between 1 and 5 and is not observed on the configuration with lowest thickness for which the studied values of H/T are higher than 5. Using Eq. V-5 to evaluate the loss in efficiency compared to a sharp crest, the maximal value of the loss is equal to 12%. Figure V-2 shows the residual losses in efficiency when the effective geometrical loss ($2T_s/L_u$) and the losses induced by the crest shape ($1-c$) have been subtracted from the losses observed by Laugier et al.. These residual losses could reach 14%.

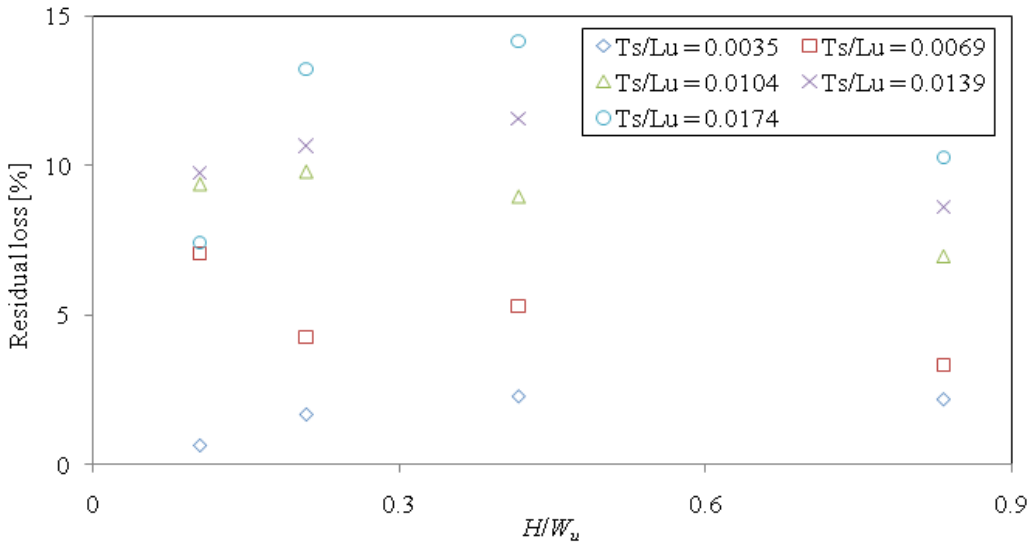

Figure V-2 Residual losses in discharge capacity measured by Laugier et al. [59] after consideration of geometrical losses and crest shape influence

The residual losses may be due to the diminution of the keys sections induced by the crest thickness. For a given head, a diminution of the inlet key section induces higher velocities. These higher velocities along the inlet key decrease the side flow (see V.5), is in favour of the apparition of a control section in the key (see V.6), and increases the head loss at the inlet key entrance (see V.7). All the phenomena induce the residual decrease of efficiency as observed on the results of Laugier et al. (Figure V-2).

Tests performed with the 1D-PKW numerical model (see XIV.2) considering thin and thick side walls, provide losses in efficiency in the same range as in the study of Laugier et al. (Figure V-3). The observed losses in efficiency could directly be linked to the free surface profile variation (Figure V-4). For low specific discharges on a high PKW (P/W_u = 1.33), the free surface profiles are close whatever the crest thickness, and the losses in efficiency are reduced (< 3%). This is mainly due to the relatively low velocities observed in these specific conditions. However, as the flow velocity increases by an increase of the specific discharge or a decrease of the weir height, the loss in efficiency increases significantly. In the same time, a variation can be seen on the free surface profile along the inlet key. Due to the increase of the flow velocity in the inlet key direction, the discharge capacity of the side crest decreases. To ensure the evacuation of the fixed specific discharge with a thick crest configuration, an increase of the water depth along the inlet key is thus necessary.

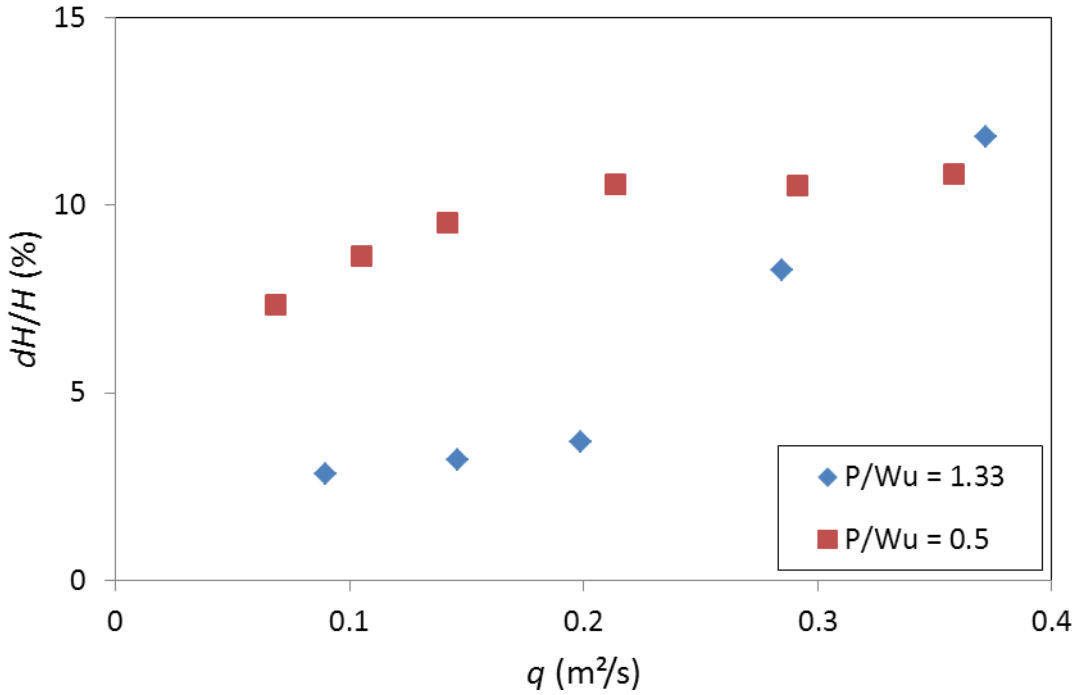

Figure V-3 Losses in efficiency measured on the 1D-PKW results for T_s/L_u passing from 0.0007 to 0.01

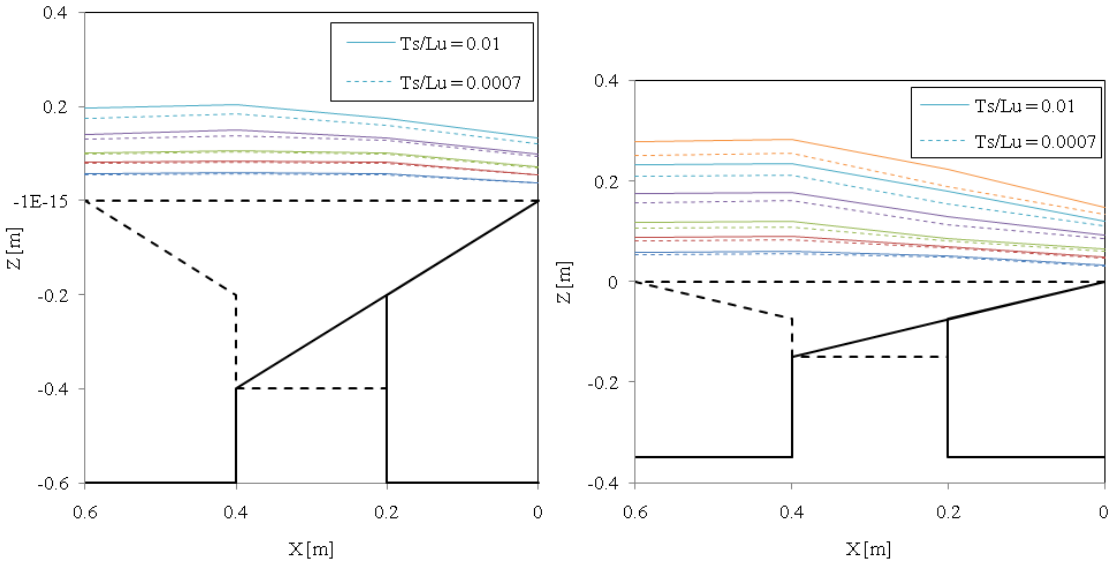

Figure V-4 Free surfaces profiles computed with the 1D-PKW model for fixed specific discharges (left - P/W_u = 1.33; right - P/W_u = 0.5)

At present, some PKW are built with variable sidewall thickness on the weir height (see XII.1). A compromise has been found with a sidewall 0.35 m thick at the basis, to ensure resistance to the maximal efforts, and 0.25 m thick at the crest, due to structural constraints (reinforcement bar covering, aggregate/cement mixing, concrete segregation, lifetime, …) [110].

In conclusion, the main influence of the crest thickness is to reduce the keys widths and thus to increase the flow velocities. Indeed, the geometrical loss in crest

length is around 2%, when losses in efficiency near 10% are observed due to the increase of flow velocities. It is thus of main interest to limit the crest thickness to the one needed for structural considerations. Regarding the crest shape, as the nappe aeration increases the discharge capacity for low heads (see IV.1), the use of upstream rounded crests should be more relevant, especially for designs performed in the scope of mitigation of the peak flow.

V.3. Crest submergence

The crest submergence by the flow in the outlet key may decrease the PKW efficiency of around 10%, considering a downstream free surface elevation corresponding to the crest one [10, 46]. The analysis of the submergence of the outlet key could be splitted in two parts: the influence on the upstream crest of the outlet key and the influence on the side wall crest efficiency.

V.3.1. Upstream crest submergence

The discharge capacity of the upstream crest is modified as long as the critical section moves downstream of its position for free flow conditions. To avoid upstream crest submergence it is thus convenient to impose a downstream slope at least equal to the critical slope (Eq. V-7) directly downstream of the upstream crest of the outlet key.

$$S_{o\,cr} = \frac{2}{3} g^{4/3} Q_o^{-2/3} K^{-2} \left(1 + 6.75 \frac{Q_o^2}{g W_o} \right)^{4/3} \qquad \text{V-7}$$

K is the Strickler coefficient and Q_o is the discharge varying along the outlet key.

As the discharge coefficient of the upstream crest is close to 0.41 (see V.2), the minimal outlet key slope to avoid the upstream crest submergence is largely under the usual slopes observed on PKW prototypes. By example, for a head of 0.3 m over a PKW with an outlet width of 0.3 m and considering a Strickler coefficient of 100, the critical slope is 0.015.

V.3.2. Side crest submergence

The effect of submergence of the side wall is observed as soon as the free surface elevation in the outlet key becomes higher than the crest one. Indeed, for thick-crested weirs, while downstream level stays under the crest one, no influence of the downstream level on the discharge capacity is observed [56]. For higher water level, the discharge coefficient has to be decreased by a submergence coefficient mainly dependent of the ratio between down- and upstream heads [105].

To avoid effects of crest submergence, the free surface level along the outlet key must stay under the crest level. This may be tuned using slopes over the critical one all

along the key. Use of parapet walls in the outlet key may also help. If the PKW is properly designed, the outlet key flow has no influence on the weir efficiency.

V.4. Nappes interactions

Two different types of nappe interaction are present on PKW: a side interference between nappes coming from side and upstream crests and a frontal interference between nappes coming from the two opposite side crests along the outlet key.

V.4.1. Lateral interference

The first one can be compared to a lateral contraction of the nappe, as observed around piles. This contraction is generally taken into account by a reduction of the effective crest length. However, the reduction for triangular pile configurations, which is the most similar to the observed contraction on PKW, is only equal to the half width of the pile, corresponding to the opposite crest thickness in this case. The reduction of effective length due to lateral interaction is thus in the range of T_s. That generally represents less than 3% of the developed length.

V.4.2. Frontal interference

The frontal interference influences the side wall crest efficiency only if the interaction zone, situated in the middle of the outlet key, is upstream of the control section in free flow conditions. From the definition of a standard weir [105], the distance between the control section and the weir crest for sharp-crest weir is close to the one situated between the upstream vertical wall and the crest for standard one, 0.28H. There should thus have no effect of the frontal interference of nappe as long as the H/W_o ratio stays under 1.8.

However, to quantify the influence of the nappe interaction on the discharge capacity, experiments have been led on a sharp crested weir (P = 0.5 m), modifying the nappe by a wall placed vertically through the downstream flume (Figure V-5).

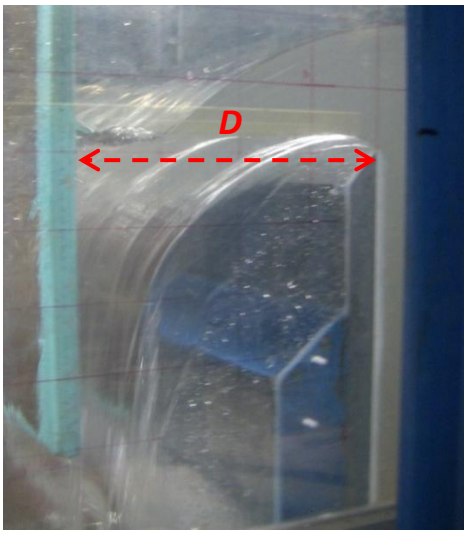

Figure V-5 Experimental sharp-crested weir influenced by a downstream vertical wall

The influence of the plate on the stage discharge curve has been investigated varying the distance D of the wall from the weir crest (D/P = 0.3, 0.4, 0.5 and ∞). Figure V-6 shows the variation of the ratio between specific discharges measured with (q) or without the wall presence (q_0) depending on the adimensional ratio between upstream head and distance between the wall and the weir crest. These results highlight the influence of the wall from H/D = 0.8, whatever the position of the wall. After this point, for increasing heads, the discharge capacity decreases quickly. Loss in efficiency of 45% are observed for H/D = 2.

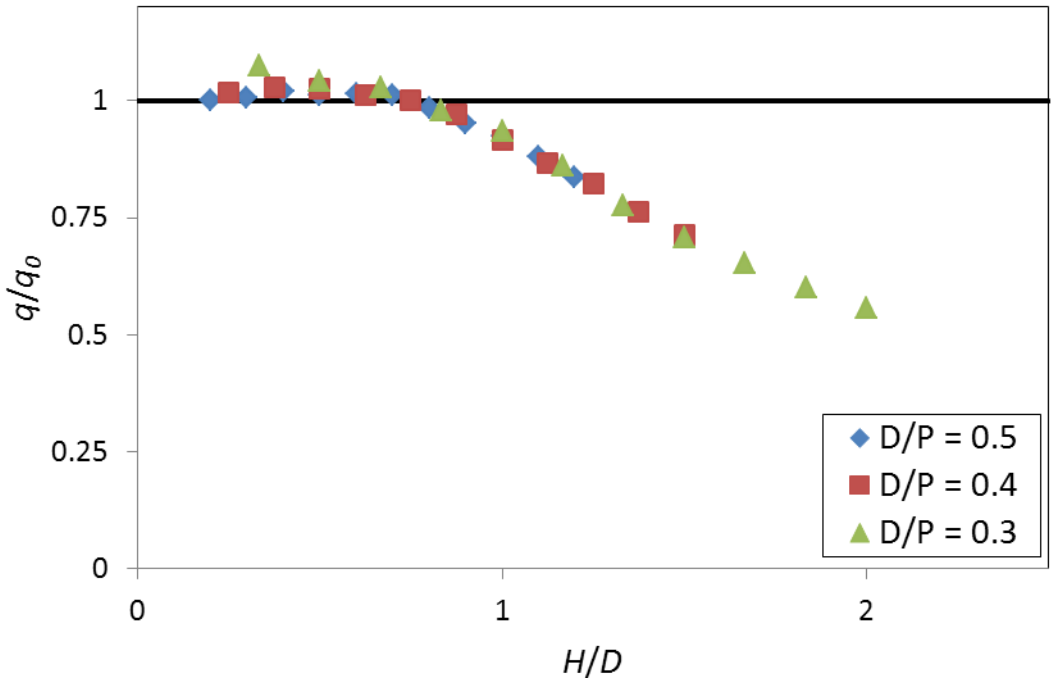

Figure V-6 Influence of the ratio between head and available space downstream a sharp crested weir on its discharge capacity

According to these results, the interaction observed on PKW between opposite side crest nappes should decrease the weir efficiency when the H/W_o ratio is higher than 0.4. However, as shown hereafter (see V.5), the head influencing the side weir discharge is lower than the upstream head as the velocity component in the inlet direction has to be ignored. Furthermore, as the side flow is not perpendicular to the side wall, the horizontal distance between the crest and the interaction zone following the nappe profile is longer than $W_o/2$. The distance D between the side crest and the interaction zone is then equal to ratio between the half outlet width $W_o/2$ and the sinus of the φ angle between the side flow and the side wall. Hager [44] proposed a formulation to compute the φ angle depending on the Froude number and the H/P ratio. Considering the water depth over the side crest as upstream head (see V.5), the maximal H/W_o ratio to avoid influence of the nappes interaction (H/D = 0.8) becomes then 2.34 for H/P = 0.5 and Fr^2 = 0.5, which are coherent values for a usual PKW design.

This is confirmed by the observation of the nappe on the sharp-crested weir when the downstream wall becomes influent (Figure V-7). In this condition, the interaction zone elevation reaches the upstream free surface level (quasi-horizontal free surface profile). This behaviour has only been observed for highest weir heights tested during the following parametric study ($P/W_u > 1.3$) and for H/W_o higher than 2.

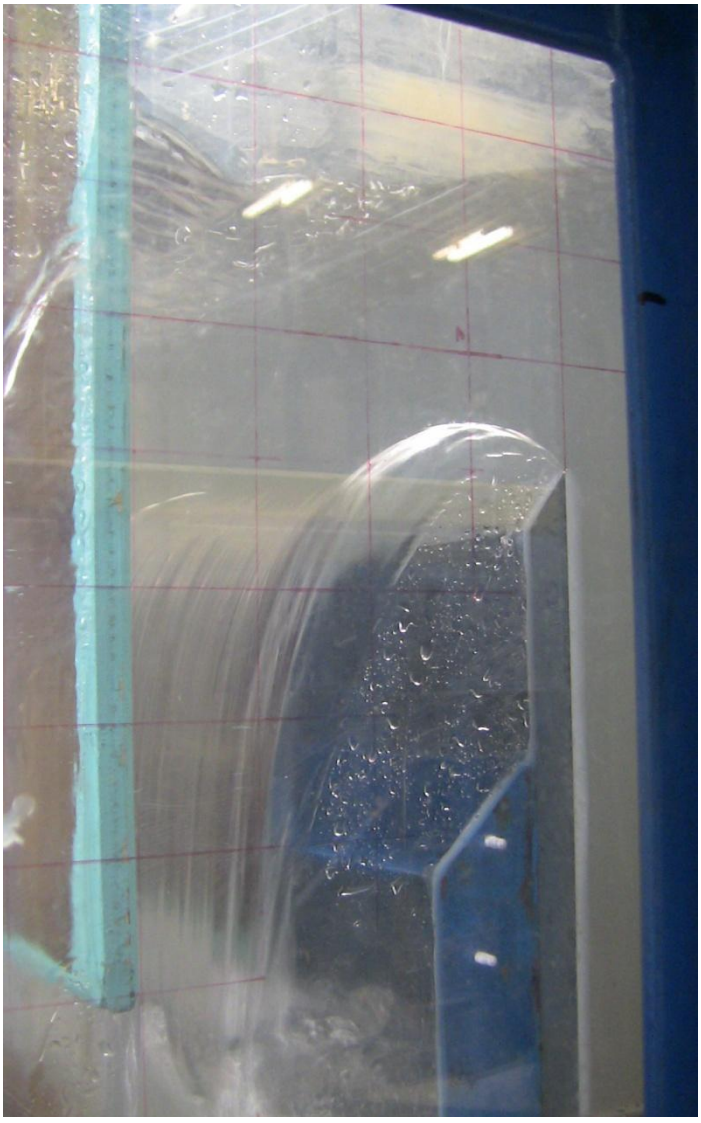

Figure V-7 View of the nappe over a sharp-crested weir influenced by a downstream wall for H/D = 0.8

The value of $H/W_o = 2$ should be considered as a maximal value for PKW design aiming to avoid the influence of the side nappes interaction. From the already built or studied prototype PKWs, the maximal ratio between design head and outlet width is 1.3 for the Dakmi 2 HPP Dam [48]. Thus, interaction between side nappes should not influence the release capacity of usual PKW designs.

V.5. Crests approach conditions

The crest of PKW can be decomposed in three parts according to different approach conditions: the downstream crest of the inlet key, which can be seen as a downstream inclined sharp-crest, the upstream crest of the outlet key, which can be seen as an upstream inclined sharp-crest, and the side wall crest, which can be seen as a lateral thick-crest.

V.5.1. Downstream crest approach conditions

As a result of the experimental study led on downstream inclined sharp-crested weirs (see XIV.1), the discharge coefficient must be corrected from the one of a traditional sharp-crested weir considering an inclination of 50°. The discharge coefficient for the downstream crest remains constant around 0.482, whatever the bottom slope or the upstream head. The downstream crest approach conditions don't influence the observed decrease in discharge capacity.

V.5.2. Upstream crest approach conditions

A similar experiment led on an upstream inclined weir has shown a decrease of the discharge coefficient of sharp-crested weir until 0.41 [53]. Since this coefficient is not modified with upstream head variations, approach conditions of the upstream crest don't influence the observed efficiency decrease of PKW.

V.5.3. Side crest approach conditions

As the main part of the discharge is provided by the side crest, the influence of the approach conditions on its efficiency is of prime importance. Hager [44] highlights that the side weir discharge is influenced by the water head as well as the weir height and the crest shape, like each plane weir. However, the water head has to be reduced to the water height over the crest, neglecting the influence of the kinetic energy in the plan parallel to the crest. Furthermore, the main channel flow velocity influences the side outflow angle which modifies the weir discharge [44]. Finally, Hager highlights an influence of the channel shape. A contraction of the main channel cross section yields to a more uniform side outflow distribution. This contraction may be took into account by a discretisation of the crest, considering no variation of the cross section along a small part of the crest. According to Hager's approach, the main parameter modifying the side crest efficiency, compared to plane weirs, is thus the velocity in the main channel. This is confirmed by several authors providing the discharge coefficient for side weirs in terms of the Froude number in the main channel [15, 44, 88, 91].

Regarding the coefficients proposed by Hager to modify the usual discharge coefficient for thick-crested weir, a variation of the Froude number along the main channel (inlet key) from 0 to 1 decreases the discharge coefficient of at least 58%, depending on upstream head and weir height. The approach flow conditions of the

side wall crest seems thus to be the main reason of the PKW efficiency decrease observed on the various tested models.

The influence of the side flow has been studied on the numerical solver Wolf1D-PKW developed for PKW modelling (see XIV.2). The mass exchanges between the inlet and outlet keys have been computed based on the Poleni formulation (Eq. V-1). In accordance with the literature on side weirs, the head considered for the side weir has been calculated neglecting the component of kinetic energy in the plan parallel to the crest. The mass exchange is thus completely defined by the discharge coefficient C_{dL} along the side crest. The value of this coefficient is largely influenced by the approach flow conditions.

A first approach is to consider the side crest as a perfect sharp-crested weir. The theoretical maximal value of the C_{dL} coefficient is 0.667. However, traditional sharp-crested weirs provide C_{dL} coefficient near 0.43 [51]. The imposition of these two values of the coefficient has thus been tested. However, discharge over a side weir doesn't exactly correspond to the discharge over a traditional sharp-crested weir. Indeed, the side discharge will be influenced by the velocity of approach, the outflow angle and the channel shape [44]. Two formulations of the C_{dL} coefficient have thus also been tested for a better approach of the side discharge. The first one is the formulation proposed by Hager [44]:

$$C_{dL} = 0.424c\left[\frac{H}{3H-2h+2w}\right]^{1/2} \qquad \text{V-8}$$

where h is the water depth in the main channel (inlet key), H is the water head considered from the bottom of the channel, w is the weir height and c the coefficient traducing the influence of the crest shape (see V.2).

The second studied formulation is the one proposed by Oertel et al. [91]:

$$C_{dL} = \frac{2}{3}\left[0.05\log\ 0.7\gamma\sqrt{Fr}\ +0.35\right] \qquad \text{V-9}$$

$$\gamma = \ 1.44 - 2.4\sqrt{Fr} + Fr\ \frac{W_i^2}{B^2}; Fr = \frac{U}{\sqrt{gh}} \qquad \text{V-10}$$

where U is the velocity in the main channel (inlet key).

The influence of the C_{dL} coefficient determination has been studied fixing the limits of horizontal integration at the key walls ("In" approach), corresponding to the more precise approach for a large use of the Wolf1D-PKW model (see XIV.2.3). The α coefficient, introduced in the integrated Navier-Stokes equations to quantify the exchange in momentum due to the side discharge, is chosen equal to one in both inlet

and outlet keys, traducing a full exchange of momentum between inlet and outlet keys. Four PKW geometries have been studied to highlight the common influence of the free variables definition with geometrical specificities of the tested model. The four tested models provide P/W_u ratios of 0.5 and 1.33 and W_i/W_o ratios of 0.796 and 1.5. These four models have also been studied in idealized conditions in laboratory to provide comparisons with the numerical results (see VIII.4). The Figure V-8 presents the comparison of the upstream heads computed with the two fixed values and the two formulations for the C_{dL} coefficient for given specific discharges on the four geometries tested in the laboratory.

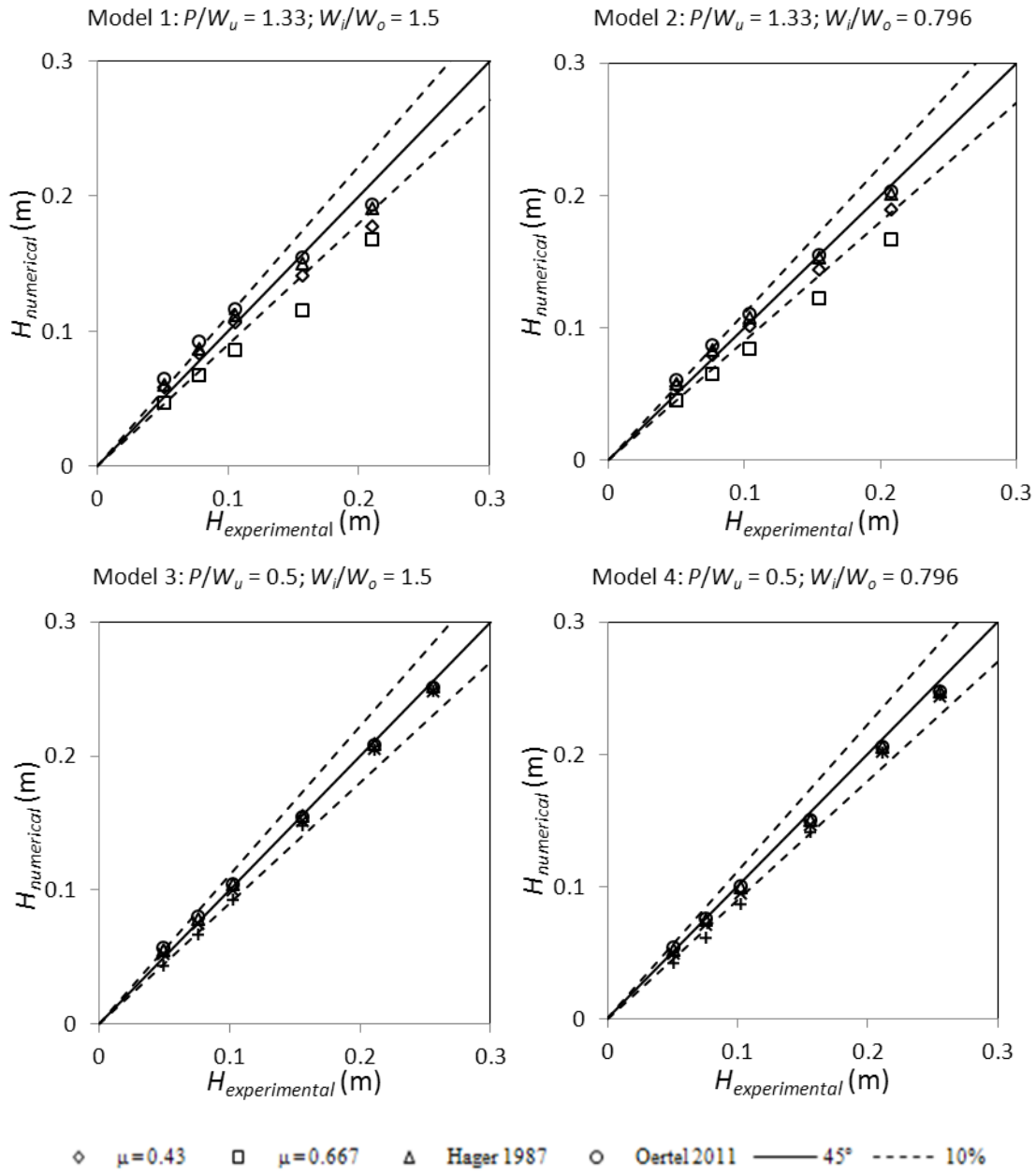

Figure V-8 Influence of the mass exchange calculation on the upstream head computed with the 1D-PKW numerical model for given discharges

For lower weir height (models 3 and 4) and high heads, the choice of the side discharge parameters values doesn't influence the computed upstream heads. This traduces the small influence of the side exchanges on the global efficiency of the PKW. Indeed, in these conditions of weir height and water head, the PKW is practically fully submerged (Figure V-9) and the side discharge is a very small part of the global discharge.

Figure V-9 PKW model 4 under a high upstream head (H = 0.256 cm)

For highest PKW height (models 1 and 2), to set the C_{dL} coefficient equal to 0.667 or 0.43 underestimates the upstream head value until respectively 20% and 15%. For these conditions of weir height and water head, the side crest works as a free weir. However, the side discharge is mainly influenced by the high flow velocity along the inlet key, reducing the efficiency of the side crest. As the two formulations of Hager and Oertel take into account the influence of the approach conditions of the side weir, they provide better evaluation of the upstream head. For the high heads, the results of the two formulations are relatively close and approach experimental results with an accuracy of 9% on the upstream head. As expected, to set the C_{dL} coefficient to 0.667 underestimates systematically the upstream head, for low heads. Indeed the value of 0.667 is an idealized theoretical value and the experimental value of the C_{dL} coefficient is close to 0.43. As, for low heads, the velocity along the inlet key is negligible, the side discharge is close to the one of a sharp-crested weir. To set the C_{dL} coefficient to 0.43 approaches the experimental upstream head with a 6% accuracy, on the four tested models. The formulation of Hager provides upstream heads relatively close to the ones obtained setting the C_{dL} coefficient to 0.43, keeping an accuracy of 10% on the experimental results. The formulation of Oertel is less relevant for low heads. Indeed, it systematically overestimates the upstream head until 17% for the highest PKW height (models 1 and 2) and 12% for the lowest one (models 3 and 4).

The main influence of the approach condition on the side crest discharge enables to explain the decrease of discharge capacity observed on PKW for increasing heads. For low heads, negligible velocities along the inlet key allow the side weir to work as a traditional sharp-crested weir, providing maximal discharge capacity and a side flow perpendicular to the inlet axis. Then, for increasing heads, the side flow becomes more

parallel to the inlet key main direction, what limits the mass exchanges between keys. This decreases the side crest and thus the global PKW efficiencies. This decrease is quicker for low weir height configurations for which the velocity increase is more important due to lower water depths. For highest heads, the PKW efficiency tends to stabilize to a similar value whatever the PKW geometry, as the side crest discharge tends to 0 due to combined effects of too important flow velocities in the inlet key direction and submergence of the side wall by the outlet flow.

V.6. Critical section

As a result of the study performed on the 1:10 scale model, the apparition of a control section in the inlet key has been highlighted for sufficiently high heads (see IV). This control section reduces the effective crest length and thus the global discharge capacity of the weir. The effective crest length depends of the PKW geometry as well as the upstream head. Indeed, it has been observed on the scale models that the control section moves upstream along the inlet key for increasing heads (see IV).

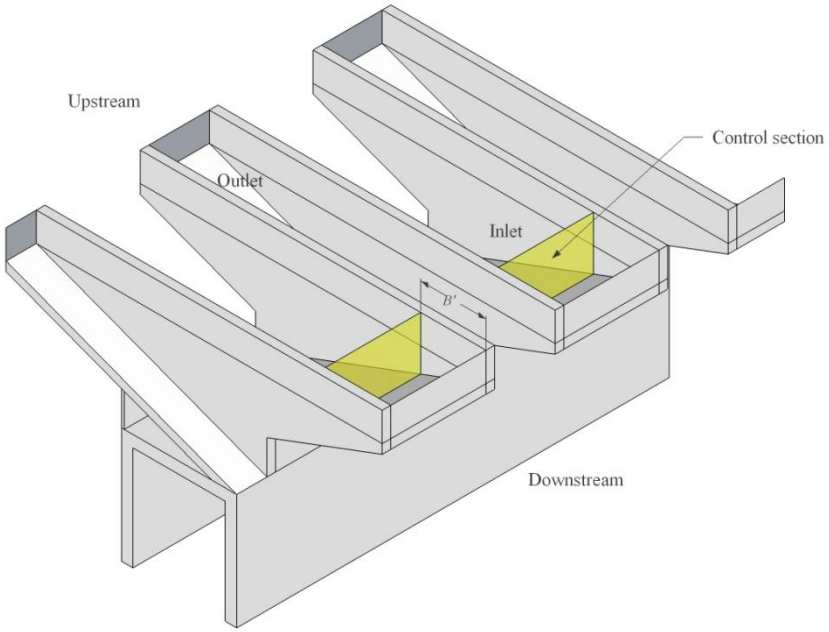

Figure V-10 Location of the control section position

As defined before, the effective crest length is completely determined, for a given PKW geometry, by the position of the control section along the inlet key *B'* (Figure V-10). As the pressure measurements on the 1:10 scale model have shown close to hydrostatic pressure profiles along the inlet key (see IV.5), the flow velocity is considered uniform along the vertical axis and the position of the control section can be determined considering the condition of critical flow.

$$Fr^2 = 1 = \frac{U^2}{gh} = \frac{q^2}{gh^3} \qquad \text{V-11}$$

This first equation links the water depth *h* to the specific discharge *q* in the control section.

The expression of the local head also links these two parameters:

$$H + P_{pi} + B'S_i = h + \frac{U^2}{2g} = h + \frac{q^2}{2gh^2} \qquad \text{V-12}$$

Combining the two equations V-11 and V-12, the water depth *h* and the specific discharge *q* at the control section can be formulated depending on the local head *H* and the position of this section *B'*.

$$h = \frac{2}{3}\ H + P_{pi} + B'S_i \qquad \text{V-13}$$

$$q = \sqrt{g\left(\frac{2}{3}\ H + P_{pi} + B'S_i\ \right)^3} \qquad \text{V-14}$$

Considering no head variation along the side crest (see V.7), three unknowns remain *h*, *q* and *B'*. To close this system, a continuity equation is used to ensure that the discharge passing through the control section is equal to the discharge passing over the crest downstream of this section. The discharge capacity of the downstream part of the crest could be calculated based on a discharge coefficient equal to 0.482. This value come from the experimental study led on sloping sharp-crested weirs (see XIV.1).

$$q_{downstream} = 0.482\sqrt{2gH^3} \qquad \text{V-15}$$

The study realized with the Wolf1D-PKW numerical model has shown that the formulation V-8 proposed by Hager [44] is relevant to compute the discharge over the side crest. In a first step, the side discharge is considered homogeneous along *B'*. Combining the expression of the side, the downstream and the critical discharges in a continuity equation, it comes:

$$0.385W_i\left(1 + \frac{P_{pi} + B'S_i}{H}\right)^{3/2} = 0.482W_i + 0.283\left(1 - \frac{2}{9\left(1 + \left(\frac{H}{T}\right)^4\right)}\right)B'\frac{\left(2 - \frac{P_{pi} + B'S_i}{H}\right)^{3/2}}{\left(5 + 2\frac{P_{pi} + B'S_i}{H}\right)^{1/2}} \qquad \text{V-16}$$

with only *B'* as unknown.

The existence of a critical section on the 1:10 scale model decreases the effective crest length up to 8%, following Eq. V-16, between upstream heads ratio *H*/*P* from 0.1 to 0.5. In the same time, the discharge through the critical section increases with head. The variation of the critical section position along the inlet key for *H*/*P* ratios between 0.1 and 0.5 decreases thus the global PKW efficiency of 5.5%, to be compared with the loss in efficiency of 40% observed on the experimental model.

The influence of the critical section observed along the inlet key cannot be neglected but seems to be of minor importance.

V.7. Head losses

The head loss induced by the flow contraction at the inlet key entrance can be compared with the head loss induced by a variable flow contraction. Considering head losses formulae proposed by Idel'Cik [50] for convergent flows, applied to the tested PKW models, it appears that the head loss is below 3% of the upstream head even for low weir height or low weir width. The head loss at inlet key entrance is thus of minor importance and the use of noses must only improve the weir capacity of a few percentage.

The head variation along the inlet key due to the exchanges between inlet and outlet keys could be neglected. Indeed, side weir theories show that the energy level stays constant along the main channel whatever the lateral discharge [44].

V.8. Conclusion

Piano Key Weir is a complex geometric structure inducing a large set of flow conditions along the different parts of the weir. Besides the difficulty of a separate observation of the different flow features, the common or opposite influence of the geometrical parameters variation on the efficiency of the weir, makes the understanding of the PKW working complex. From former researches and observations, six factors are identified to affect the global discharge capacity of PKW: the crest shape and thickness, the crest submersion, the nappes interactions, the approach conditions, the critical section position along the inlet key and the head losses at inlet key entrance.

From the studies discussed before, the main parameter influencing the weir efficiency is the approach conditions of the side wall crest. The decrease of the effective head on the side wall and the inclination of the lateral flow, due to the longitudinal flow velocity along the inlet key, allow to explain the main part of the stage-discharge curves observed on tested models. It is thus of prime importance to decrease the flow velocity along the inlet key for the best PKW design.

The crest shape mainly influences the PKW working at low heads. In order to limit the observed decrease in efficiency for low heads, rounded crests have to be preferred on prototypes designed for flow mitigation.

Effects of the critical section appearance along the inlet key seem to be of secondary importance, modifying only of around 5% the PKW efficiency.

In the same way, the consideration of the crest thickness and the lateral nappe interferences only decrease the effective crest length in the range of 3%. Head losses also affect the upstream head of less than 3% on studied models. However, as the crest thickness decreases the keys widths it has to stay limited.

Finally, effects of the crest submergence and of the frontal nappe interaction can be avoided by the design of sufficiently sloped and wide outlet keys.

VI. Parametric studies definition

VI.1. Main geometrical parameters of PKW [39]

Considering the results and the observations from the 1:10 scale model study (see IV) and the flow behaviour of the PKW (see V), four main geometrical parameters can be distinguished from the large set of parameters induced by the complex geometry of PKW: the crest length, the weir height, the keys widths and the overhangs lengths.

VI.1.1. Crest length

The crest length seems to be the main parameter for PKW. Indeed, it defines the relative length L/W and so the maximal efficiency of the weir for low heads. The influence of the L/W ratio has been studied by several authors [61, 66, 94]. As expected, for low heads, the gain in efficiency is in the range of the L/W ratio increase. However, for higher heads, the differences tend to decrease. Lempérière et al. [69] proposed values of this ratio between 4 and 5 as a reasonable compromise between discharge capacity and structural cost increases.

As this parameter has already been extensively studied and as its main influence is, as expected, only to increase the effective weir length, this parameter has not been studied in the present parametric study. However, the other geometrical parameters have been tested with L/W values in the range proposed by Lempérière et al., and the separated influences of each part of the crest have been decomposed in all the theoretical and analytical approaches presented hereafter.

VI.1.2. Weir height

On the 1:10 scale model, the flow contraction at the inlet key entrance and the apparition of a control section in the downstream part of the key have been identified as the two main reasons of the observed efficiency decrease with increasing heads. As the increase of the weir height decreases the flow velocities along the inlet key, it must increase significantly the PKW efficiency.

The influence of the vertical aspect ratio P/W_u has been studied by several authors [61, 94]. All confirm the interest in increasing weir height in terms of discharge capacity for ratio values between 0.3 and 0.9. However, two different ways enable to modify the weir height of the PKW: increasing the key slopes or adding vertical extensions, called parapet walls, on the weir crest. Before this research, all studies have been realized modifying simultaneously the weir height and the keys slopes. In the present parametric study, the two approaches are studied separately to isolate the influences of the weir height and the keys slopes. The range of P/W_u ratios studied has been extended from 0.3 to 2, and the influence of both weir height and keys slopes has been examined on the different parts of the weir crest.

VI.1.3. Keys width

As the increase of the inlet key width decreases the flow velocities along the inlet key, it must also increase significantly the PKW efficiency. However, the increase of the inlet width, for given weir width and crest length, induces a decrease of the outlet width. A too narrow outlet key may be unable to evacuate the outlet flow under supercritical conditions and may so decrease the global weir efficiency. An optimal value of the W_i/W_o ratio must thus be found between inlet width increase and outlet resilience capacity.

In previous studies, Ouamane and Lempérière [93-95] noted the interest to expand the inlet key width against outlet one, or increase the W_i/W_o ratio. Pushing this last reasoning in the extreme, it would be upstream sloping straight weir. The discharge coefficient of straight weir, similar to that of a traditional spillway (see XIV.1), is well below those measured on the PKW. Similarly, pushing the reverse reasoning in the extreme, the weir becomes a downstream sloping sharp crested weir (Figure VI-1), for which the discharge coefficient is, once again, well below those measured on standard models of PKW (see XIV.1). It can, therefore, be expected to find an optimal ratio of widths, between these extremes, offering the best working of the spillway.

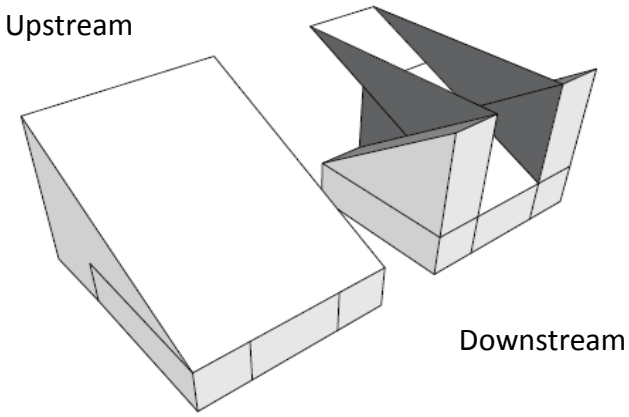

Figure VI-1 Comparison of a classical PKW with the extreme case of a unique outlet key

Le Doucen et al. [61] defined the optimal value of W_i/W_o between 1.25 and 1.5 regarding hydraulic aspects. However, their studies were limited to type A PKW and they showed poor differences for W_i/W_o ratios between 0.8 and 2. In the present parametric study, the influence of the W_i/W_o ratio has been studied on both type A and B PKWs. The range of studied ratios is between 0.5 and 2 for type A models and between 0.54 and 2.33 for type B models.

VI.1.4. Overhangs lengths

The position of the overhangs influences the inlet and outlet key slopes and cross section. As the side crest efficiency is influenced by these slopes and cross sections, modifying flow velocities along the keys, the position of the overhangs influences significantly the PKW discharge. The use of upstream overhangs increases the inlet cross section what must increase the weir capacity. However, it decreases in the same time the outlet cross section and slope, what may limit its resilience capacity. The use of downstream overhangs increases this resilience capacity of the outlet key but decreases the inlet cross section, what may decrease the weir efficiency. The optimal ratio between up- and downstream overhangs lengths must thus be balanced to increase the inlet cross section assuring a sufficient release capacity of the outlet key.

Ouamane and Lempérière [94] have shown that a type B model of PKW, using only upstream overhangs, is approximately 12% more efficient than a type A model, using symmetric up- and downstream overhangs. However, they show that a PKW with longer upstream overhangs and shorter downstream ones is less efficient than model using symmetric overhangs. Furthermore, no comparison has been done with downstream balanced overhangs. In the present study, the influence of the overhangs is studied displacing the basis both up- and downstream, modifying the B_o/B_i ratio in a range between 0 and infinity.

VI.2. Preliminary design method [80]

At this stage of the study, the hydraulic design of a PKW was mainly performed on the basis of experimental knowledge and numerical models, used to design an initial geometry, which was then studied on scale models and modified step by step following the ideas of the project engineers [63].

By exploitation of existing experimental results, a preliminary design method for PKW has been developed and is presented here. To limit the experimental studies, the design method aims at approaching as well as possible the final project design, compromise between hydraulic optima, respect of project constraints and cost effective building.

The design method is based on the project constraints (discharge, reservoir levels, available space …) and on extrapolation of existing experimental results from a reference scale model. By the study of the different possibilities to scale the reference model, the final design is defined depending on project engineer's interests (increase of the security level, increase of the reservoir capacity, decrease of the structure dimensions …).

The method can be resumed in four steps: Choice of a reference model; Scaling of the geometric and hydraulic characteristics of the reference model, corresponding with different number of PKW-units; Isolation of the designs enabled to respond to the

project constraints; Optimization of the design based on structural, economic and/or hydraulic criteria, depending on the project engineer's interests.

VI.2.1. Basis elements

The elements necessary to the design method are categorized in project elements (single notations) and reference model elements (notations with *). The project elements are the hydraulic and geometric specificities of the project (discharge, maximal head and available width). Regarding the reference model, a release capacity curve, issued from experimental tests, is necessary as well as the geometric characteristics of the tested model.

VI.2.2. Scaling for various number of PKW-units

Based on the project elements, different efficient designs may exist. The first step of the method aims at defining these different possibilities as a function of the number of PKW-units in the structure, by scaling of the geometric and hydraulic parameters of the reference model.

The PKW-unit width W_u is defined as a function of the number of PKW-units N_u and the available width for the project W:

$$W_u = \frac{W}{N_u} \qquad \text{VI-1}$$

The scale of the project model x is then defined as the ratio between the widths of PKW-elements on the project W_u and on the reference model W_u^*.

$$x = \frac{W_u}{W_u^*} \qquad \text{VI-2}$$

Applying this scale on the design water head H, the corresponding head on the reference model H^* is:

$$H^* = \frac{H}{x} \qquad \text{VI-3}$$

The discharge coefficient C_{dw}, of the Poleni equation (Eq. IV-1), usually used to characterize weirs efficiency, is a non-dimensional number. There is thus no scaling on its value and the C_{dw} value of the project model for the design head H is equal to the C_{dw}^* value of the reference model at the corresponding head H^* (Eq. VI-4).

$$C_{dw}\ \ H\ = C_{dw}^*\ \ H^* \qquad \text{VI-4}$$

Inserting Eqs. VI-1 to VI-4 in the Poleni equation IV-1, a relation between the head and the discharge is obtained for the project model depending on the hydraulic

and geometric characteristics of the reference model (W_u* and C_{dw}*), the project constraint (W) and the number of PKW-units on the project.

$$Q = C_{dw}^{*} W \sqrt{2gH^3} \text{ with } C_{dw}^{*} = f\left(\frac{HW_u^{*} N_u}{W}\right) \qquad \text{VI-5}$$

This relation enables to compute the head/discharge curve of the PKW for each value of N_u.

If the discharge coefficient of the reference model is not known for the corresponding head, its value is calculated by interpolation in-between the existing values. The accuracy of the design method is thus directly linked to the experimental tests accuracy and to the number of available results for the reference model.

VI.2.3. Verification of project constraints

By drawing the head/discharge curves defined by Eq. VI-5 for different numbers of PKW-units and limiting these curves to head and discharge values under the design head and over the design discharge, zero, one or several designs may respond to the project constraints.

VI.2.4. Technico-economic optimization of the PKW design

If more than one design responds to the project constraints, the second step of the method is then to optimize remaining parameters depending on the project engineer's interests, to clearly define the final design. By application of the scale factor to the reference model dimensions X*, the project model dimensions X are completely defined (Eq. VI-6), permitting the optimization of the final design including structural, economic or hydraulic criteria.

$$X = xX^{*} \qquad \text{VI-6}$$

The last step of a complete design is to validate the preliminary design by exploitation of a scale model representing the complete project integration. The scale model enables to take into account project specificities and local effects (piers, abutments, …).

VI.2.5. Applications

To illustrate the proposed preliminary design method, it has been applied to a new PKW project on a large gravity dam and to a rehabilitation project.

VI.2.5.1. New dam project

The characteristics of the new PKW project are summarized in Table VI-1. Considering preliminary flood mitigation calculations in the reservoir, the design discharge should be around 4000 m³/s, what represents a specific discharge of 40 m³/s/m to be evacuated for a maximal head of 4.5 m. Traditional Creager weirs are

unable to achieve this goal. Due to the restricted place and the necessary placement of the weir on the dam crest, the PKW seems to be a good solution to ensure the dam safety. For building considerations, the overhangs length is limited to 5 m by the project engineers. The overhangs length is a common constraint for PKW projects. Building considerations, as the limit length of crane, structural considerations, as the quantity of steel necessary to the concrete reinforcement, and stability considerations, as the response of the structure to seism, may limit the overhangs length.

Table VI-1 – Project dam and spillway characteristics

Type	Gravity dam
Available crest length	100 m
Maximal head	4.5 m
Maximal overhangs length	5 m

The first step of the PKW design is to choose a reference model. Regarding the existing experimental results in the literature, three models seem to be suitable for an efficient design: the model B from Ho Chi Minh [46], a model from Biskra [92] and the model 2 from Liège [73]. The geometric characteristics of these three models are given in Table VI-2 and the experimental results are summarized on Figure VI-2 in terms of discharge coefficient C_{dw}^* depending on the non-dimensional ratio between the water head H^* and the weir height P^*.

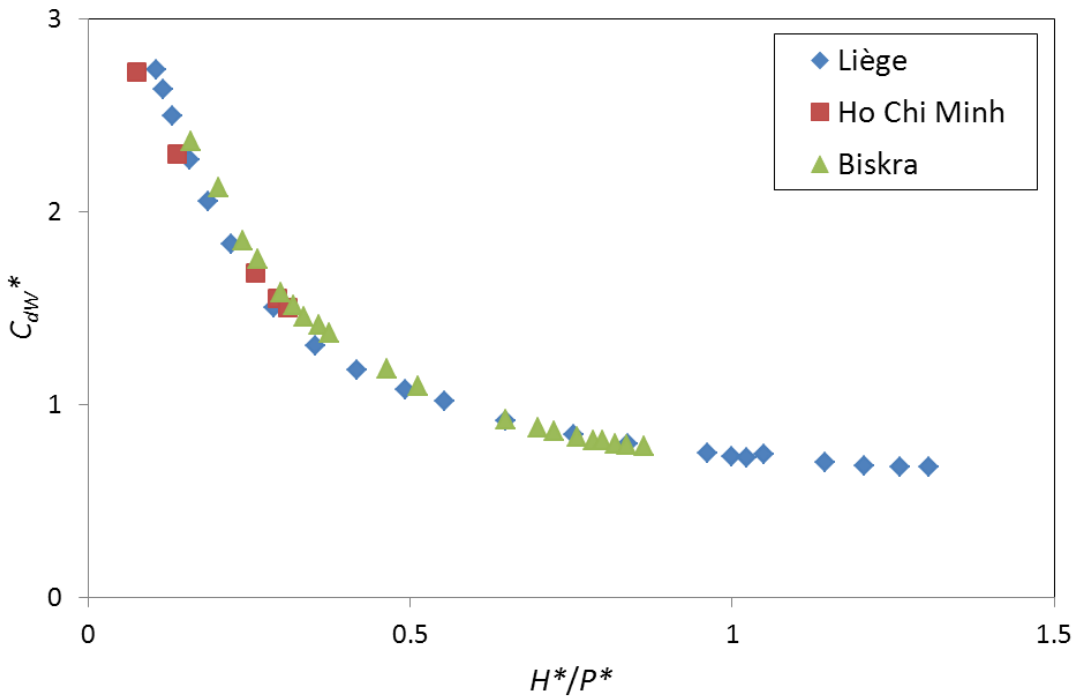

Figure VI-2 Non-dimensional head/discharge curves of reference models

Table VI-2 – Geometric characteristics of the reference models

	Ho Chi Minh	Biskra	Liège
W_u* (m)	0.2	0.165	0.2
P* (m)	0.22	0.155	0.2
W_i* (m)	0.12	0.09	0.12
W_o* (m)	0.08	0.075	0.08
B_i* (m)	0.15	0.103	0
B_o* (m)	0.15	0.103	0.25
B* (m)	0.6	0.412	0.5

The limited number of results for the Ho Chi Minh model should decrease the accuracy of the design method. The two other models show similar efficiency, but the one from Liège uses only upstream overhangs longer than those on the Biskra model. Due to the constraint on the overhangs length, the model from Biskra is chosen as the reference model. The influence of the choice of the reference model is discussed in VI.2.6, confirming the performance of the Biskra model compared to Liège and Ho Chi Minh models.

Considering a 10 units PKW, the width of each unit is 10 m (Eq. VI-1), what represents a scale ratio of 60.6 between the project and the reference model (Eq. VI-2). The corresponding design head on the reference model is equal to 0.074 m (Eq. VI-3). By interpolation in-between the experimental results, the discharge coefficient of the PKW for the design head is equal to 1.16 (Eq. VI-4). A PKW with 10 units placed on the crest of the projected dam enables to discharge 4900 m³/s (Eq. VI-5). However, the overhangs length of this PKW is 6.2 m (Eq. VI-6). A 10-units PKW is thus unable to respect the project constraints. The project characteristics, calculated considering 10 to 17 PKW-units, are represented in Table VI-3. Applying the Eqs. VI-3 to VI-5 for varying values of the upstream head H, the head discharge curves could be drawn for each value of N_u (Figure VI-3).

Table VI-3 – Project characteristics for various N_u values

N_u	10	11	12	13	14	15	16	17
W_u (m)	10	9.1	8.3	7.7	7.1	6.7	6.2	5.9
P (m)	9.4	8.5	7.8	7.2	6.7	6.3	5.9	5.5
W_i (m)	5.5	5	4.5	4.2	3.9	3.7	3.4	3.2
W_o (m)	4.5	4.1	3.8	3.5	3.2	3.0	2.8	2.7
$B_i = B_o$ (m)	6.2	5.7	5.2	4.8	4.5	4.2	3.9	3.8
B (m)	25	22.7	20.8	19.2	17.8	16.6	15.6	14.7
C_{dw}[1]	1.16	1.08	1.02	0.96	0.9	0.87	0.83	0.8
Q[1] (m³/s)	4900	4562	4300	4038	3820	3673	3508	3371
V_c (m³)	966	878	805	743	690	644	604	568

[1] for H = 4.5 m

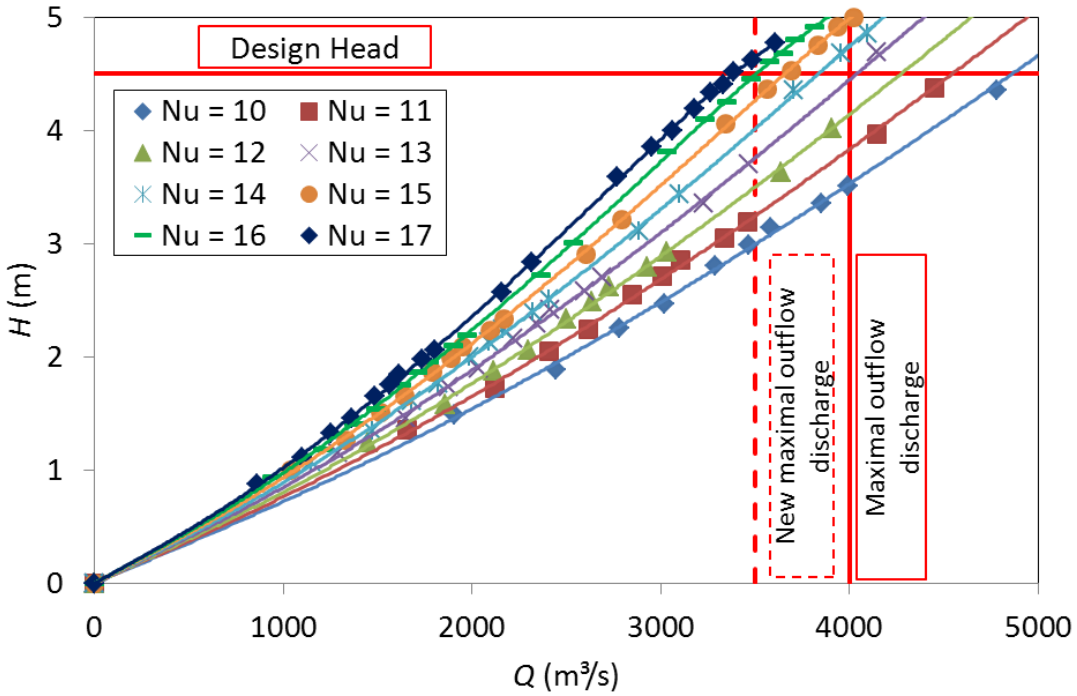

Figure VI-3 Project head/discharge curves for various N_u values with the Biskra model as reference

Regarding project constraints, the single acceptable solution is the one considering 13 PKW-units (For N_u > 13, the discharge capacity is not enough, and for N_u < 13, the overhangs are too long). However, the design discharge of 4000 m³/s has been calculated considering the flood mitigation provided with a weir working as an ogee crested weir. The PKW discharge for low heads is significantly higher than ogee-crested weir discharge, what improves the flood mitigation by the reservoir. As the proposed method provides the complete head/discharge curves for all studied geometries, the spillway design discharge could be re-evaluated considering the new expected flood mitigation. Regarding the curve provided for the 16 units PKW, the design discharge is reduced to 3500 m³/s.

Many solutions exist to ensure the discharge of 3500 m³/s under a head of 4.5 m ($N_u \leq 16$). However, solutions with less than 13 PKW units involve overhangs longer than 5 m, what is over the technical constraint of the project. Four solutions, with N_u between 13 and 16, enable thus to ensure the safety of the dam, respecting the constraints of reservoir level and overhangs length.

The final optimization of the design depends on the project engineer's interests. Considering the direct link between the weir cost and the material quantities necessary to its building, the economic optimum can be defined based on the volume of concrete in the structure V_c (Table VI-3). Regarding construction costs, the solution with 16 PKW-units seems thus to be the best design.

However, economic optimum is not only dependent of the construction costs. The limitation of the weir height, also involving a 16 units PKW design, enables the reservoir filling earlier during the weir construction, what limit the total building time and thus the project costs. Increasing the normal reservoir level may also involve economic interests (increasing the head for hydropower plant by example). Increasing the reservoir level of 0.5 m limits the acceptable designs to those with 13 or 14 PKW-units. Increasing the weir discharge capacity, by reducing the number of PKW-units, enables mitigation of floods with higher occurrence what may reduce damage costs of extreme floods.

The optimal design could thus be the design responding to technical (W = 100 m and $B_{o\,max}$ = $B_{i\,max}$ = 5 m) and hydraulic constraints (Q = 3500 m³/s, H_{max} ≤ Maximal reservoir level) and assuring economic interests (Minimal V_c value with P_{max} = 7 m and normal reservoir level increased by 0.5 m). In this case, the final design considers 14 PKW-units.

VI.2.5.2. Rehabilitation project

The preliminary design method has also been used on a rehabilitation project, to optimize the PKW design regarding the project engineer's interests. Let us consider a dam project with features as summarized in Table VI-4. A gated weir is already situated on the dam crest. However, its discharge capacity is insufficient regarding to the update of the design discharge calculation. To increase the global discharge capacity, a complementary weir is studied and the PKW option is envisaged. The discharge to release on the PKW at maximal reservoir level is 400 m³/s. The specific discharge is thus 11.5 m³/s/m, to be evacuated under a head of 2 m.

Table VI-4 – Dam and spillway characteristics

Type	Gravity dam
Available crest length	35 m
Maximal head	2 m
Distance between existing gated weir crest and normal reservoir level	6 m

From the different available results from the literature [46, 61, 72], the model from Biskra [94] has been chosen as the reference model. As shown before, this model presents efficient geometric and hydraulic characteristics, and a large set of available results, which increases the method accuracy. The geometric characteristics of the model are given in Table VI-2 and the experimental results are summarized in Figure VI-2 in terms of discharge coefficient C_{dw}* of the Poleni equation depending on the ratio between the water head H* and the weir height P*.

Considering a 5-units PKW, the width of each unit is 7m (Eq. VI-1), what represents a scale ratio of 42.4 between the project and the reference model (Eq.

VI-2). The corresponding design head on the reference model is 0.0471 m (Eq. VI-3). By interpolation in-between the experimental results, the discharge coefficient of the PKW for the design head is equal to 1.56 (Eq. VI-4). A PKW with 5 units placed on the crest of the dam enables to discharge 685 m³/s (Eq. VI-5). A 5-units PKW enables thus to respect the project constraints.

The project characteristics calculated for N_u varying from 5 to 11 are presented in Table VI-5. Figure VI-4 shows the head/discharge curves calculated for these N_u values. Many solutions exist to ensure the dam safety. An optimization of the design on different parameters is thus possible.

Table VI-5 – Project characteristics for various N_u values

N_u	5	6	7	8	9	10	11
W_u (m)	7	5.9	5	4.4	3.9	3.5	3.1
P (m)	6.6	5.5	4.7	4.1	3.7	3.3	3
W_i (m)	3.8	3.2	2.7	2.4	2.1	1.9	1.7
W_o (m)	3.2	2.7	2.3	2	1.8	1.6	1.4
$B_i = B_o$ (m)	4.4	3.6	3.1	2.7	2.4	2.2	2
B (m)	17.5	14.6	12.5	10.9	9.7	8.7	7.9
C_{dw}[1]	1.56	1.39	1.26	1.14	1.05	0.97	0.9
Q[1] (m³/s)	685	611	554	502	461	427	397
V_c (m³)	267	223	191	167	149	134	122

[1] for H = 2 m

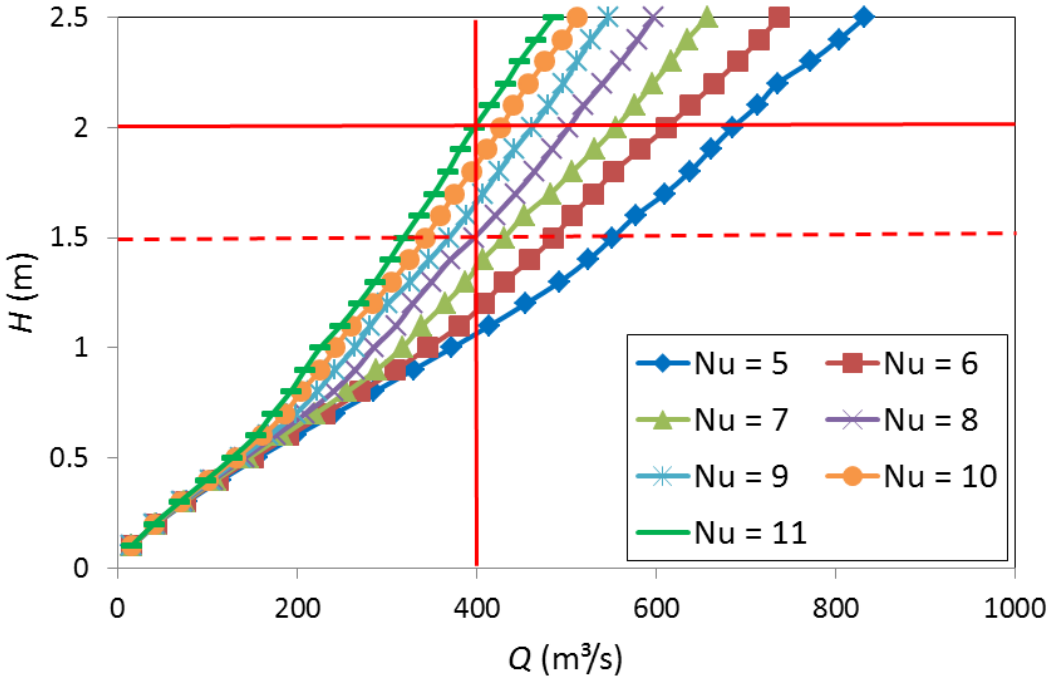

Figure VI-4 Project head/discharge curves for various N_u values with the Biskra model as reference

The increase of the normal reservoir level enables increasing the hydropower capacity. A first optimization could thus consist in the limitation of the maximal head to 1.5 m, enabling to increase by 0.5 m the normal reservoir level and limiting the solutions to N_u values under 8 (Figure VI-4).

A second optimization could concern the structural constraints. By limitation of the basis position of the PKW 0.5 m over the gated weir crest, the reservoir and the existing weir stays partially usable during the construction. So, there is no need of deviation building and the hydroelectric power plant could stay working during the PKW building. The weir height is thus limited under 6 m, what involve N_u values over 6 (Table VI-5).

The final choice between the two last solutions could be realized to minimize the necessary volume of concrete (Table VI-5). The PKW design considering 7 units is so finally the best, corresponding with project constraints and engineers interests. With the lowest concrete volume, this design enables to ensure a discharge of 400 m³/s under a head of 1.5 m, allowing an increase of the hydropower production.

Other designs may be optimum considering other criteria for optimization. For instance, a 5-units PKW ensures a higher level of security, and a 10-units PKW enables the use of prefabricated elements due to the smaller size of the alveoli.

VI.2.6. Influence of the reference model

As mentioned before, the accuracy of the proposed design method lies on the experimental tests accuracy and on the number of available results for the reference model. The choice of the reference model is thus of high importance. In the application presented before, the Biskra model has been favoured to Ho Chi minh and Liège ones.

Regarding the new dam project application, the head/discharge curves given by application of Eqs. VI-3 to VI-5 with the Ho Chi Minh model as reference (Figure VI-5) show non-physical phenomenon for heads approaching 4.5 m. For this range of head, the weir discharge begins to decrease with increasing heads. This phenomenon results from the extrapolation of the available experimental C_{dW}^{*} values for heads 2 times higher than the maximal corresponding head studied on the reference model. These results highlight the importance of choosing a reference model with a wide range of available results near the corresponding design head.

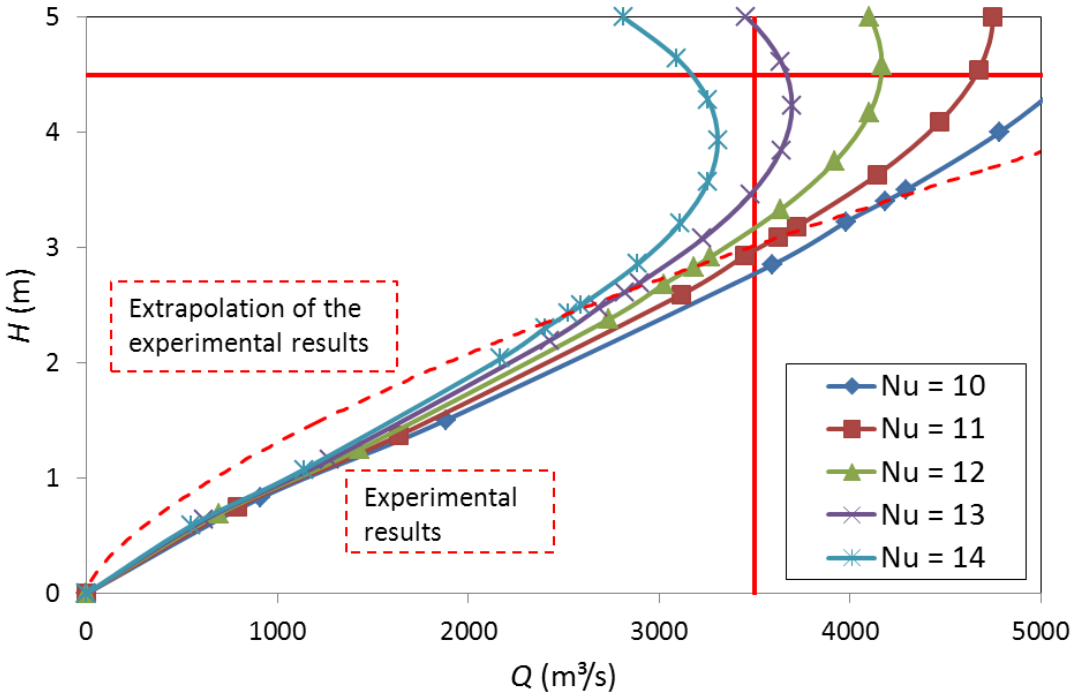

Figure VI-5 Project head/discharge curves for various N_u values with the Ho Chi Minh model as reference (Dotted line – separation between interpolation in-between the available reference results and extrapolation over the available reference results)

Regarding the head/discharge curves given by application of Eqs. VI-3 to VI-5 with the Liège model as reference (Figure VI-6), more geometries than with using the Biskra model are able to release a discharge of 3500 m³/s under a head of 4.5 m (Table VI-6). However, even with the 17 unit PKW, which is the solution with the smallest dimensions, the upstream overhang length is equal to 7.35 m. Using the Liège model as a reference provides thus no available solution. The choice of the reference model must be consistent with the project constraints. Considering a project constraint on the overhangs length favours a reference model with symmetric overhangs.

Table VI-6 – Project characteristics for various N_u values with the Liège model as reference

N_u	10	11	12	13	14	15	16	17
W_u (m)	10	9.1	8.3	7.7	7.1	6.7	6.2	5.9
P (m)	10	9.1	8.3	7.7	7.1	6.7	6.2	5.9
W_i (m)	6	5.5	5	4.6	4.3	4	3.7	3.5
W_o (m)	4	3.6	3.3	3.1	2.8	2.7	2.5	2.4
B_o (m)	12.5	11.4	10.4	9.6	8.9	8.3	7.8	7.4
B (m)	25	22.7	20.8	19.2	17.9	16.7	15.6	14.7
C_{dw}[1]	1.14	1.08	1.03	0.99	0.94	0.9	0.87	0.84
Q[1] (m³/s)	4808	4548	4366	4168	3965	3802	3666	3536
V_c (m³)	1033	939	860	794	738	688	645	607

[1] for H = 4.5 m

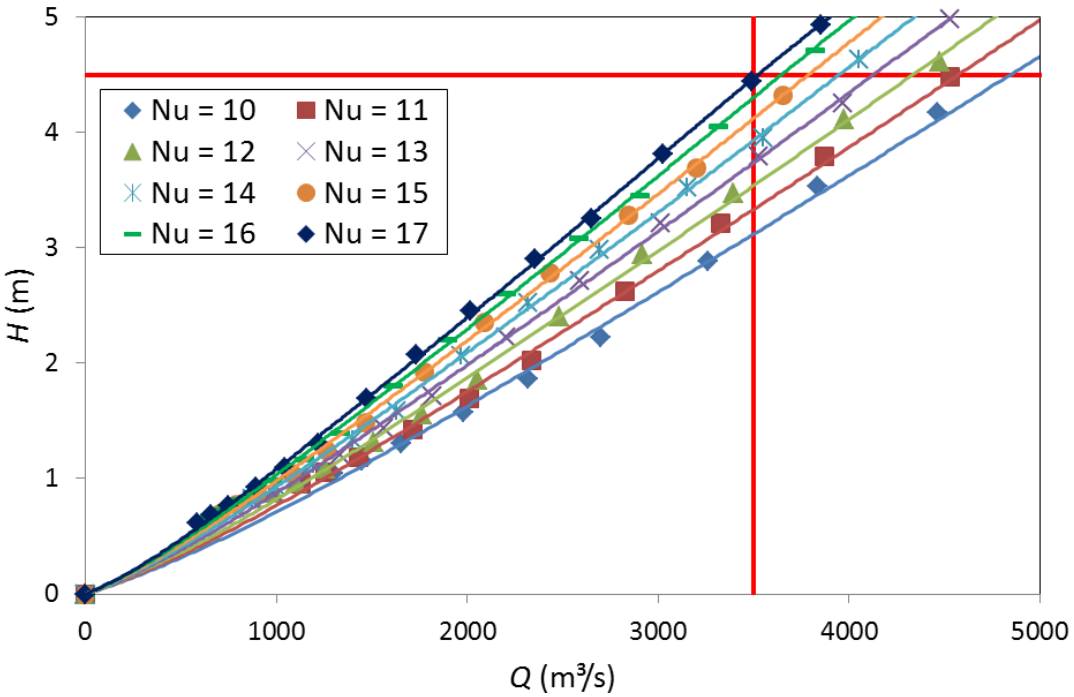

Figure VI-6 Project head/discharge curves for various N_u values with the Liège model as reference

VI.3. Method for parametric studies

The parametric studies presented hereafter have been realized following a systematic method.

In a first time, the scale of the models has been determined based on the experimental flume dimensions and the discharge capacity of the two pumps available. To achieve this goal, the preliminary design method presented here above has been used on a reference model chosen as the more efficient from the existing results in literature. Taking a security on the obtained results, the tested models and discharges will be able on the existing facility. The flume width has been decreased at 0.75 m using convergent. 2.5 PKW-units have been studied on each model enabling the observation of the flow in both half inlet and outlet keys, and the measurements along the full ones.

In a second time, the range of variation of each parameter has been determined using the first version of the 1D-numerical model developed based on the experimental results of the 1:10 scale model and validated on existing experimental results from the literature (see XIV.2).

For each parameter, the various geometries have been placed in the experimental flume and studied in three different ways. Firstly, a stage/discharge curve of each geometry has been realized. Then, measurements of the free surface level have been realized along the inlet key for particular upstream heads. For the

same heads, extensive observations of the flow behaviour along the different part of the weir have also been realized.

Combining results and observations with theoretical assumptions issued from the literature, an analytical approach of the stage/discharge curve has then been realized for each parameter. A comparison of the analytical, numerical and experimental approaches is then realized.

Finally design advices are given for the determination of the optimal values of each parameter. These advices include pure hydraulic interests studied here but also technical and economic interests gained from prototype studies realized at the laboratory and exchanges with project engineers and PKW owners.

VII. On the influence of the PKW height [85]

VII.1. Introduction

To test the influence of PKW height, several models with varying height, providing varied bottom slopes of the inlet and outlet keys, have been studied in a first time. In a second time, to highlight the relative influence of the weir height and the keys slope, several models have been tested with and without parapet walls, providing variants characterized by either the same bottom slopes or the same total height.

In each part of the study of the PKW height influence, the scale models have been exploited to provide stage discharge curves and free surfaces profiles for varied upstream heads. The experimental results enable then the development of an analytical formulation of the discharge capacity of PKW. For models with simultaneous variation the weir height and the keys slope, a comparison to the numerical results provided by the Wolf1D-PKW solver has also been realized. This has not been realized on the models with parapet walls as the flow behaviour around the vertical extension may be badly represented by the 1D solver. Design advices are finally given taking into account all the results obtained from the experimental, numerical and analytical approaches.

VII.2. Experimental set-up

In the first part of the study of weir height influence, 7 PKW models with varying height, providing varied bottom slopes of the inlet and outlet keys, have been studied. The inlet/outlet widths ratio W_i/W_o of all models is 1.5, the ratio between the total length of the crest L and the width of the weir W is 5, and the two overhangs are symmetric and equal to the third of the side crest length B. Table VII-1 and Figure VII-1 give the values of the geometrical parameters of the 7 tested models. P_i/W_u ratios are 0.33, 0.5, 0.67, 0.8, 1, 1.33, 2.

Table VII-1 – Dimensions of PKW models with varying height and keys slope

W	0.75 m
L	3.75 m
$P_i = P_o$	0.1; 0.15; 0.2; 0.24; 0.3; 0.4; 0.6 m
P_d	0.2 m
W_u	0.3 m
W_i	0.165 m
W_o	0.105 m
T_s	0.015 m
$T_i = T_o$	0 m
B	0.6 m
$B_i = B_o$	0.2 m

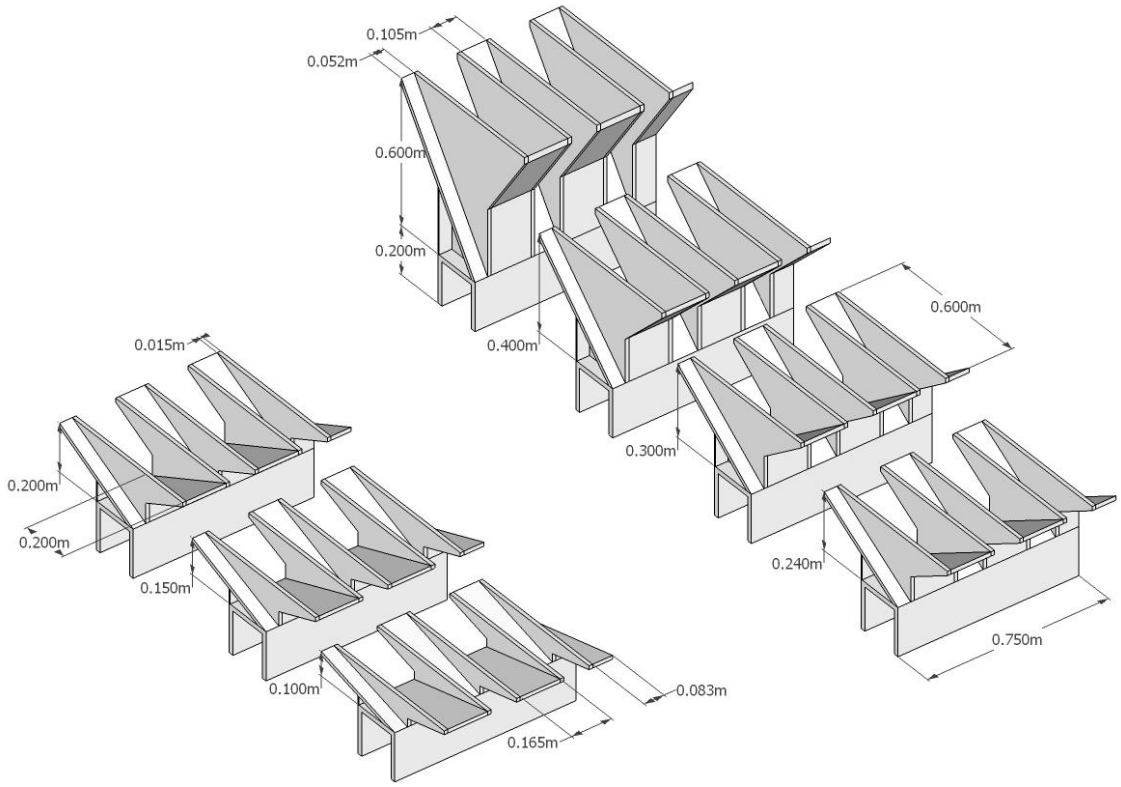

Figure VII-1 Experimental layout of PKW models with varying height and keys slope

In the second part of the study, 6 models, providing 14 variants of PKW, have been studied to highlight the relative influence of parapet walls and of other geometric parameters. Models have been tested with and without parapet walls, providing variants characterized by either the same bottom slopes or the same total height, while varying values have been used for inlet/outlet widths ratio, developed length ratio and slopes of the keys. The characteristics of these variants are given in Table VII-2 and Figure VII-2.

Table VII-2 – Dimensions of studied variants with or without parapet walls

Model	Variant	W (m)	L (m)	P_i (m)	P_r (m)	P_d (m)	W_u (m)	W_i (m)	W_o (m)	T_s (m)	$T_i = T_o$ (m)	B (m)	$B_i = B_o$ (m)
1	1	0.6	2.34	0.525	0	0.2	0.4	0.18	0.18	0.02	0.024	0.63	0.184
	2			0.625	0.1						0.02		
2	1			0.135	0	0.59					0.024		
	2			0.235	0.1	0.59					0.02		
	3			0.235	0	0.49					0.024		
3	1	0.75	3.75	0.4	0	0.2	0.3	0.165	0.105	0.015	0	0.6	0.2
	2			0.45	0.05						0.003		
4	1			0.4	0			0.105	0.165		0		
	2			0.45	0.05						0.003		
5	1			0.15	0			0.165	0.105		0		
	2			0.2	0.05						0.003		
	3			0.2	0						0		
6	1			0.15	0			0.105	0.165		0		
	2			0.2	0.05						0.003		

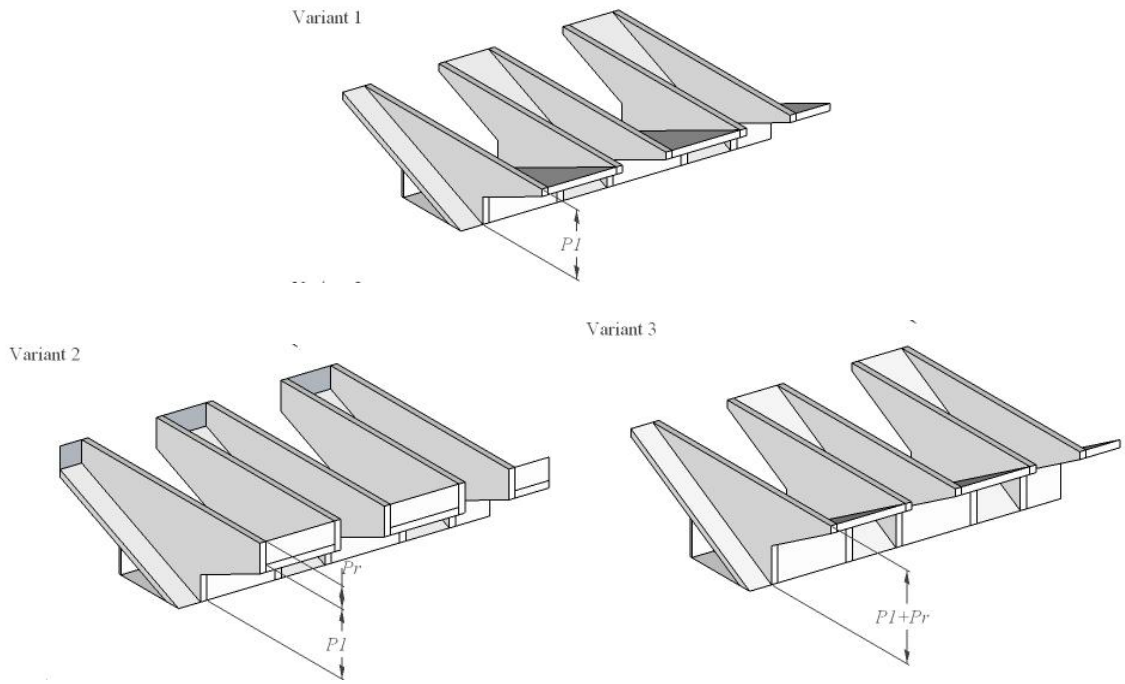

Figure VII-2 Experimental layout of studied variants

The variant 1 of model 1 corresponds to the 1:10 scale model depicted before (see IV). The variants 1 of model 3 and 5 correspond to the models studied in the first part of the weir height study for P_i/W_u ratios respectively of 1.33 and 0.5. Finally, the variant 3 of model 5 corresponds to the model studied for a P_i/W_u ratio of 0.67.

VII.3. Influence of the PKW height [77-79]

The experimental study of the effect of PKW height has been carried out in four ways: effect of bottom slope variations on the release capacity of the downstream part of the crest (see XIV.1), hysteresis effect considering rising or decreasing water heads, effect of weir height variations on its global discharge capacity and effect of weir height variations on the free surface profiles. Based on these experimental results, analytical and numerical approaches have been applied and design advices are provided.

VII.3.1. Head-discharge curve

VII.3.1.1. Influence of air entrainment

With variations of the upstream head, variations of the air entrainment can be observed on the tested models. The study on the 1:10 scale model highlighted the variation of the nappe shape, from a leaping or an adherent nappe to a springing one, for very low heads ($H/T < 0.4$). For high heads, the transition from fully aerated nappes to non-aerated ones can also be observed (Figure VII-3). This transition is observed, on the four smallest models ($P_i/W_u < 0.8$), for the same range of the ratio between the upstream head H and the crest height P_T, around 0.55. For highest models ($P_i/W_u > 0.8$), the nappes are still fully aerated even for the highest heads studied.

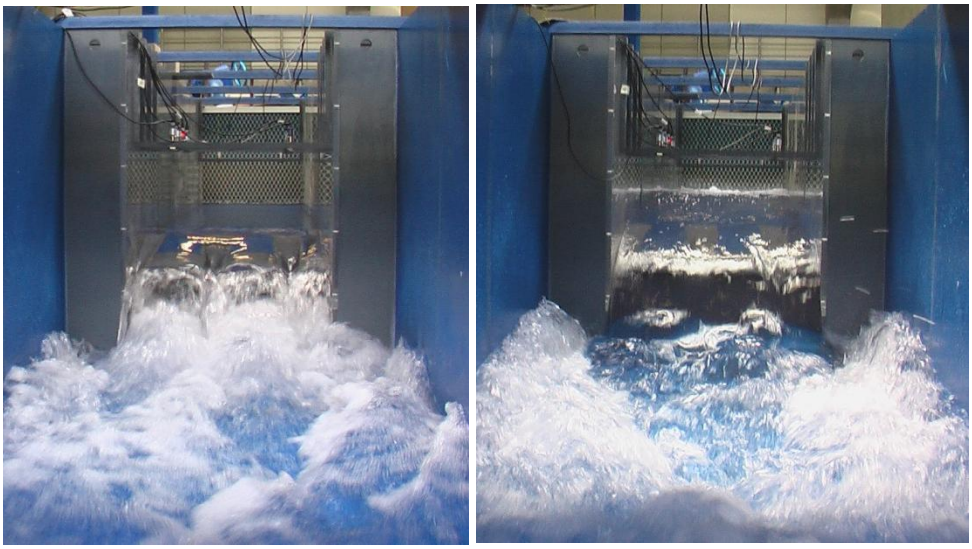

Figure VII-3 Variation of the air entrainment for high heads (P_i = 0.1 m, left – H/P_T = 0.51, right – H/P_T = 1.05)

The air entrainment may influence the discharge capacity of the weir. The transition heads highlighted before may thus be modified. Indeed, the air entrainment influences the pressure profile along the nappes, and so the flow behaviour over the weir. Considering heads just under or just over this transition, the flow behaviour is thus not the same. Hysteresis effects may occur when considering rising or decreasing heads. However, the comparison of the head/discharge curves of the tested PKW considering rising or decreasing heads shows no difference, despite variation of the nappe aeration (Figure VII-4). This result, confirmed for all of the tested geometries, allows the study of a particular head whatever the way it is reached.

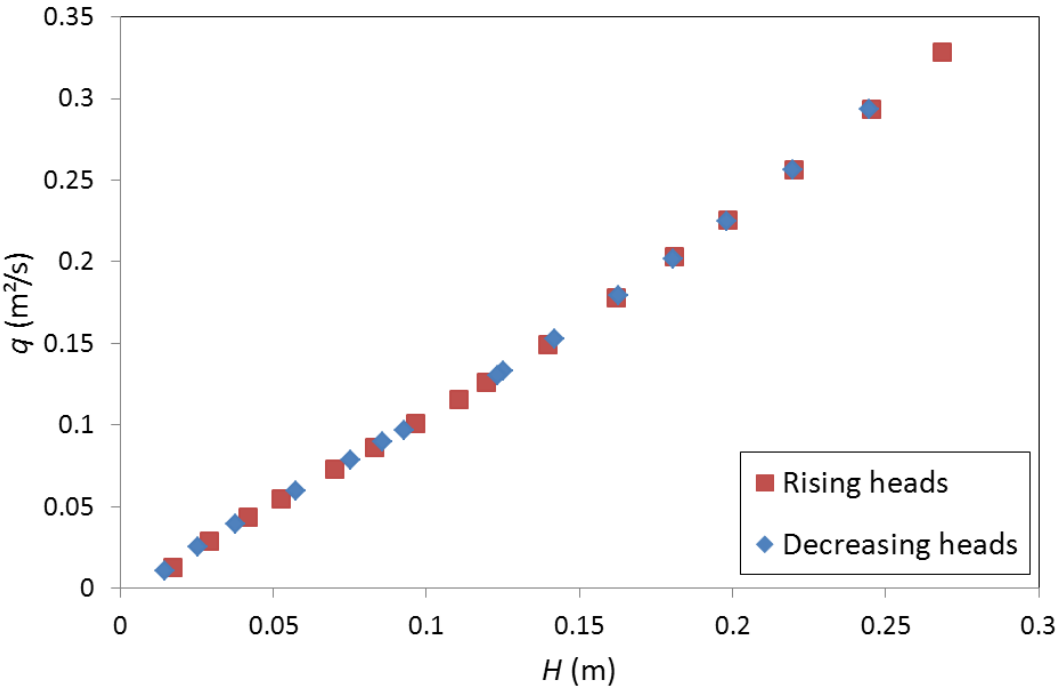

Figure VII-4 Head/discharge curves of the PKW (P_i = 0.1 m) considering rising or decreasing heads

VII.3.1.2. Influence of the weir height on the stage/discharge curve

The Figure VII-5 shows the variation of the specific discharge q on the tested PKW depending on the weir height P for different values of the upstream head H.

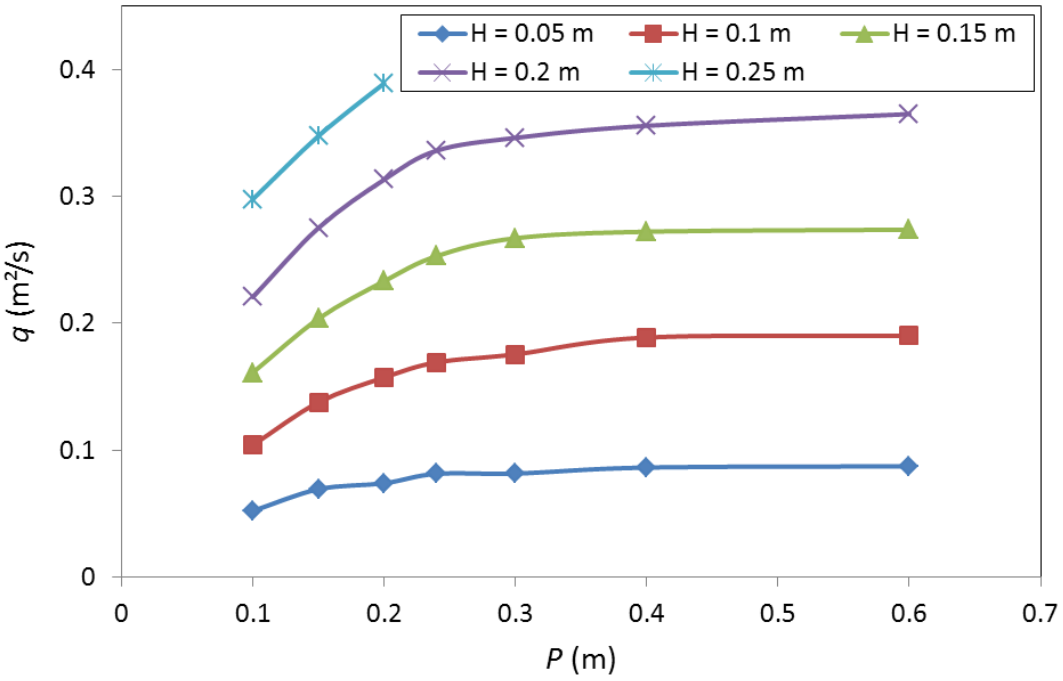

Figure VII-5 Evolution of the discharge with the PKW height for different heads

As expected, increasing the PKW height, and so the inlet key cross section, increases the global release capacity of the weir. However, there is a limit over which increasing this height doesn't improve anymore the release capacity of the PKW. This limit increases with increasing heads between P = 0.4 and 0.6 m, corresponding to S_i between 1 and 1.5.

VII.3.1.3. Comparison with literature

Le Doucen [61] proposed to represent the results of discharge capacity in terms of the ratio between PKW and sharp-crested weir (see II.1.1) release capacity q_{PKW}/q_{SCW} depending on the ratio of the head on the weir height H/P. He assumes that this representation allows homogeneity of the curves for varying slopes S_i between 0.36 and 0.8. However, the results of the present study highlight an optimum of efficiency with regard to the H/P ratio for S_i = 0.375, and an important decrease for S_i higher than 0.75 or lower than 0.25 (Figure VII-6). As long as the weir height varies from a model to another, a representation with H/P ratio in abscissa doesn't highlight the hydraulic optimal geometry (S_i = 1.5). Furthermore, a too straight range of values of the studied parameter may mask some conclusions on the efficiency of valuable PKW designs.

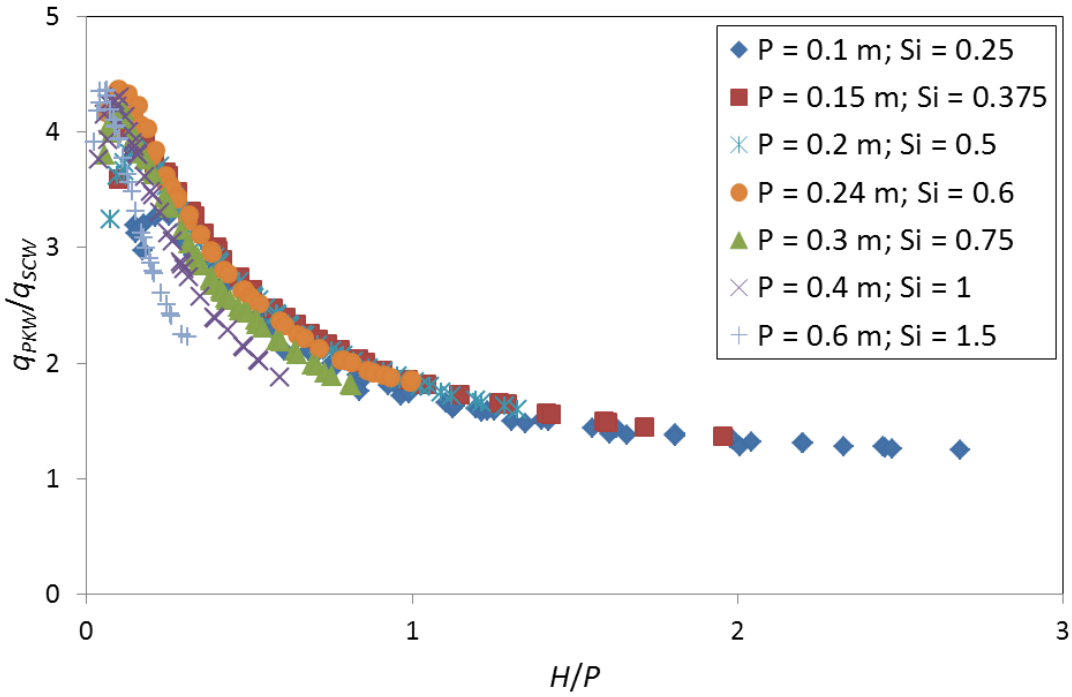

Figure VII-6 Comparison of the efficiency of the tested PKW depending on the H/P ratio

VII.3.2. Free surface profile

VII.3.2.1. Inlet key profile

Regarding free surface profiles measured in the middle of the inlet key, the free surface elevation, measured from the crest one, generally decreases from the upstream to the downstream ends of the key (Figure VII-7). Considering negligible head losses along the key (see V.7), this decrease traduces an increase of the flow velocity.

For low head (Figure VII-7 – (a)), the free surface profiles in the different tested models are similar except for S_i = 0.25. For all the models, the velocity increase, related to a free surface decrease, is only observed on the downstream crest, traducing the negligible flow velocity along the inlet key. However, for S_i = 0.25, non-negligible velocities are developed along the key, traduced by an important lowering of the free surface level. The flow velocity variation along the inlet key direction and the lowering of the free surface level, both decrease consequently the discharge capacity of the side crest and thus the global PKW efficiency (Figure VII-8).

For higher heads (Figure VII-7 – (b) to (d)), two free surface profiles can be distinguished depending on the inlet key slope.

For low key slopes ($S_i \leq 0.6$), an important lowering of the free surface level is observed at the inlet key entrance (X = 0.4 m), traducing the velocity increase induced by the flow contraction. This free surface lowering is as much important as the weir is higher. Then, from the inlet key entrance to its downstream, a constant decrease of

the free surface level is observed. This decrease is as much important as the key slope is lower, traducing higher velocities. The higher longitudinal velocities and the correspondent lowering of free surface level decrease the side crest efficiency and so the discharge of lowest weir configurations (Figure VII-8).

For high key slopes ($S_i \geq 0.75$), the lowering of the free surface level at the inlet key entrance is still observed. However, this free surface lowering is as much important as the weir is lower. From the inlet key entrance to its downstream, a small increase of the free surface level is observed before a quasi-horizontal free surface. This increase, mainly observed for highest heads, may correspond to the passage of the recirculation zones, observed on the 1:10 scale model (see IV.6), which increase the flow velocity at the inlet key entrance. The horizontal free surface traduces the negligible influence of the bottom slope on the flow velocity. This negligible influence of the bottom slope is also observed on stage-discharge curves (Figure VII-8).

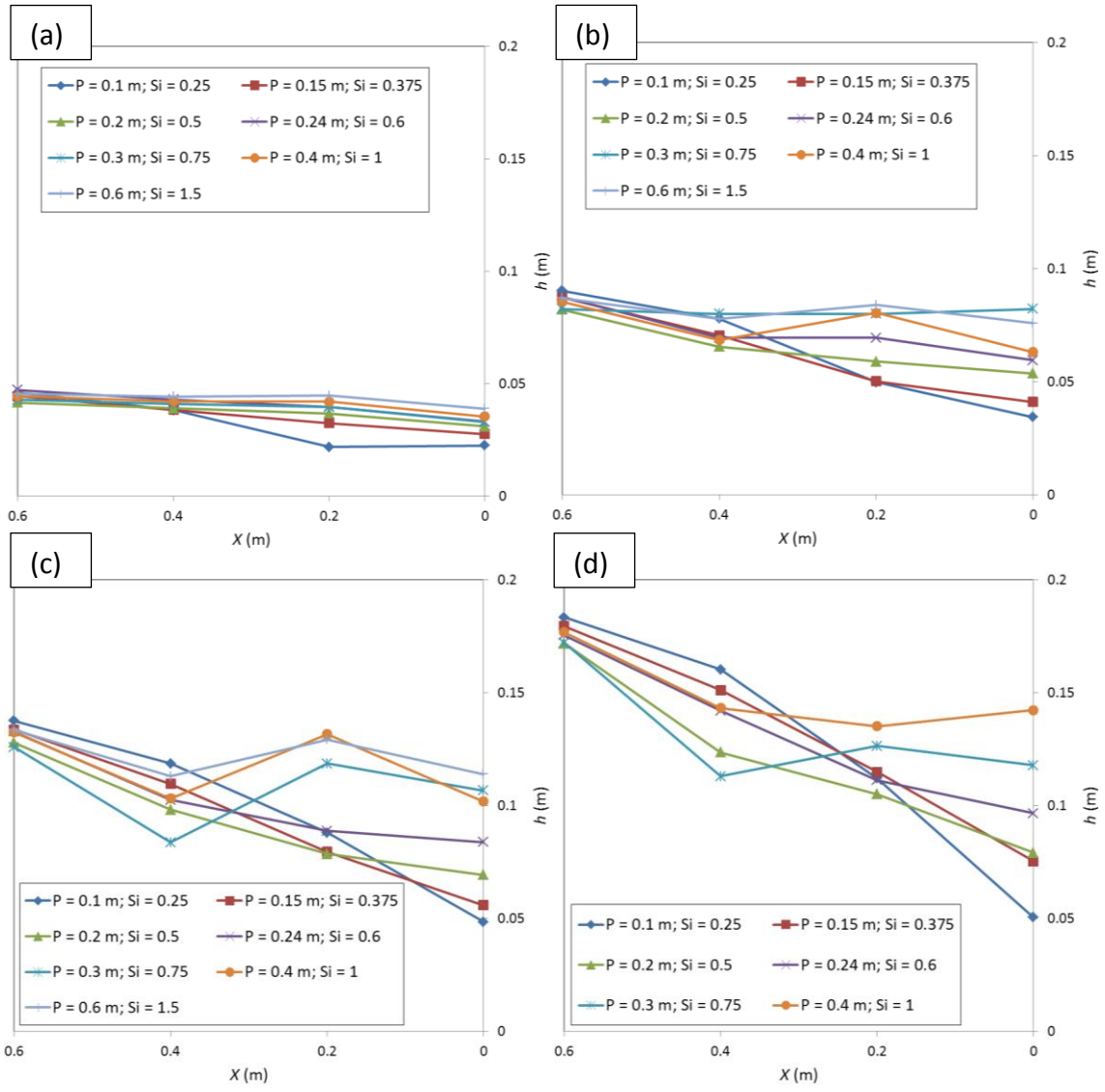

Figure VII-7 Free surface profiles in the middle of the inlet key for varied upstream heads: (a) H = 0.05 m; (b) H = 0.1 m; (c) H = 0.155 m; (d) H = 0.21 m

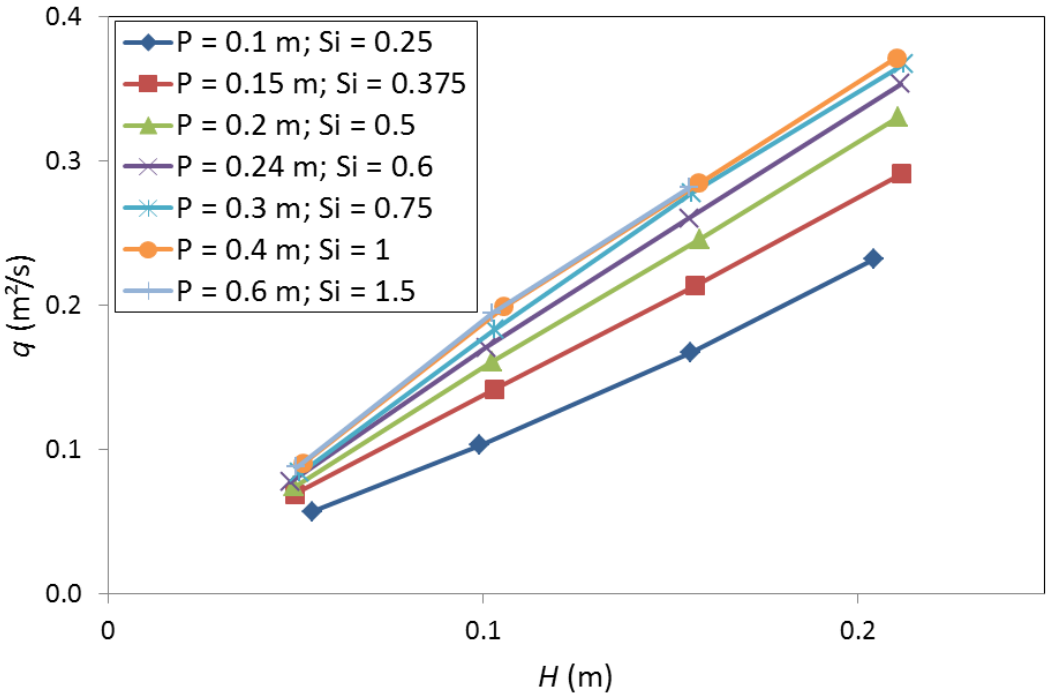

Figure VII-8 Stage-discharge curves of the tested models

The observation of the flow along the half inlet key (Figure VII-11) confirms the flow behaviours developed here before. For low heads, the free surface is close to horizontal excepted for P = 0.1 m (S_i = 0.25) (Figure VII-9).

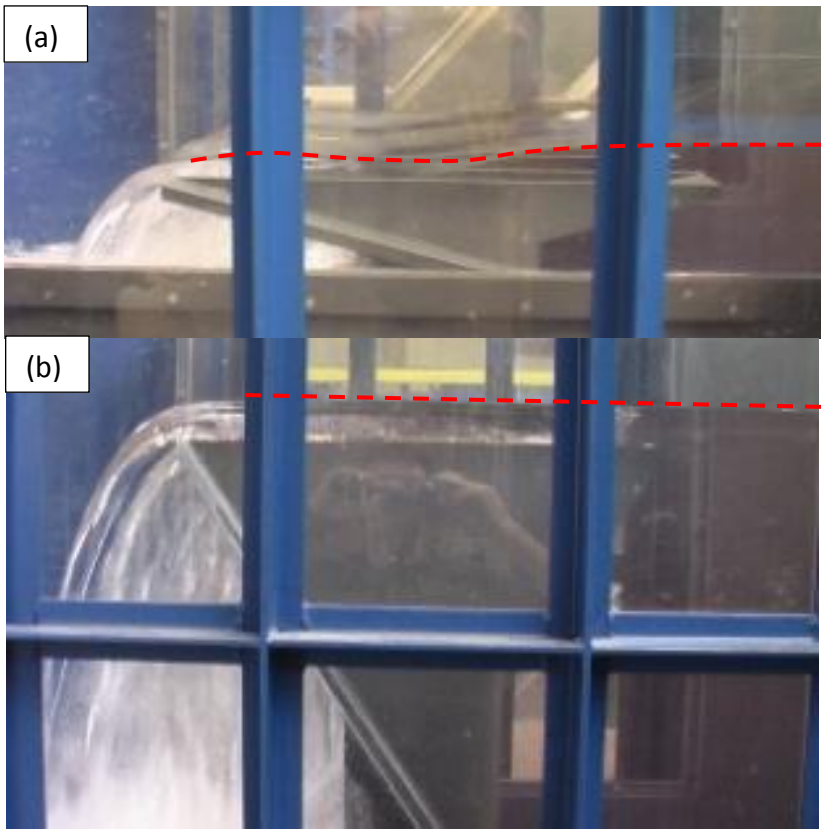

Figure VII-9 View of the inlet free surface variation for H = 0.05 m; P = (a) – 0.1 m; (b) – 0.6 m

For higher heads and low weir height, a constant decrease of the free surface level is observed from the inlet entrance to its downstream (Figure VII-10 – (a)). For high heads and high weir height, a decrease of the free surface level is still observed at the inlet entrance (Figure VII-10 – (b)). However, the free surface profile in the downstream part of the key is close to horizontal. For highest weir height (P = 0.6 m; S_i = 1.5), a small increase of the free surface level is observed on the downstream part of the key (Figure VII-10 – (c)). That may be caused by the influence of the bottom slope on the downstream crest behaviour, modifying the nappe shape and the velocity profile over the crest.

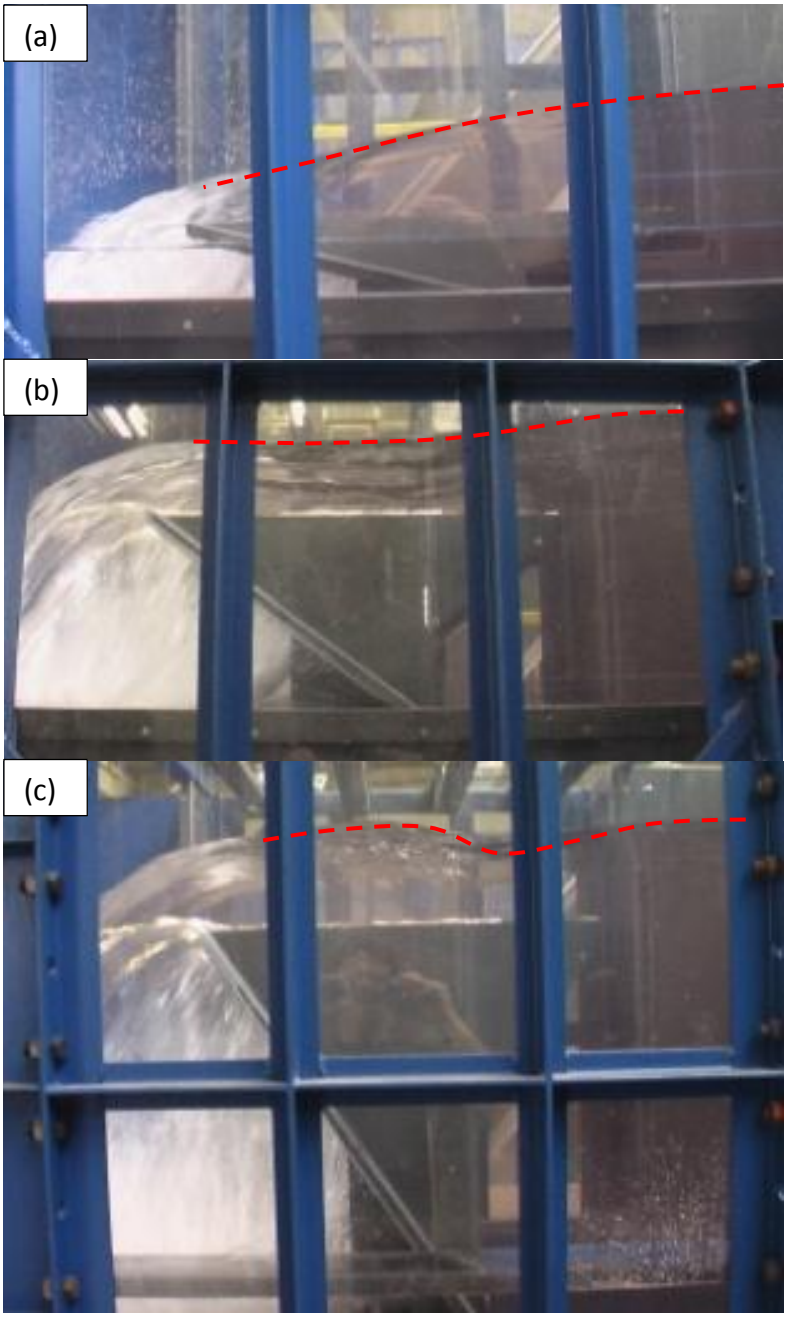

Figure VII-10 View of the inlet free surface variation for H = 0.155 m; P = (a) – 0.1 m; (b) – 0.3 m; (c) – 0.6 m

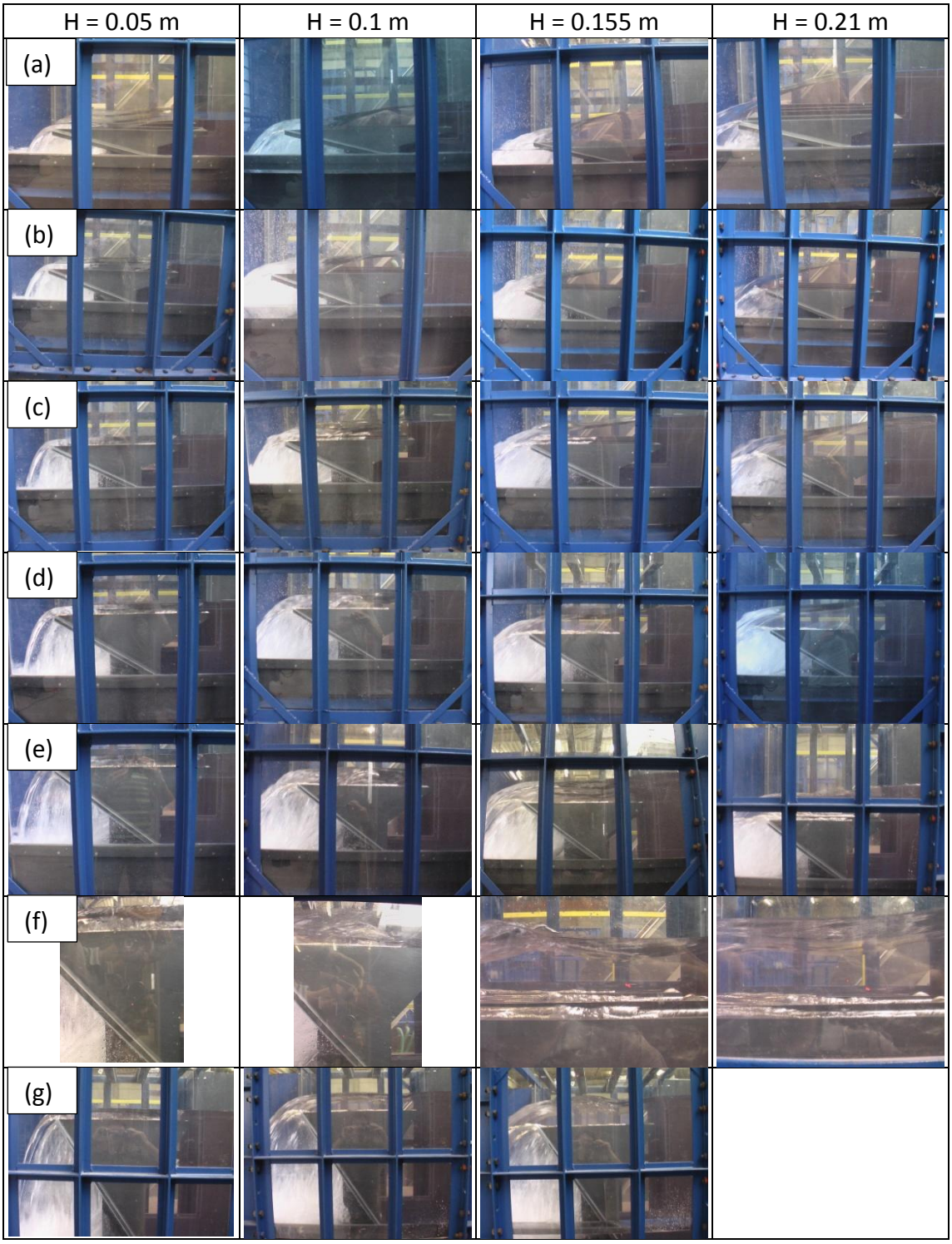

Figure VII-11 View of the inlet free surface variation with head: P = (a) – 0.1 m; (b) – 0.15 m; (c) – 0.2 m; (d) – 0.24 m; (e) – 0.3 m; (f) – 0.4 m; (g) – 0.6 m

VII.3.2.2. Outlet key profile

Regarding free surface profiles along the outlet key (Figure VII-12), the influence of the outlet key flow on the weir efficiency is dependent of the weir height and the upstream head.

Figure VII-12 View of the outlet free surface variation with head: P = (a) – 0.1 m; (b) – 0.15 m; (c) – 0.2 m; (d) – 0.24 m; (e) – 0.3 m; (f) – 0.4 m; (g) – 0.6 m

For high weir heights (P > 0.4 m; S_o > 1), whatever the upstream head, the outlet flow is still well aerated and seems to stay supercritical (Figure VII-13 – (c)). It plays no role on the PKW discharge efficiency.

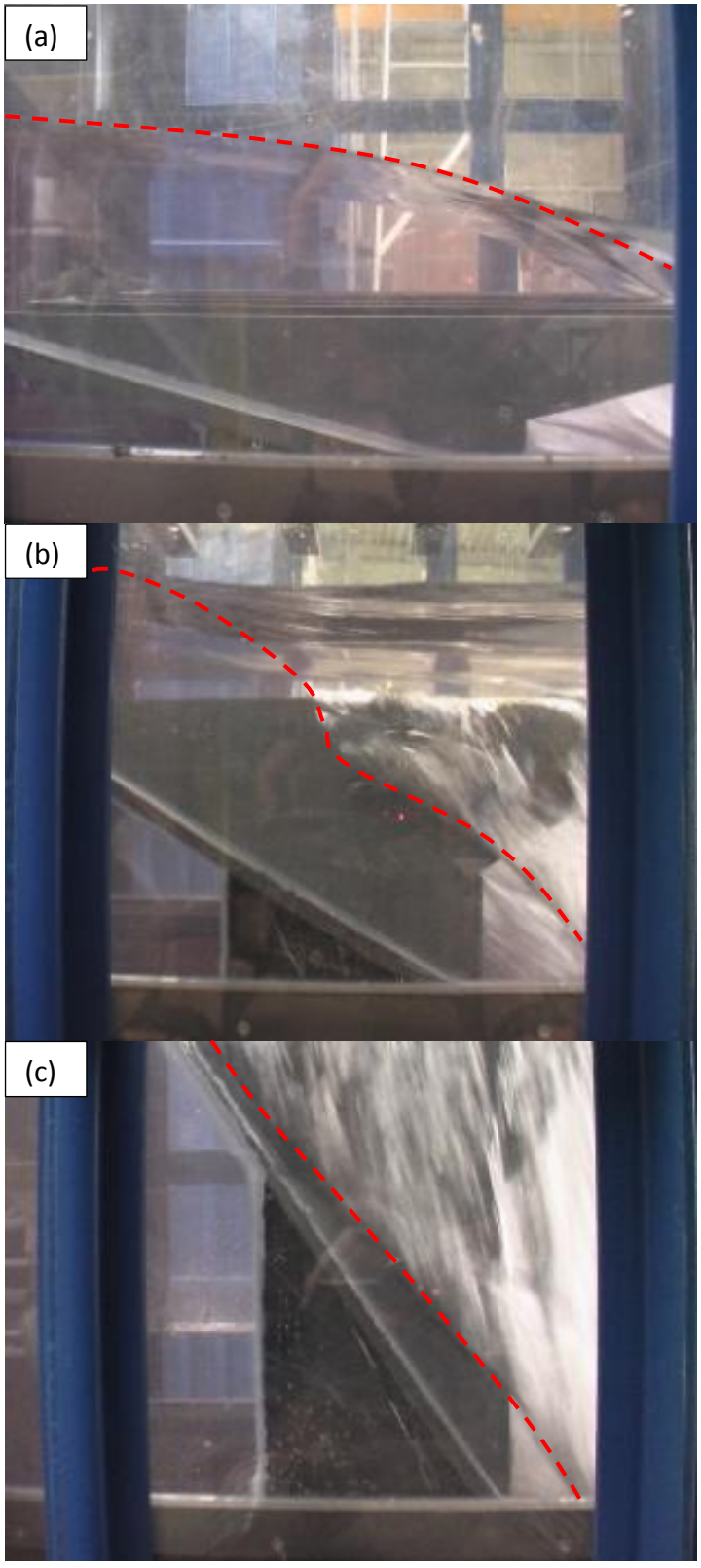

Figure VII-13 View of the outlet free surface variation for H = 0.155 m; P = (a) – 0.1 m; (b) – 0.24 m; (c) – 0.6 m

For low weir height (P < 0.15 m; S_o < 0.375), the outlet key slope is no more sufficient to ensure supercritical flow (Figure VII-13 – (a)). The resilience capacity of the outlet key manages the upstream crest efficiency. Furthermore, as the flow becomes subcritical the outlet free surface level passes over the crest level along a non-negligible part of the side wall. For highest heads, the whole side crest is submerged by the outlet flow. That reduces significantly the side crest discharge.

For intermediate weir heights (0.15 m < P < 0.4 m, 1 < S_o < 0.375), the outlet flow behaviour is dependent of the upstream head. For low heads, the outlet key slope stays over the critical one and the outlet flow seems have no influence on the weir efficiency. For high heads, the outlet key slope becomes lower than the critical one. The outlet resilience capacity manages then the upstream crest efficiency and a part of the side crest is submerged (Figure VII-13 – (b)).

The outlet key flow behaviour enables to explain the observed inlet key behaviour for high heads. For low weir heights, as the outlet flow highly reduced the side crest discharge and as the inlet key slope reduces constantly the inlet cross section, the flow velocity along the inlet key increases constantly what decreases the free surface level. For high weir heights, the decrease of the inlet cross section is compensated by the decrease of the inlet discharge induced by the side crest, assuring a quasi-constant flow velocity along the key and a quasi-horizontal free surface profile.

VII.3.2.3. Transverse profile

Regarding the transverse free surface profile (Figure VII-14), no influence of the weir height can be observed for heads until 0.15 m.

Indeed, the W_i/W_o ratio seems sufficient to ensure that the side nappes interference zone is still under the crest level and so play no role in the PKW efficiency (Figure VII-15 – (a)). However, for highest weir heights the interference zone level increases to reach the crest level (Figure VII-15 – (b)). This may be due to smaller velocities along the inlet key. Indeed, smaller longitudinal velocities increase the side crest efficiency and so the side nappe length. This phenomenon is accentuated for H = 0.2 m. The transverse free surface profile on highest PKWs (P > 0.4 m; S_i > 1) is near the horizontal.

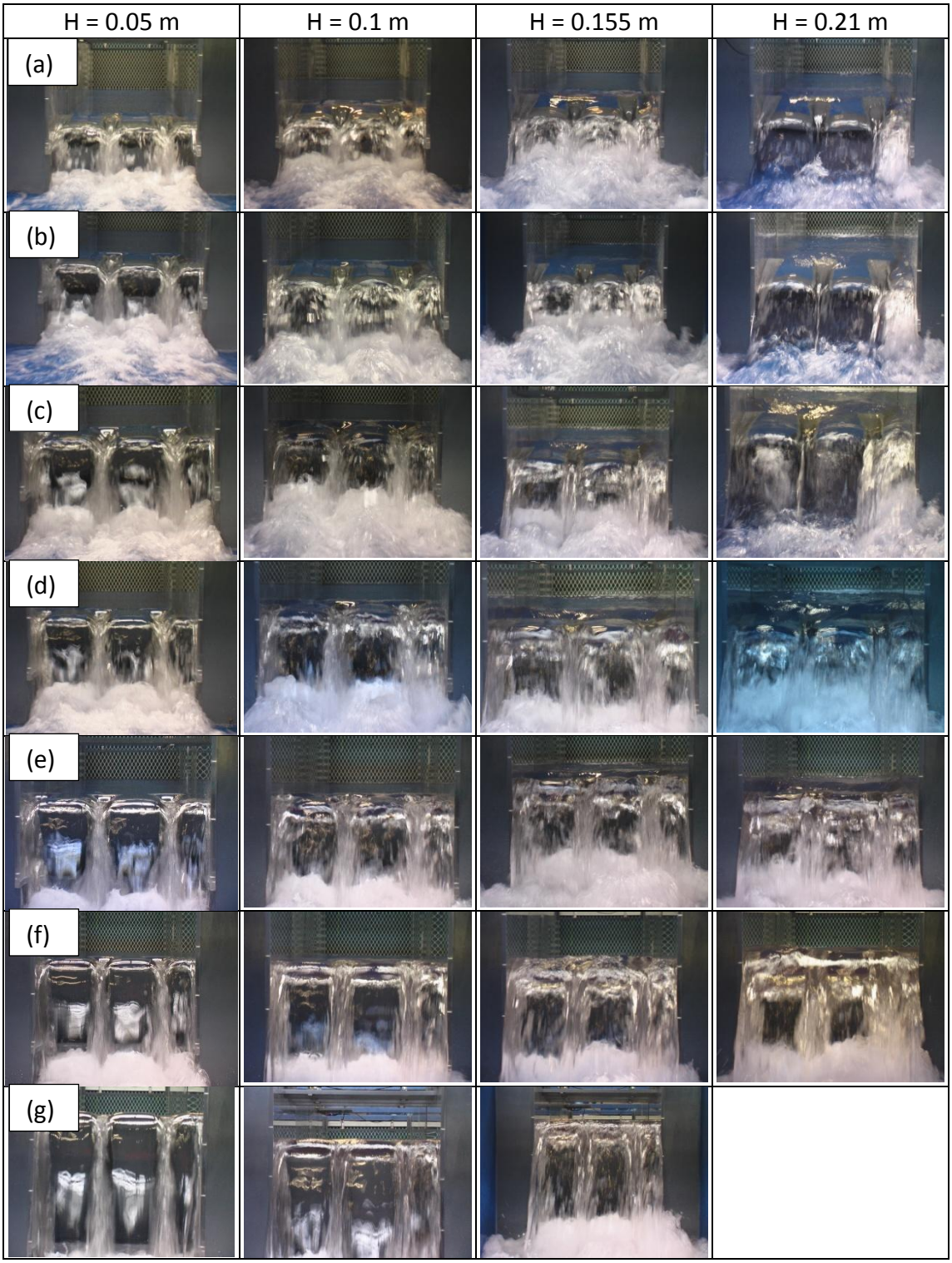

Figure VII-14 View of the transverse free surface profile variation with head: P = (a) – 0.1 m; (b) – 0.15 m; (c) – 0.2 m; (d) – 0.24 m; (e) – 0.3 m; (f) – 0.4 m; (g) – 0.6 m

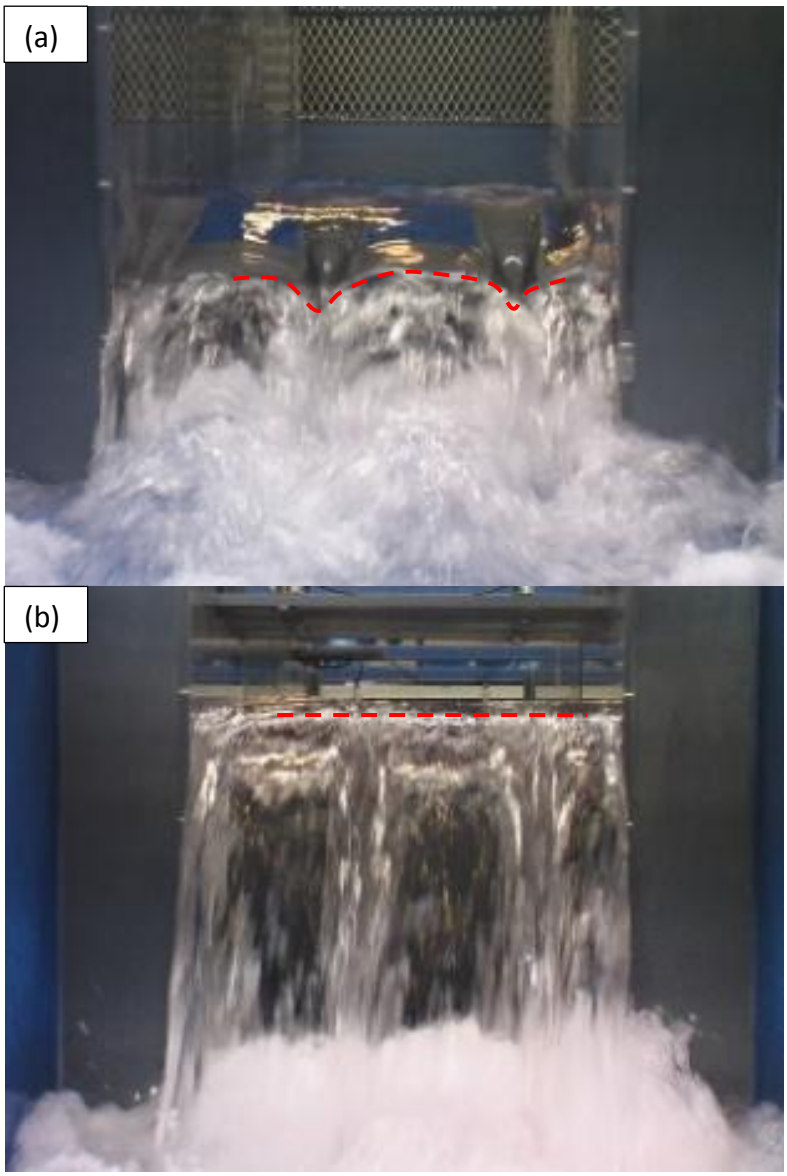

Figure VII-15 View of the transverse free surface variation for H = 0.155 m; P = (a) – 0.1 m; (b) – 0.6 m

For highest heads and low weir heights, even if the transverse free surface profile seems to play no role in the PKW efficiency, the PKW height influences the air entrainment downstream of the weir. As the weir height decreases and the head increases, no more air entrainment is observed under the downstream nappes (Figure VII-16). This phenomenon may induce negative pressure on the structure. Furthermore, the energy dissipation along the weir is largely decreased, what may induce some problems on the downstream dissipation structure. Low PKWs would thus need artificial aeration structures when high PKW geometries are sufficient to ensure nappe aeration.

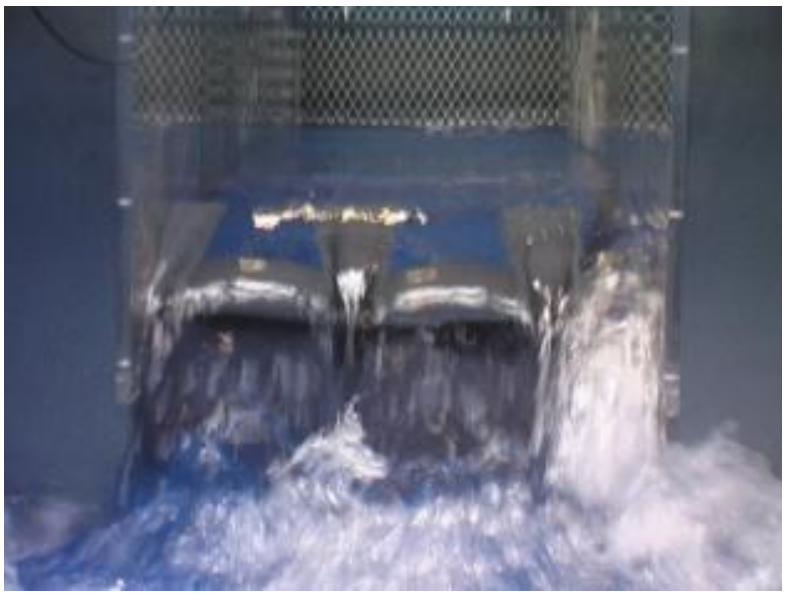

Figure VII-16 View of the downstream nappe aeration for H = 0.2 m and P = 0.1 m

VII.3.3. Analytical approach

In order to help the optimization of future PKW designs, an analytical approach has been initiated. The approach of the effect of the inlet key height and slope on the PKW release capacity has thus been realized combining the results of the studies led on sharp crested inclined weirs (see XIV.1) and on the PKWs with varied weir heights, keeping in mind the conclusions of the study on the 1:10 scale model of PKW. Based on these results, the specific discharge q over a PKW geometry can be seen as the addition of 3 components: the discharge evacuated on the upstream crest of the outlet key q_u, only influenced by the approaching weir height P_T and the upstream head H, the one evacuated on the downstream part of the inlet key q_d, influenced by the weir height P and the upstream head H, and the discharge released on the side crest in-between the inlet and the outlet keys q_s, influenced by the side wall height and the water height varying along the inlet key. The specific discharge of a PKW geometry could thus be calculated by:

$$q = q_u \frac{W_o}{W_u} + q_d \frac{W_i}{W_u} + q_s \frac{2B}{W_u} \qquad \text{VII-1}$$

Regarding the results of the inclined sharp-crested weirs study (see XIV.1), the discharge on the downstream crest is only depending on the weir height P and the water head H and can be calculated combining the SIA equation [107] and the Boussinesq correction [16] for an inclination of 50° (see XIV.1):

$$q_d = 0.445\left(1 + \frac{1}{1000H + 1.6}\right)\left(1 + 0.5\left(\frac{H}{H+P}\right)^2\right)\sqrt{2gH^3} \qquad \text{VII-2}$$

Assuming the same behaviour for the upstream crest, the discharge could be calculated using the same equations with an inclination of -50°. However, for the

upstream crest, the approaching weir height P_T must be considered from the bottom of the flume adding the weir and dam heights P and P_d:

$$q_u = 0.374\left(1+\frac{1}{1000H+1.6}\right)\left(1+0.5\left(\frac{H}{H+P_T}\right)^2\right)\sqrt{2gH^3} \qquad \text{VII-3}$$

For the side crest, the SIA equation [107] can be used considering the water height along the inlet key as the head and correcting the discharge to take into account of the flow inertia in the inlet key direction [44]. Approximating the water height by a linear variation from the upstream head H to the critical height $0.67H$ respectively at the upstream and downstream ends of the side crest, the discharge on the side crest could be calculated as:

$$q_s = 0.41\left(1+\frac{1}{833H+1.6}\right)\left(1+0.5\left(\frac{0.833H}{0.833H+P_e}\right)^2\right)\left(\frac{P_e^{\alpha}+\beta}{0.833H+P_e{}^{\alpha}+\beta}\right)\sqrt{2gH^3} \qquad \text{VII-4}$$

where α and β are parameters depending on the weir geometry. P_e is the mean side wall height calculated by:

$$P_e = P_T\frac{B_o}{B}+\frac{P}{2}\left(1-\frac{B_o}{B}\right) \qquad \text{VII-5}$$

The third corrective coefficient of Eq. VII-4 takes into account the influence, on the side crest discharge, of the flow inertia in the inlet key direction. It makes the side crest discharge tend to the one of a sharp-crested weir when the PKW height tends to infinity, corresponding with negligible longitudinal velocity. It also ensures that the side crest discharge becomes negligible when the head tends to infinity, corresponding with very high longitudinal velocity.

A least square approach on the experimental results enables defining the values of the two parameters α and β depending on the inlet key slope:

$$\alpha = \frac{0.7}{S_i^2}-\frac{3.58}{S_i}+7.55 \qquad \text{VII-6}$$

$$\beta = 0.029\,\mathrm{e}^{-\frac{1.446}{S_i}} \qquad \text{VII-7}$$

The Figure VII-17 shows the comparison between the specific discharges computed with Eqs. VII-1 to VII-7 and the experimental results. It highlights that the

experimental results are approached with an accuracy of 10% except for very low heads where effects of the nappe transition are not taking into account.

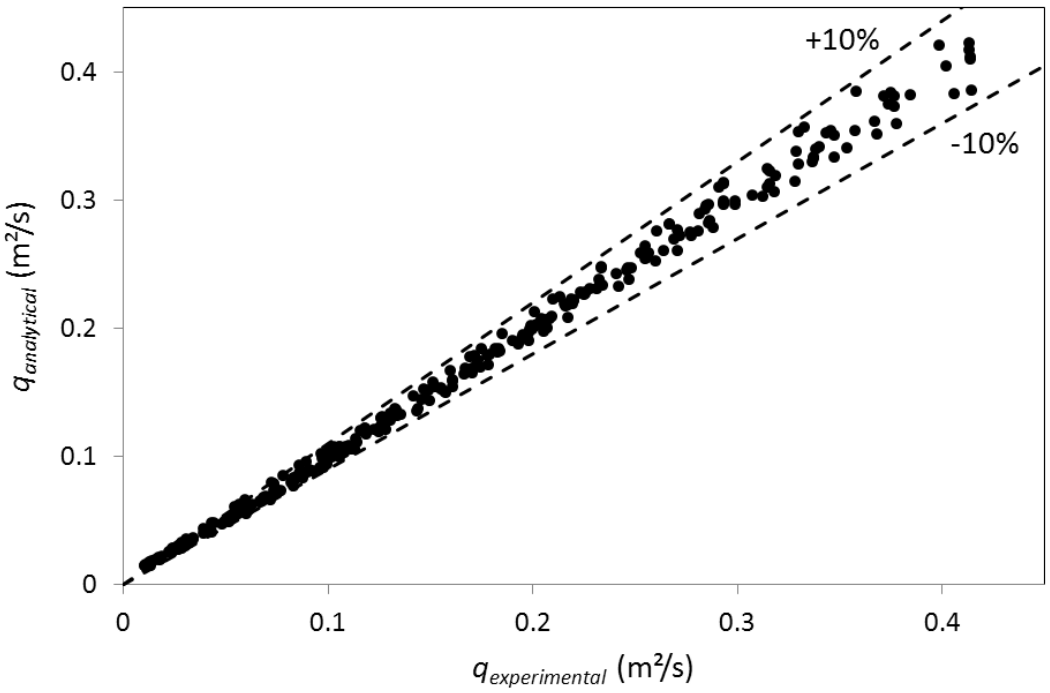

Figure VII-17 Comparison of the specific discharges computed by Eqs. VII-1 to VII-7 and experimental results

The proposed analytical formulation can be compared with the experimental results obtained by Le Doucen [61]. However, attention must be paid on the crest shape. Indeed, Le Doucen used quarter-round crest when the proposed formulation is developed for a sharp crest. Results of experiments led on labyrinth weirs with varied crest shapes shows that a quarter-round crest provides discharges near 9% higher than a sharp crest [42]. The comparison of the experimental results of Le Doucen, obtained for the same ratios B_o/B_i = 1 and L/W = 5 than the present experiments and varied W_i/W_o ratios, with the analytical formulation, applying a 1.09 coefficient to take into account the variation of the crest shape, is shown on Figure VII-18.

The accuracy of the analytical approach, compared with the results of Le Doucen, is still 10% whatever the variation of the ratio between the inlet and the outlet keys widths. This highlights the low influence of this ratio on the value of the two parameters α and β of the proposed analytical formulation. However, the accuracy of the formulation is mainly managed by the results obtained for the highest values of this ratio (W_i/W_o = 2 and 1.6). For these ratios, the precision of the analytical approach tends to reach 10% with increasing discharges and decreasing slopes.

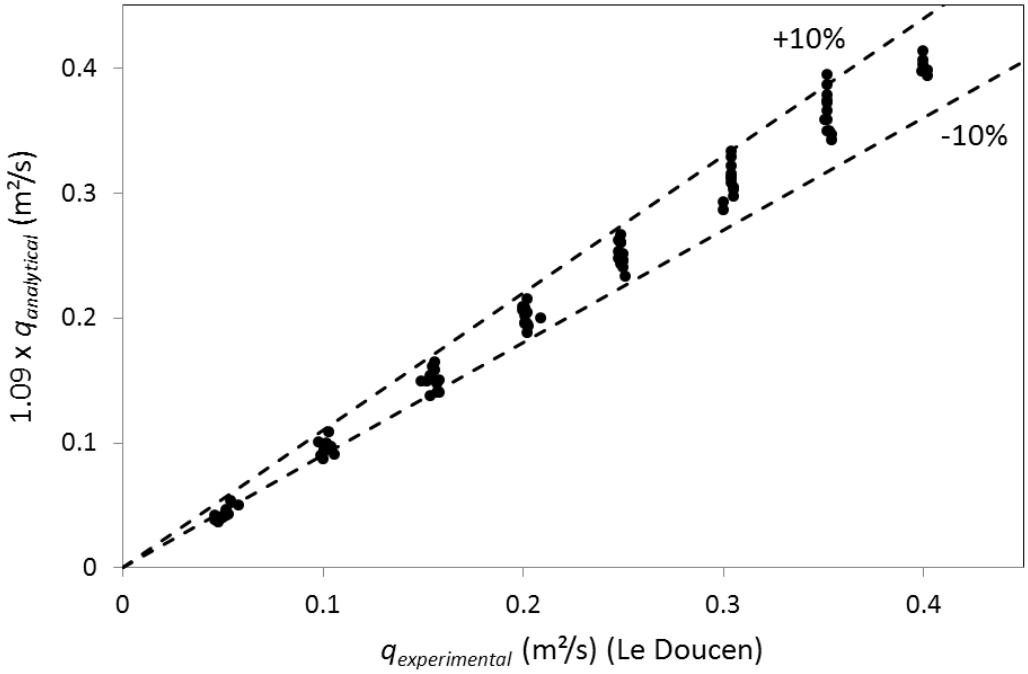

Figure VII-18 Comparison of the specific discharges computed by Eqs. VII-1 to VII-7 with experimental results of Le Doucen [61]

VII.3.4. Numerical approach

The experimental models have also been modelled numerically using the enhanced version of Wolf1D-PKW (see XIV.2). Even if the numerical approach gives results with an accuracy of 10%, the results are systematically less accurate than the ones of the analytical approach (Figure VII-19). The analytical approach has thus to be preferred for pre-design.

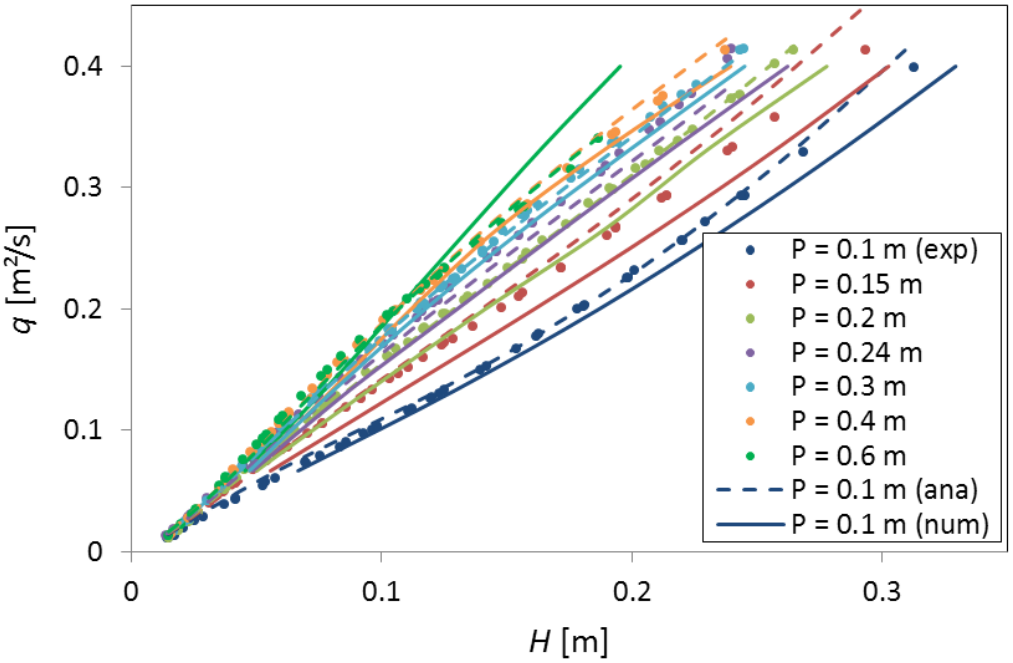

Figure VII-19 Comparison between stage discharge curves obtains from experimental, analytical and numerical approaches

However, the interest of the 1D numerical solver is to give information on the free surface profiles and on the position of the critical section, that had been observed moving along the inlet key on the 1:10 scale model (see IV).

VII.3.4.1. P = 0.4 m

Figure VII-20 and Table VII-3 show the comparison between the free surface profiles along the inlet and outlet keys computed with the enhanced version of Wolf1D-PKW for a high weir height (P = 0.4 m; S_i = 1) and the experimental results.

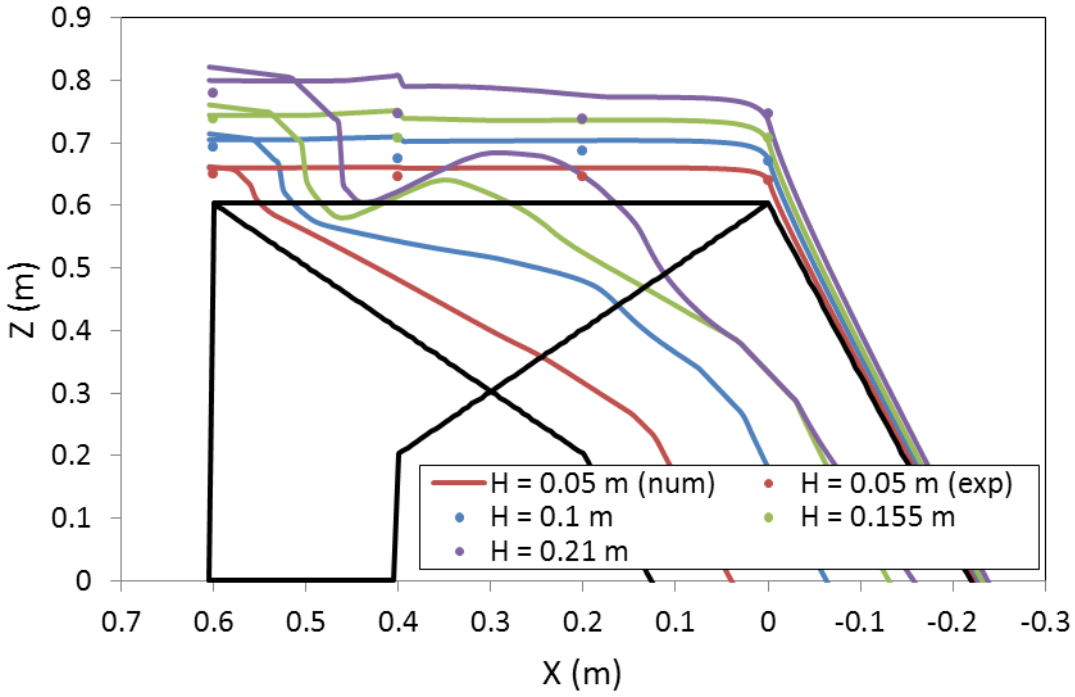

Figure VII-20 Comparison between measured free surface level and profiles provided by Wolf1D-PKW for P = 0.4 m

Table VII-3 – Comparison of experimental and numerical results for P = 0.4 m

X (m)	H (m)	$\Delta h/h$ (%)	X (m)	H (m)	$\Delta h/h$ (%)
0.6	0.05	22.9	0.2	0.05	30.9
	0.1	13		0.1	18.7
	0.155	4.9		0.155	0.3
	0.21	10.9		0.21	27.9
0.4	0.05	31.3	0	0.05	3.5
	0.1	38.8		0.1	7.9
	0.155	30.9		0.155	3.8
	0.21	31.3		0.21	6.5

Regarding the inlet free surface profile, the upstream (X = 0.6 m) and downstream (X = 0 m) levels are in agreement with experimental results. However, the decrease observed in free surface level at the inlet entrance (X = 0.4 m) on scale models is not represented by the numerical solver. This decrease comes from the

progressive lateral contraction of the flow under the upstream overhangs and from the quick vertical contraction at the key entrance. However, the flow solver considers only the inlet width to model the inlet key. There is thus no lateral contraction considered. In further developments, the Wolf1D-PKW solver should include the consideration of compounded cross sections.

Regarding the outlet free surface profile, the upstream part is in agreement with observations made on the scale model with a flow quickly passing by a critical depth. However, the hydraulic jump observed on the numerical results for highest heads (Figure VII-21) is not observed on the scale model. This may come from the longitudinal transfer of the flow between inlet and outlet keys. Indeed, the solver considers well the side flow inclination in the calculation of the mass and momentum transfers between the keys. However, the transfers are realized perpendicularly to the side crest. Practically, the transfer follows the side flow inclination that is non-negligible for high heads. That phenomenon decreases the discharges along the outlet key and delay the apparition of the hydraulic jump observed on the numerical model. This hydraulic jump, moving the free surface level over the side crest one, enables to explain the PKW loss in efficiency observed, for high heads, on numerical results compared with the experimental ones (Figure VII-19).

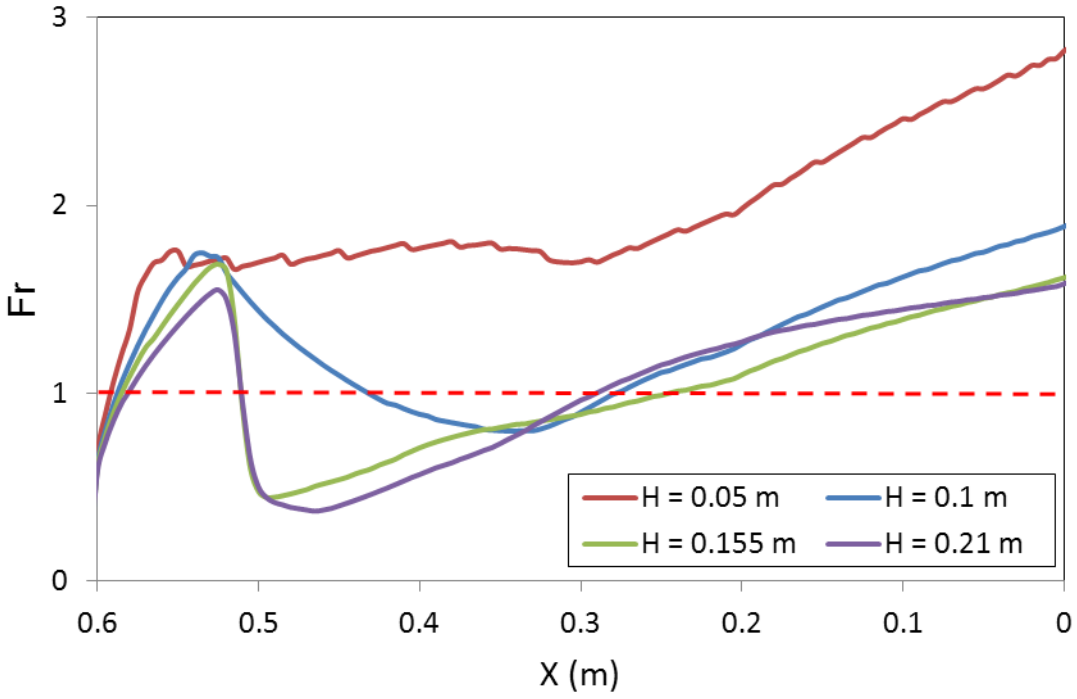

Figure VII-21 Variation of the Froude number along the outlet key for P = 0.4 m

VII.3.4.2. *P* = 0.15 m

Figure VII-22 and Table VII-4 show the comparison between the free surface profiles along the inlet and outlet keys computed with Wolf1D-PKW for a low weir height (P = 0.15 m; S_i = 0.375) and the experimental results.

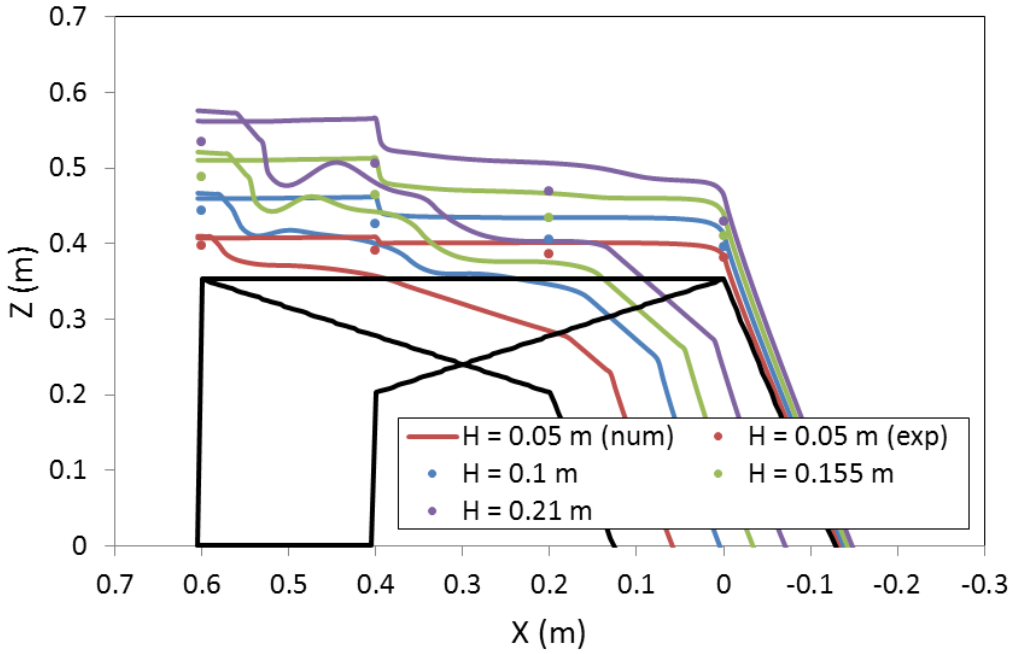

Figure VII-22 Comparison between measured free surface level and profiles provided by Wolf1D-PKW for P = 0.15 m

Table VII-4 – Comparison of experimental and numerical results for P = 0.15 m

X (m)	*H* (m)	Δ*h*/*h* (%)	*X* (m)	*H* (m)	Δ*h*/*h* (%)
0.6	0.05	23.1	0.2	0.05	49
	0.1	18.5		0.1	56.7
	0.155	16.4		0.155	41.4
	0.21	15.3		0.21	32.5
0.4	0.05	29.5	0	0.05	11.8
	0.1	22.9		0.1	13
	0.155	18.3		0.155	18.7
	0.21	15.7		0.21	14.6

The inlet free surface profiles are this time closer from the free surface profiles obtained from the experiments at the inlet entrance (*X* = 0.4 m). Indeed, as the weir height decreases, the influence of the transversal flow contraction decreases and the one of the vertical contraction increases. As the flow solver computes well the vertical contraction, despite the lateral one, it is more efficient for low weir heights.

Regarding the outlet keys, the shape of the free surface profiles are closer from the ones observed on the scale model than for the high weir. As the weir height decreases, the transfer way between inlet and outlet keys decreases, and so the longitudinal transfer length. The assumption of a transfer perpendicular to the side wall becomes thus more accurate for low weirs.

VII.3.4.3. Control section on the inlet key

The free surface profiles in the downstream part of the inlet key are not affected by the simplifications of the flow solver, whatever the upstream head or the weir

height. The numerical results may thus help in the analysis of the control section position along the key. Figure VII-23 shows the variation of the distance *B'* between the downstream crest and the control section of the inlet key regarding head and weir height.

For high weir heights ($P \geq 0.3$ m; $S_i \geq 0.75$), the control section is located on the downstream crest. Flow velocities are sufficiently low in the inlet key to avoid apparition of supercritical flows. The weir height plays no role on the discharge capacity (Figure VII-8).

For low weir heights ($P \leq 0.15$ m; $S_i \leq 0.375$), the control section of the inlet key moves upstream to reach a maximum distance from the downstream crest for a H/P ratio approximately equal to 1.5. Then, for increasing heads, the control section moves downstream. Flow velocities along the inlet key become higher than the critical one due to the low water depth in the downstream part of the inlet key. However, for high heads, the submergence of the side crest by the outlet flow decreases the inlet key discharge and so the velocities, what moves the control section downstream. The PKW discharge capacity decrease observed with decreasing weir height is so less important for high heads than for low heads (Figure VII-8).

For intermediate weir heights, the studied heads are not sufficiently high to observe the maximum displacement of the control section along the inlet key. The discharge capacity decreases continuously with weir height and upstream head (Figure VII-8).

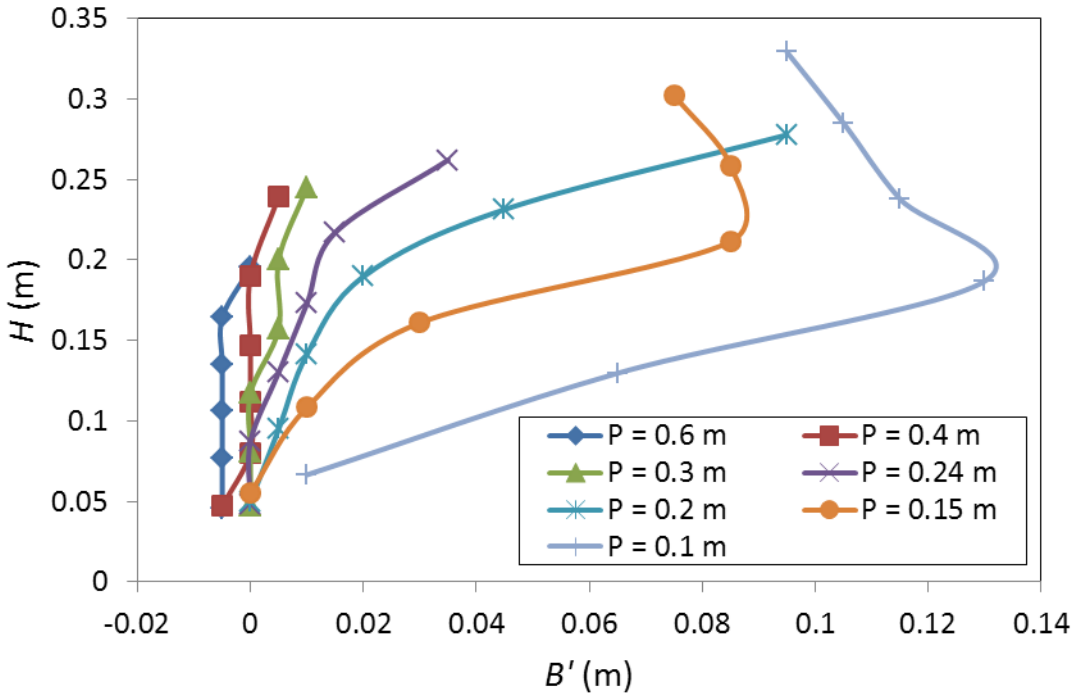

Figure VII-23 Variation of the inlet control section position with head and weir height – numerical results

VII.3.5. Design considerations

By derivation of the proposed analytical formulation, the optimal slope, in terms of discharge capacity, is between 1.1 and 1.2, for the tested values of the other non-dimensional ratios (L/W = 5, W_i/W_o = 1.5, B_o/B_i =1, B_o/B = 0.33) (Figure VII-24). However, 95% of the maximum discharge capacity is already provided with slopes between 0.4 and 0.8 depending on the upstream head.

Even if the hydraulic criterion encourages increasing the bottom slope of the PKW, modification of the geometry involves technical and economic consequences that designers have to deal with. The optimization of the structure may change depending on the large set of design criteria varying with the project constraints.

By example, assuming that the global cost of a PKW building is directly proportional to the volume of the structure, the optimal geometry, considering economic interests, is the one which provides, for a given head, the highest discharge Q per cubic meter of concrete $V_{concrete}$ necessary to build a PKW-unit. In this case the optimal geometry varies with the design head between S_i = 0.3 to 0.35 (Figure VII-24).

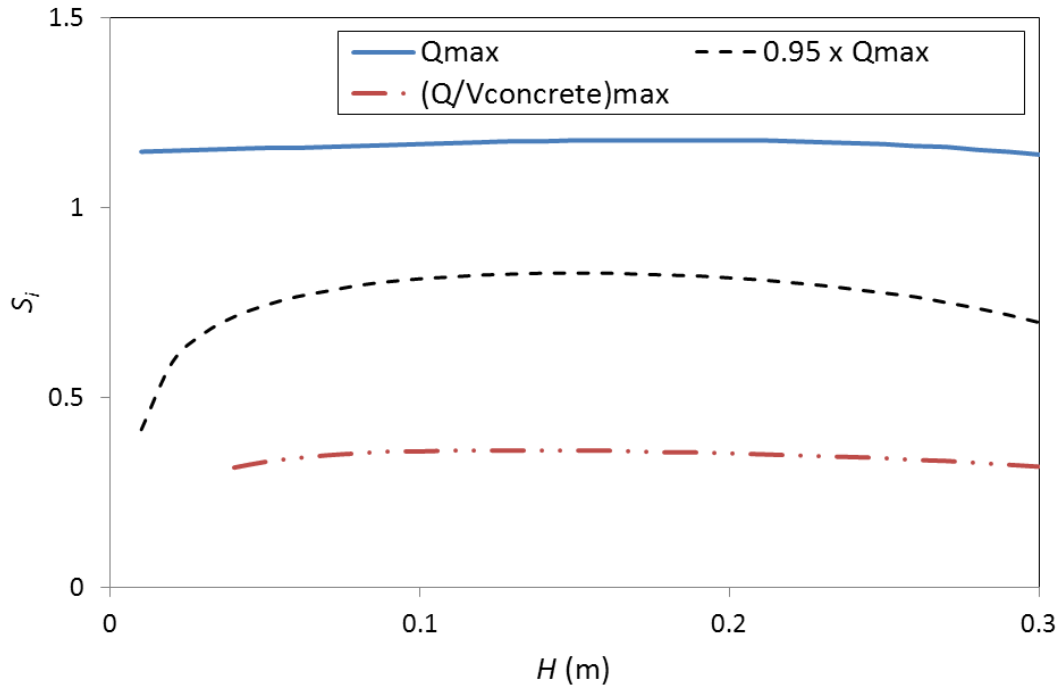

Figure VII-24 Variation of the optimal slope with the head for varied design criteria

If the designer wishes to maximize the reservoir use during the PKW building, in a rehabilitation project, he has to look for the geometry able to release the design discharge for a minimal value of the sum of the weir height P and the necessary head H. In this case the optimal geometry involves the smallest slopes (Figure VII-25).

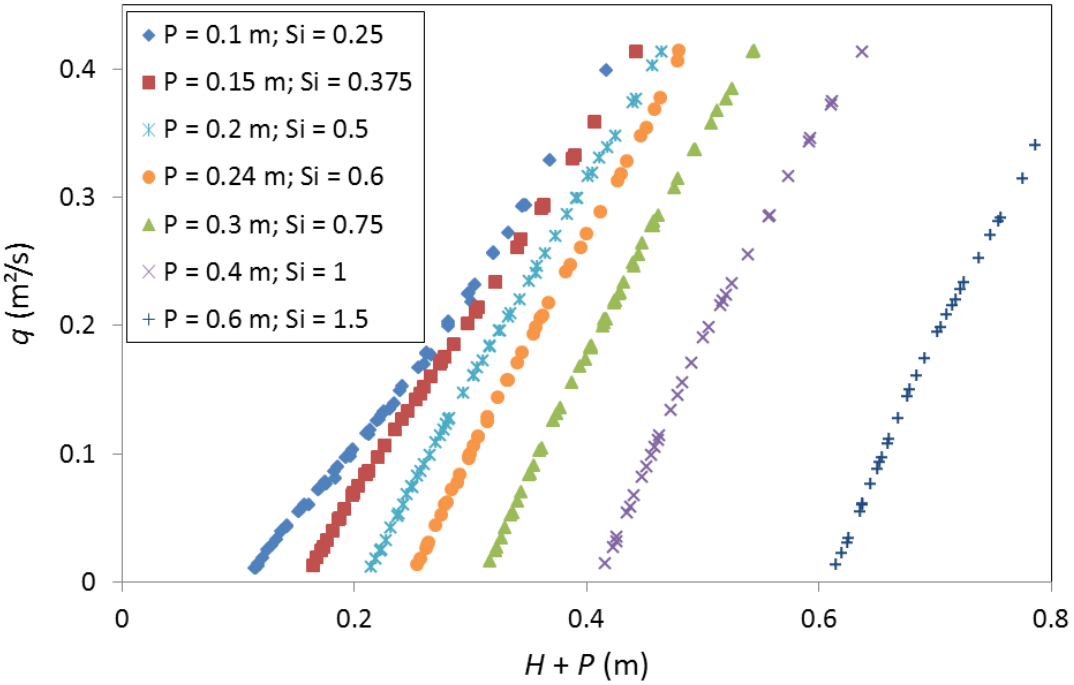

Figure VII-25 Comparison of the head plus weir height/discharge curves for tested models

Combining the hydraulic, technical and economic aspects, a bottom slope of the inlet key of 0.375 seems to be the best solution for PKW. This optimal value may be slightly modified by the variation of the other geometric ratios kept constant in this part of the study (W_i/W_o, B_o/B_i, L/W).

For high design heads, a technico-economic optimal slope may become higher considering the need in artificial aeration systems on downstream crests for low slopes.

VII.4. Influence of the parapet walls [84]

From the study of the weir height influence, an optimal value of the weir height has been defined. Ouamane and Lempérière [93] also demonstrated the interest in increasing the weir height to increase its discharge capacity. However, in their study, as in the one presented here before, the weir height and the keys slope are modified in the same time. This doesn't enable to draw conclusions on the separate influence of these two parameters. The study of the weir height influence alone can be realized using vertical extensions placed over the weir crest, called parapet walls [98]. These extensions enable to increase the height of a given PKW geometry, without modification of the keys slopes.

The influence of parapet walls has been tested while optimizing the hydraulic efficiency of PKW. Leite Ribeiro et al. [65] show that the use of parapet walls on the Etroit dam PKW increases its discharge capacity by up to 15%. However, the efficiency of such structures has only been studied on a single PKW configuration, with or

without parapet walls, changing the total weir height and keeping the keys slopes constant. Furthermore, in the same range of weir heights, modifying the PKW height by changing the inclination of inlet and outlet keys bottom slopes induces similar variations in the discharge capacity (see VII.3). Consequently, it is not so clear yet whether a PKW with parapet walls is more efficient than a standard one having the same total height or not.

From existing studies, the influence of the keys slopes remains not defined. In most cases of PKW use, the total weir height is fixed by the normal level of the reservoir and structural considerations on the main dam body that impose the toe elevation of the weir. It is thus of primary practical interest to distinguish the influence of the weir height, which confronts the structural and hydraulic interests, and the one of the keys slopes, which are parameters for the hydraulic optimization of the structure.

Several PKW configurations have been tested with or without parapet walls, providing models with same height and varying slopes as well as models with same slopes and varying height. This double approach enables to distinguish the effect of PKW height from the one of keys slopes, and to provide practical guidelines on the use of parapet walls.

VII.4.1. Head-discharge curve

VII.4.1.1. Variation of the weir height

The comparison of the specific discharges q, regarding the weir width for given upstream heads, depending on the weir height at constant keys slope is shown in Figure VII-26 for varied W_i/W_o, L/W and $S_i = S_o$ values. For each model, the specific discharges measured on variant 2 and variant 1 are compared. The variant 2 has the same geometry as variant 1 except for the weir height which is increased using parapet walls (Table VII-2).

Practically no variation of the weir efficiency is observed when the P/W_u ratio is increased between 1.3 and 1.5 (models 1, 3 and 4). These values of the P/W_u ratio are closed to the optimal value of 1.33 determined from the study of PKW models varying simultaneously height and keys slope (see VII.3). As the P/W_u ratio decreases below the optimal value, the influence of the weir height becomes more and more important (models 2, 5 and 6). The maximal increase in efficiency is obtained from the variation of P/W_u from 0.34 to 0.59. It reaches 28%.

This suggests that the use of a parapet wall to increase weir height is relevant when the weir height is far below the optimal weir height. However, the same increase in efficiency is observed for the same variation of the P/W_u ratio on the models varying simultaneously weir height and keys slopes (see VII.3). The keys slope seems thus to

have no influence on the PKW discharge capacity, as the gain in efficiency observed increasing the weir height is similar considering a constant or a variable keys slope.

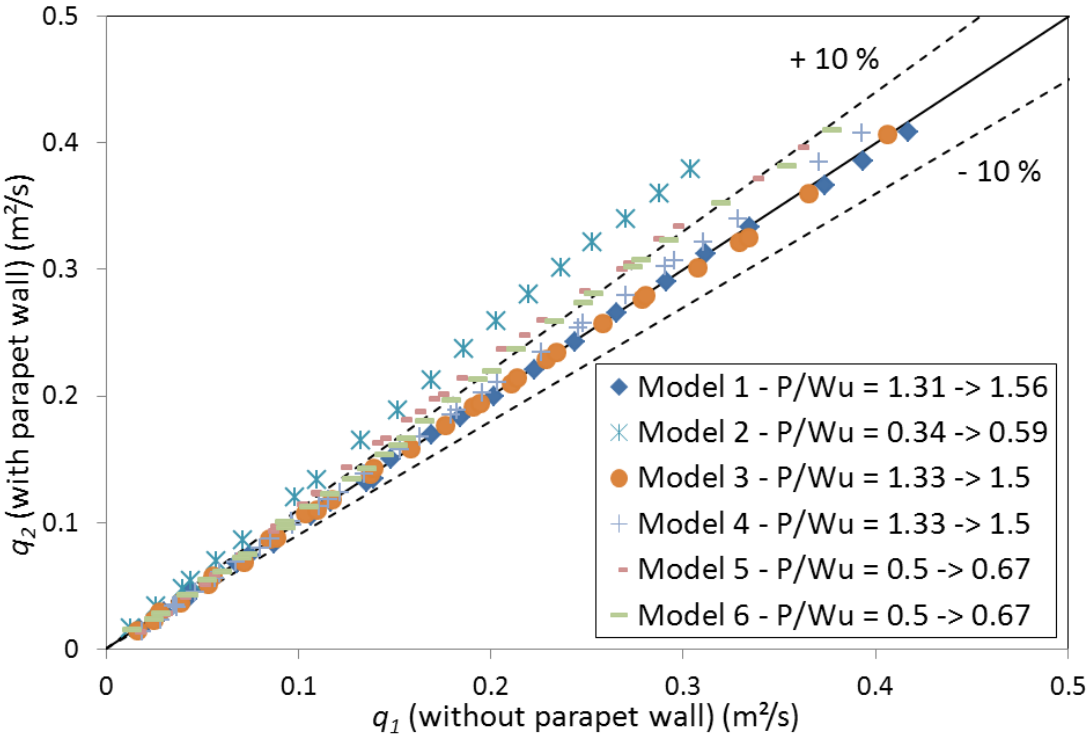

Figure VII-26 Weir height influence on relative specific discharges with constant keys slope (variants 2/1)

VII.4.1.2. Variation of the keys slope

Figure VII-27 shows the comparison of specific discharges over the weir for given upstream heads depending on the keys slope with constant weir height for varied W_i/W_o, L/W and $S_i = S_o$ values. For each model, the specific discharges measured on variant 2 and variant 3 are compared. The variant 3 has the same geometry as variant 2 except for the keys slope which is increased to avoid the use of parapet walls.

The variation of the keys slope has practically no influence on the PKW efficiency. The variation of the specific discharge, varying only the keys slope, is less than 7% for model 2 and less than 3% for model 5.

As expected after the analysis of Figure VII-26, the parapet walls enhance the PKW discharge only if they increase the total PKW height to tend to its optimal value. There is thus no direct effect on the discharge capacity of the keys slope but well of the ratio between the total weir height and the length of the keys. For PKW with a low height or considering high upstream heads, the increase of the keys slope seems more relevant. In these cases, the limitation of the weir efficiency comes from the discharge capacity of the outlet key that is increased as the outlet key slope increases, increasing flow velocities. For low heads and sufficiently high weir height, the PKW efficiency is mainly managed by the Froude number along the inlet key (see IV.6). As the lower keys

slope provides higher water depths along the keys, it decreases the flow velocities and the Froude number, increasing the global efficiency of the weir.

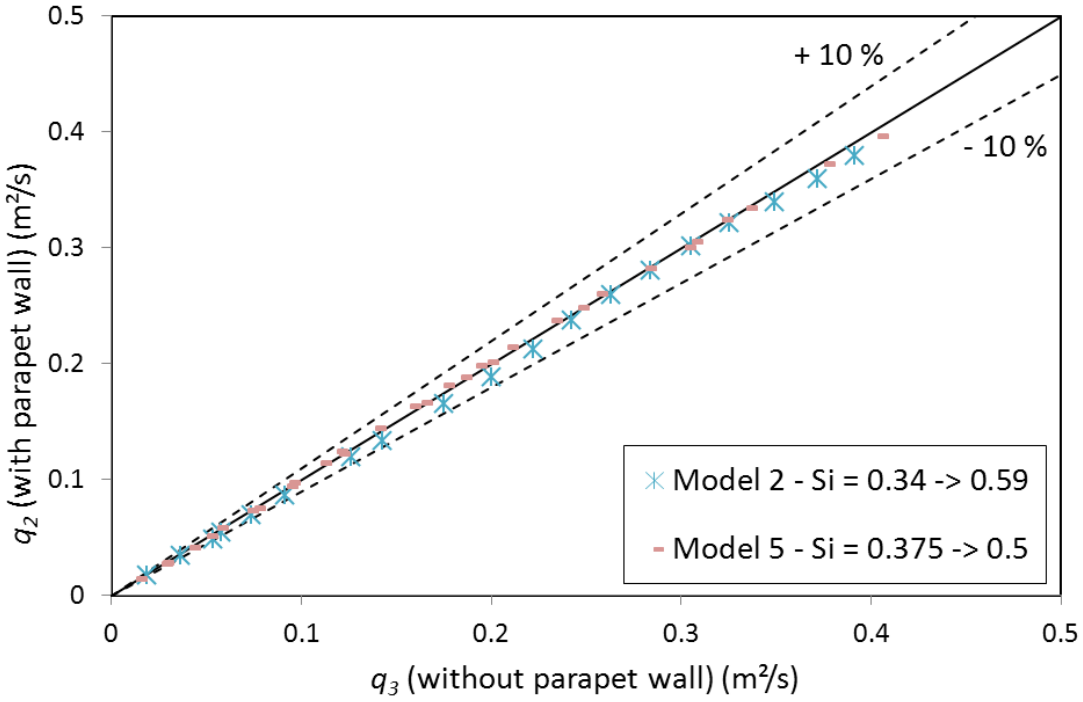

Figure VII-27 Keys slope influence on relative specific discharges with constant weir height (variants 2/3)

VII.4.2. Free surface profile

VII.4.2.1. Inlet key profile on model 5

Figure VII-28 shows the free surface profiles in the centre of the inlet key for the three variants of model 5 considering low, normal and high upstream heads of respectively 0.05, 0.15 and 0.24 m.

The comparison of the free surface profiles for variants 2 and 3 of model 5 highlights that the use of a parapet wall, while keeping constant the total weir height, influences only the downstream part of the inlet key. Indeed, the maximal difference observed between surface profiles of the two models remains below 0.005 m except on the downstream crest where it reaches 0.017 m for the intermediate and the highest upstream heads. Since these two models have similar stage-discharge curves, it may be deduced that above a threshold upstream head, the downstream part of the inlet key has no more influence on the PKW discharge capacity. This observation is in agreement with the statement of the development for high heads of a control section in the inlet key, upstream of the inlet apex, which controls the discharge on the downstream part of the weir (see IV.6).

The comparison of the free surface profiles for variants 1 and 2 of model 5 highlights the influence of the parapet walls, which increase the total weir height. For an upstream water head of 0.24 m, the free surface is higher (up to 0.015 m) without

parapet walls except on the downstream crest (- 0.033 m). However for this value of the upstream head, there is no more influence of the downstream part of the inlet key due to the presence of the control section upstream the inlet key apex. The model with a higher free surface along the side crest has a lower discharge capacity. That means that the side discharge is not directly dependent on the water height over the side crest but also of the velocity in the inlet key direction. The side crest discharge capacity is reduced due to inertia effect, depending on the velocity in the direction of the inlet key. In variant 1, even if the water head along the side crest is higher than in variant 2, the velocity in the direction of the inlet key is more important due to lower water depths in the inlet key provided by a lower total weir height. This higher velocity in the direction of the inlet key decreases the side crest discharge and, in turn, the discharge capacity of the PKW.

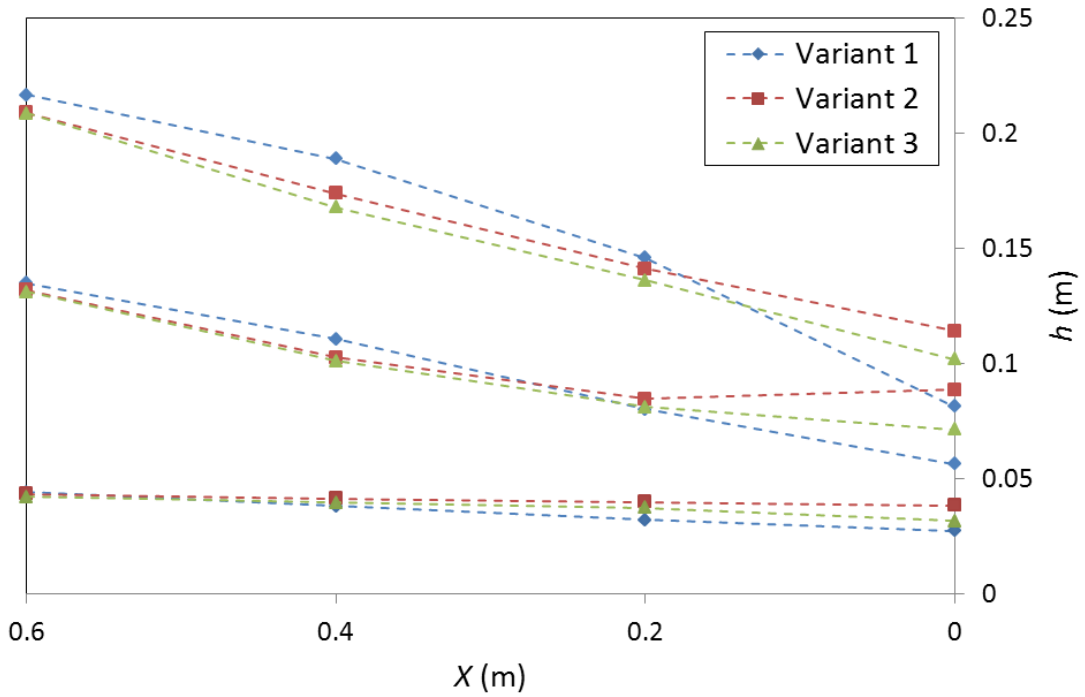

Figure VII-28 Influence of the parapet wall on free surface profiles of model 5

The observation of the flow along the half inlet key (Figure VII-30) confirms the flow behaviours developed here before.

For variant 1, a continuous decrease of the free surface level is observed from the inlet entrance to its downstream (Figure VII-29 – (a)). For variant 2 and 3, a quicker decrease is observed at the inlet entrance before a lower decrease on the downstream part of the crest (Figure VII-29 – (b) and (c)). The free surface level at the downstream crest is higher on variant 2 than variant 3. That may be due to the vertical ending wall that modifies the downstream crest behaviour, modifying the nappe shape and the velocity profile over the crest.

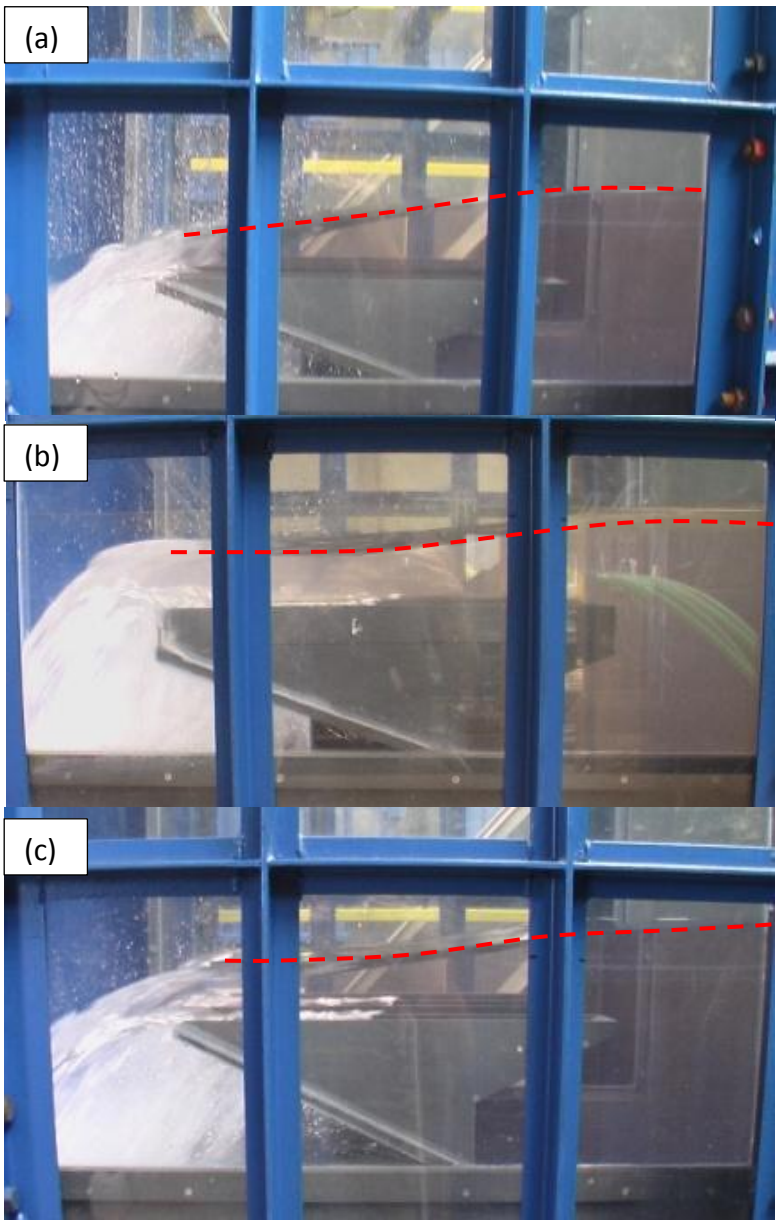

Figure VII-29 View of the inlet free surface variation for H = 0.15 m on model 5: (a) – variant 1; (b) – variant 2; (c) – variant 3

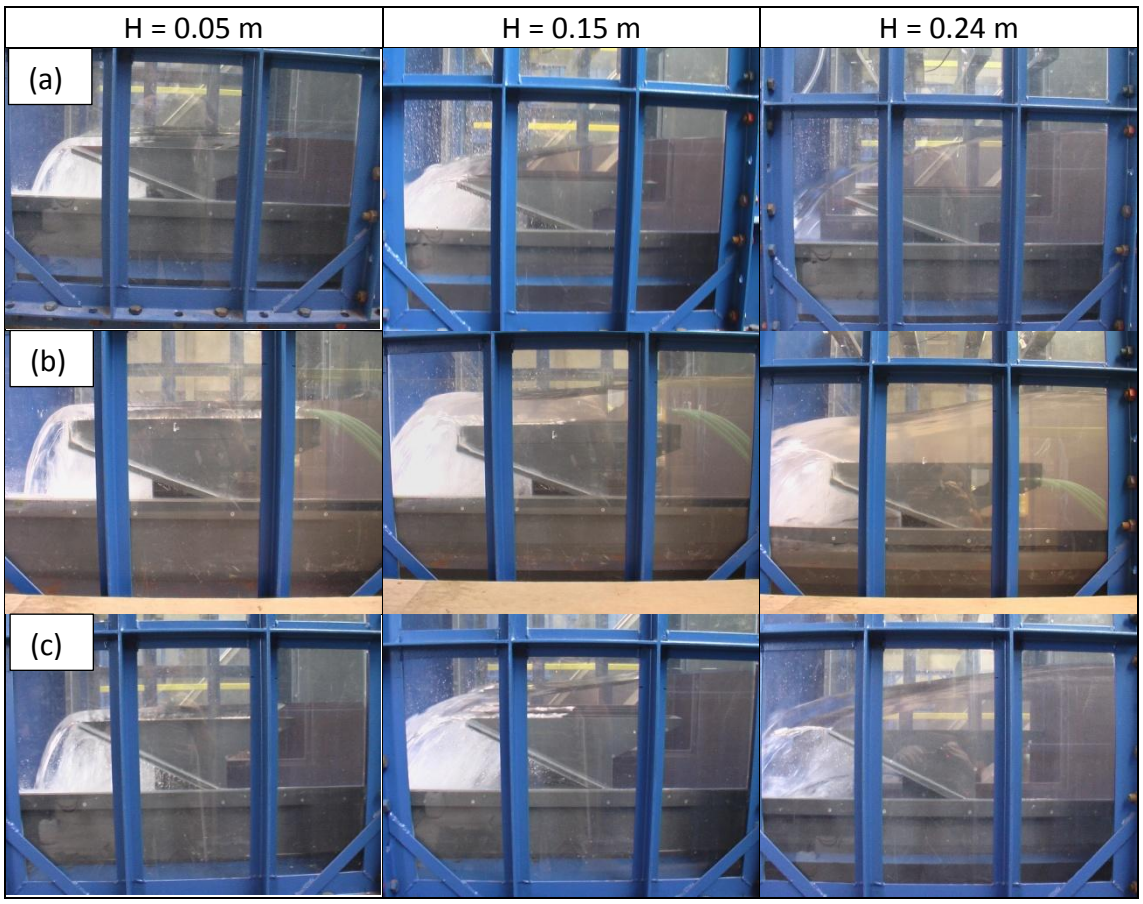

Figure VII-30 View of the inlet free surface variation with head for model 5: (a) – variant 1; (b) – variant 2; (c) – variant 3

VII.4.2.2. Outlet key profile on model 5

Regarding the free surface profiles along the outlet key (Figure VII-33), the influence of the outlet key flow on the weir efficiency is only dependent of the weir height and the upstream head.

The use of parapet walls in variant 2 enables supercritical flows for low heads (Figure VII-31).

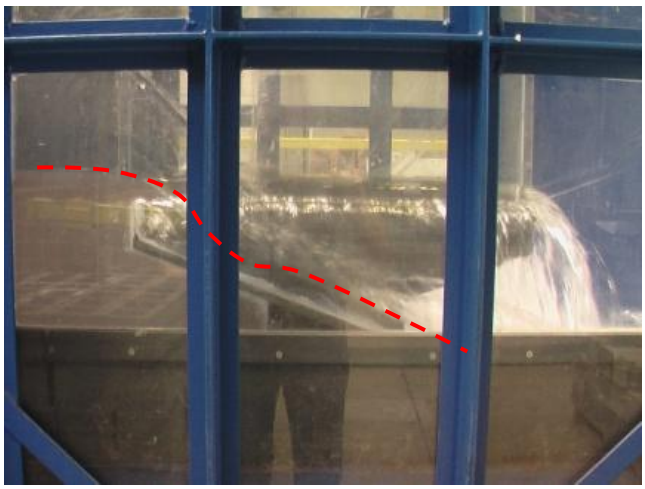

Figure VII-31 View of the outlet free surface for H = 0.05 m on variant 2 of model 5

The use of parapet walls also decreases the length of submerged side crest for high heads on variant 2 compared to variant 1 (Figure VII-32 – (a) and (b)).

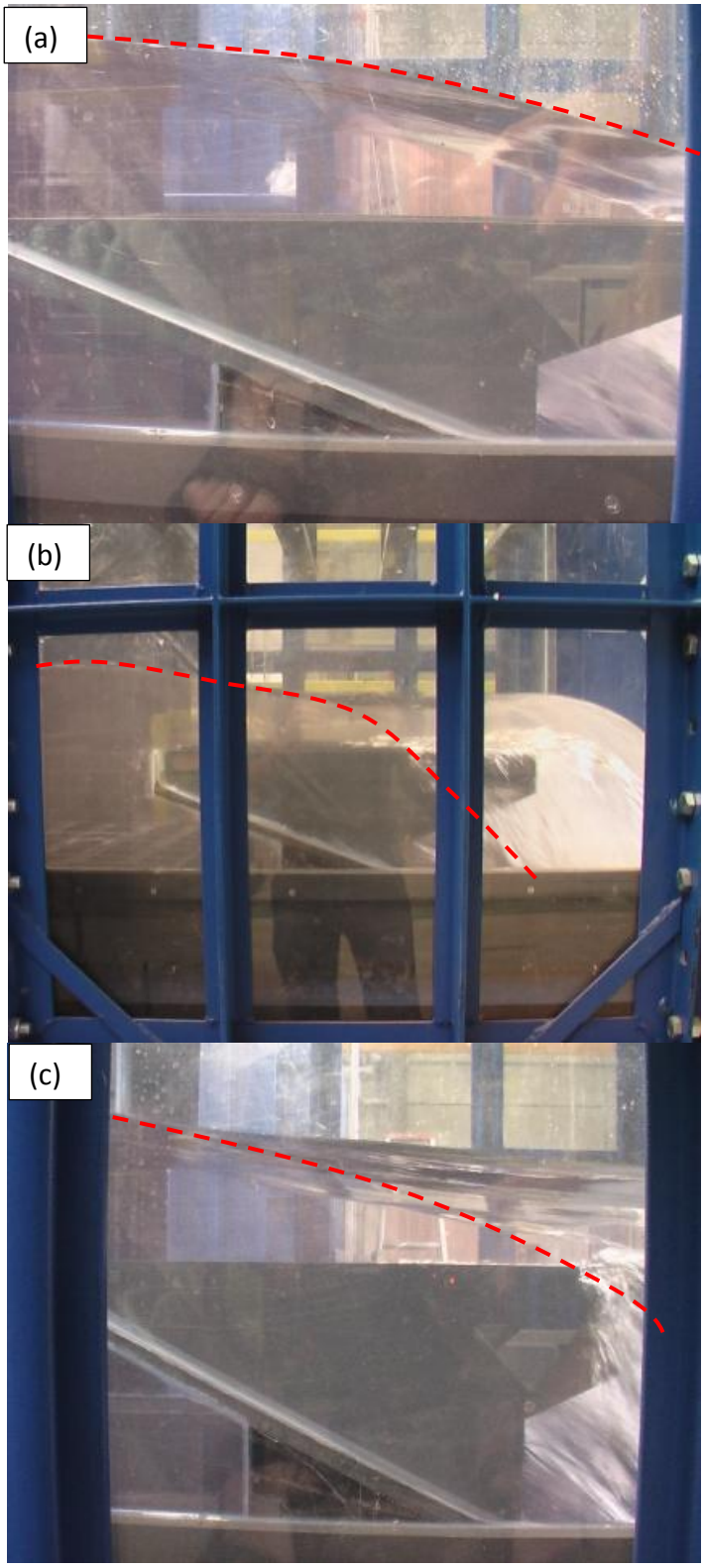

Figure VII-32 View of the outlet free surface variation for H = 0.15 m on model 5: (a) – variant 1; (b) – variant 2; (c) – variant 3

However, the comparison of the variants 2 and 3 doesn't show any variation in the outlet flow behaviour (Figure VII-32 – (b) and (c)). As long as the outlet flow becomes subcritical, the upstream crest stays managed by the outlet resilience capacity. The transition from supercritical to subcritical is realized for similar upstream head. The length of side crest submergence is similar whatever the variant 2 or 3 and whatever the upstream head.

The outlet key flow behaviour enables one more time explaining the observed inlet key behaviour. For variant 1, as the outlet flow highly reduces the side discharge and as the inlet key slope reduces constantly the inlet cross section, the flow velocity along the inlet key increases continuously what decreases the free surface level. For variant 2 and 3, the decrease of the inlet cross section is compensated, on its downstream part, by the decrease of the inlet discharge induced by the side crest, assuring quasi-constant flow velocity along the key and a free surface profile near to horizontal.

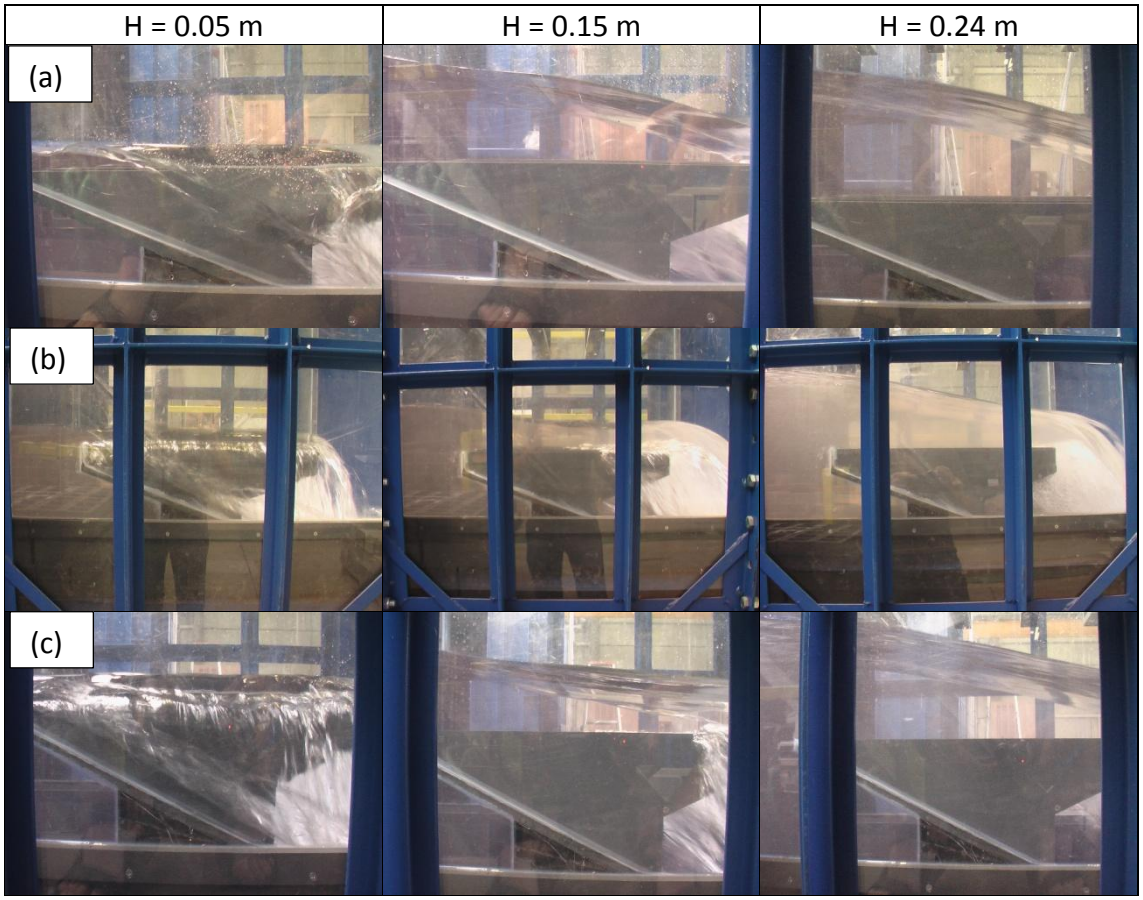

Figure VII-33 View of the outlet free surface variation with head for model 5: (a) – variant 1; (b) – variant 2; (c) – variant 3

VII.4.2.3. Transverse profile on model 5

Regarding the transverse free surface profiles (Figure VII-36), no influence of the weir height can be observed.

The W_i/W_o ratio is sufficient to ensure that the side nappes interference zone is still under the crest level and thus play no role on the PKW efficiency (Figure VII-34 – (a)). However, the presence of parapet walls modifies the side nappe profile. As the vertical extension increases the nappe length, the interference zone level increases (Figure VII-34 – (b)). The interference zone reaches the crest level for highest heads. The transverse free surface profile becomes then quasi-horizontal.

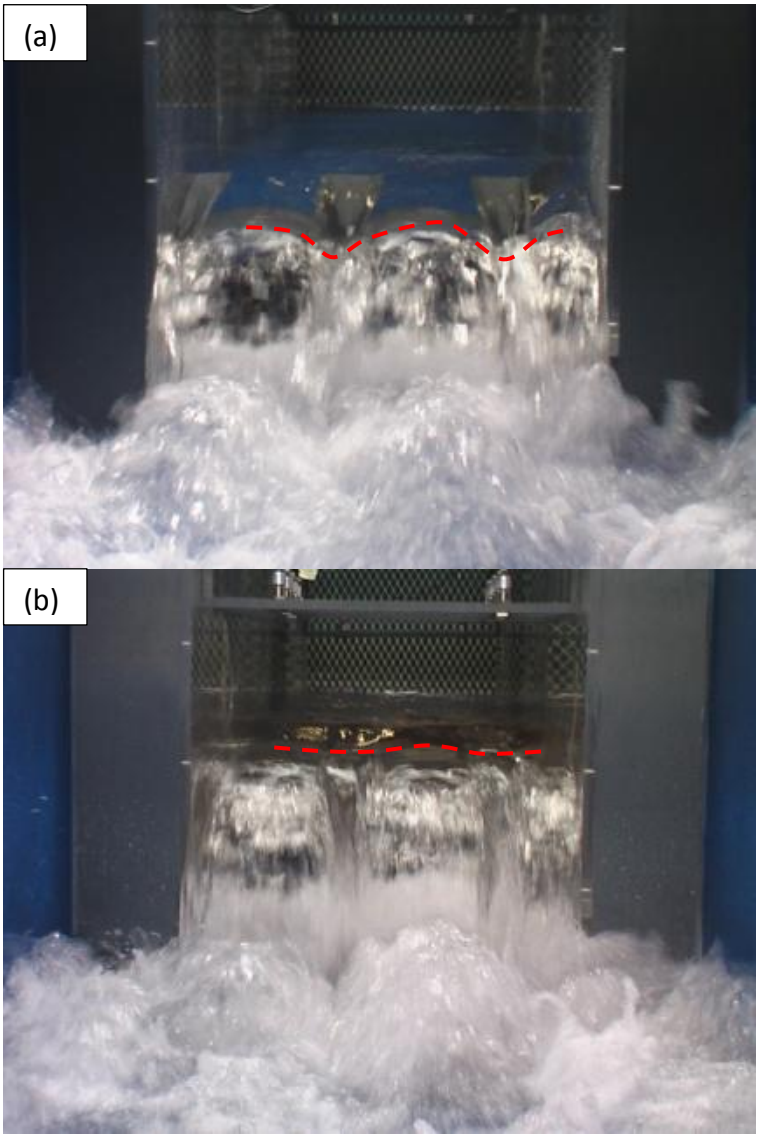

Figure VII-34 View of the transverse free surface variation for H = 0.15 m on model 5: (a) – variant 1; (b) – variant 2

The presence of parapet walls also modifies the downstream aeration (Figure VII-35). As the vertical extensions increase the nappes length and level on the side and downstream crests, they also modify the air entrainment. The use of parapet walls enables the use of low heighted PKW without any artificial aeration system.

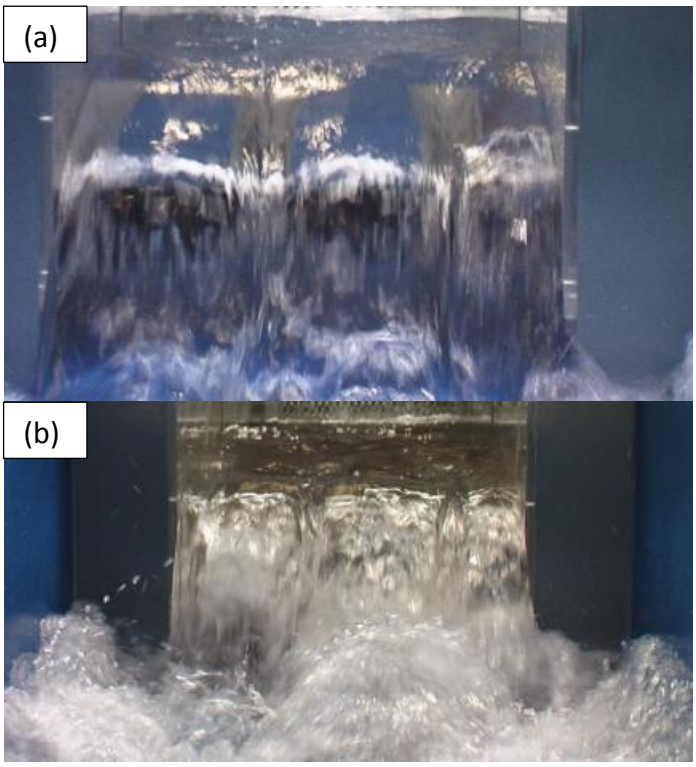

Figure VII-35 Variation of the air entrainment for H = 0.24 m on model 5: (a) – variant 1; (b) – variant 2

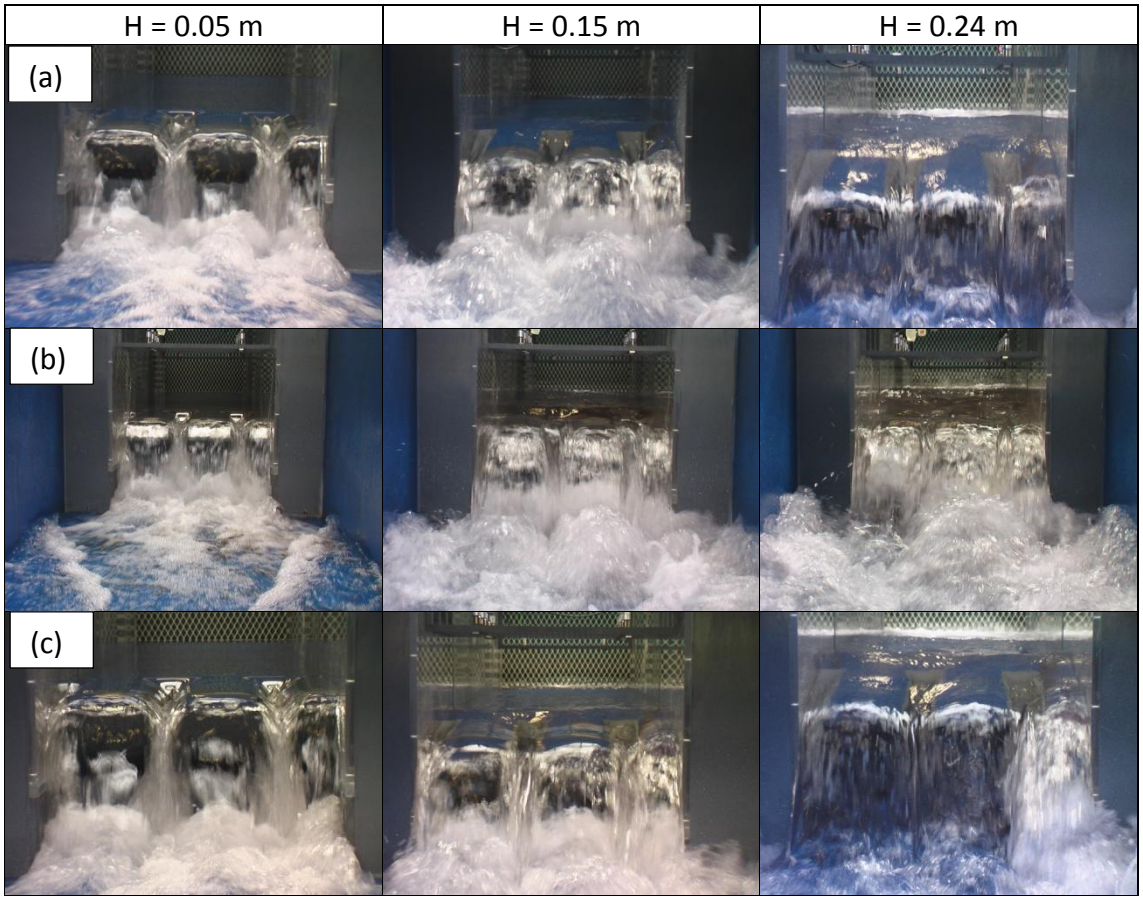

Figure VII-36 View of the transverse free surface variation with head for model 5: (a) – variant 1; (b) – variant 2; (c) – variant 3

VII.4.2.4. Inlet key profile on model 3

Figure VII-37 shows the free surface profiles in the centre of the inlet key for the two variants of model 3 considering upstream heads of 0.05 m, 0.15 m and 0.24 m.

The influence of the parapet walls, increasing the total weir height, is only visible in the downstream part of the inlet key. The total weir height of the model without parapet walls is important enough to reduce the longitudinal velocity. The height increase, induced by the parapet walls, doesn't modify significantly this velocity and the side discharge is mainly influenced by the water height over the side crest. Once more, even if the free surface profiles vary on the downstream part of the inlet key, for the intermediate and the highest upstream heads, it doesn't change the PKW discharge capacity, due to the presence of a control section upstream of this zone.

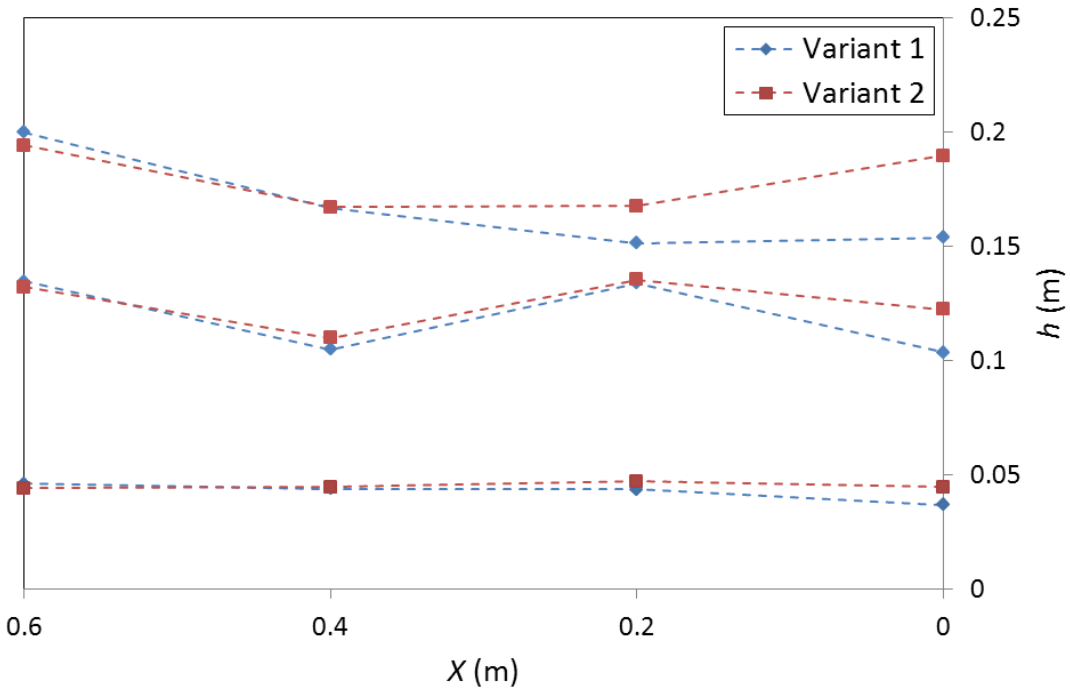

Figure VII-37 Influence of the parapet walls on free surface profiles of model 3

The observation of the flow along the half inlet key (Figure VII-38) confirms one more time the flow behaviours developed here before. For the two variants, a quick decrease is observed at the inlet entrance before a quasi-horizontal free surface on the downstream part of the key. The free surface level at the downstream crest is higher on variant 2 than on variant 1. It may be due, one more time, to the vertical wall that modifies the downstream crest behaviour, modifying the nappe shape and the velocity profile over the crest.

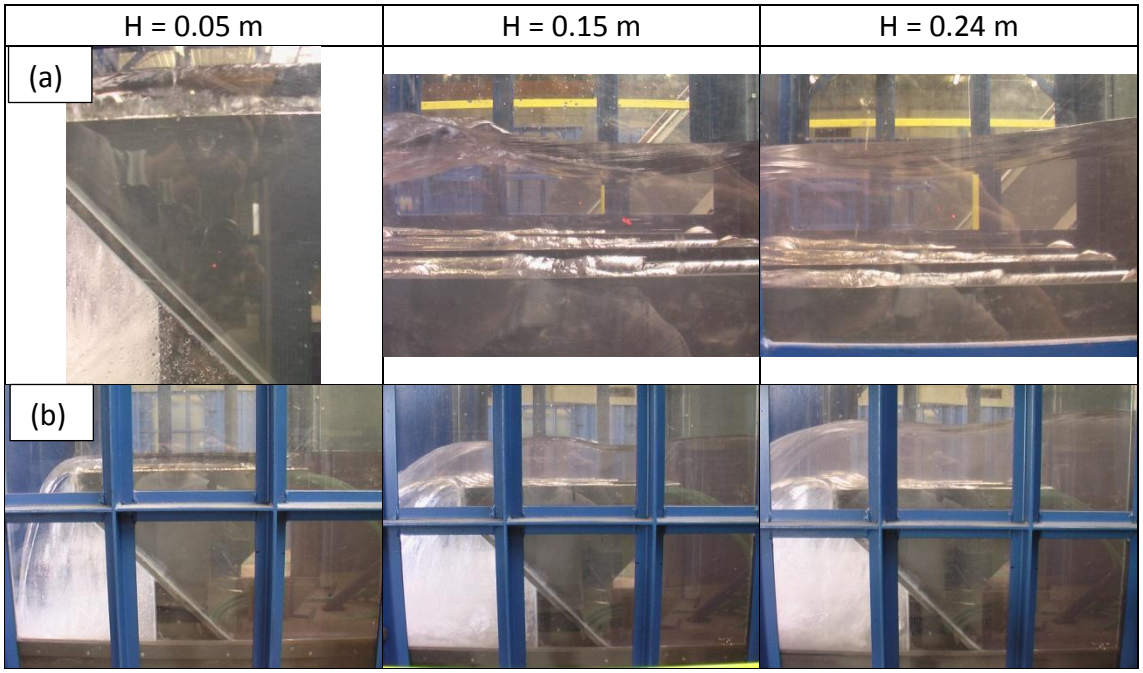

Figure VII-38 View of the inlet free surface variation with head for model 3: (a) – variant 1; (b) – variant 2

VII.4.2.5. Outlet key profile on model 3

Regarding the free surface profiles along the outlet key (Figure VII-39), the influence of the outlet key flow on the weir efficiency is still negligible whatever the variant. Indeed, this time the weir height is sufficient to ensure supercritical flows along the outlet key whatever the upstream head or the variant.

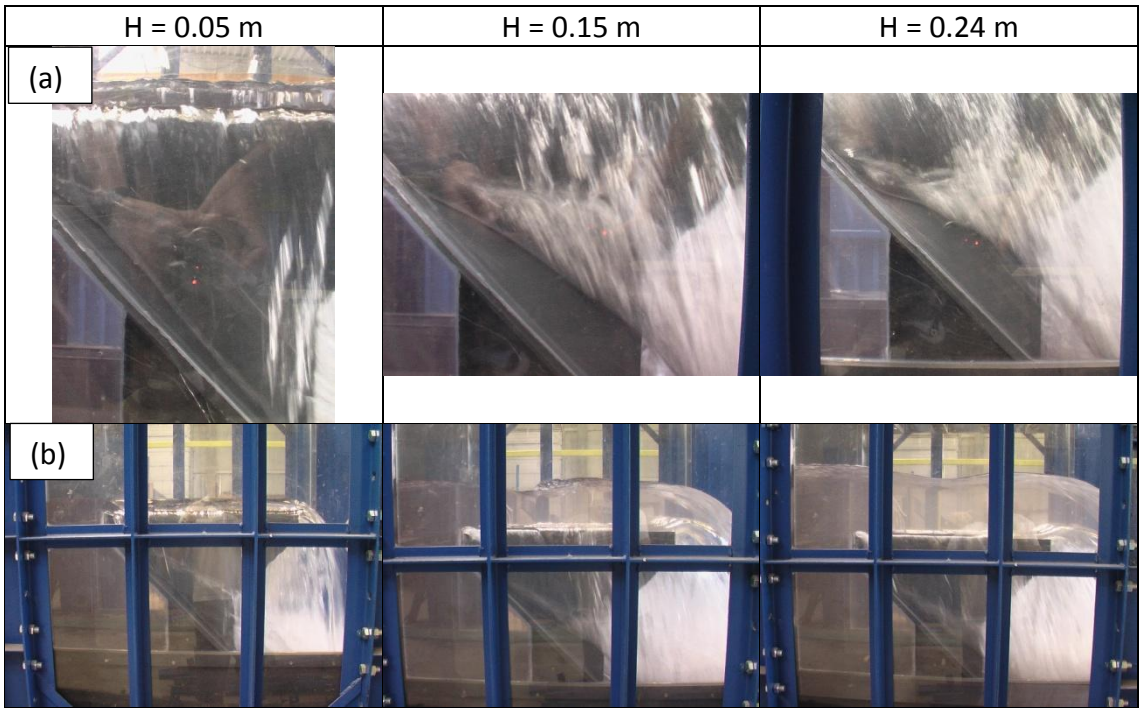

Figure VII-39 View of the outlet free surface variation with head for model 3: (a) – variant 1; (b) – variant 2

VII.4.2.6. Transverse profile on model 3

Regarding the transverse free surface profile (Figure VII-40), no influence of the weir height can be observed. The W_i/W_o ratio is sufficient to ensure that the side nappes interference zone is still under the crest level and so play no role on the PKW efficiency for low heads.

However, for the highest heads, the interference zone level increases to reach the crest level on both variants. This may be due, one more time, to smaller velocities along the inlet key, increasing the side crest efficiency and so the side nappe length. The transverse free surface profile becomes then near to horizontal.

Furthermore, the presence of parapet walls modifies the side nappe profile. The vertical extension, increasing the inlet cross section, increases moreover the nappe length and level, what increases even more the interference zone level for variant 2 than for variant 1. For H = 0.24 m and variant 2, the interference zone becomes thus higher than the inlet free surface level and seems slightly to perturb the inlet flow (Figure VII-41).

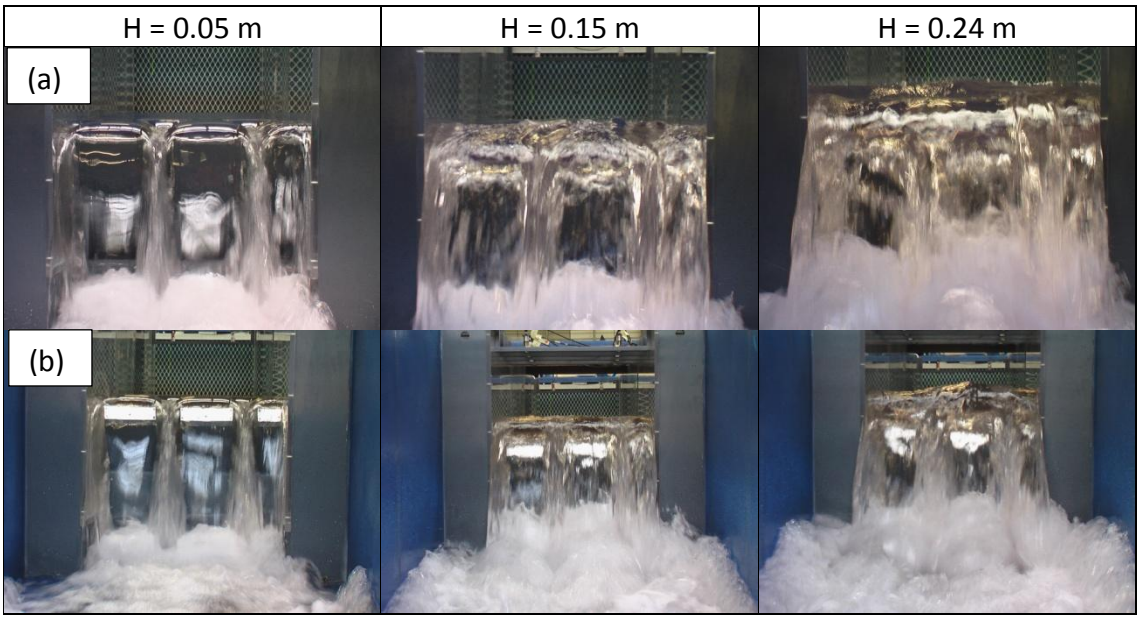

Figure VII-40 View of the transverse free surface variation with head for model 3: (a) – variant 1; (b) – variant 2

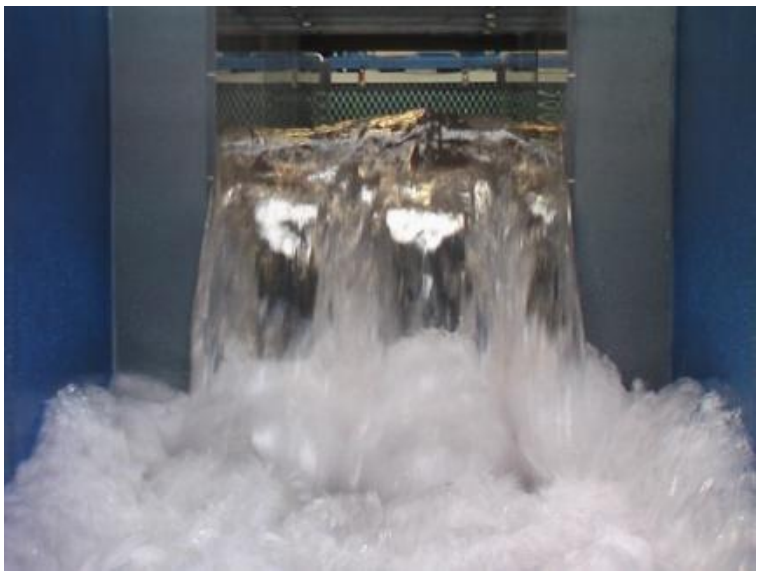

Figure VII-41 View of the transverse free surface variation for H = 0.24 m on variant 2 of model 3

VII.4.3. Analytical approach

The comparison of the present experimental results, obtained on 14 tested variants considering weir height and keys slope variations separately, with the analytical formulation developed in VII.3.3 is shown on Figure VII-42.

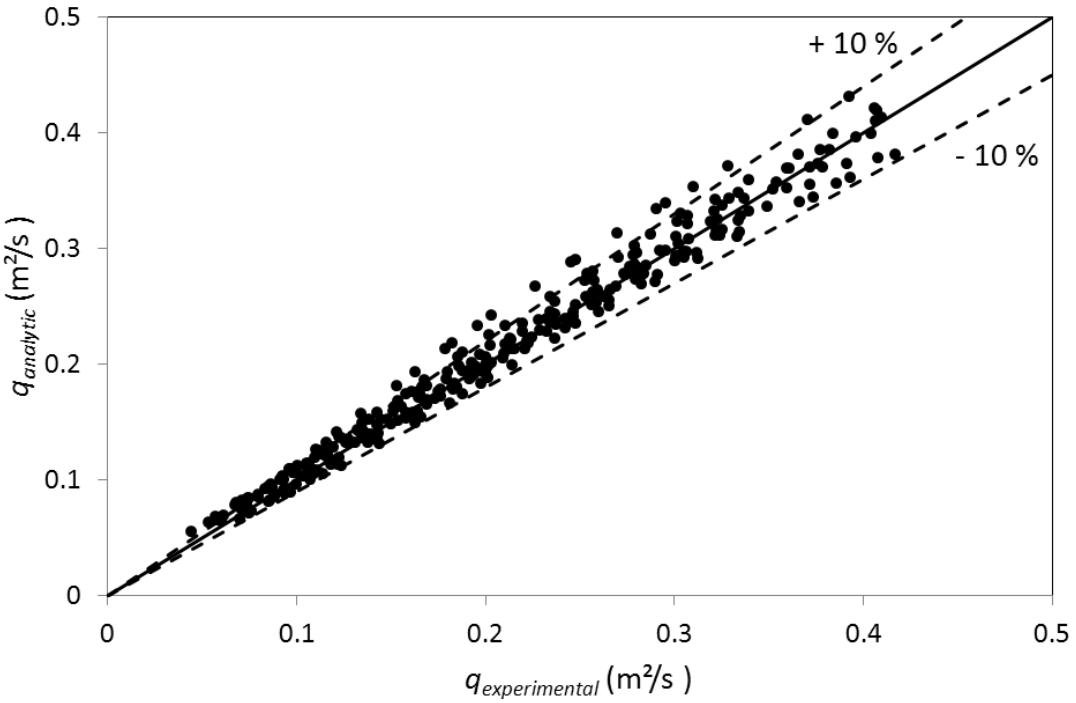

Figure VII-42 Comparison of experimental results and analytical formulation

It highlights the efficiency of the formulation (less than 10% error) for almost all tested geometries, whatever variations of L/W, W_i/W_o, P/W_u, S_i and S_o. Only the first variant of model 4 is less satisfactory approached by the formulation (errors until 17%). This highlights the influence of the very low value of the W_i/W_o ratio (0.67) on

the side crest efficiency, what is not taken into account by the analytical formulation. Further studies must help to confirm this influence (see VIII.4). However, different parametric studies have defined the optimal value of W_i/W_o between 1 and 1.5 regarding hydraulic, structural and economic aspects [61, 73, 94, 97].

VII.4.4. Design considerations

The results obtained from the 14 variants of PKW highlight the main importance of the weir height. When the vertical aspect ratio P/W_u decreases below its optimal value of 1.33, the efficiency of the weir decreases quickly (until 30% for P/W_u decreasing from 1.33 to 0.5). The keys slopes are of minor importance, only allowing a few percentage of discharge increase. A more important outlet key slope will be preferred, for low height geometries, as it increases the resilience capacity of the outlet key. For sufficiently high weir geometries, the definition of the optimal keys slopes must be balanced between the low gain in efficiency obtained with parapet walls, decreasing the inlet key slope, and the increase of the cost resulting of the complexity of the structure using parapet walls. Furthermore, the height of the parapet walls has to be limited to keep the interest of upstream overhang use, which limits the flow velocity at the inlet key entrance and so gives to the PKW a better discharge capacity than a labyrinth weir with same horizontal shape.

As the practical design of PKW is based on project constraints which most of the time impose the weir height (normal reservoir level, structural characteristics of the dam …), it is more convenient and cost effective to use standard PKW, without parapet walls. However, parapet walls provide a good opportunity for future PKW rehabilitations, enabling in some cases to increase the discharge of the initial PKW geometry by up to 20% by a limited increase of the maximal reservoir level. Parapet walls must thus be conserved and studied as safety works for future.

VII.5. Conclusion

The study of the 14 variants providing models with varying only the keys slope or the weir height enables to conclude to the main influence on the discharge capacity of the weir height compared to the keys slope influence.

The study of the 7 models, with varying weir height and keys slope, aims at defining varied optimal PKW heights function of the project interests. Regarding pure hydraulic, a P/W_u ratio of 1.33 is optimal. According to technico-economic interest, a P/W_u ratio close to 0.5 seems more relevant.

The study of the free surface profiles enables to explain the hydraulic interest in increasing the weir height until a limit.

For low weir height ($P/W_u < 0.5$), the discharge capacity of the PKW is mainly managed by the resilience capacity of the outlet key. The outlet free surface level

passes over the crest level along a non-negligible part of the side wall. That reduces significantly the side crest discharge.

For high weir height (P/W_u > 1.33), the discharge capacity of the PKW is only managed by the inlet key flow velocity. Indeed, the outlet flow stays supercritical for the studied upstream heads, and thus plays no role on the crest efficiency. As the inlet key cross section is then sufficient to provide negligible flow velocities the weir height doesn't more influence the discharge capacity.

For intermediate weir heights (0.5 < P/W_u < 1.33), the outlet flow behaviour depends of the upstream head. For low heads, the outlet key slope stays over the critical one and the PKW efficiency is mainly managed by the flow velocity along the inlet key, modifying the side crest efficiency. For high heads, the outlet key slope becomes lower than the critical one. The outlet resilience capacity manages then the upstream crest efficiency and a part of the side crest is submerged.

The exploitation of the Wolf1D-PKW solver enables to highlight the influence of the PKW height on the position of the control section on the inlet key. For high weir heights ($P/W_u \geq 1$), the control section is located on the downstream crest. For low weir heights ($P/W_u \leq 0.5$), the control section of the inlet key moves upstream to reach a maximum distance from the downstream crest for H/P ratio approximately equals to 1.5. Then, for increasing heads, the control section moves downstream. For intermediate weir heights (0.5 < P/W_u < 1), the studied heads are not sufficiently high to observe the maximum displacement of the control section along the inlet key.

Finally, based on the experimental results, an analytical formulation of the discharge capacity of PKW has been developed. It predicts all the experimental results with an accuracy of 10 %.

VIII. On the influence of the keys widths [85]

VIII.1. Introduction

As the results presented in VII have shown various optimal PKW heights regarding pure hydraulic or technico-economic considerations, the influence of the keys widths has been studied considering two PKW heights corresponding respectively to these two optima. For each weir height, models with varied ratio between inlet and outlet keys widths have been tested. Before these tests with a type A weir, the influence of the W_i/W_o ratio had been studied on PKW models with only upstream overhangs (type B), according to the available results from a former experimental study led at the University of Liège [53].

As the study of the type B PKW had been realized before the other experiments, the approach of the study differs a little from the one followed in VII, VIII.4 and IX. The influence of the keys widths is only studied based on the stage discharge curves. An analytical formulation stays proposed. However, it differs from the one developed based on the others parametric studies. Design advices are thus provided based on the analysis of the discharge efficiency and of the developed analytical formulation.

For the type A PKW with varying keys widths, the same approach as the one used for the study of the models with varying height has been followed (see VII). Experimental, analytical and numerical ways are explored based on the stage discharge and the free surface profiles measurements to finally provide design advices.

VIII.2. Experimental set-up

For the type B PKW, six geometries of PKW with varying keys widths (W_i/W_o = 0; 0.54; 0.82; 1.5; 2.33; ∞) has been tested on a single PKW-unit. The ratio between the total length of the crest and the width of all weirs is 6, and the only upstream overhang has a length equals to the half of the whole side crest length. Table VIII-1 and Figure VIII-1 give the values of the geometrical parameters of the six tested models.

Table VIII-1 – PKW type B models with varying keys widths dimensions

W	0.2 m
L	1.2 m
$P_i = P_o$	0.2 m
P_d	0.2 m
W_u	0.2 m
W_i	0; 0.065; 0.085; 0.115; 0.135; 0.2 m
W_o	0.2; 0.125; 0.105; 0.075; 0.055; 0 m
T_s	0.005 m
$T_i = T_o$	0 m
B	0.5 m
B_o	0.25 m
B_i	0 m

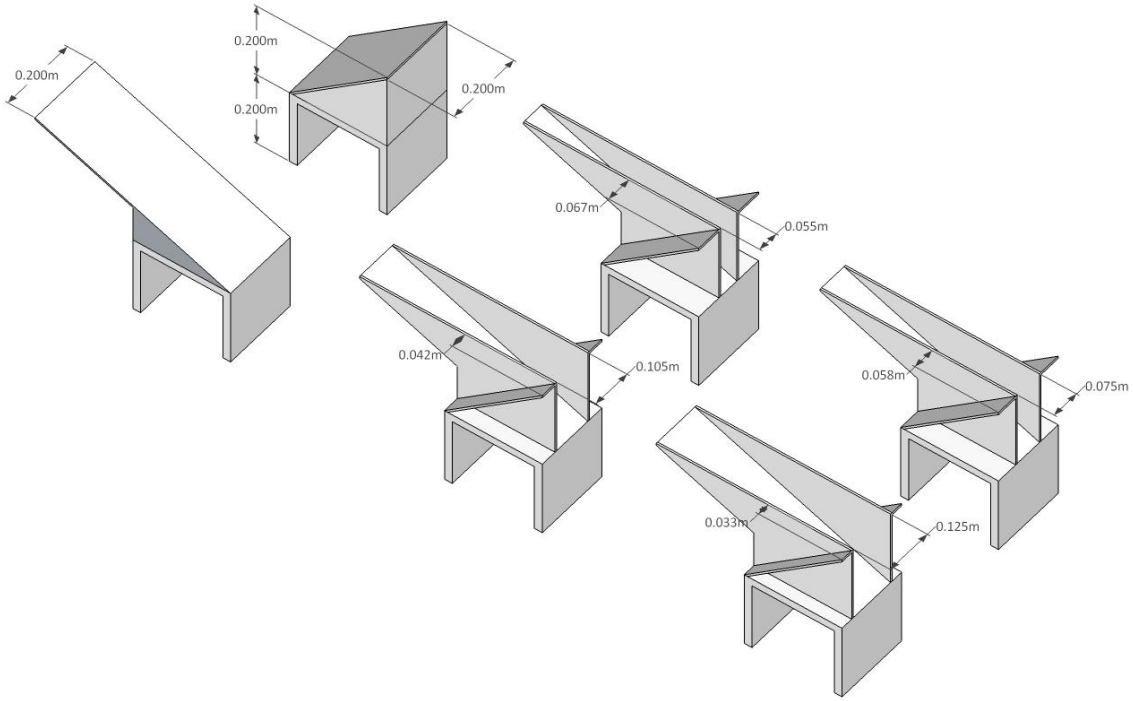

Figure VIII-1 Experimental layout of PKW type B models with varying keys widths

On the type A PKW, for the two weir heights (P/W_u = 1.33; 0.5) corresponding respectively to the hydraulic and a technico-economic optimum, seven models of PKW, with varied ratios between inlet and outlet keys widths (W_i/W_o = 0.5; 0.667; 0.796; 1; 1.256; 1.5; 2), have been tested. The ratio between the total length of the crest and the width is 5 for all weirs, and the two overhangs are symmetric (type A) with a length equal to the third of the whole side crest length. Table VIII-2 and Figure VIII-2 give the values of the geometrical parameters of the 14 tested models.

Table VIII-2 – PKW type A models with varying keys widths dimensions

	Hydraulic optimal height	Technico-economic optimal height
W	0.75 m	
L	3.75 m	
$P_i = P_o$	0.4 m	0.15 m
P_d	0.2 m	
W_u	0.3 m	
W_i	0.085; 0.105; 0.118; 0.135; 0.152; 0.165; 0.185 m	
W_o	0.185; 0.165; 0.152; 0.135; 0.118; 0.105; 0.085 m	
T_s	0.015 m	
$T_i = T_o$	0 m	
B	0.6 m	
$B_i = B_o$	0.2 m	

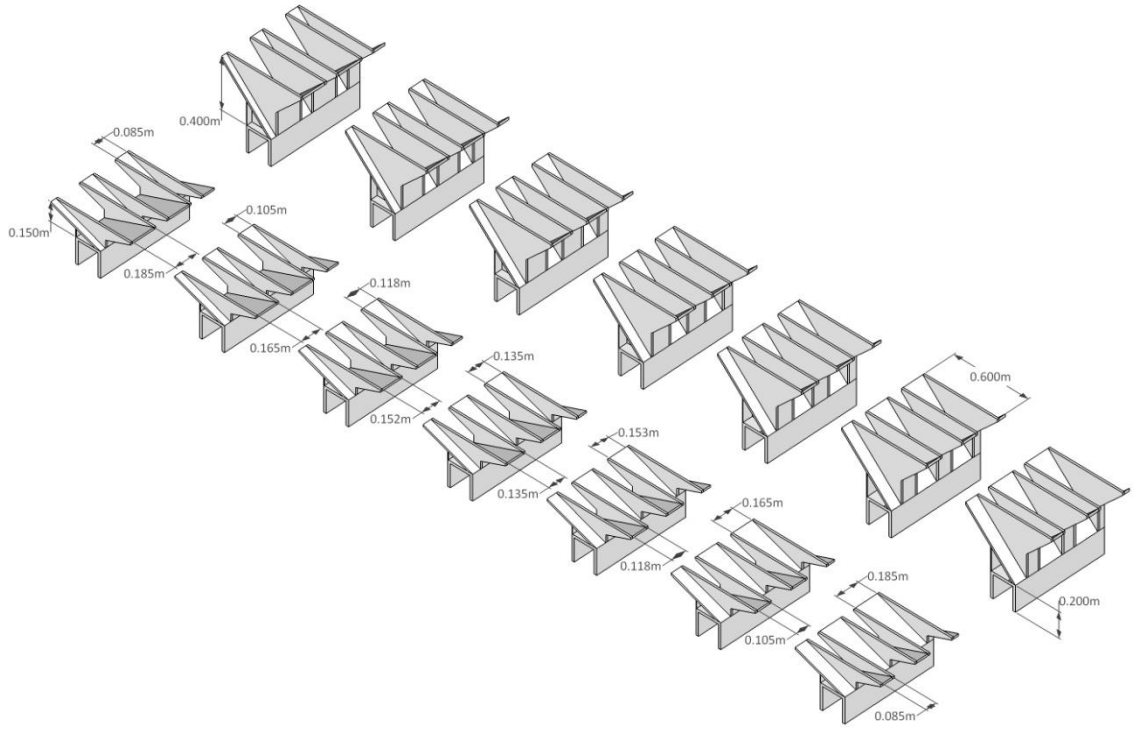

Figure VIII-2 Experimental layout of PKW type A models with varying keys widths

VIII.3. Influence of the inlet/outlet keys widths ratio for type B PKW [72, 73]

VIII.3.1. Head-discharge curve

For the six type B models, Figure VIII-3 shows the variation of the specific discharge q as a function of the upstream head H. The results obtained for W_i/W_o ratios varying between 0.54 and 1.5 are similar. However, a more precise observation allows distinguishing the optimal ratio function of the upstream head.

For low heads, the W_i/W_o ratio of 1.5 gives the best discharge capacity from the studied geometries. For higher heads, ratios of 0.82 and 0.54 become more relevant. As expected, an optimal W_i/W_o ratio exists. However, this optimal value varies with the upstream head.

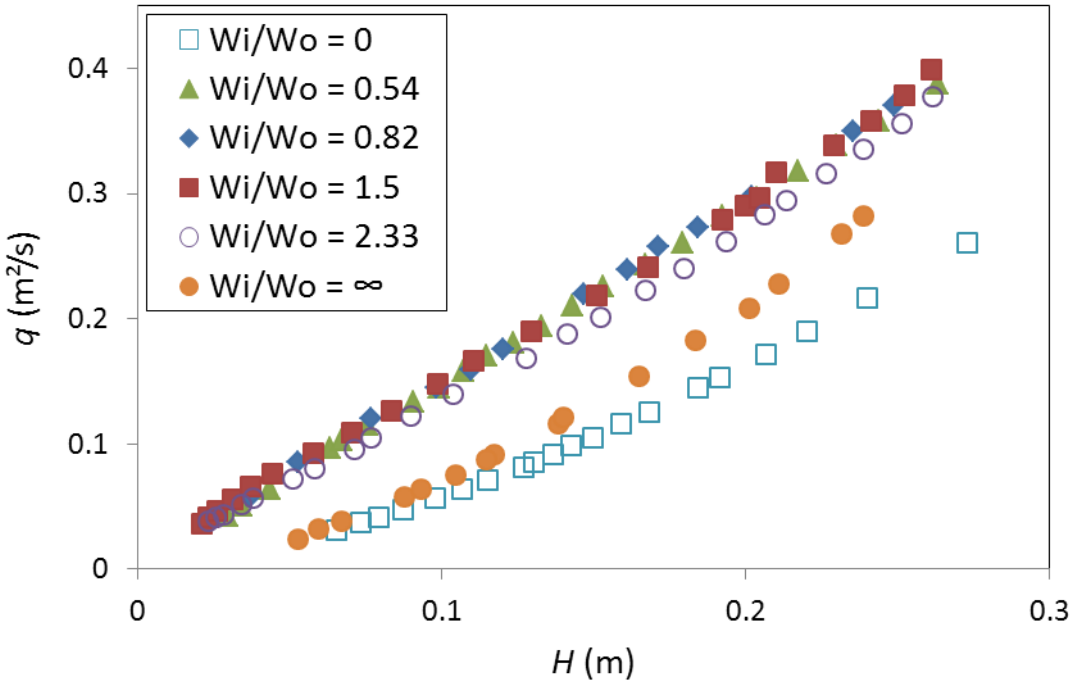

Figure VIII-3 Head/discharge curves of the PKW type B models

VIII.3.2. Analytical approach

To construct an analytical equation linking the discharge coefficient C_{dw} to the geometrical parameters of the PKW, a semi-empirical formulation has been developed on the basis of reasoning on the physics of the flow, before the setting of the parameters to the experimental results.

By separating the contributions of each upstream $C_{dw\,u}$, downstream $C_{dw\,d}$ and side $C_{dw\,s}$ part of the crest to the global discharge, a formulation of the global discharge coefficient C_{dw} has been proposed:

$$C_{dw} = C_{dw\,u} + C_{dw\,d} + C_{dw\,s} \qquad \text{VIII-1}$$

Introducing corrective factors to take into account interactions between these various parts of the crest, it gets a formulation which settings have been fitted on the basis of the experimental results.

The contribution of the upstream crest (Eq. VIII-2) is calculated based on the discharge coefficient determined on the case of the single outlet key (W_i/W_o = 0). The following three terms of the equation are introduced to take into account respectively the relative width of the outlet key, the lateral nappe contraction, as well as the variation of this contraction with the longitudinal flow velocity. The influence of the lateral contraction of the nappe is represented by the relative width of the outlet key quantifying the discharge passing over the upstream crest compared with the one passing over the side crest. As the importance of this contraction varies with the flow velocity, the last term will be depending on it. For a constant discharge coefficient this flow velocity is proportional to the root of the load *H*.

$$C_{dw\,u} = \underbrace{0.414}_{\text{Discharge coefficient}} \underbrace{\frac{W_o}{W_u}}_{\text{Relative width}} \underbrace{\frac{W_o}{W_u}}_{\text{Lateral flow contraction}} \underbrace{\frac{\left(\frac{H}{P}\right)^{0.5} + \frac{W_o}{W_u}}{\left(\frac{H}{P}\right)^{0.5} + 1}}_{\text{Variation of the lateral contraction with flow velocity}} \qquad \text{VIII-2}$$

As for the upstream crest, the contribution of the downstream crest (Eq. VIII-3) is calculated based on the discharge coefficient determined on the case of the single inlet key ($W_i/W_o = \infty$). These experimental results highlight that, in this case, the influence of the vertical contraction of the nappe due to the water head is not negligible. The second term of the equation takes into account the influence of the head upstream of the weir on the downstream discharge coefficient. The two other terms are introduced respectively to take into account the relative width of the inlet key and the variation of the head between upstream and downstream part of the key. This head variation is only depending on the upstream head and of the weir geometry.

$$C_{dw\,d} = \underbrace{0.476}_{\text{Discharge coefficient}} \underbrace{\left(1 + 0.125\left(\frac{H}{P}\right)^{1-0.373\,W_i/W_o\,^{-0.1}}\right)}_{\text{Vertical flow contraction}} \qquad \text{VIII-3}$$

$$\underbrace{\frac{W_i}{W_u}}_{\text{Relative width}} \underbrace{\left(\frac{H}{P}\right)^{-0.56\,W_i/W_o\,^{-0.1}}}_{\text{Variation of the head}}$$

Finally, the side crest contribution (Eq. VIII-4) is calculated based on the Dominguez formulation for side weirs considering the vertical nappe contraction due to the head [17]. As for the calculation of the downstream contribution, the third and fourth terms of the equation are introduced to take respectively into account the relative crest length and the head variation along the weir. As for the upstream contribution, the two last terms are introduced to take into account the lateral contraction of the nappe due to the interference between upstream and side flows.

$$C_{dw\,s} = \underbrace{0.985}_{\text{Discharge coefficient}} \underbrace{\left(0.4 + 0.272\left(\frac{H}{P}\right)^{0.451\,W_i/W_o\,^{-0.1}}\right)}_{\text{Vertical flow contraction}} \underbrace{\frac{B}{W_u}}_{\text{Relative width}} \qquad \text{VIII-4}$$

$$\underbrace{\left(\frac{H}{P}\right)^{-0.56\,W_i/W_o\,^{-0.1}}}_{\text{Variation of the head}} \underbrace{\frac{W_i}{2W_u}}_{\text{Lateral flow contraction}} \underbrace{\frac{\frac{W_o}{2W_u}}{\left(\frac{H}{P}\right)^{0.5} + 1}}_{\text{Variation of the lateral contraction with flow velocity}}$$

It is important to note that the study focused on the variation of the ratio of the keys widths. The parameters of the Eqs. VIII-2 to VIII-4 have been fitted based on the experimental data. They are thus only valid for a relative length L/W = 6, a vertical aspect ratio P/W_u = 1 and a single upstream overhang. For different conditions, the shape of the formulation would remain valid but should again be fitted.

Results of Eq. VIII-1 are in good agreement with the experimental results, as can be seen on the Figure VIII-4. The maximum relative error (Table VIII-3) between the discharges calculated by equations VIII-1 to VIII-4 and the ones measured on the six tested models is 11.4% for a specific discharge of 0.055 m²/s.

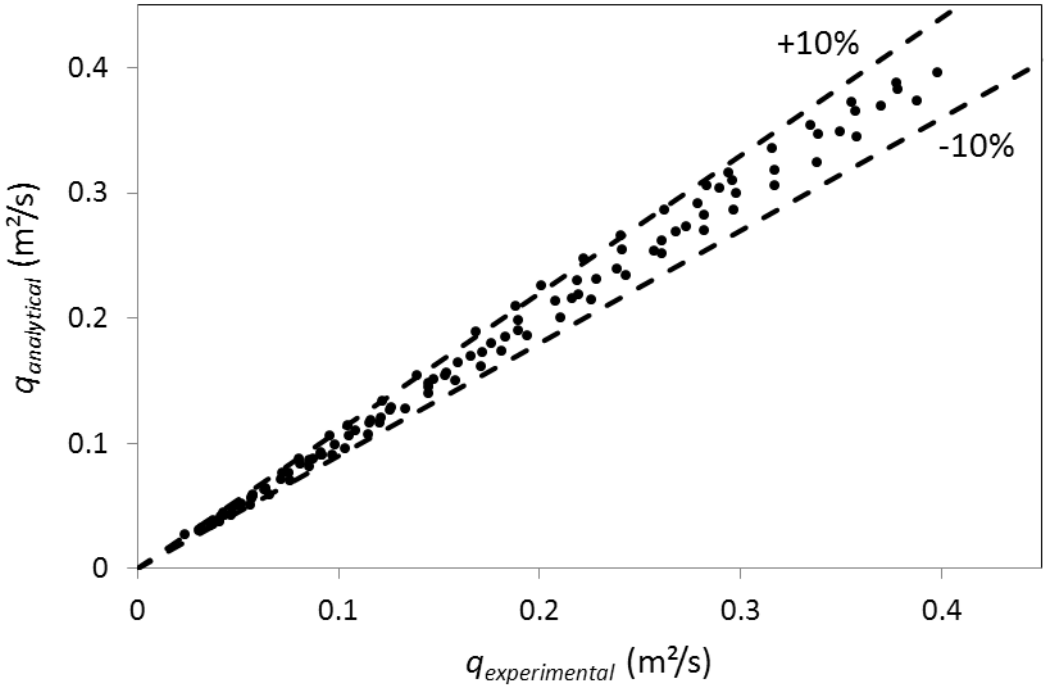

Figure VIII-4 Comparison of the specific discharges computed by Eqs. VIII-1 to VIII-4 and experimental results

Table VIII-3 – Maximal relative error between analytical and experimental C_{dw}

W_i/ W_o	Maximal relative error
0	2.1%
0.54	8.5%
0.82	5.5%
1.5	11.4%
2.33	11.1%
∞	2.6%

The derivation of Eq. VIII-1 enables to determine the optimal keys widths ratio as a function of the upstream head (Figure VIII-5). As expected, the optimal value of W_i/W_o varies with the head. It reaches a maximum around 1.4 for H/P near 0.5. For

$H/P < 0.5$, the optimal W_i/W_o ratio decreases with the upstream head. At contrary, for $H/P > 0.5$, the optimal W_i/W_o ratio decreases with increasing heads.

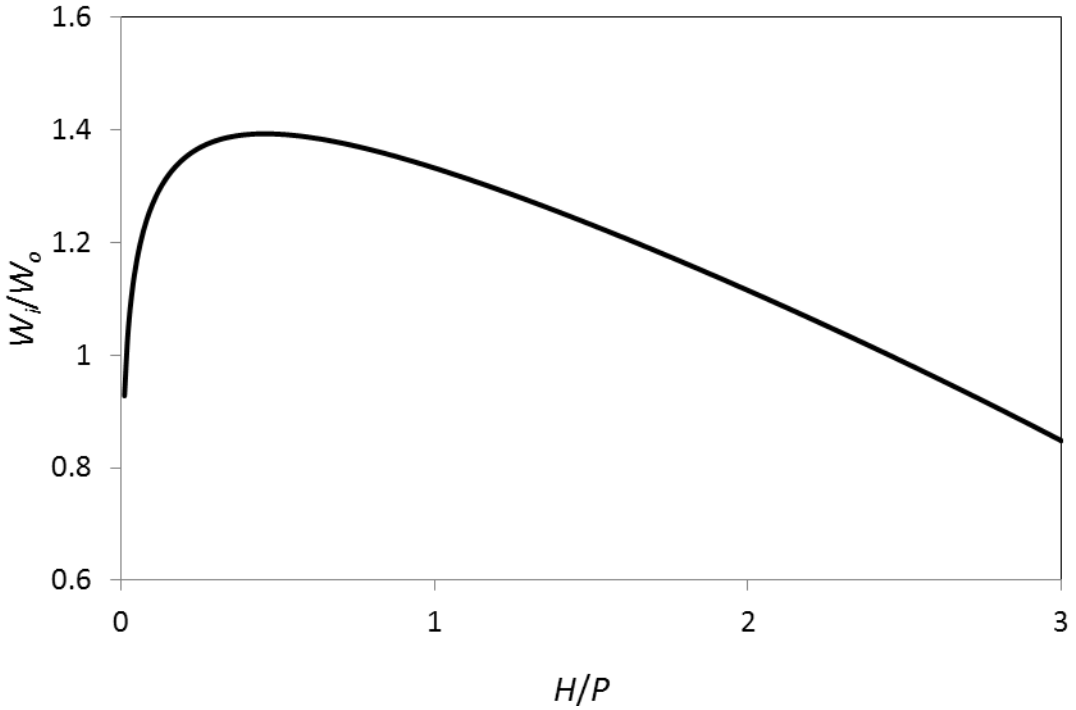

Figure VIII-5 W_i/W_o ratios for an optimal use of studied PKW depending on the adimensional head

VIII.3.3. Design considerations

The hydraulic optimal keys widths ratio W_i/W_o for type B PKW seems to be between 1.2 and 1.4 depending on the upstream head. However, varying this ratio between 0.54 and 1.5 modifies the PKW discharge capacity of only a few percents (Figure VIII-3). The interest in W_i/W_o ratio study for prototype designs is thus depending on the hydraulic knowledge of the weir emplacement as well as the economic interests of the project. For a PKW project on a dam for which designers are confident in the design discharge and head calculations, the study of the optimization of the keys widths ratio seems relevant. However, for projects with larger uncertainties on hydraulic data, the definition of the optimal W_i/W_o ratio is no more so easy and the cost of the study necessary to its determination may become higher than the real gain obtained on weir performances. For such projects, keeping the W_i/W_o ratio equal to 1 seems relevant as this favours the use of prefabricated elements.

VIII.4. Influence of the inlet/outlet keys widths ratio for PKW type A [83]

VIII.4.1. Head-discharge curve

As the basic structure of a PKW considers symmetric inlet and outlet keys, the influence of the variation of the W_i/W_o ratio on the type A PKW has been studied by comparison with the efficiency of the basic geometry considering a ratio $W_i/W_o = 1$.

VIII.4.1.1. Hydraulic optimal PKW height

Considering the optimal weir height for hydraulic considerations (Figure VIII-6), the model with $W_i/W_o = 2$ is upto 8% more efficient than the basic geometry for lowest heads. However, for high heads, it becomes less relevant, providing similar discharges than the basic geometry. For high heads, models with $W_i/W_o = 1.256$ and 1.5 are more efficient even if the gain in discharge is lower than 5% of the discharge provided by the basic geometry. For W_i/W_o ratios under 1, the discharge capacity of the weir decreases constantly compared with the basic geometry, whatever the ratio between head H and PKW-unit width W_u. A PKW with an outlet key which is 2 times larger than the inlet key is upto 18% less efficient than a basic symmetric geometry.

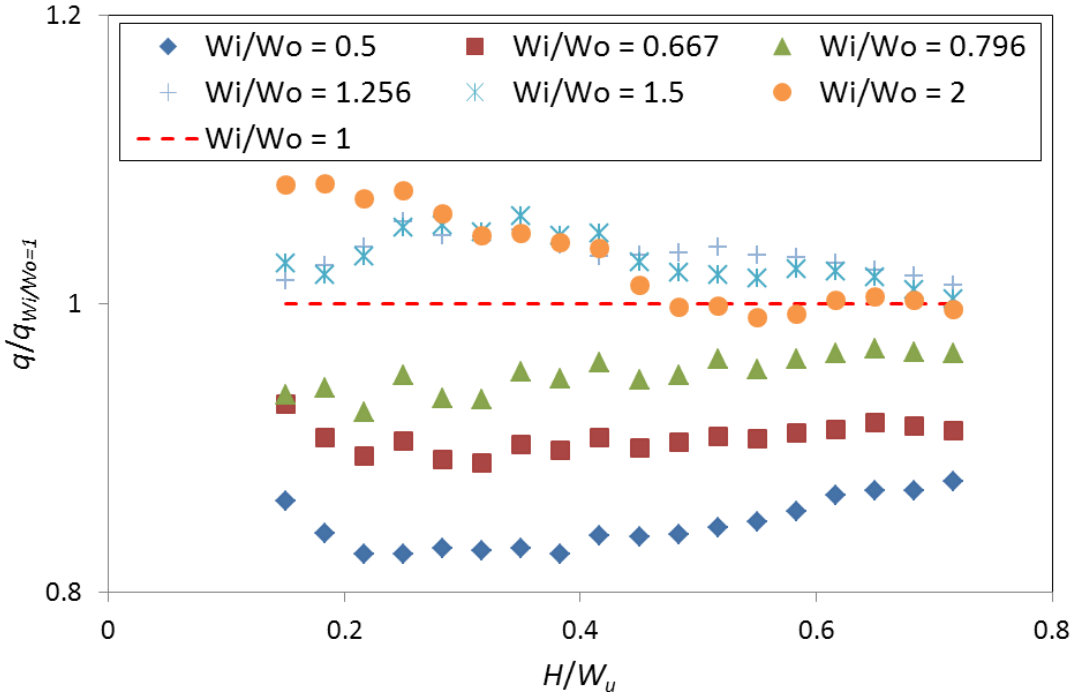

Figure VIII-6 Comparison of the specific discharges provided by PKWs with various W_i/W_o ratios considering the hydraulic optimal weir height

VIII.4.1.2. Technico-economic optimal PKW height

Considering the optimal weir height for technico-economic considerations (Figure VIII-7), the model with $W_i/W_o = 2$ is no more relevant. For low heads, it provides similar discharges than the basic geometry and for higher heads it becomes upto 3% less efficient. For low heads, models with $W_i/W_o = 1.256$ and 1.5 are more

efficient, delivering upto 6% more discharge than the basic geometry. For high heads, even if they remain more efficient than the basic geometry, the gain in discharge is lower than 1%. For W_i/W_o ratios under 1, the observed decrease in efficiency is in the same range as for models with hydraulic optimal height considering low heads. However, for high heads, this decrease becomes less important.

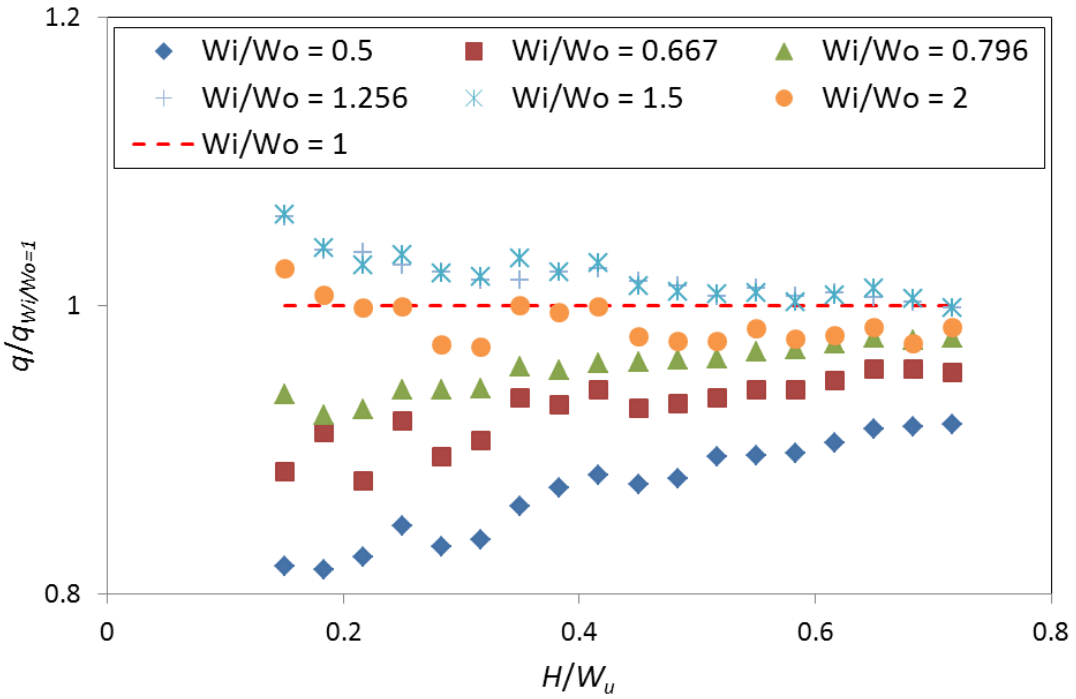

Figure VIII-7 Comparison of the specific discharges provided by PKWs with various W_i/W_o ratios considering a technico-economic optimal weir height

VIII.4.1.3. Relative influence of weir height and keys widths variations

It is important to keep in mind that the influence of the weir height stays of prime importance. The comparison of the specific discharges evacuated by the models considering a technico-economic ($q_{T\text{-}E}$) or a hydraulic (q_H) optimization of the weir height shows that the first ones are between 15 and 30% less efficient than the second ones (Figure VIII-8). This loss in efficiency is all the more important as the W_i/W_o ratio increases.

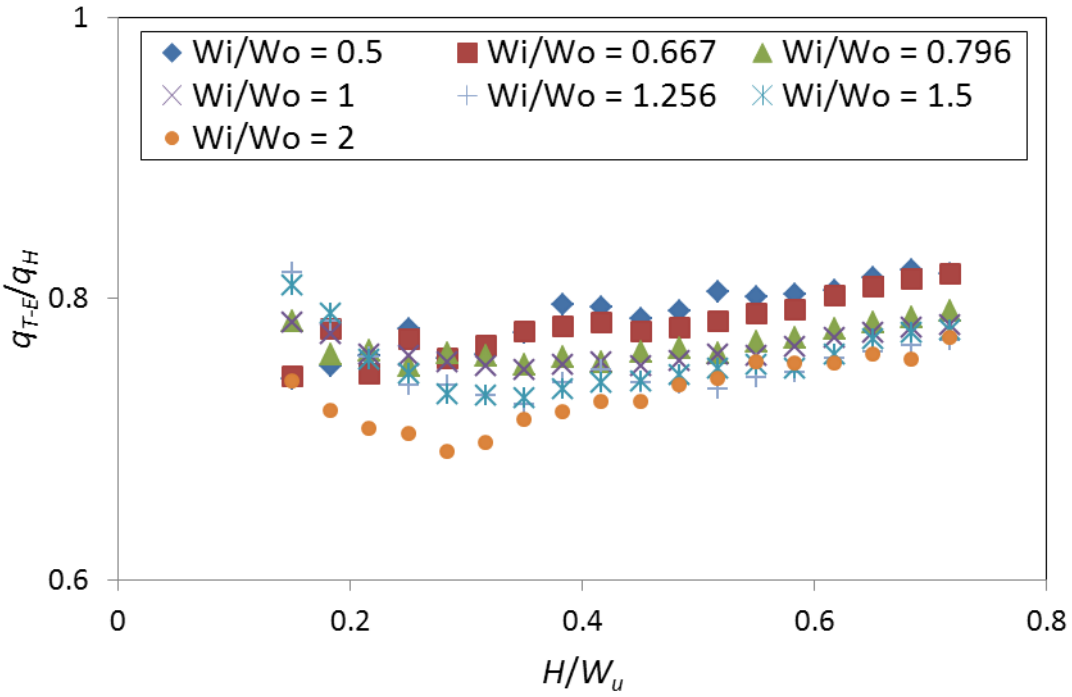

Figure VIII-8 Comparison of the specific discharges provided by PKWs with various W_i/W_o ratios considering a technico-economic or hydraulic optimal weir height

VIII.4.2. Free surface profile

VIII.4.2.1. Inlet key profile for hydraulic optimization of the weir height

Regarding the free surface profiles measured in the middle of the inlet key for the models with varying keys widths, the free surface level decreases from the upstream to the downstream ends of the key (Figure VIII-9 and Figure VIII-17). Considering negligible head losses along the key, this decrease traduces once again an increase of the flow velocity (see VII.3.2). For all the tested models, an important lowering of the free surface level is observed at the inlet key entrance, traducing the velocity increase induced by the flow contraction at this specific location. This free surface lowering is all the more important as the weir is higher and the inlet key width is smaller. For high heads and low inlet key widths this decrease provides too important free surface slopes to allow the measurements of the free surface elevation with the electronic probes. As shown before (see VII.3.2), the free surface behaviour downstream of the inlet key entrance is different considering the hydraulic optimal height of the PKW (Figure VIII-9) or a technico-economic one (Figure VIII-17).

Considering the hydraulic optimization of the weir height (Figure VIII-9), a small increase of the free surface level is observed from the inlet key entrance before a quasi-horizontal free surface to its downstream. This increase may correspond to the flow velocity decrease after the passage of the recirculation zones, observed on the 1:10 scale model (see IV.6). As long as the energy is considered constant along the side crest [44] (see V.7), the quasi-horizontal free surface traduces a constant flow velocity

along the inlet key. However, this flow velocity is all the more important as the inlet key width is smaller, lowering the free surface level from one model to another.

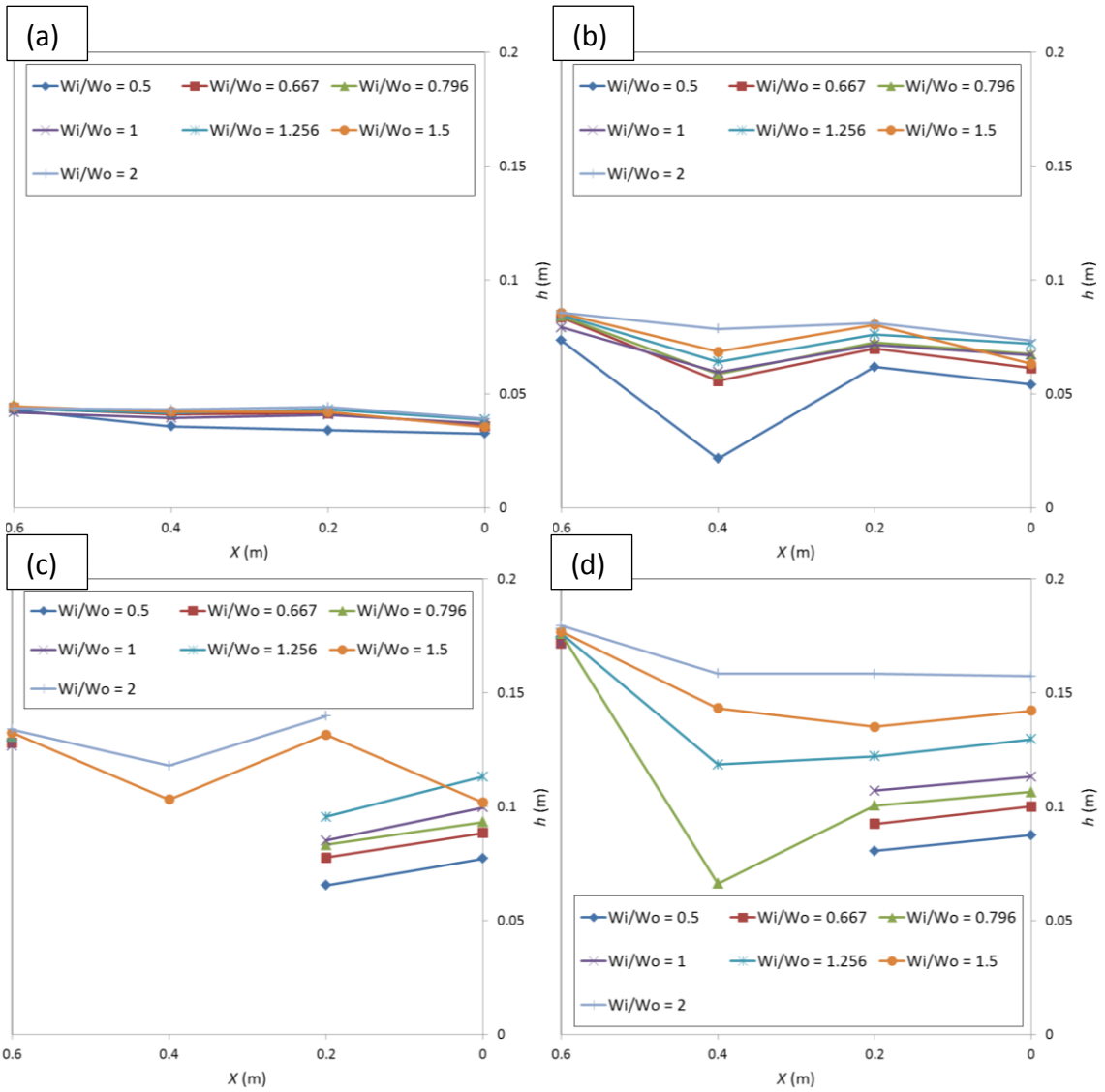

Figure VIII-9 Free surface profiles in the middle of the inlet key for hydraulic optimal PKW height: (a) H = 0.05 m; (b) H = 0.1 m; (c) H = 0.155 m; (d) H = 0.21 m

The observation of the inlet free surface profiles (Figure VIII-11) confirms the measurements, showing an important decrease of the free surface level at the inlet key entrance, due to the flow contraction and the consequent velocity increase. This decrease is all the more important as the inlet key width decreases (Figure VIII-10). On the downstream part of the key, the free surface profiles become quasi-horizontal, traducing no velocity variation along the key.

For W_i/W_o < 1, the combined influence of the velocity increase and the free surface lowering is directly highlighted on the PKW stage-discharge curve, as it decreases the side crest efficiency (Figure VIII-12). For W_i/W_o ≥ 1, the stage-discharge curves are not significantly modified, even if the varied free surface levels traduce

variations of the inlet key flow velocity. That may highlight the negligible influence of this lower velocity on the side crest efficiency.

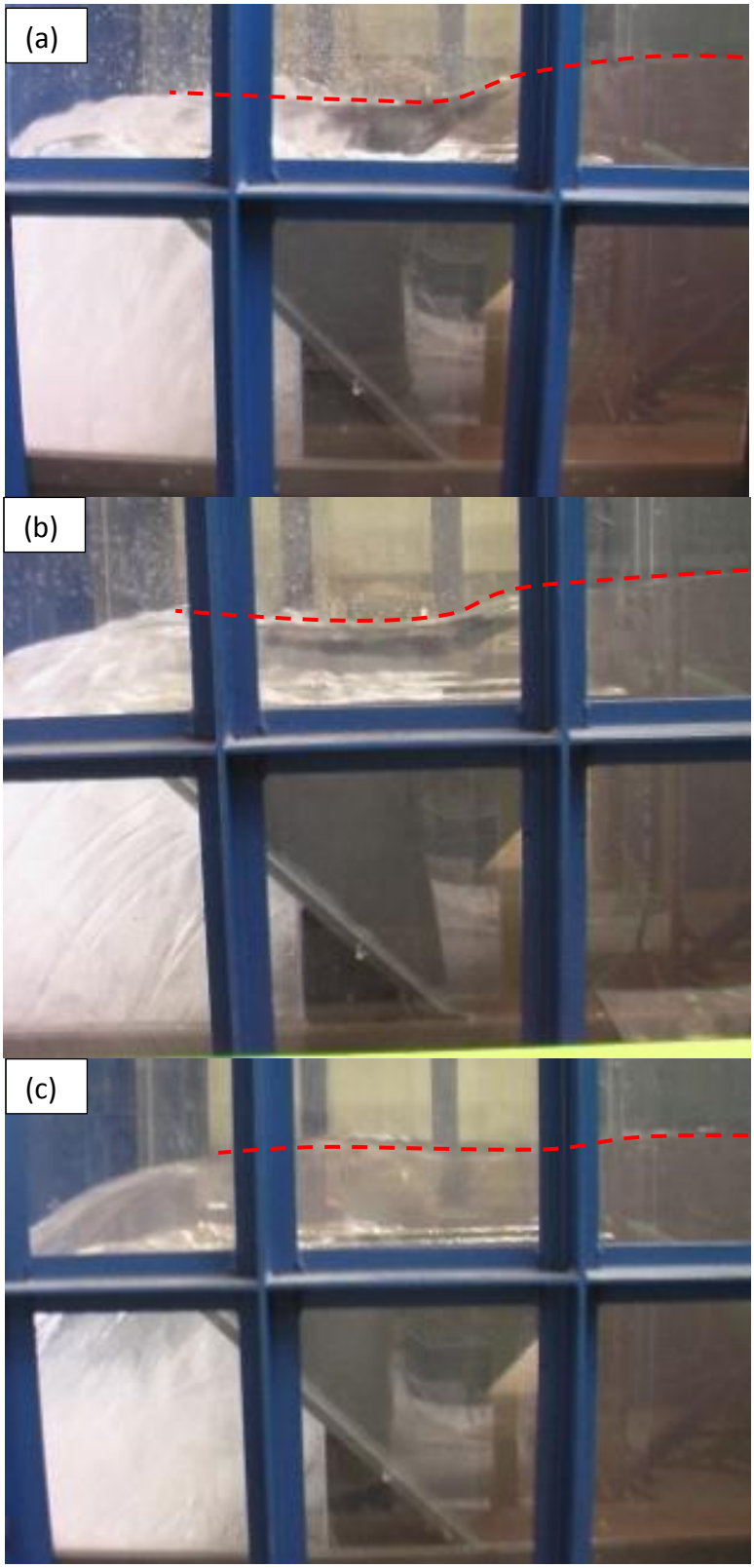

Figure VIII-10 View of the inlet free surface variation for hydraulic optimal weir height and H = 0.155 m: W_i/W_o = (a) – 0.5; (b) – 1; (c) – 2

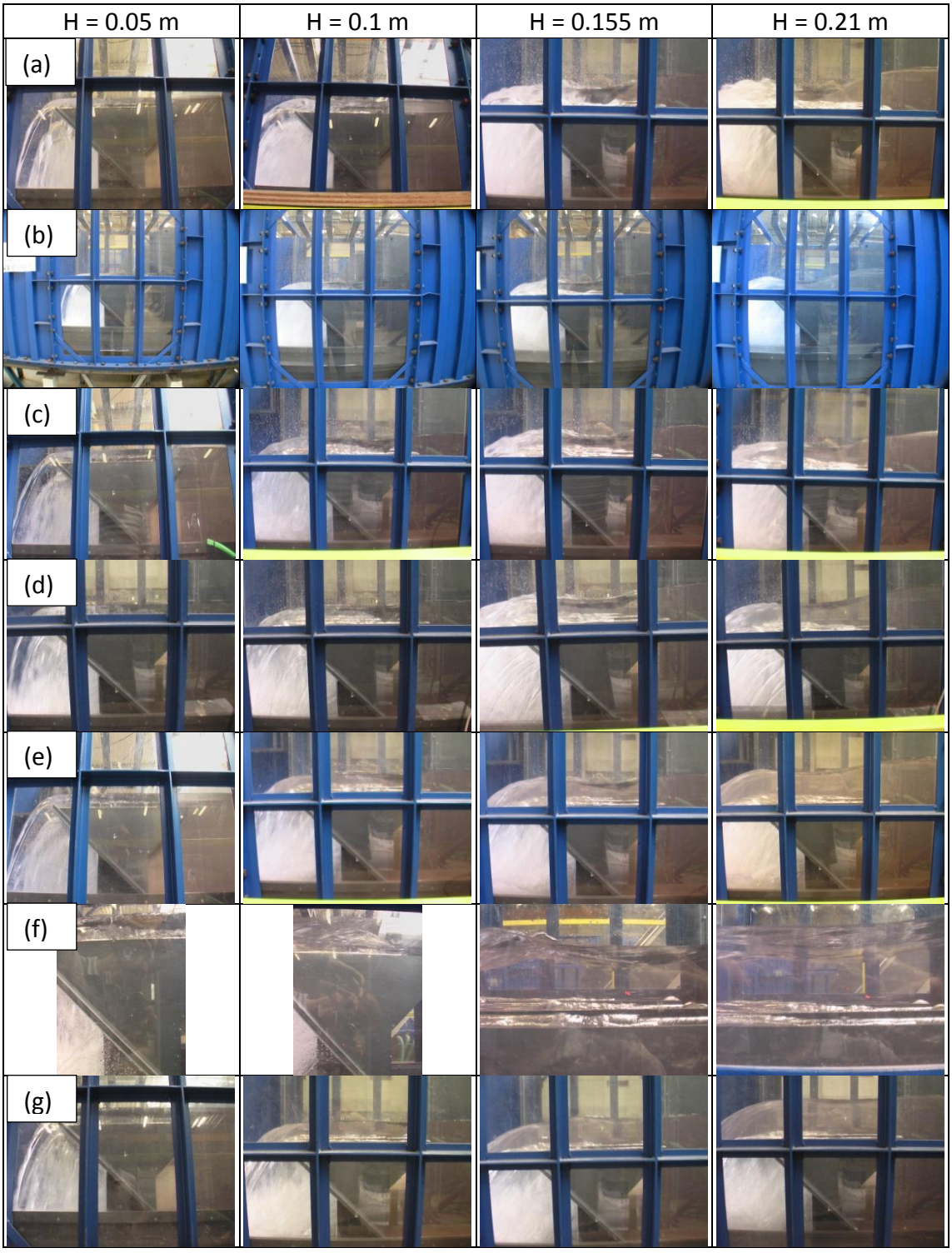

Figure VIII-11 View of the inlet free surface variation with head for hydraulic optimal weir height: W_i/W_o = (a) – 0.5; (b) – 0.667; (c) – 0.796; (d) – 1; (e) – 1.256; (f) – 1.5; (g) – 2

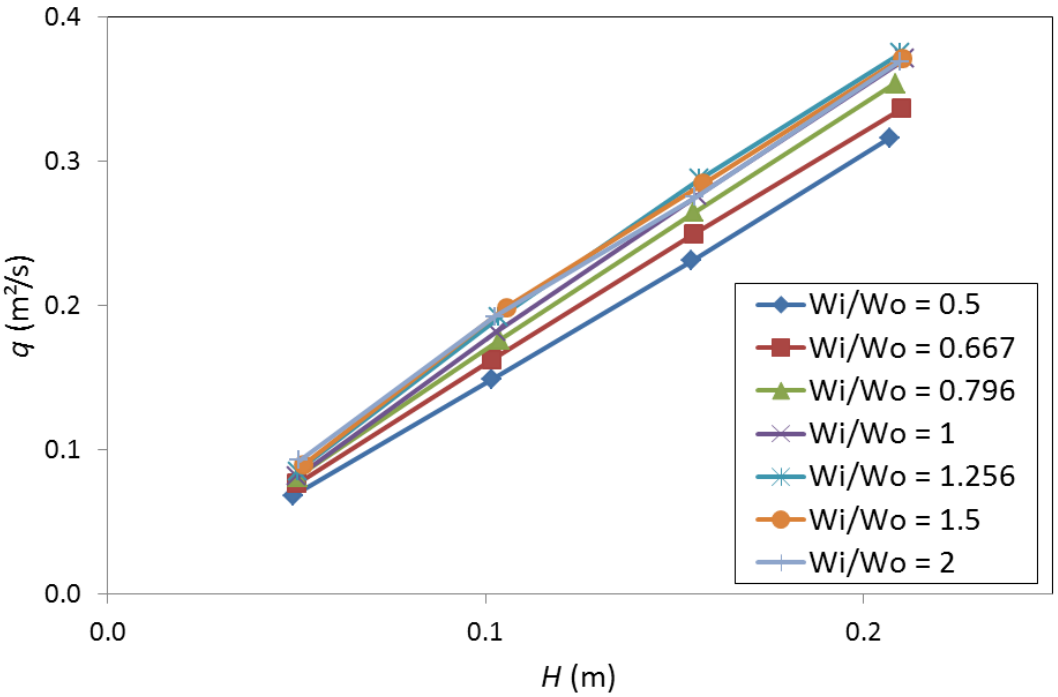

Figure VIII-12 Stage-discharge curves of the tested models with hydraulic optimal PKW height

VIII.4.2.2. Outlet key profile for hydraulic optimization of the weir height

The observation of the free surface profiles along the outlet key (Figure VIII-14) highlights supercritical flows whatever the outlet key width. The outlet flow plays no role on the upstream or side crest efficiency and is thus unable to explain the non-variation of the PKW efficiency whatever the modification of the inlet key flow behaviour for W_i/W_o higher than 1 (Figure VIII-13).

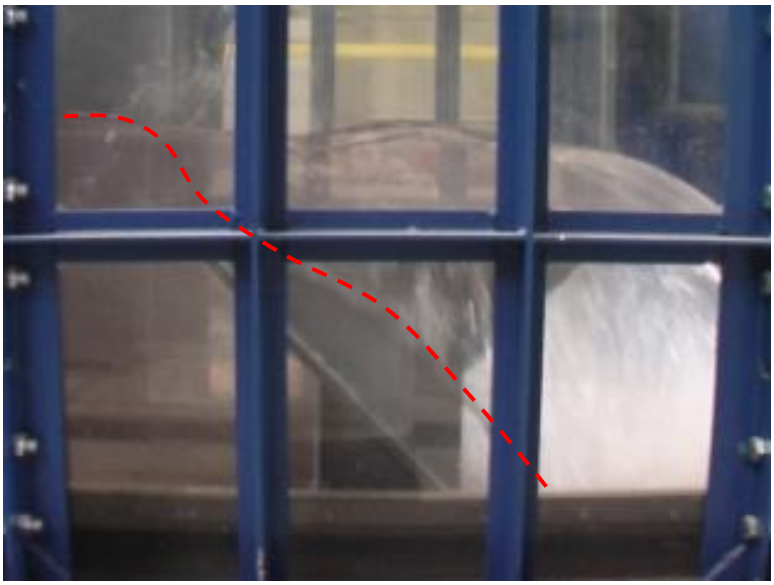

Figure VIII-13 View of the outlet free surface profile for hydraulic optimal weir height: H = 0.21 m; W_i/W_o = 2

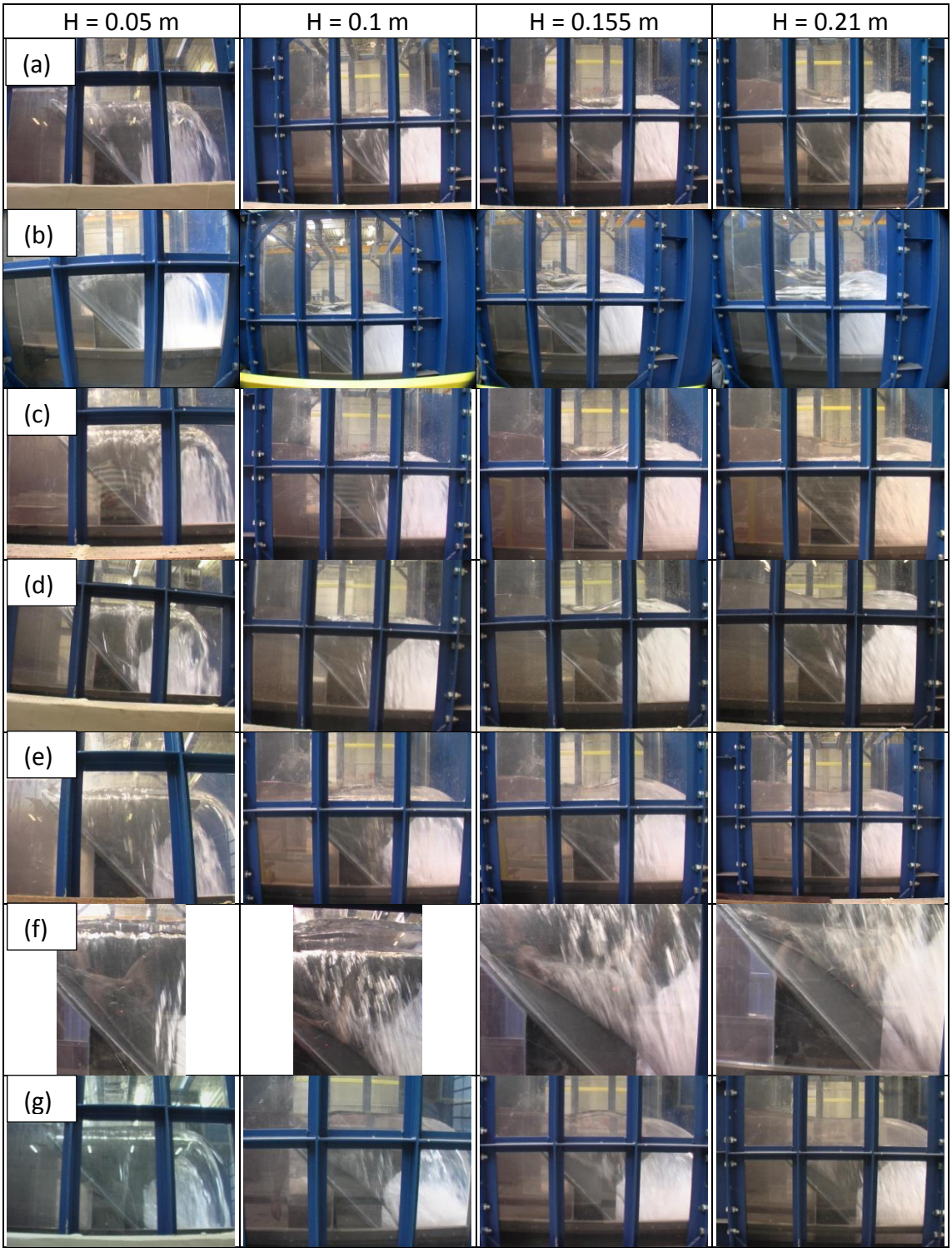

Figure VIII-14 View of the outlet free surface variation with head for hydraulic optimal weir height: W_i/W_o = (a) – 0.5; (b) – 0.667; (c) – 0.796; (d) – 1; (e) – 1.256; (f) – 1.5; (g) – 2

VIII.4.2.3. Transverse profile for hydraulic optimization of the weir height

Regarding the transverse free surface profiles for varied W_i/W_o ratios (Figure VIII-15), the nappe over the side crest seems less aerated for $W_i/W_o \geq 1$ (no more white water - Figure VIII-16), even if the outlet key slope is sufficient to avoid side crest submergence. This is induced by the interference zone between the nappes coming

from opposite side crests. Reducing the outlet key width, this interference zone moves upstream the crest level, what reduces more and more the side crest discharge capacity.

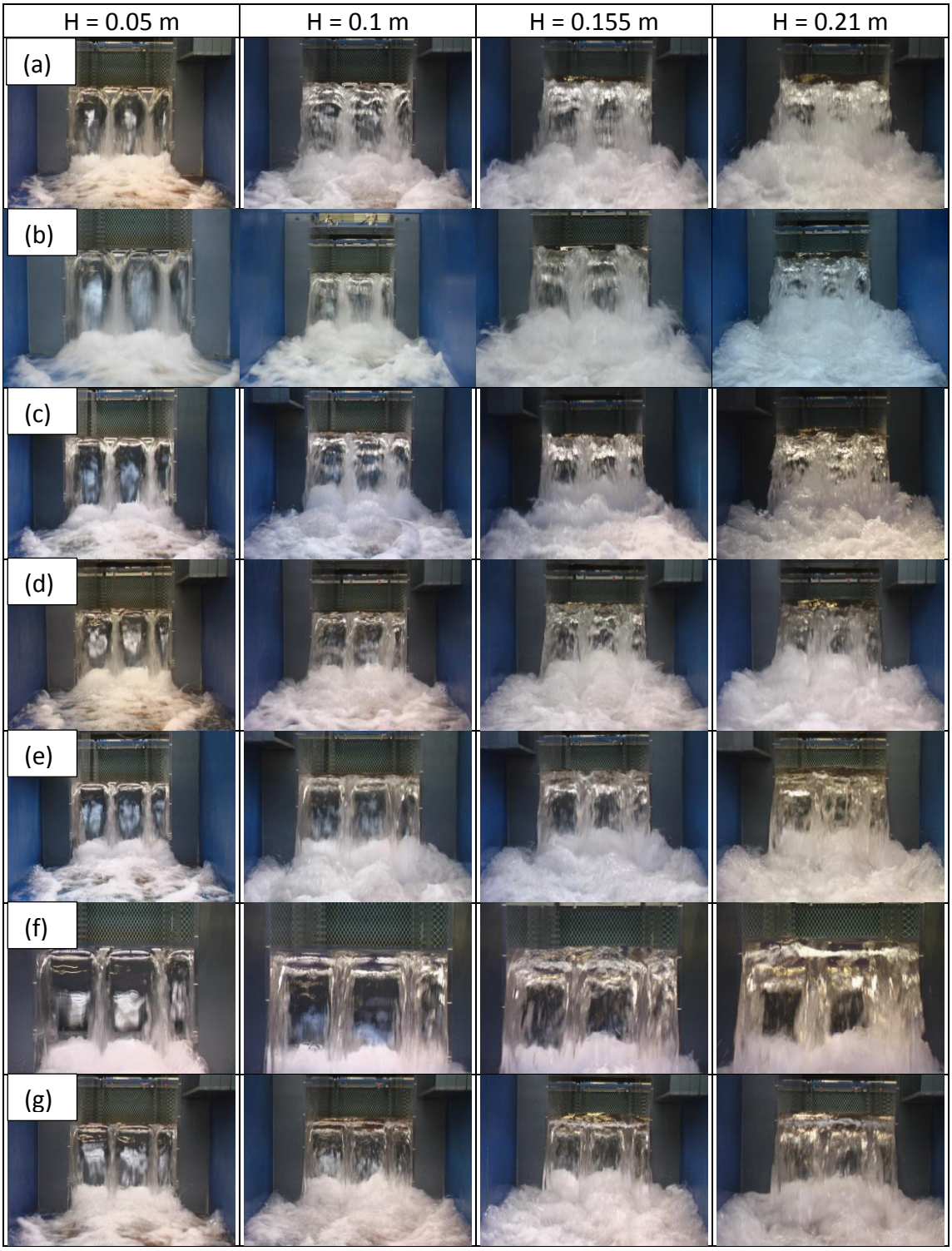

Figure VIII-15 View of the transverse free surface variation with head for hydraulic optimal weir height: W_i/W_o = (a) – 0.5; (b) – 0.667; (c) – 0.796; (d) – 1; (e) – 1.256; (f) – 1.5; (g) – 2

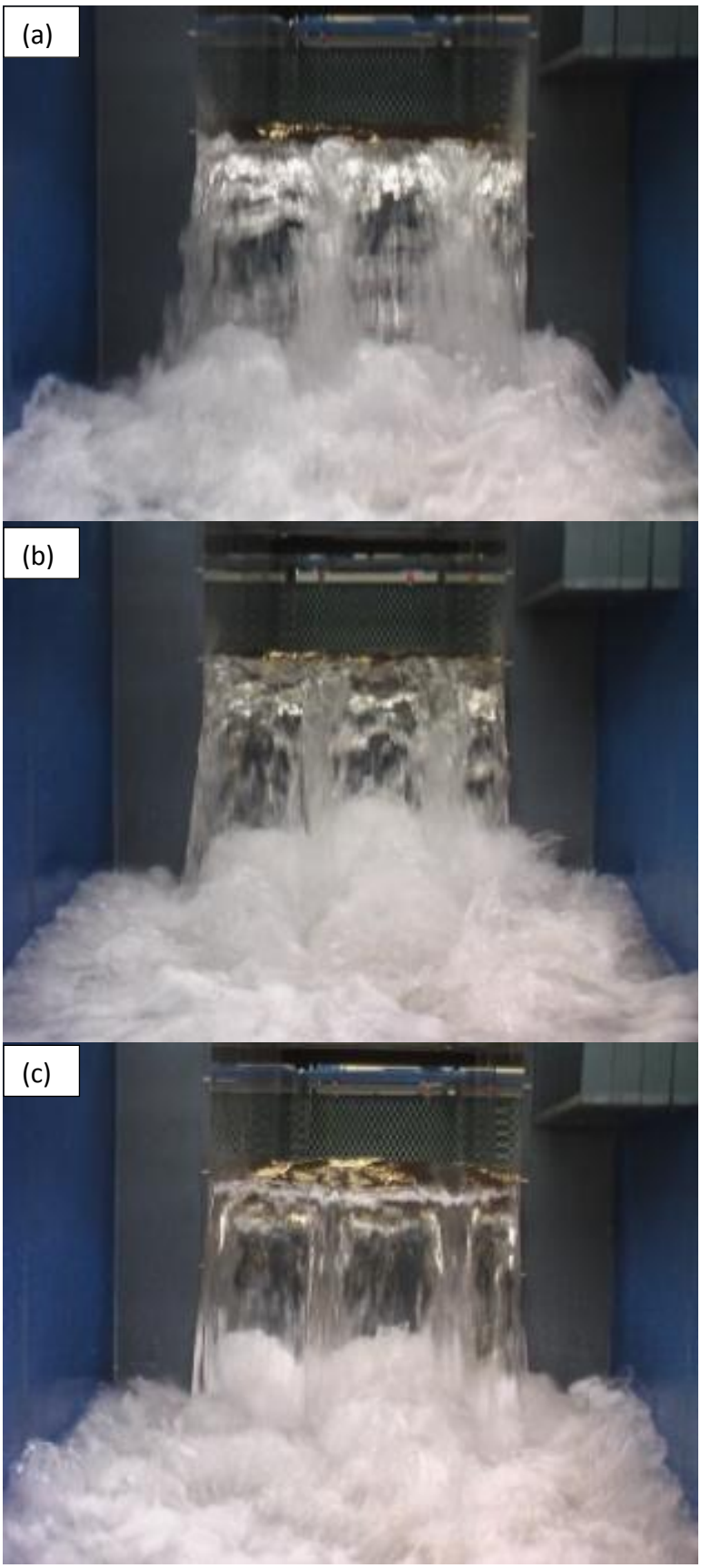

Figure VIII-16 View of the transverse free surface variation for hydraulic optimal weir height and H = 0.155 m: W_i/W_o = (a) – 0.5; (b) –1; (c) – 2

For W_i/W_o until 1.5, the increase in side crest efficiency due to lower flow velocities and higher free surface level along the inlet key stays more important than the decrease created by the interference between opposite nappes. The PKW discharge capacity increases with the W_i/W_o ratio. For W_i/W_o ratios increasing over 1.5, the nappes interference becomes of main importance and the PKW discharge capacity decreases.

VIII.4.2.4. Inlet key profile for technico-economic optimization of the PKW height

Considering a technico-economic optimization of the weir height, a constant decrease of the measured free surface level is observed from the inlet key entrance to its downstream (Figure VIII-17). This decrease is all the more important as the inlet key width is smaller, traducing higher velocities. For smallest inlet key widths, the decrease provides one more time too important free surface slope to allows a correct free surface measurement.

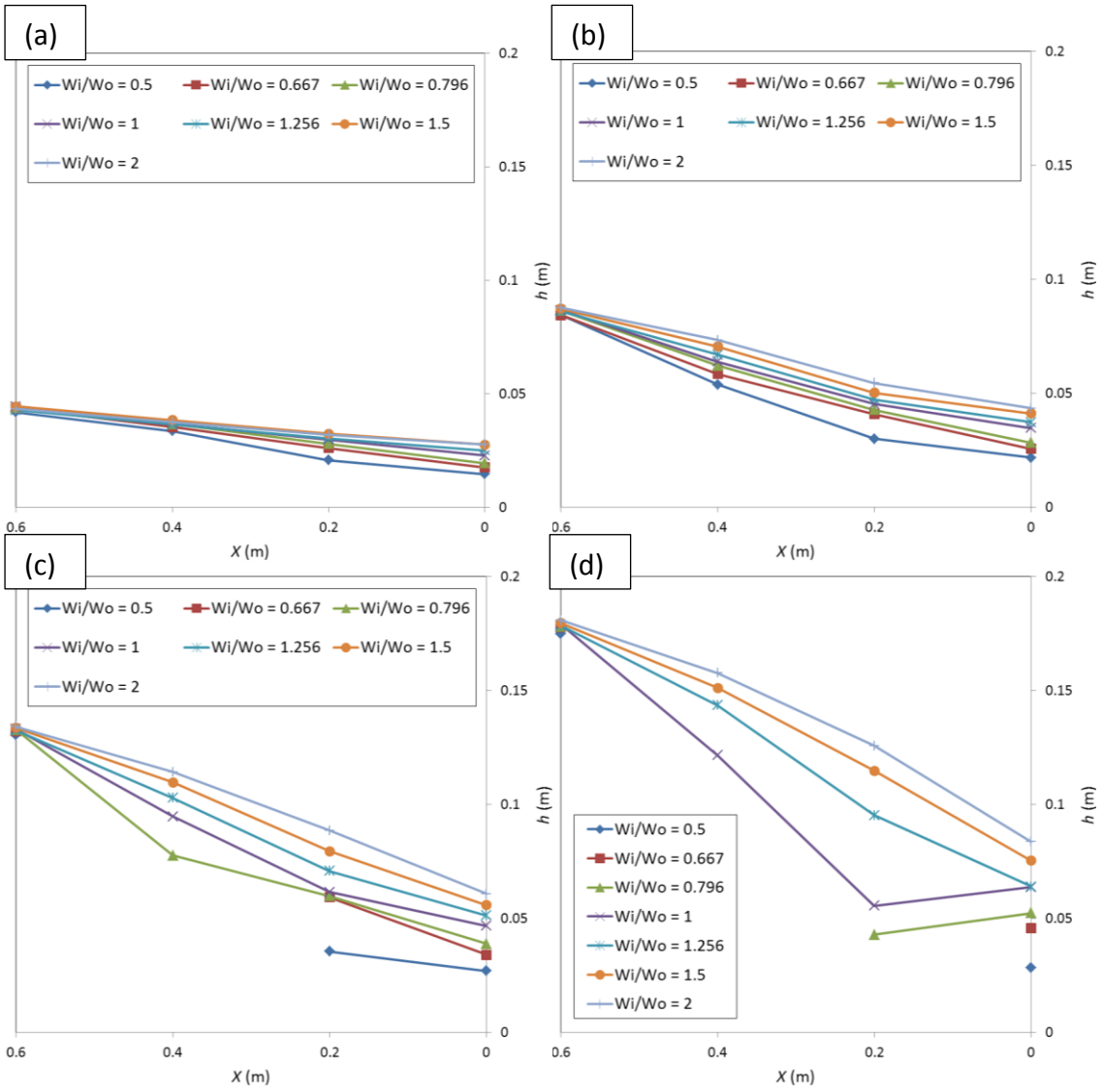

Figure VIII-17 Free surface profiles in the middle of the inlet key for technico-economic optimal PKW height: H = (a) 0.05 m; (b) 0.1 m; (c) 0.155 m; (d) 0.21 m

The observation of the free surface profiles along the inlet key (Figure VIII-18) confirms the measured flow characteristics.

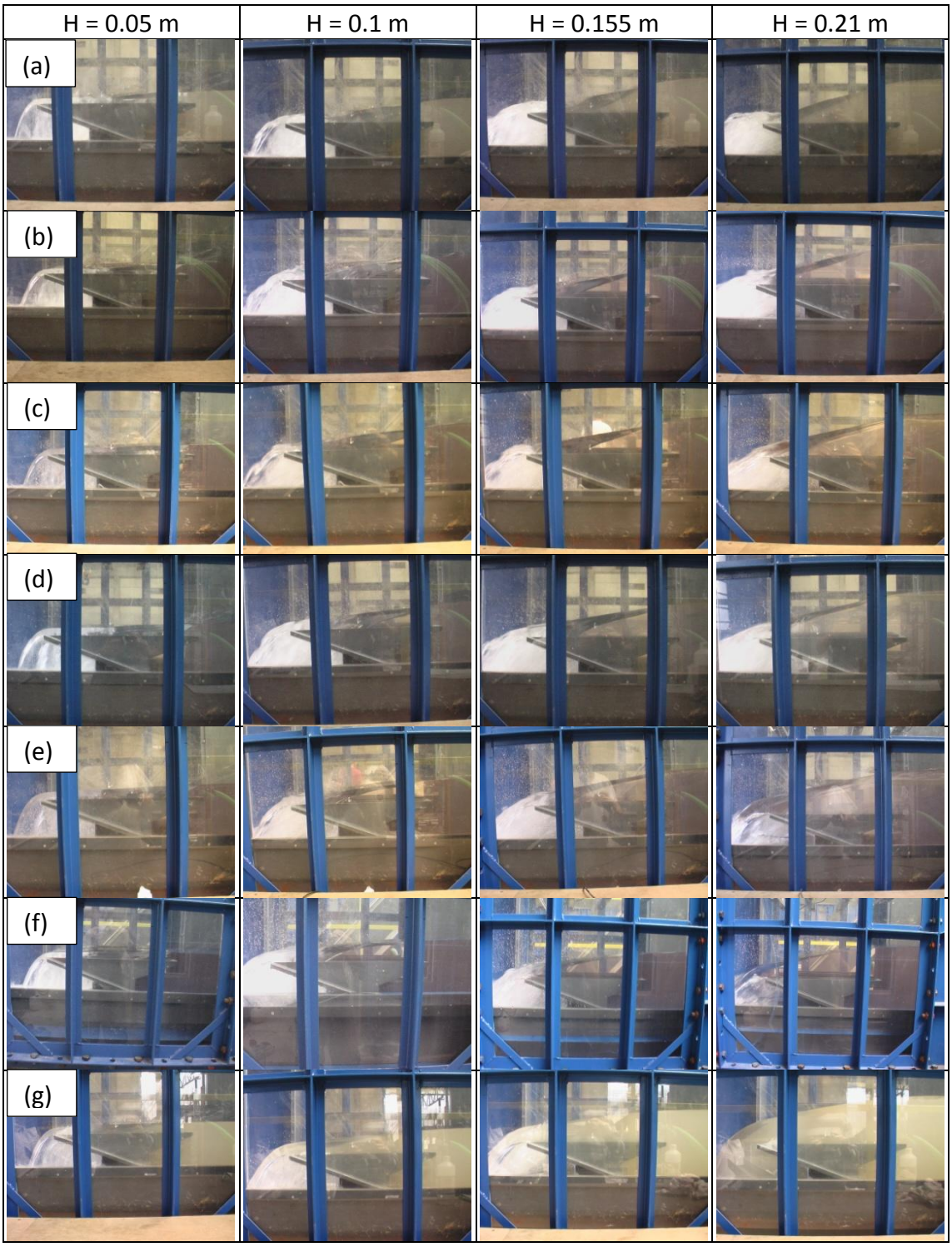

Figure VIII-18 View of the inlet free surface variation with head for technico-economic optimal weir height: W_i/W_o = (a) – 0.5; (b) – 0.667; (c) – 0.796; (d) – 1; (e) – 1.256; (f) – 1.5; (g) – 2

The free surface level decreases continuously from the inlet key entrance to its downstream apex. The slope of the free surface is all the more important as the inlet key width decreases.

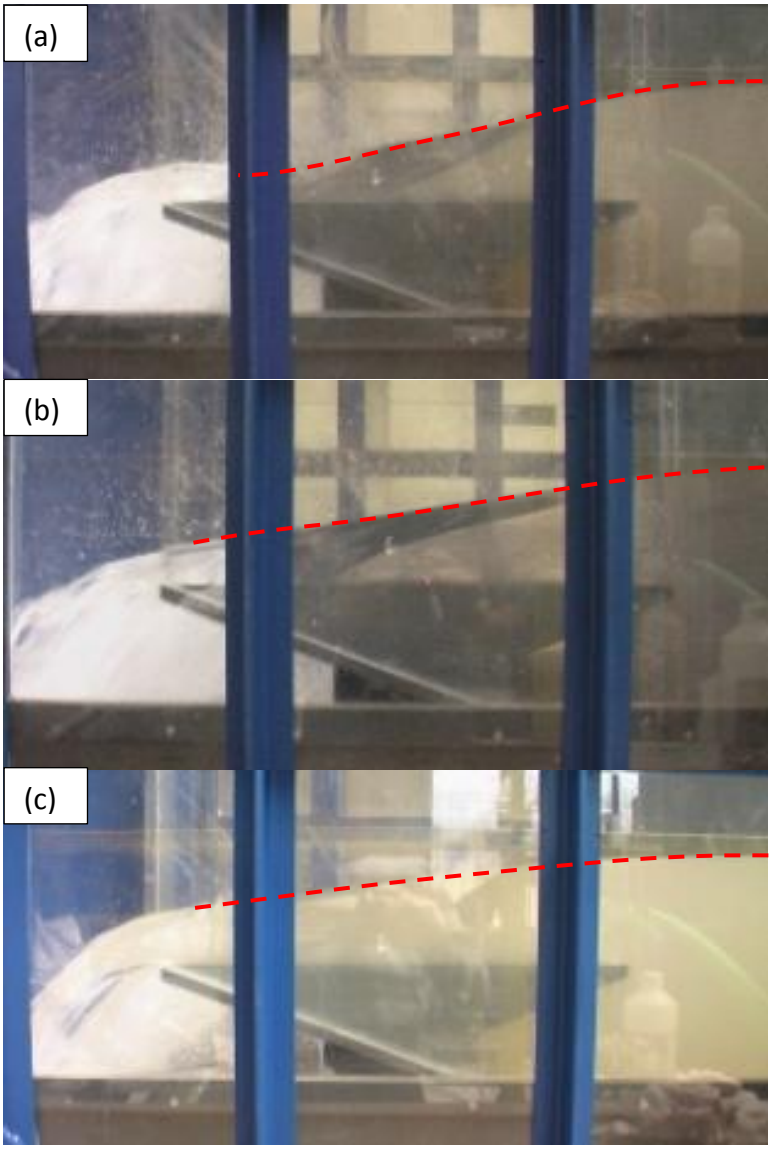

Figure VIII-19 View of the inlet free surface variation for technico-economic optimal weir height and H = 0.155 m: W_i/W_o = (a) – 0.5; (b) –1; (c) – 2

For $W_i/W_o < 1$, the higher longitudinal velocities and the correspondent lowering of the free surface level decrease the side crest efficiency and so the PKW discharge (Figure VIII-20). For $W_i/W_o \geq 1$, even if the free surface level increases for increasing W_i/W_o ratio, traducing lower inlet key velocities, the stage discharge curve doesn't change significantly. The flow velocity along the inlet key seems thus to have no influence on the side crest efficiency.

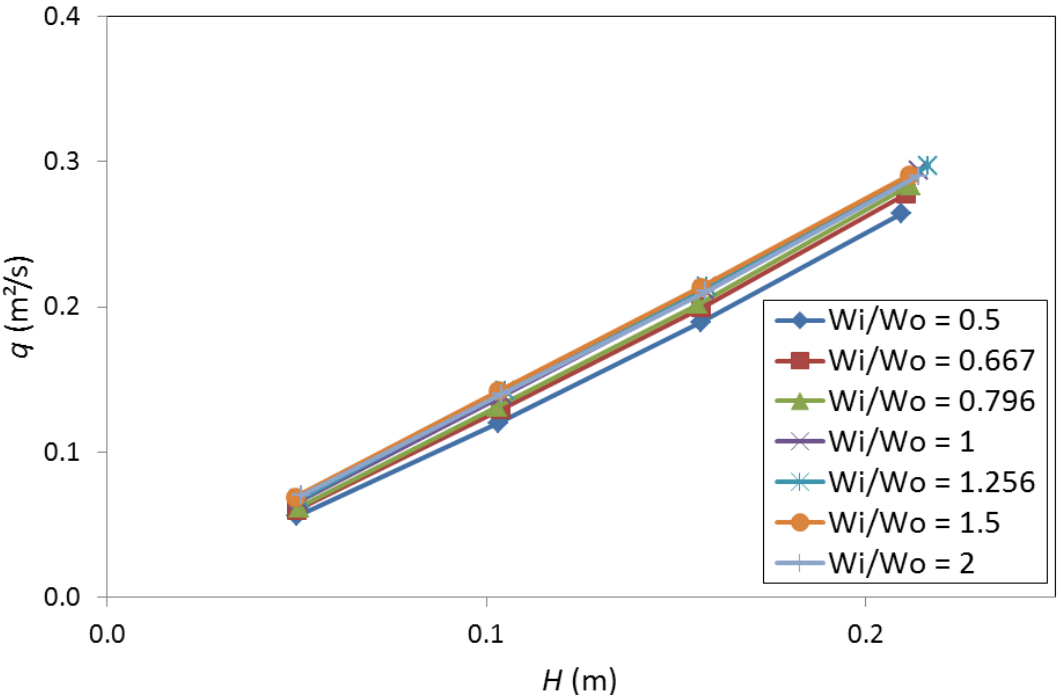

Figure VIII-20 Stage-discharge curves of the models with technico-economic optimal PKW height

VIII.4.2.5. Outlet key profile for technico-economic optimization of the weir height

Regarding the free surface profiles along the outlet key (Figure VIII-22), subcritical flows are observed on all tested models (Figure VIII-21 – (b)) excepted for the lowest head on the largest outlet key width (Figure VIII-21 – (a)). The subcritical outlet flow decreases the upstream crest efficiency. Furthermore, the free surface level rises over the side crest one on a non-negligible part of the side wall, what decreases the side crest efficiency on this part.

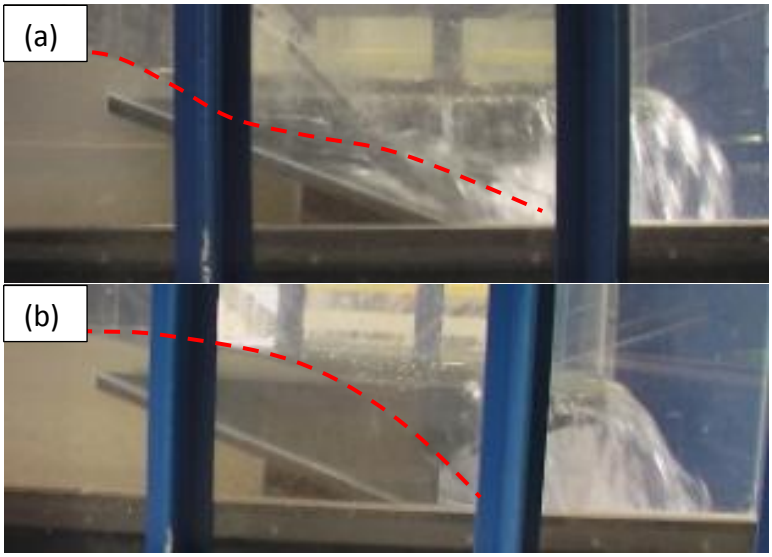

Figure VIII-21 View of the outlet free surface variation for technico-economic optimal weir height and H = 0.05 m: W_i/W_o = (a) – 0.5; (b) –2

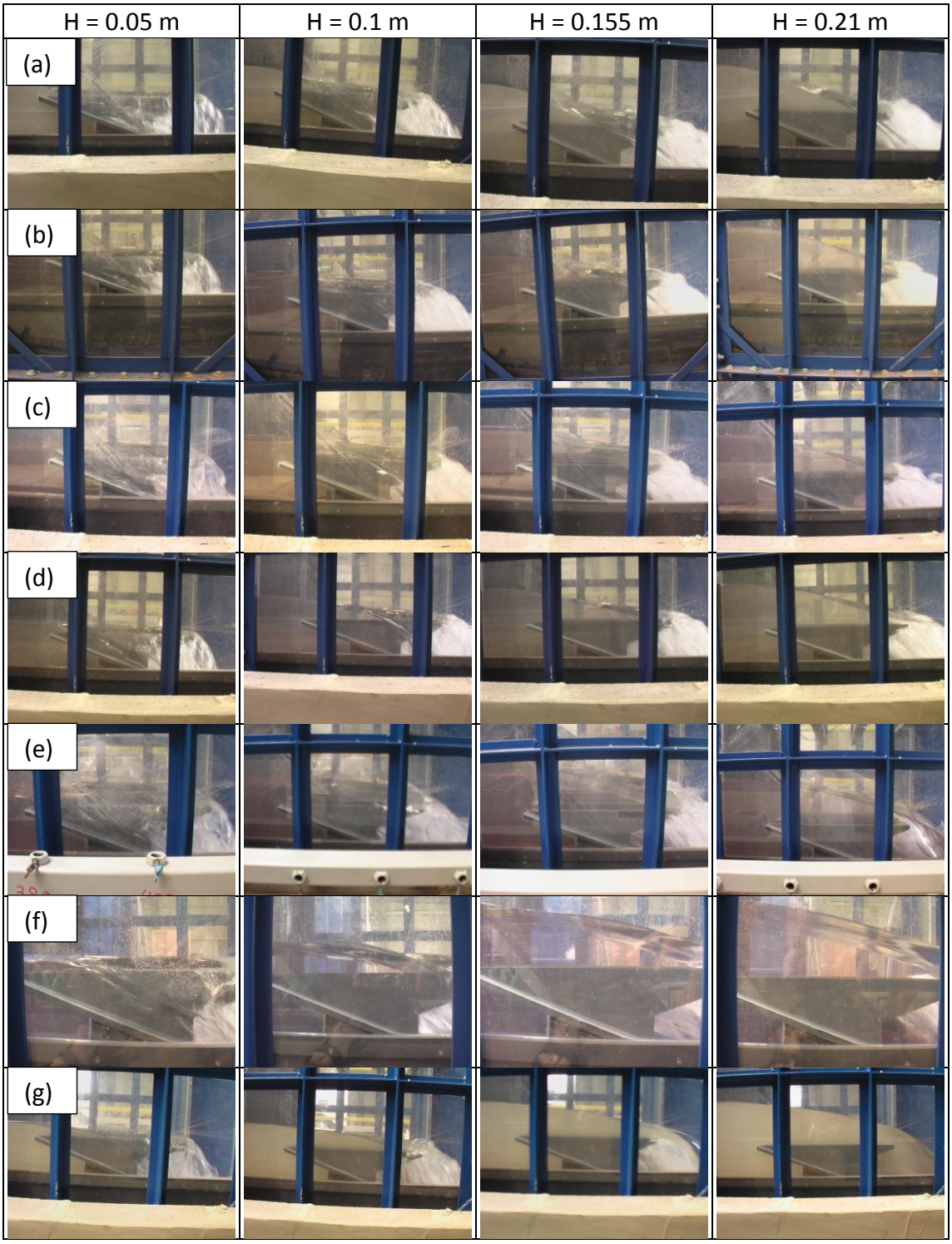

Figure VIII-22 View of the outlet free surface variation with head for technico-economic optimal weir height: W_i/W_o = (a) – 0.5; (b) – 0.667; (c) – 0.796; (d) – 1; (e) – 1.256; (f) – 1.5; (g) – 2

As the submerged side crest length increases with decreasing outlet key widths, the outlet key flow behaviour enables to explain the variation of stage discharge curves for varied W_i/W_o ratios (Figure VIII-20). For $W_i/W_o < 1.5$, the increase in side crest efficiency due to lower flow velocities and higher free surface levels along the inlet key stays more important than the decrease created by the partial submergence

of the side crest by the outlet flow. The PKW discharge capacity increases with the W_i/W_o ratio. For W_i/W_o ratios increasing over 1.5, the length of submerged crest becomes of main importance and the PKW discharge capacity decreases.

VIII.4.2.6. Transverse profile for technico-economic optimization of the weir height

Furthermore, the observation of the transverse free surface profiles (Figure VIII-24) enables to highlight one more time the influence of the interference zone between side nappes. The elevation of this zone rises with decreasing outlet widths. For highest W_i/W_o ratios and highest heads, the interference zone reaches the side crest level and decreases more the side crest efficiency.

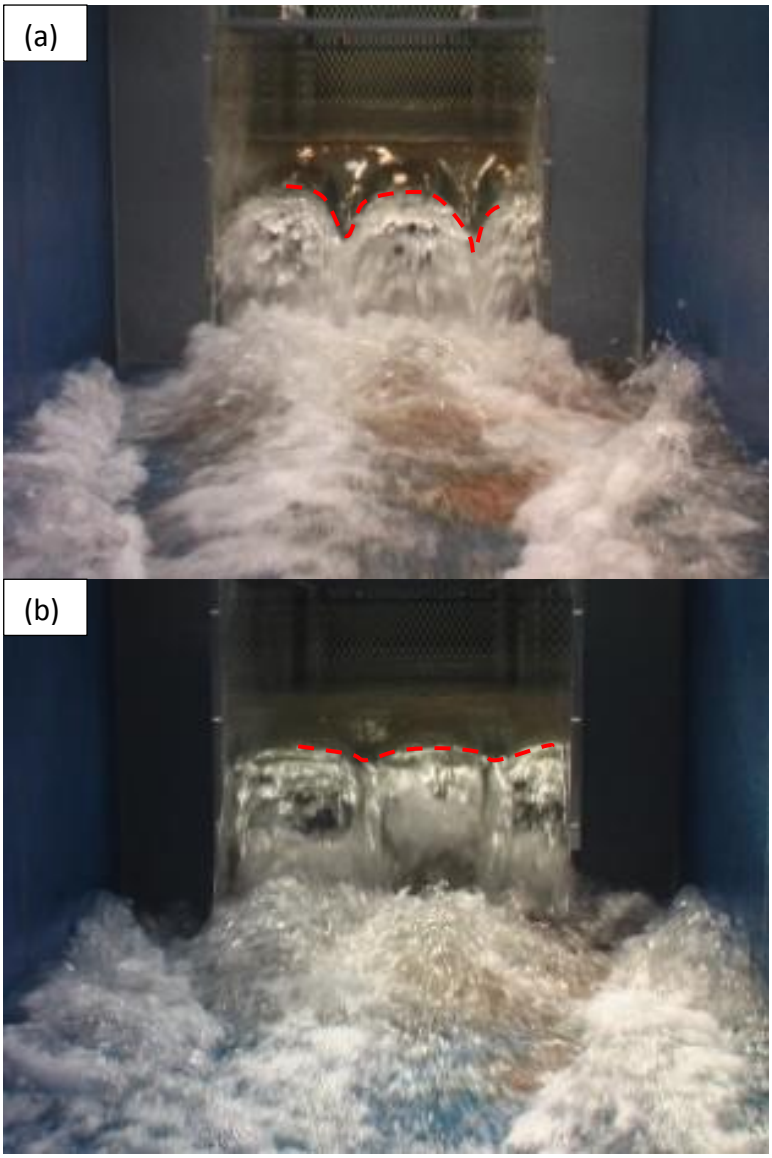

Figure VIII-23 View of the transverse free surface variation for technico-economic optimal weir height and H = 0.155 m: W_i/W_o = (a) – 0.5; (b) –2

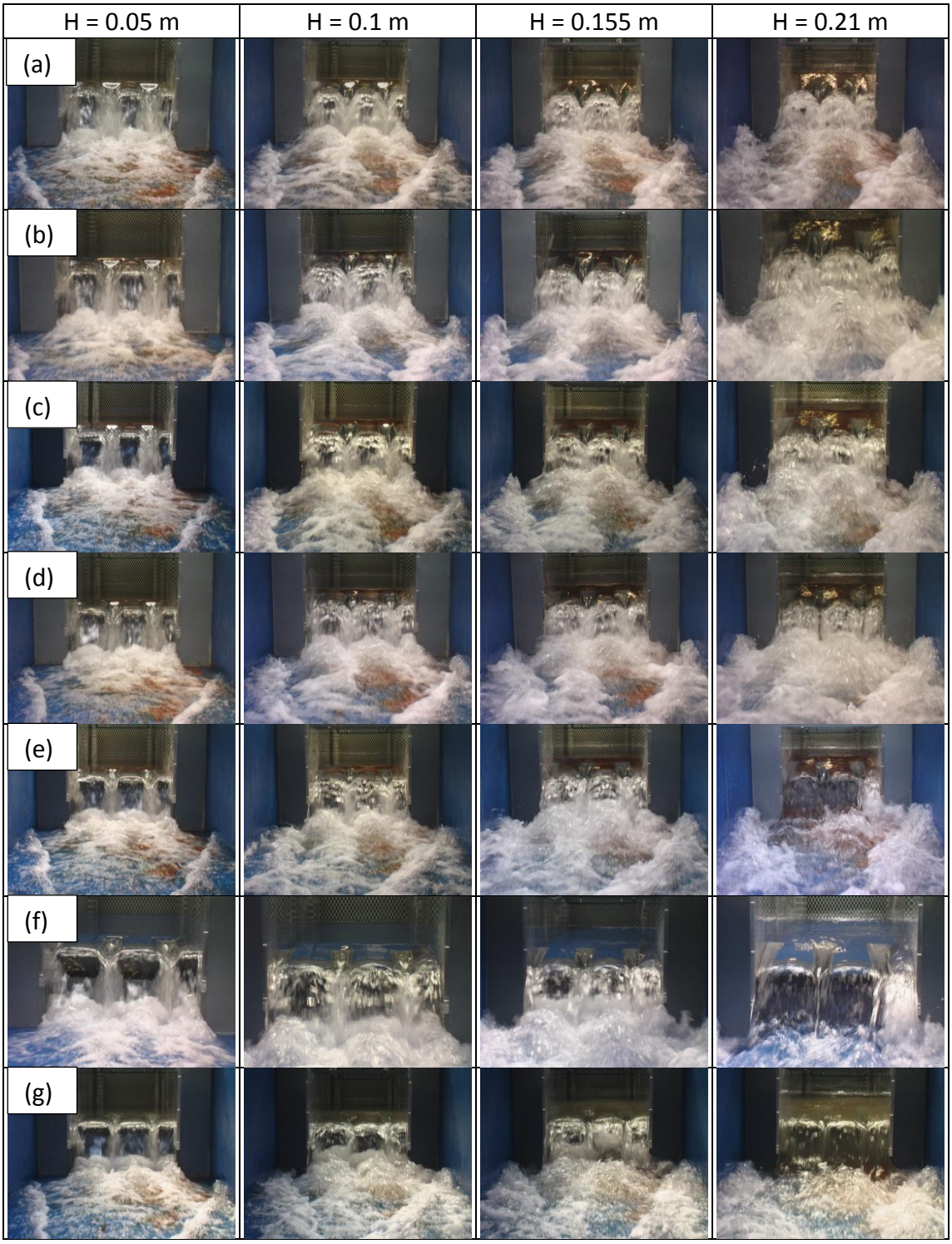

Figure VIII-24 View of the transverse free surface variation with head for technico-economic optimal weir height: W_i/W_o = (a) – 0.5; (b) – 0.667; (c) – 0.796; (d) – 1; (e) – 1.256; (f) – 1.5; (g) – 2

The observation of the transverse profiles allows also highlighting the influence of the W_i/W_o ratio on the nappe aeration. Models with lower outlet widths ($W_i/W_o \geq 1.256$) are no more aerated for high heads and the downstream nappe becomes leaping (Figure VIII-25). Artificial aerators are thus needed to avoid the negative effect of the negative pressure and the nappe beat on the structure.

Figure VIII-25 No more air entrainment and leaping nappe on the PKW for H = 0.21 m and W_i/W_o = 2

VIII.4.2.7. Comparison between the Froude number and the water depth influences

The influence of the W_i/W_o ratio is supposed to be mainly related to the inlet key width influence. Larger is the inlet key, less important are the velocities along it for the same discharge. The diminution of the longitudinal velocity increases the water height (considering a given head) and limits the apparition of a critical section in the inlet key. The position of the critical section is related to the Froude number Fr calculated using Eq. VIII-5 where Q_i is the discharge varying along the inlet key and h is the water depth along the inlet key. As the position of the critical section is related to a Froude number equal to 1, the efficiency of the weir is linked to $h^{1.5}$ following Eq. VIII-5.

$$\mathrm{Fr} = \frac{Q_i}{W_i\sqrt{gh^3}} \qquad \text{VIII-5}$$

Hager [44] prescribes to consider the water depth over the side crest in the main channel as the upstream head to calculate the discharge on a side weir. The increase of the water depth h along the inlet key increases thus the side discharge q_s, which is linked to $(h - w)^{1.5}$ following the traditional Poleni equation for weir corrected considering Hager's assumption (Eq. VIII-6), where C_{dL} is the discharge coefficient related to the crest length and w is the side wall height.

$$q_s = C_{dL}\sqrt{g\ \ h-w\ ^3} \qquad \text{VIII-6}$$

However, Hager prescribes also formulations of C_{dL} as a function of the Froude number in the main channel (inlet key). Higher Froude number values, characterizing higher flow velocities, decrease the C_{dL} value, as the main flow deviation is more difficult.

Table VIII-4 and Table VIII-5 show the comparison between mean ratios of the water depths and of the side heads, and the specific discharge ratio measured on the various tested models for low and high heads respectively.

The mean ratios of flow depths are closer from the specific discharge ratios than the side heads ones. This comparison enables to conclude to a main influence of the water depth along the inlet key. That traduces the influence of the Froude number and thus the longitudinal velocity. However, for high heads and high values of the W_i/W_o ratio, some differences exist between the water depth ratios and the specific discharge ratios. These differences are all the more important as the W_i/W_o ratio or the head increases. The differences observed may be linked to the nappes interferences, observed on higher PKW models (Figure VIII-15), and to the partial submergence of the side crest by the outlet key flow, observed on lower ones (Figure VIII-22).

Regarding low heads or high weir height for which the water depths ratios are well correlated with the specific discharges ratios, there is no modification of the outlet key flow behaviour whatever the value of the W_i/W_o ratio. There is thus no variation of the side crest flow behaviour that is mainly managed by the inlet key flow conditions.

Table VIII-4 Comparison of the mean ratios of water depths and of side heads along the inlet key with the specific discharges ratios for H/W_u = 0.167

W_i/W_o	$(h/h_{Wi/Wo=1})^{1.5}$	$(h\text{-}w/h\text{-}w_{Wi/Wo=1})^{1.5}$	$q/q_{Wi/Wo=1}$
Hydraulic optimal PKW height			
0.5	0.93	0.82	0.85
0.667	0.99	1.03	0.92
0.796	1.03	1.08	0.94
1.256	1.03	1.08	1.02
1.5	1.03	1.17	1.02
2	1.05	1.16	1.08
Technico-economic optimal PKW height			
0.5	0.85	0.69	0.82
0.667	0.90	0.82	0.90
0.796	0.94	0.92	0.93
1.256	1.04	1.04	1.05
1.5	1.07	1.07	1.05
2	1.10	1.13	1.02

Table VIII-5 Comparison of the mean ratios of water depths and of side heads along the inlet key with the specific discharges ratios for $H/W_u = 0.667$

W_i/W_o	$(h/h_{Wi/Wo=1})^{1.5}$	$(h\text{-}w/h\text{-}w_{Wi/Wo=1})^{1.5}$	$q/q_{Wi/Wo=1}$
Hydraulic optimal PKW height			
0.5	0.83	0.74	0.87
0.667	0.91	0.87	0.92
0.796	0.94	0.91	0.97
1.256	1.09	1.14	1.02
1.5	1.18	1.27	1.01
2	1.29	1.48	1.00
Technico-economic optimal PKW height			
0.5	0.63	0.59	0.92
0.667	0.78	0.76	0.96
0.796	0.88	0.78	0.98
1.256	1.10	1.44	1.00
1.5	1.17	1.61	1.01
2	1.27	1.85	0.98

However, for high heads or low weir height for which the correlation between the water depths ratios and the specific discharges ones is less relevant, variations of the outlet key width influence on the side crest flow behaviour has been observed with varying values of the W_i/W_o ratio. The side crest efficiency becomes mainly managed by the outlet key flow conditions, decreasing the efficiency of the weir as the W_i/W_o ratio increases.

This phenomenon may also explain the shape of the curves of Figure VIII-6 and Figure VIII-7. For the high weir configuration, the bottom slope of the outlet key is sufficiently high to avoid side crest submergence whatever the outlet key width. That is traduced by relatively constant values of the specific discharges ratios on Figure VIII-6, excepted for higher W_i/W_o ratios for which the influence of the nappes interferences could be observed. The PKW efficiency for a weir height hydraulically optimized is thus mainly managed by the Froude number value along the inlet key.

For the low weir configuration, the bottom slope of the outlet key is no more sufficient to avoid the side crest submersion. This time, decreasing the outlet key width increases the crest submersion and so decreases the efficient length of the side crest. For very high heads, the efficient length of the side crest is reduced to zero and the efficiency of the PKW is only depending on its global height and width whatever the value of the W_i/W_o ratio. This is traduced on Figure VIII-7 by values of the specific discharges ratios near the ones observed on Figure VIII-6 for low heads, and tending to 1 for very high heads. The PKW efficiency for a weir height technico-economically

optimized is thus mainly managed by the Froude number value along the inlet key for low heads, and by the capacity of flow conveyance along the outlet key for high heads.

VIII.4.3. Analytical approach

Regarding the analytical formulation developed in VII.3.3, the discharge capacity of the models with W_i/W_o lower than 1 is poorly predicted (accuracy reaching 20%). From the observations made on the experimental models with varying keys widths, this may come from the influence of the inlet key width on the side crest discharge which is not taken into account in the former analytical formulation.

The equation VII-4 of the side crest discharge must be corrected adding a term depending on the square of the inlet width. Indeed, according to Hager [44], the discharge over a side weir (here the side crest) is managed by the square of the Froude number along the main channel (here the inlet key). And the Froude number is directly proportional to the inlet width (Eq. VIII-5). The corrective term must be equal to 1 for infinite key width, providing negligible flow velocities, and to 0 for inlet width tending to 0, providing infinitely high velocities. The corrective term can thus be written as:

$$K_{W_i} = 1 - \frac{\gamma}{\gamma + W_i^2} \qquad \text{VIII-7}$$

where γ is a parameter which has been fitted on the experimental results obtained on the four models with hydraulically optimized height and $W_i/W_o \leq 1$. These models are the only ones able to isolate the influence of the inlet width from the one of the outlet width, as the outlet flow remains supercritical and thus has no influence on the global discharge. γ can thus be expressed as a function of the W_i/W_o ratio by:

$$\gamma = -0.0038\frac{W_i}{W_o} + 0.0055 \qquad \text{VIII-8}$$

Considering this corrective term, the discharge capacity of the models with low weir height and low outlet width becomes poorly predicted (accuracy reaching 15%). Regarding the experimental observations, this may be due to the influence of the outlet key width and slope on its resilience capacity which decreases the efficient length of the side crest. A corrective term is thus to apply to the relative side crest length in equation VII-1, depending on the ratio between upstream head and outlet width that characterizes the combine effect of outlet key submergence and lateral nappes interference. For H/W_o lower than a limit value L_1, there is no influence of the outlet key on the flow over the side crest and the corrective term must be equal to 1. For H/W_o higher than a second limit value L_2, the side crest is fully submerged by the outlet flow and no more side discharge is observed. The corrective term has then to be equal to 0. For intermediate values, the effective side crest length varies with H/W_o.

The corrective coefficient K_{Wo} could thus be defined to ensure the continuity of its values and of its derivatives for the two limits L_1 and L_2.

$$K_{W_o} = 1 \qquad \text{for } \frac{H}{W_o} \le L_1$$

$$K_{W_o} = \frac{2}{L_2 - L_1{}^3}\left(\frac{H}{W_o}\right)^3 - \frac{3\ L_2 + L_1}{L_2 - L_1{}^3}\left(\frac{H}{W_o}\right)^2 + \frac{6L_2L_1}{L_2 - L_1{}^3}\left(\frac{H}{W_o}\right) + \frac{L_2^2\ L_2 - 3L_1}{L_2 - L_1{}^3} \qquad \text{for } L_2 \ge \frac{H}{W_o} \ge L_1 \qquad \text{VIII-9}$$

$$K_{W_o} = 0 \qquad \text{for } \frac{H}{W_o} \ge L_2$$

The values of the two limits are directly related to the outlet key slope which influences the outlet flow regime. The following expressions have been fitted on the experimental results.

$$L_1 = 0.24S_o + 0.51 \qquad \text{VIII-10}$$

$$L_2 = 4.8S_o + 3.2 \qquad \text{VIII-11}$$

The corrected discharge equation can be written as:

$$q = q_u \frac{W_o}{W_u} + q_d \frac{W_i}{W_u} + q_s \frac{2B}{W_u} K_{W_o} \qquad \text{VIII-12}$$

with q_u and q_d expressed respectively by Eqs. VII-3 and VII-2, and q_s expressed by:

$$q_s = 0.41\left(1 + \frac{1}{833H + 1.6}\right)\left(1 + 0.5\left(\frac{0.833H}{0.833H + P_e}\right)^2\right)\left(\frac{P_e^{\alpha} + \beta}{0.833H + P_e{}^{\alpha} + \beta}\right)K_{W_i}\sqrt{2gH^3} \qquad \text{VIII-13}$$

The comparison of the specific discharges computed by these corrected formulations with the experimental discharges measured on the 14 tested models with varied keys widths is shown on Figure VIII-26. It highlights that the experimental results are approached with an accuracy of 10%.

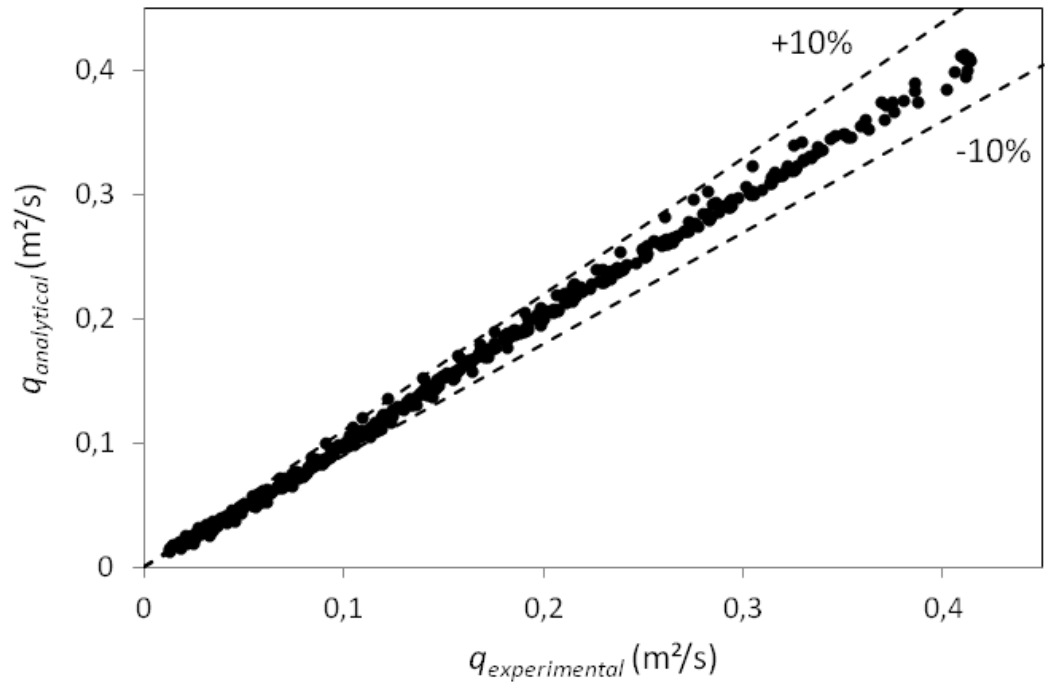

Figure VIII-26 Comparison of the specific discharges computed by the analytical formulation and experimental results of the Type A models with varying keys widths

The proposed analytical formulation can be one more time compared with the experimental results obtained by Le Doucen [61]. The comparison of the experimental results of Le Doucen, obtained for the same ratio B_o/B_i = 1 than the present experiments and varied ratios L/W = 3 to 7, W_i/W_o = 0.5 to 2, and P_i/P_o = 0.72 to 1.4, with the corrected analytical formulation is shown on Figure VII-18.

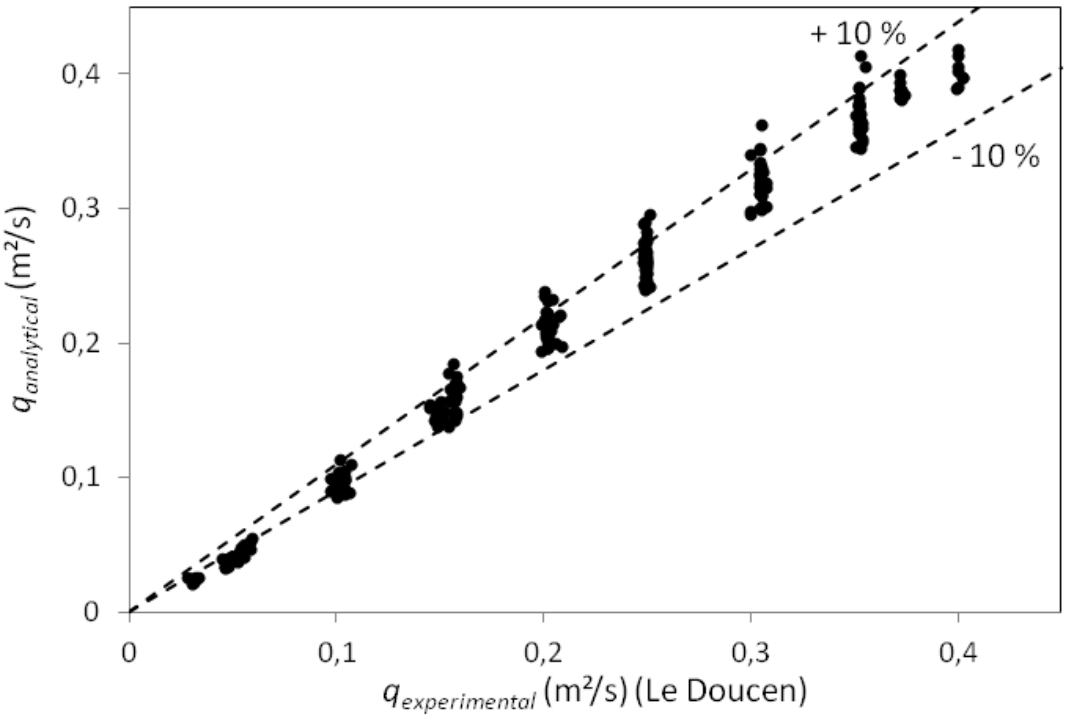

Figure VIII-27 Comparison of the specific discharges computed by the analytical formulation and experimental results of Le Doucen [61]

The accuracy of the analytical approach is in the order of 10% for almost all the geometries. However, for outlet slopes of 0.36 and highest values of W_i/W_o, the accuracy of the analytical approach falls down to 15%. This traduces the bad definition of the limits L_1 and L_2 for low outlet slopes. Indeed the definition of the variation of these limits with the key slope has been realized considering only two different slopes. The definition of these limits will probably be enhanced after analysis of the results obtained on models with varying overhangs position, what modifies keys slopes (see IX.3.3).

VIII.4.4. Numerical approach

As for the models with varied heights, the tested models with varied keys widths have been modelled numerically using the enhanced version of Wolf1D-PKW (see XIV.2).

VIII.4.4.1. Hydraulic optimization of the PKW height

Considering hydraulic optimization of the weir height, the accuracy of the numerical model is around 10% for discharge capacity prediction (Figure VIII-28). For W_i/W_o < 1, both numerical and analytical approaches provide similar results. For W_i/W_o > 1, the analytical formulation becomes more relevant regarding the comparison with experimental results.

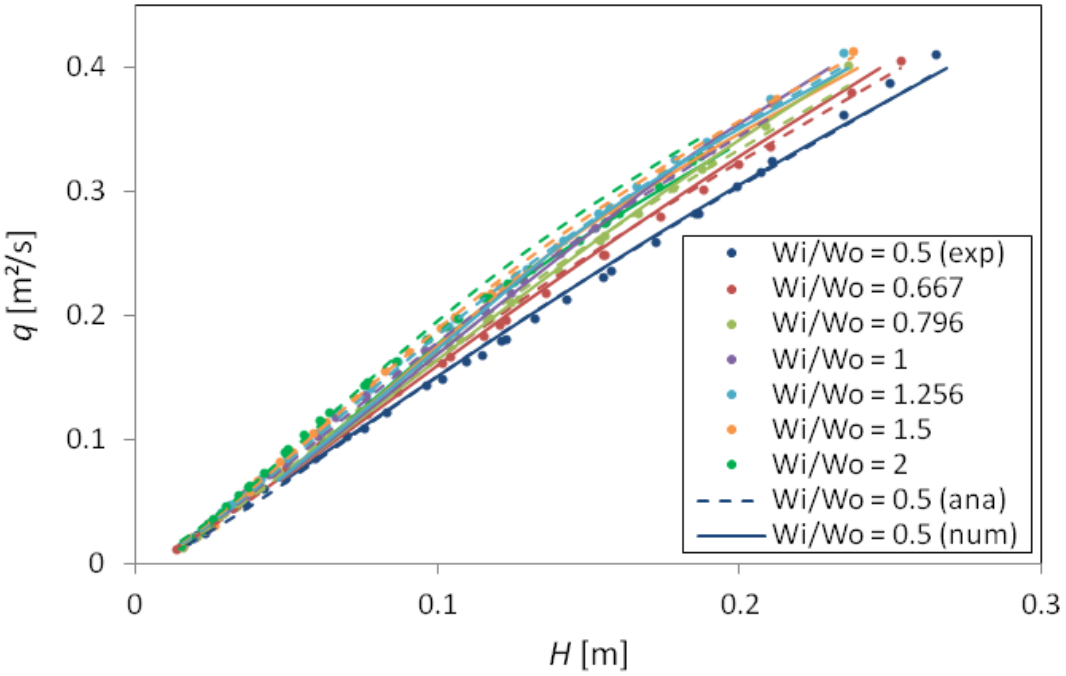

Figure VIII-28 Comparison between stage discharge curves obtained from experimental, analytical and numerical approaches for hydraulic optimal weir height

However, the interest of the 1D numerical solver is again to provide additional information on the free surface profiles and on the position of the critical section along the inlet key.

VIII.4.4.1.1. W_i/W_o = 1.5

Figure VIII-29 and Table VIII-6 show the comparison between the free surface profiles along the inlet and outlet keys computed with the enhanced version of Wolf1D-PKW for W_i/W_o = 1.5 and the experimental results.

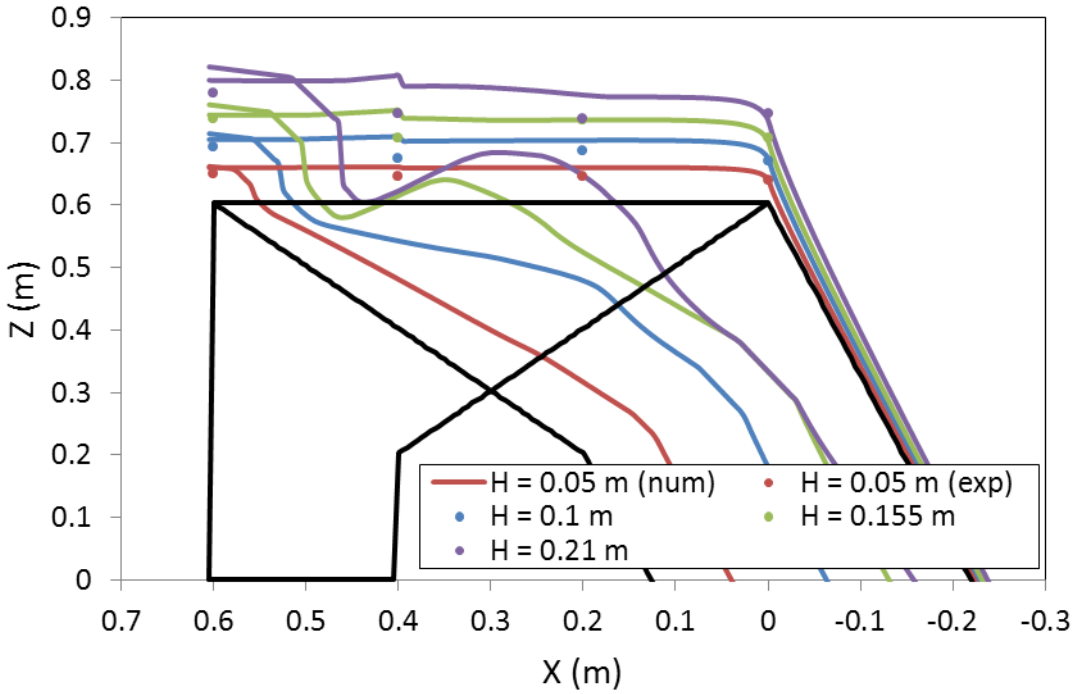

Figure VIII-29 Comparison between measured free surface level and profiles provided by Wolf1D-PKW for W_i/W_o = 1.5 and hydraulic optimal weir height

Table VIII-6 – Comparison of experimental and numerical results for W_i/W_o = 1.5 and hydraulic optimal weir height

X (m)	*H* (m)	Δ*h*/*h* (%)	*X* (m)	*H* (m)	Δ*h*/*h* (%)
0.6	0.05	22.9	0.2	0.05	30.9
	0.1	13		0.1	18.7
	0.155	4.9		0.155	0.3
	0.21	10.9		0.21	27.9
0.4	0.05	31.3	0	0.05	3.5
	0.1	38.8		0.1	7.9
	0.155	30.9		0.155	3.8
	0.21	31.3		0.21	6.5

Regarding the inlet free surface profile, the upstream (*X* = 0.6 m) and downstream (*X* = 0 m) levels agree with the experimental results. However, the decrease observed in free surface level at the inlet entrance (*X* = 0.4 m) on scale models is not represented by the numerical solver. That decrease comes from the progressive lateral contraction of the flow under the upstream overhangs and from the quick vertical contraction at key entrance. However, the flow solver considers only the inlet width to model the inlet key. There is thus no lateral contraction considered. In

further developments, as already mentioned, the Wolf1D-PKW solver should include the consideration of compounded cross sections.

Regarding the outlet free surface profile, the upstream part is in agreement with the observations made on the scale model with a flow quickly passing by a critical depth. However, the hydraulic jump observed on the numerical results for the highest heads (Figure VIII-30) is not observed on the scale model. This may come from the longitudinal transfer of the flow between inlet and outlet keys. Indeed, the solver considers well the side flow inclination in the calculation of the mass and momentum transfers between the keys. However, the transfers are realized perpendicularly to the side crest. Practically, the transfer follows the side flow inclination which is non-negligible for high heads. That phenomenon decreases the discharge along the outlet key and delays the apparition of the hydraulic jump observed on the numerical model. This hydraulic jump, moving the free surface level over the side crest one, enables to explain the PKW loss in efficiency observed, for high heads, on numerical results compared with the experimental ones (Figure VIII-28).

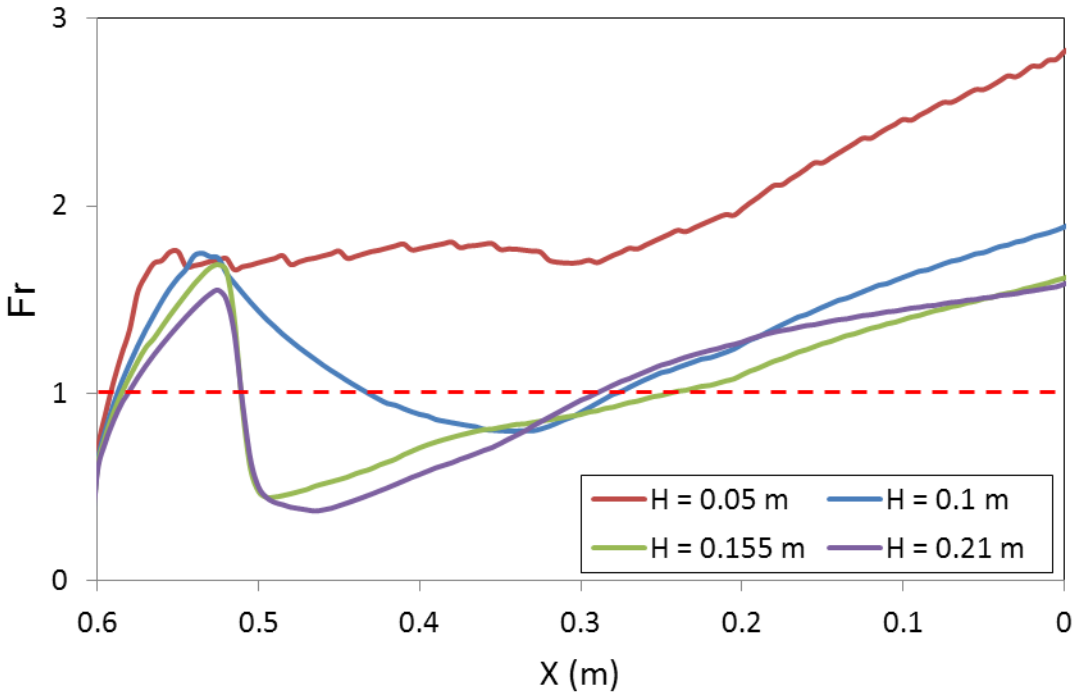

Figure VIII-30 Variation of the Froude number along the outlet key for W_i/W_o = 1.5 and hydraulic optimal weir height

VIII.4.4.1.2. W_i/W_o = 1

Figure VIII-31 and Table VIII-7 show the comparison between the free surface profiles along the inlet and outlet keys computed with Wolf1D-PKW for W_i/W_o = 1 and the experimental results.

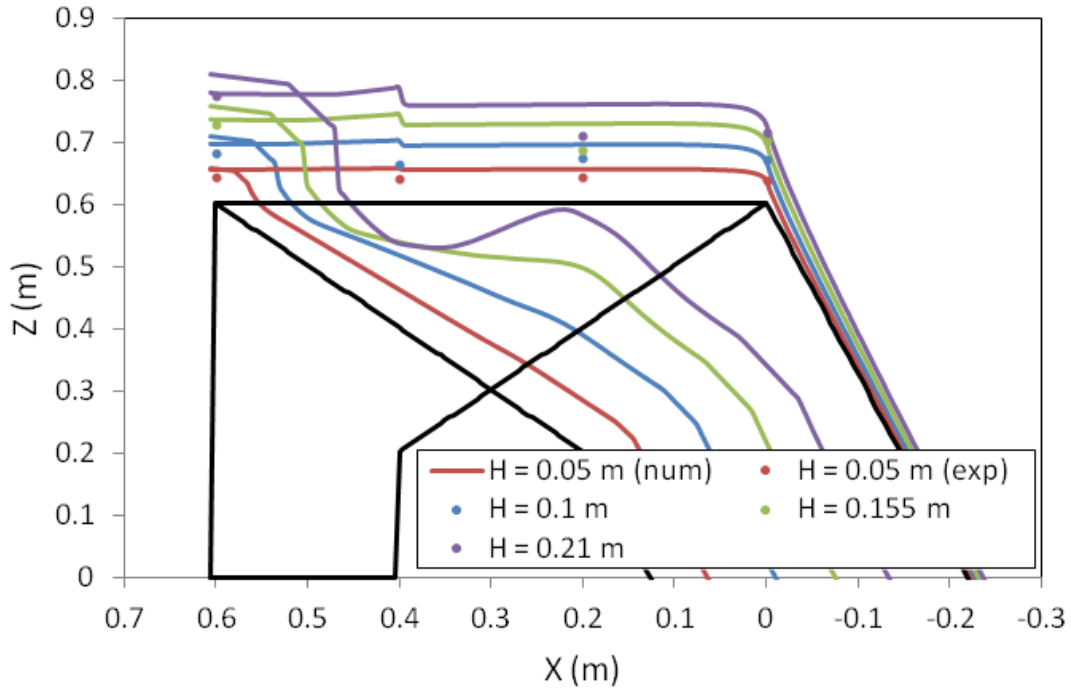

Figure VIII-31 Comparison between measured free surface level and profiles provided by Wolf1D-PKW for W_i/W_o = 1 and hydraulic optimal weir height

Table VIII-7 – Comparison of experimental and numerical results for W_i/W_o = 1 and hydraulic optimal weir height

X (m)	*H* (m)	Δ*h*/*h* (%)	*X* (m)	*H* (m)	Δ*h*/*h* (%)
0.6	0.05	25.7	0.2	0.05	30.4
	0.1	17		0.1	28.1
	0.155	4.7		0.155	48.5
	0.21	1.4		0.21	46.3
0.4	0.05	35.2	0	0.05	3.3
	0.1	53		0.1	0.8
	0.155	-		0.155	2.8
	0.21	-		0.21	10.3

Even if the lateral contraction at inlet key entrance (*X* = 0.4 m) becomes more influent for decreasing W_i/W_o ratios, the comparison of the inlet free surface profiles computed with the numerical solver and measured on the tested model is still similar. The experimental results are approached with only 1% less accuracy than on model with W_i/W_o = 1.5. One more time, the upstream (*X* = 0.6 m) and downstream (*X* = 0 m) levels are well represented. However, the surface decrease at the inlet entrance is underestimated on the numerical results.

Regarding the outlet keys profiles, one more time, a hydraulic jump is observed for the highest head on the numerical results (Figure VIII-32) that are not observed on the tested model. However, the outlet free surface remains under the crest level (Figure VIII-31) and the hydraulic jump doesn't more influence the side discharge. This

enables to explain the better approach of experimental discharges for W_i/W_o < 1 (Figure VIII-28).

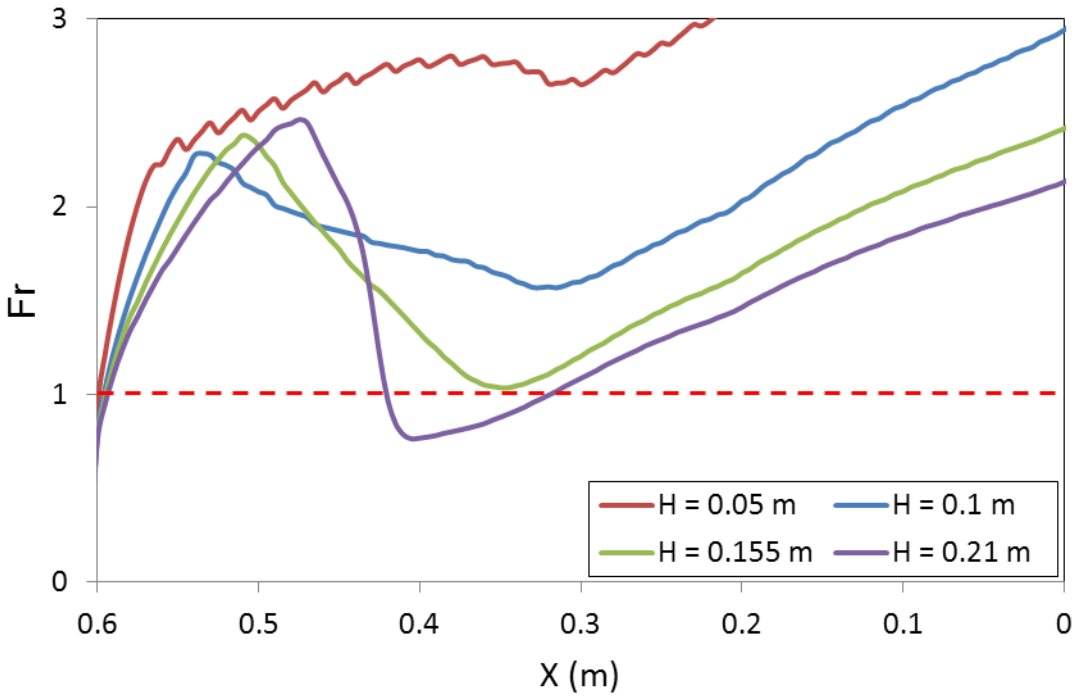

Figure VIII-32 Variation of the Froude number along the outlet key for W_i/W_o = 1 and hydraulic optimal weir height

VIII.4.4.1.3. W_i/W_o = 0.667

Figure VIII-33 and Table VIII-8 show the comparison between the free surface profiles along the inlet and outlet keys computed with Wolf1D-PKW for W_i/W_o = 0.667 and the experimental results.

Table VIII-8 – Comparison of experimental and numerical results for W_i/W_o = 0.667 and hydraulic optimal weir height

X (m)	*H* (m)	Δ*h*/*h* (%)	*X* (m)	*H* (m)	Δ*h*/*h* (%)
0.6	0.05	15.2	0.2	0.05	22.6
	0.1	3.9		0.1	22.6
	0.155	2.2		0.155	50.8
	0.21	3.7		0.21	56
0.4	0.05	25.5	0	0.05	2
	0.1	52.8		0.1	3.9
	0.155	-		0.155	4.8
	0.21	-		0.21	5.7

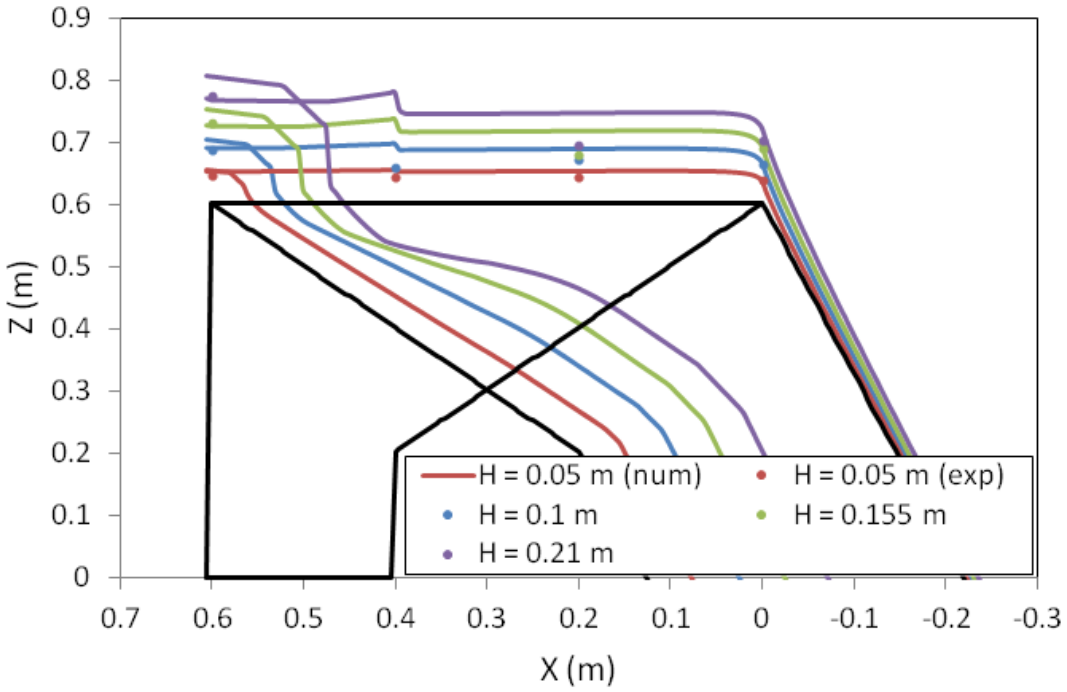

Figure VIII-33 Comparison between measured free surface level and profiles provided by Wolf1D-PKW for W_i/W_o = 0.667 and hydraulic optimal weir height

The experimental results are approached with the same accuracy than on model with W_i/W_o = 1. The upstream (X = 0.6 m) and downstream (X = 0 m) levels are still well represented. The surface decrease at the inlet entrance (X = 0.4 m) is still not sufficient on the numerical results.

Regarding the outlet keys profiles, the outlet width becomes sufficiently high to avoid apparition of a hydraulic jump even for high heads.

VIII.4.4.1.4. Control section on the inlet key

As the free surface profiles in the downstream part of the inlet key are not affected by the simplifications of the flow solver, whatever the upstream head or the keys widths, the numerical results may help to the determination of the control section position along the key.

Figure VIII-34 shows the variation of the distance B' between the downstream crest and the control section of the inlet key with head and keys widths.

For $W_i/W_o > 1$, the control section in the inlet key stays on the downstream crest. Flow velocities are sufficiently low to avoid apparition of supercritical flows. The keys widths play limited role on the discharge capacity (Figure VIII-6).

For $W_i/W_o < 1$, the control section of the inlet key moves upstream with increasing heads. Flow velocities along the inlet key become higher than critical one due to the small inlet width combined with low water depths in the downstream part

of the key. The discharge capacity decreases continuously with the inlet width (Figure VIII-6).

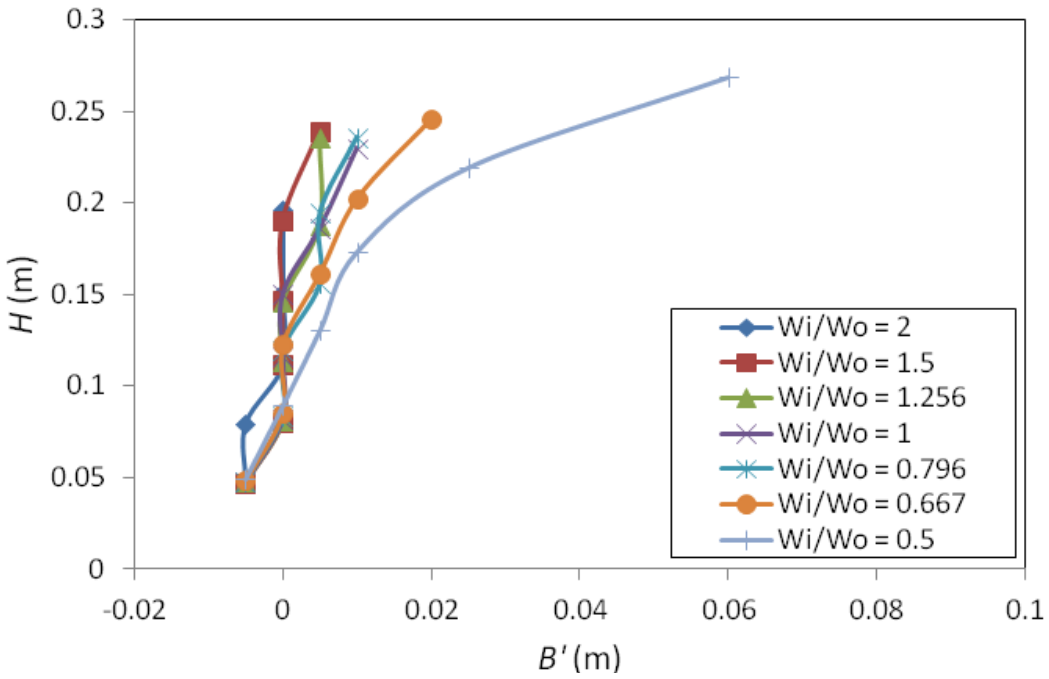

Figure VIII-34 Variation of the inlet control section position with head and keys widths for hydraulic optimal weir height

VIII.4.4.2. Technico-economic optimization of the PKW height

Considering a technico-economic optimization of the weir height, the accuracy of the numerical model stays around 10% (Figure VIII-35).

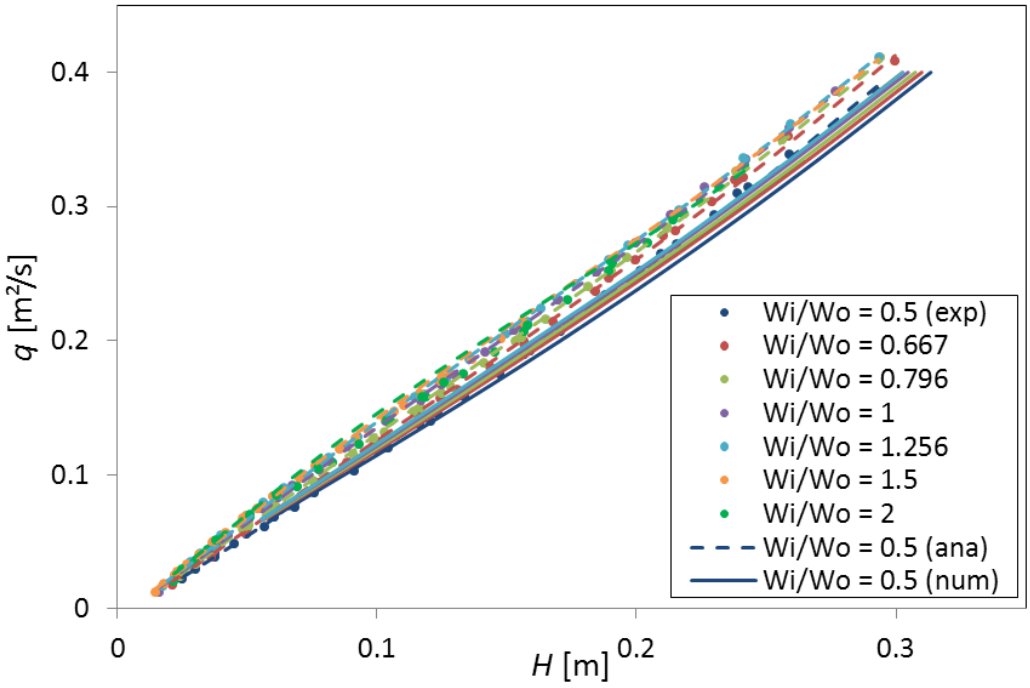

Figure VIII-35 Comparison between stage discharge curves from experimental, analytical and numerical approaches for technico-economic optimal height

However, the numerical results systematically under-estimate the experimental ones, even if the influence of the W_i/W_o ratio remains similar. The analytical results are in better agreement with the experimental ones.

One more time, the interest of the 1D numerical solver is to give information on the free surface profiles and on the position of the critical section along the inlet key.

VIII.4.4.2.1. W_i/W_o = 1.5

Figure VIII-36 and Table VIII-9 show the comparison between the free surface profiles along the inlet and outlet keys computed with the enhanced version of Wolf1D-PKW for W_i/W_o = 1.5 and the experimental results.

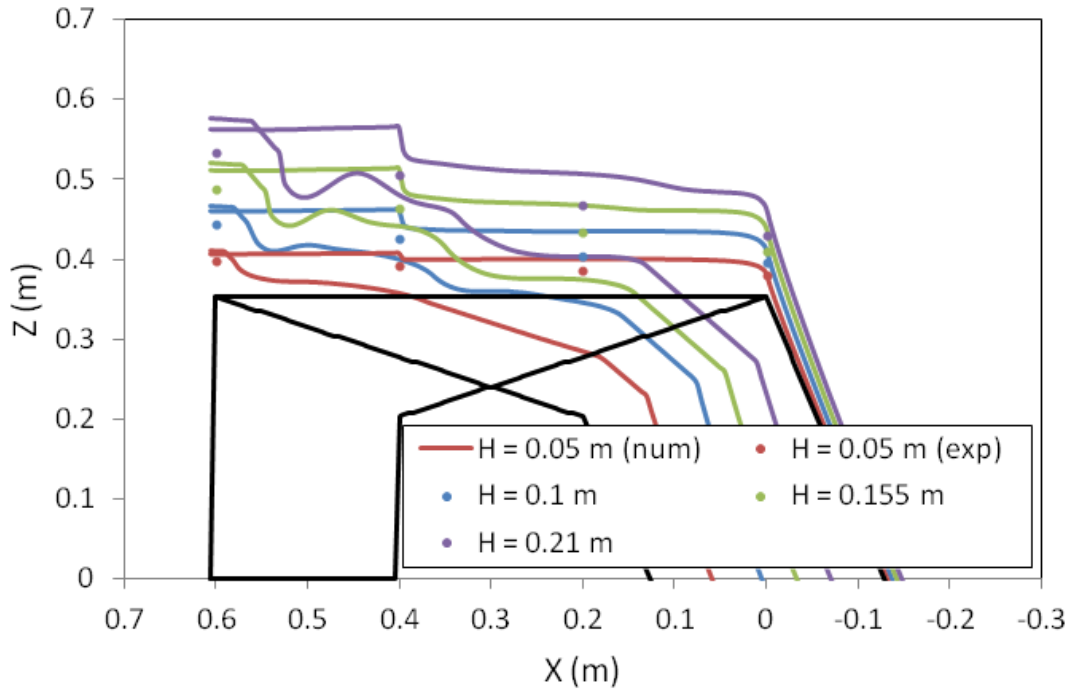

Figure VIII-36 Comparison between measured free surface level and profiles provided by Wolf1D-PKW for W_i/W_o = 1.5 and technico-economic optimal weir height

Table VIII-9 – Comparison of experimental and numerical results for W_i/W_o = 1.5 and technico-economic optimal weir height

X (m)	*H* (m)	Δ*h*/*h* (%)	*X* (m)	*H* (m)	Δ*h*/*h* (%)
0.6	0.05	23.1	0.2	0.05	49
	0.1	18.5		0.1	56.7
	0.155	16.4		0.155	41.4
	0.21	15.3		0.21	32.5
0.4	0.05	29.5	0	0.05	11.8
	0.1	22.9		0.1	13
	0.155	18.3		0.155	18.7
	0.21	15.7		0.21	14.6

The inlet free surface profiles are this time closer from the experimental results at the inlet entrance (X = 0.4 m). The influence of the transversal flow contraction decreases and the one of the vertical contraction increases, as the weir height is decreased. As the flow solver computes well the vertical contraction, and not the lateral one, it is more efficient for low weir heights.

Regarding the outlet keys, the free surface profiles are closer from the ones observed on the scale models than for the hydraulic optimal weir height. As the weir height decreases, the transfer way between the inlet and outlet keys decreases, and so the longitudinal transfer length. The assumption of a transfer perpendicular to the side wall becomes thus more accurate for low weirs.

VIII.4.4.2.2. $W_i/W_o = 1$

Figure VIII-37 and Table VIII-10 show the comparison between the free surface profiles along the inlet and outlet keys computed with Wolf1D-PKW for W_i/W_o = 1 and the experimental results.

One more time, even if the lateral contraction at inlet key entrance (X = 0.4 m) becomes more influent for decreasing W_i/W_o ratios, the comparison of inlet free surface profiles computed with the numerical solver and measured on the tested model is similar.

Regarding the outlet keys profiles, the enlargement of the key enables a more quickly decrease of the free surface level, as observed on the experimental models.

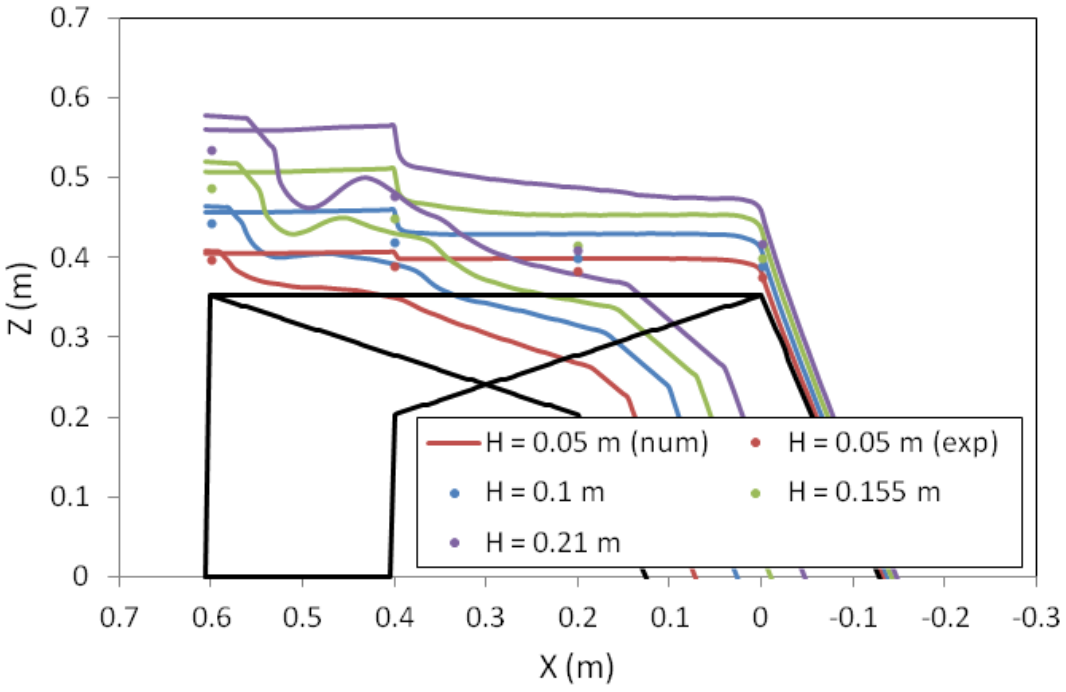

Figure VIII-37 Comparison between measured free surface level and profiles provided by Wolf1D-PKW for W_i/W_o = 1 and technico-economic optimal weir height

Table VIII-10 – Comparison of experimental and numerical results for W_i/W_o = 1 and technico-economic optimal weir height

X (m)	H (m)	$\Delta h/h$ (%)	X (m)	H (m)	$\Delta h/h$ (%)
0.6	0.05	14.4	0.2	0.05	49.3
	0.1	14.4		0.1	61.5
	0.155	13.1		0.155	59.4
	0.21	13.8		0.21	138.4
0.4	0.05	25.9	0	0.05	27.2
	0.1	25.4		0.1	14.7
	0.155	27.5		0.155	21.9
	0.21	37		0.21	16.3

VIII.4.4.2.3. W_i/W_o = 0.667

Figure VIII-38 and Table VIII-11 show the comparison between the free surface profiles along the inlet and outlet keys computed with Wolf1D-PKW for W_i/W_o = 0.667 and the experimental results.

The experimental results are approached with the same accuracy than on model with W_i/W_o = 1 and 1.5 along the inlet key except on the downstream crest (X = 0 m).

Regarding the outlet keys profiles, increasing one more time the outlet width enables quicker decrease of the free surface level.

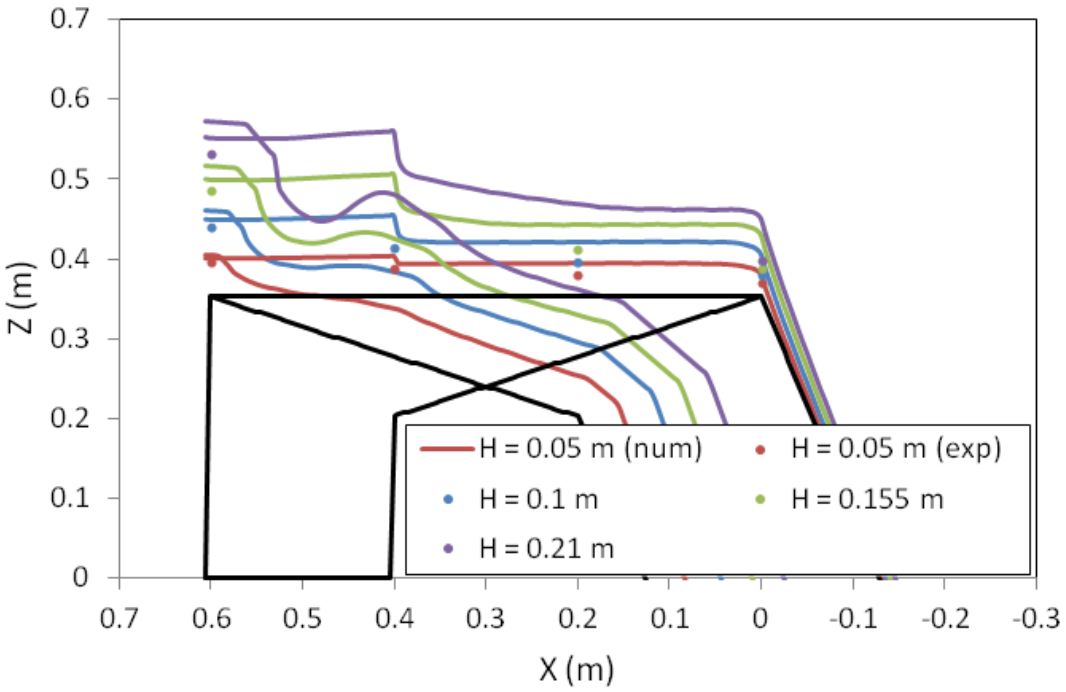

Figure VIII-38 Comparison between measured free surface level and profiles provided by Wolf1D-PKW for W_i/W_o = 0.667 and technico-economic optimal weir height

Table VIII-11 – Comparison of experimental and numerical results for W_i/W_o = 0.667 and technico-economic optimal weir height

X (m)	*H* (m)	$\Delta h/h$ (%)	*X* (m)	*H* (m)	$\Delta h/h$ (%)
0.6	0.05	8.4	0.2	0.05	57
	0.1	11.2		0.1	63.1
	0.155	9.2		0.155	50.2
	0.21	11.1		0.21	-
0.4	0.05	21.6	0	0.05	53.5
	0.1	26.6		0.1	34.9
	0.155	-		0.155	32.3
	0.21	-		0.21	33.7

As for technico-economic optimization of the weir height the discharge is mainly managed by the resilience capacity of the outlet key, a small increase of the free surface level may vary significantly the side crest discharge and thus the global weir efficiency. As the mass transfer is considered perpendicular to the side crest, a small increase of the free surface along the outlet key is provided by the solver. It decreases the efficient side crest length, what enables to explain the systematic underestimation of the discharge by the numerical approach (Figure VIII-35).

VIII.4.4.2.4. Control section on the inlet key

As the free surface profiles in the downstream part of the inlet key are not affected by the simplifications of the flow solver, whatever the upstream head or the keys widths, the numerical results may help to the determination of the control section position along the key. Figure VIII-39 shows the variation of the distance *B'* between the downstream crest and the control section of the inlet key with head and keys widths.

For the technico-economic optimal weir height, the control section of the inlet key moves upstream to reach a maximum distance from the downstream crest for a *H*/*P* ratio approximately equal to 1.5, whatever the keys widths. Then, for increasing heads, the control section moves downstream. Flow velocities along the inlet key become higher than the critical one due to the low water depths in the downstream part of the inlet key. However, for high heads, the submergence of the side crest by the outlet flow decreases the inlet key discharge and so the velocities, what moves the control section downstream. The position of the control section is all the more upstream as the W_i/W_o ratio decreases, decreasing the inlet key cross section.

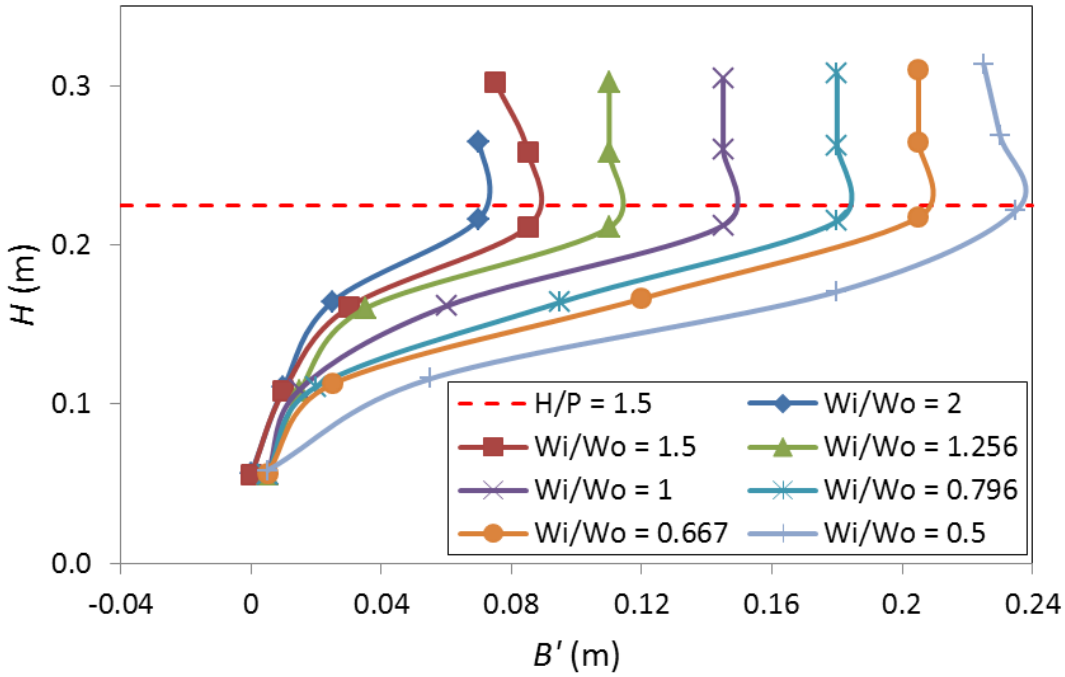

Figure VIII-39 Variation of the inlet control section position with head and keys widths for technico-economic optimal weir height

VIII.4.5. Design considerations

Until now, the value of the H/W_u ratios for the design of the existing projects of PKW varies between 0.18 and 0.25 for dams rehabilitations in Europe [110], and between 0.35 and 0.55 for rehabilitations as well as new dams projects in Asia [22, 48]. Regarding the above mentioned results for these ranges of H/W_u ratios, W_i/W_o ratios between 1.25 and 1.5 must be used to obtain an optimal discharge capacity whatever the optimization of the weir height. However, in dam projects for which the economic interest is of prime importance (development projects by example) and with a large number of PKW-units, the use of a symmetric geometry, which encourages the use of precast elements, is relevant. This economic PKW geometry, using simultaneously a low weir height and symmetric keys, decreases the maximal discharge by 30% compared to the hydraulically optimized geometry, but by less than 2% considering a technico-economic optimized PKW height.

Furthermore, the use of larger inlet apex enhances the air entrainment under the downstream nappe for low weir heights. This avoids cavitation and nappe beat problems and helps to a better energy dissipation along the structure without need of artificial aerators.

VIII.5. Conclusion

The study of the 6 type B and the 14 type A models with varying keys widths enables to conclude to an optimal W_i/W_o ratio close to 1.25. However, variations of this ratio between 1 and 1.5 don't change significantly the discharge capacity of the PKW. For a PKW design based on pure hydraulic, a ratio of 1.25 is optimal. According

to technico-economic interests, a symmetric configuration seems more relevant as it enables the use of precast elements.

Based on the results obtained on the type B PKW, a specific analytical formulation of the discharge capacity has been developed. This predicts the experimental results with accuracy close to 10 %.

The study of the free surface profiles on the type A models enables to explain the hydraulic interest in approaching a W_i/W_o ratio of 1.25.

Considering the hydraulic optimal weir height (P/W_u = 1.33), the outlet key flow stays supercritical and doesn't influence the crest efficiency. However, as the outlet key width decreases, the interference zone between nappes coming from the opposite side crests rises. For W_i/W_o until 1.5, the increase in side crest efficiency due to lower flow velocities and higher free surface level along the inlet key stays more important than the decrease created by the interference between opposite nappes. The PKW discharge capacity increases with the W_i/W_o ratio. For W_i/W_o ratios increasing over 1.5, the nappes interference becomes of main importance and the PKW discharge capacity decreases.

Considering a technico-economic optimal weir height (P/W_u = 0.5), the outlet key flow is this time subcritical and influences the side crest efficiency. For $W_i/W_o < 1.5$, the increase in side crest efficiency due to lower flow velocities and higher free surface levels along the inlet key stays more important than the decrease created by the partial submergence of the side crest by the outlet flow. The PKW discharge capacity increases with the W_i/W_o ratio. For W_i/W_o ratios increasing over 1.5, the length of submerged crest becomes of main importance and the PKW discharge capacity decreases. Furthermore, as the outlet key width decreases, the interference zone between nappes decreases even more the side crest efficiency.

Models with low weir height (P/W_u = 0.5) and low outlet widths ($W_i/W_o \geq 1.256$) have also shown problems of aeration. For high heads, no more aeration is observed under the weir and the downstream nappe becomes leaping. Artificial aerators are thus needed to avoid the effect of the negative pressure and the nappe beat on the structure.

The exploitation of the Wolf1D-PKW solver, on the type A models, enables to highlight the influence of the keys widths on the position of the control section on the inlet key. For the high weir height (P/W_u = 1.33), the control section stays located on the downstream crest except for highest heads on the model with the lowest inlet key width. For the low weir height (P/W_u = 0.5), the control section of the inlet key moves upstream to reach a maximum distance from the downstream crest for a H/P ratio

approximately equal to 1.5. The maximum distance is all the longer as the inlet key width decreases.

Finally, based on the experimental results of type A models, the analytical formulation of the discharge capacity of PKW has been enhanced. It predicts all the experimental results with an accuracy of 10 %.

IX. On the influence of the overhangs lengths [85]

IX.1. Introduction

As for the study of keys widths influence on type A PKW (see VIII), the influence of the overhangs position has been studied considering two PKW heights corresponding respectively to the hydraulic and a technico-economic optimum.

The same methodology as the one used for the study of the type A models with varying height (see VII) and varying keys widths (see VIII) has been applied. Experimental, analytical and numerical approaches are explored successively, focusing on the stage discharge curves and the free surface profiles measurements to finally provide design advices.

IX.2. Experimental set-up

For both weir heights (P/W_u = 1.33; 0.5) corresponding respectively to the hydraulic and a technico-economic optimum, five models of PKW, with varied ratios between upstream and downstream overhangs lengths (B_o/B_i = 0 – type C; 0.333; 1 – type A; 3; ∞ - type B), have been tested. The ratio between the total length of the crest and the width of all weirs is 5, the ratio between the inlet and outlet keys widths is equal to 1.5, and the base length is equal to the third of the whole side crest length. Table IX-1 and Figure IX-1 give the values of the geometrical parameters of the 10 models tested.

Table IX-1 – PKW models with varying overhangs lengths dimensions

	Hydraulic optimal height	Technico-economic optimal height
W	0.75 m	
L	3.75 m	
$P_i = P_o$	0.4 m	0.15 m
P_d	0.2 m	
W_u	0.3 m	
W_i	0.165 m	
W_o	0.105 m	
T_s	0.015 m	
$T_i = T_o$	0 m	
B	0.6 m	
B_o	0.4; 0.3; 0.2; 0.1; 0 m	
B_i	0; 0.1; 0.2; 0.3; 0.4 m	

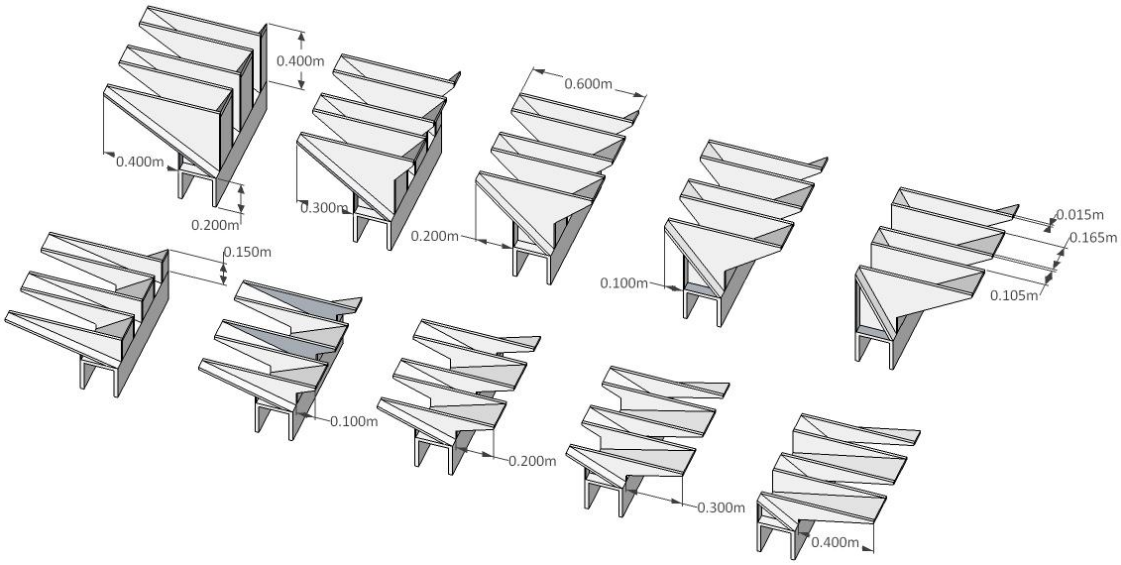

Figure IX-1 Experimental layout of PKW models with varying overhangs lengths

IX.3. Influence of the upstream/downstream overhangs lengths ratio

IX.3.1. Head-discharge curve

The most largely used structure of a PKW considers symmetric up- and downstream overhangs. The influence of the variation of the B_o/B_i ratio has thus been studied by comparison with the efficiency of the basic geometry considering a ratio $B_o/B_i = 1$ (Type A).

IX.3.1.1. Hydraulic optimization of the PKW height

Considering the optimal weir height for hydraulic considerations (Figure IX-2), the model with $B_o/B_i = 3$ is around 10% more efficient than the basic geometry. Even if, for low heads, the model with only upstream overhangs ($B_o/B_i = \infty$ - type B) seems relevant. With increasing heads, its released discharge is similar to the one of the symmetric model. For B_o/B_i ratios lower than 1, the discharge capacity of the weir decreases constantly compared with the basic geometry, whatever the ratio between the head H and the PKW-unit width W_u. A PKW with only downstream overhangs ($B_o/B_i = 0$ – type C) is up to 10% less efficient than the basic symmetric geometry.

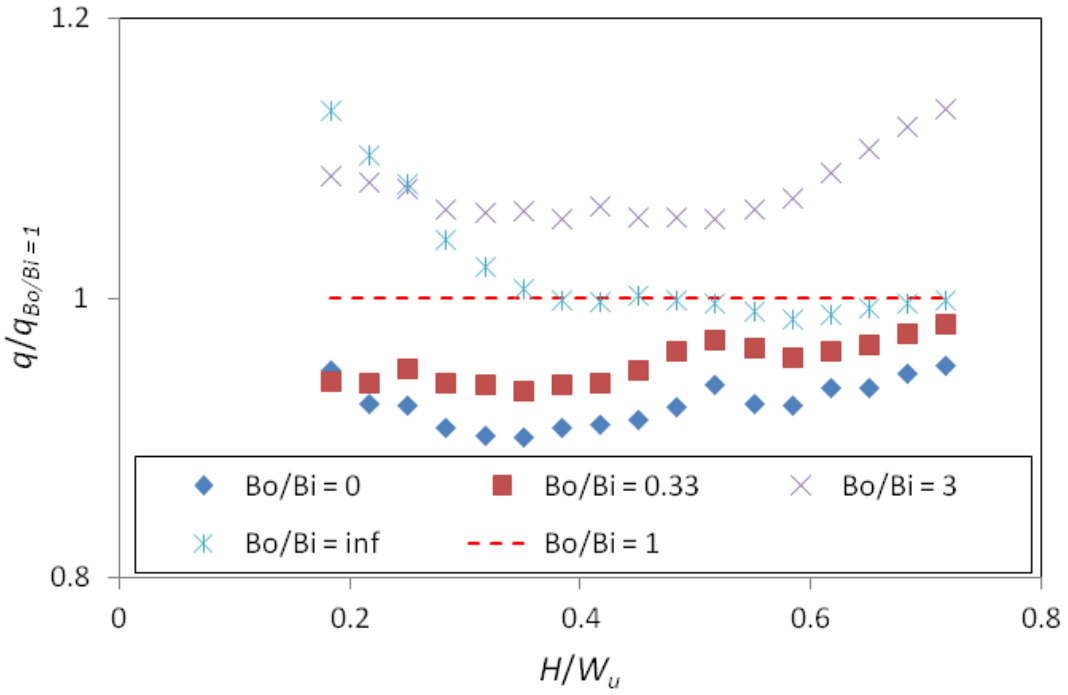

Figure IX-2 Comparison of the specific discharges provided by PKWs with various B_o/B_i ratios considering the hydraulic optimal weir height

IX.3.1.2. Technico-economic optimization of the PKW height

Considering an optimal weir height for technico-economic considerations (Figure IX-3), the model with $B_o/B_i = 3$ is no more relevant.

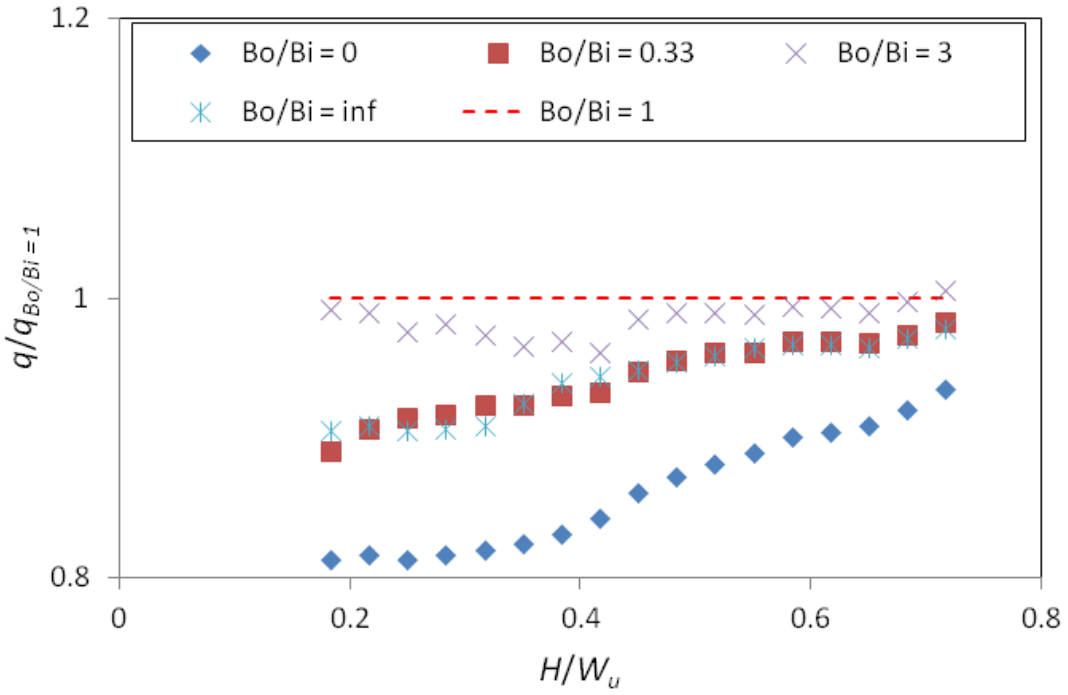

Figure IX-3 Comparison of the specific discharges provided by PKWs with various B_o/B_i ratios considering a technico-economic optimal weir height

For low heads, it provides discharges until 5% lower than the basic geometry, and for higher heads, it releases similar discharges. The model with only upstream

overhangs is also no more relevant. The loss in efficiency compared with the symmetric model is all the more important as the upstream head decreases. The loss in efficiency reaches 10% for lowest heads and only 1% for highest ones. For B_o/B_i ratios under 1, the observed decrease in efficiency is this time influenced by the upstream head. For low heads, the decrease reaches until 20% for the model with only downstream overhangs. For high heads, the release capacity is closer from the one of the symmetric model.

IX.3.1.3. Relative influence of weir height and overhangs lengths variations

One more time, it is important to keep in mind that the influence of the weir height is of prime importance. The comparison of the specific discharges evacuated by the models considering a technico-economic ($q_{T\text{-}E}$) or a hydraulic (q_H) optimization of the weir height shows that the first ones are between 20 and 40% less efficient than the second ones (Figure IX-4). The loss in efficiency is all the more important as the overhangs are non-symmetric. The influence of the weir height is thus more important on Type B and C PKWs.

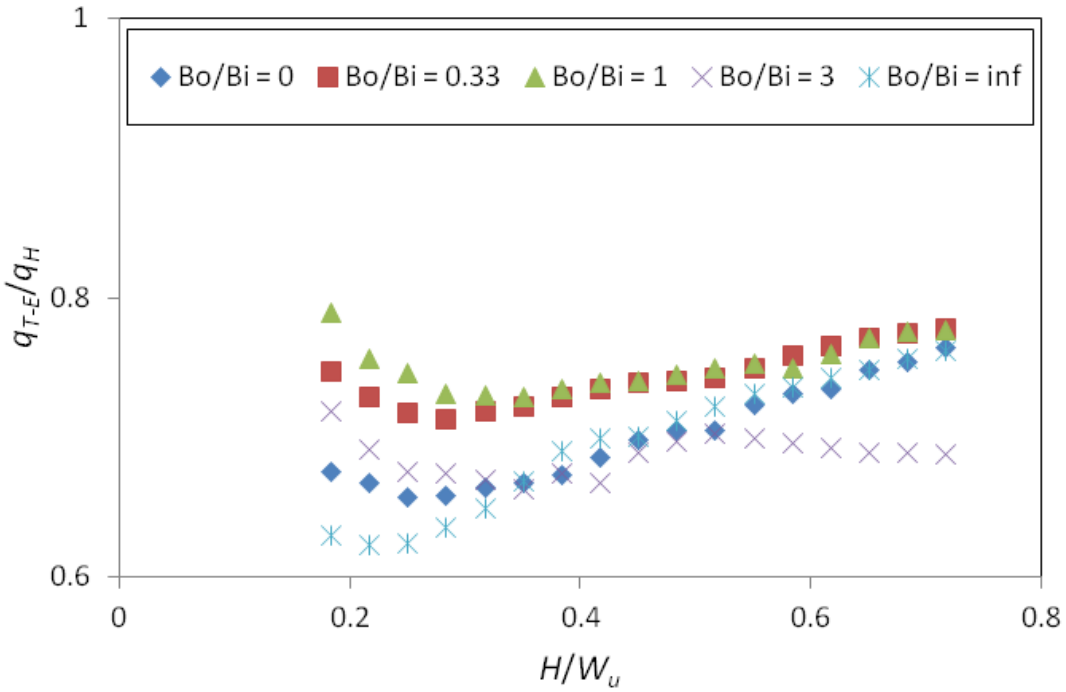

Figure IX-4 Comparison of the specific discharges provided by PKWs with various B_o/B_i ratios considering a technico-economic or hydraulic optimal weir height

IX.3.2. Free surface profile

IX.3.2.1. Inlet key profile for hydraulic optimization of the PKW height

Regarding the free surface profiles measured in the middle of the inlet key for the models with the hydraulic optimization of the weir height, they stays relatively close to the horizontal (Figure IX-5). However, for low heads ($H \leq 0.155$ m), a decrease

of the free surface level is observed at the downstream end, traducing an increase of the flow velocity. For high heads ($H \geq 0.155$ m), a free surface decrease is observed at inlet entrance, traducing the velocity increase induced by the flow contraction. This free surface lowering is all the more important as the upstream overhangs length decreases. For the model without upstream overhangs, this decrease provides too important free surface slopes to allow a correct measurement of the free surface with the ultrasound sensors.

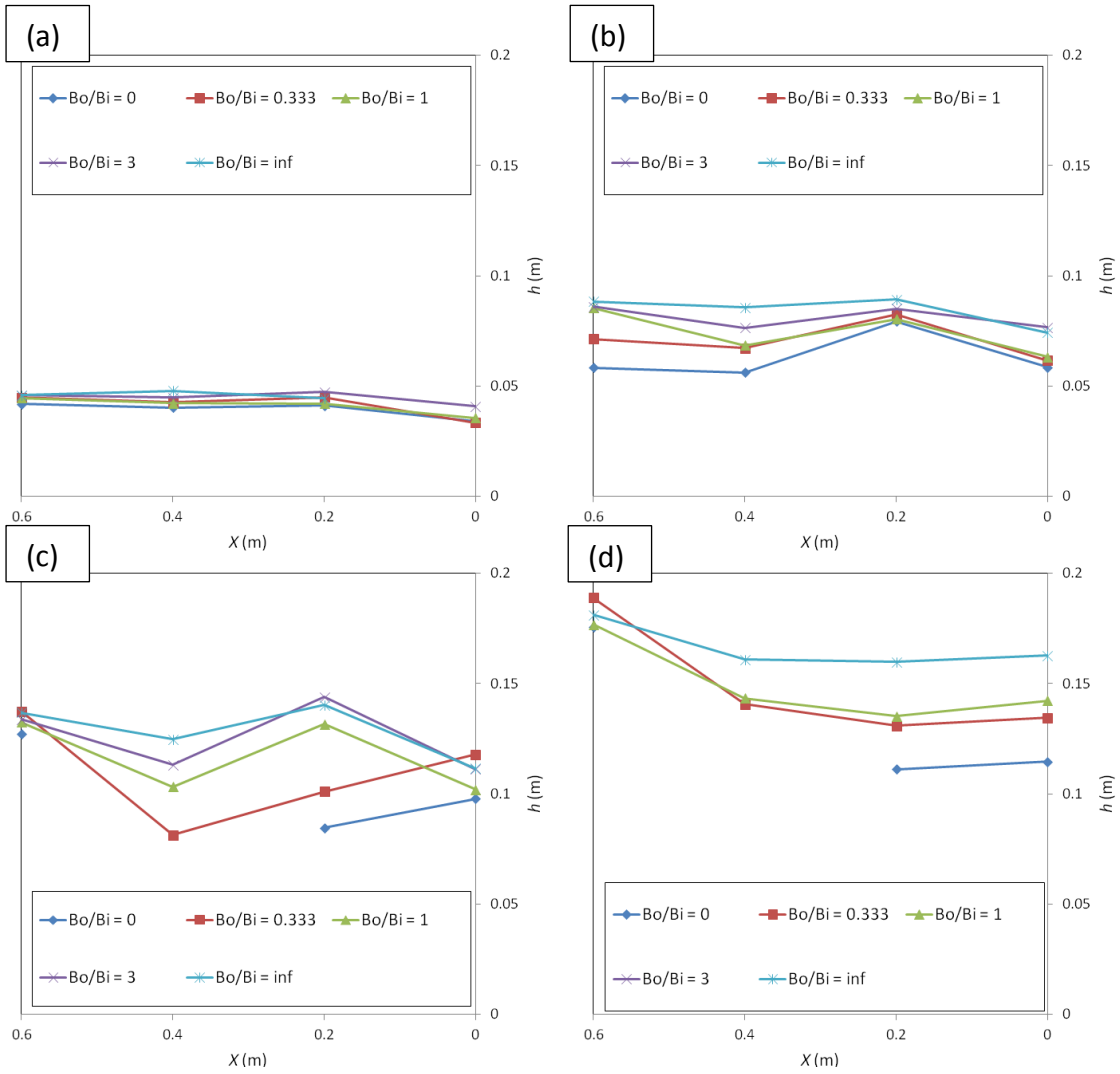

Figure IX-5 Free surface profiles in the middle of the inlet key for hydraulic optimal PKW height: (a) H = 0.05 m; (b) H = 0.1 m; (c) H = 0.155 m; (d) H = 0.21 m

The observation of the inlet free surface profiles (Figure IX-8) confirms the measurements, showing a decrease of the free surface level at the inlet key entrance, due to the flow contraction and to the substantial velocity increase. This decrease is all the more important as the upstream overhangs length decreases (Figure IX-6). On the downstream part of the key the free surface profile is near the horizontal (Figure IX-6), traducing no velocity variation along the key.

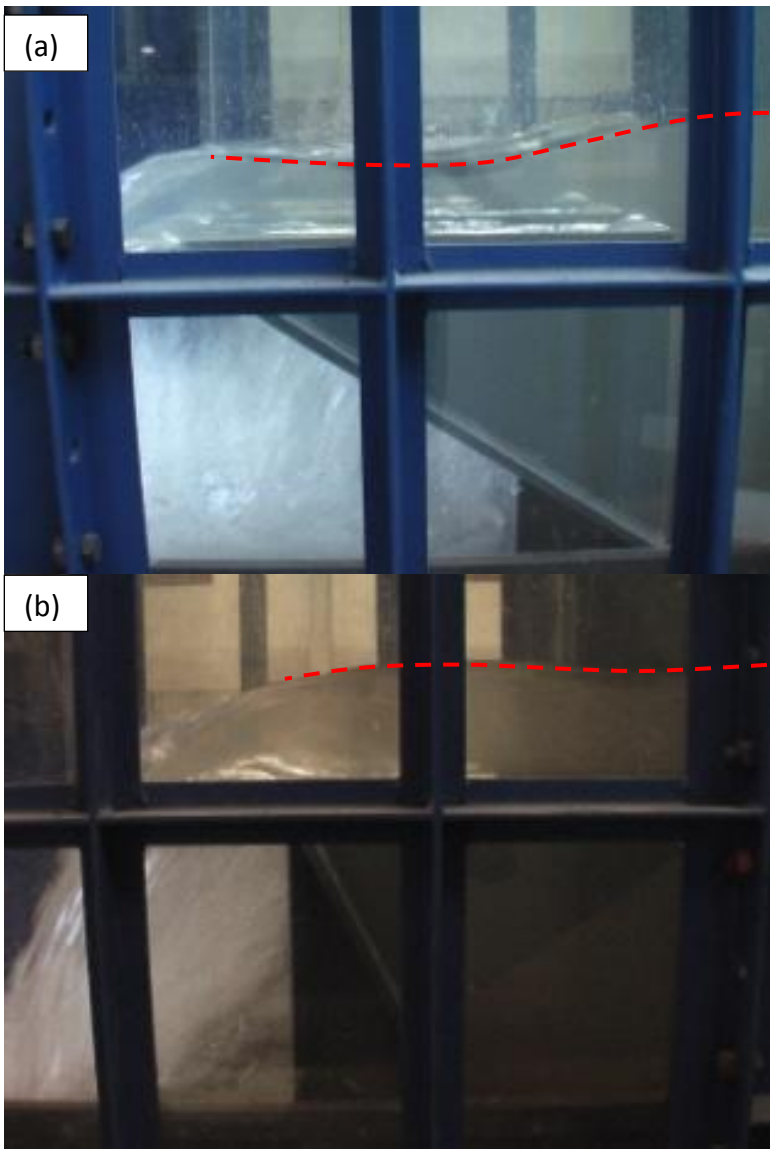

Figure IX-6 View of the inlet free surface variation for hydraulic optimal weir height and H = 0.155 m: B_o/B_i = (a) – 0; (b) –∞

For $B_o/B_i \leq 3$, the combined influence of the velocity increase and the free surface lowering is directly highlighted on the PKW stage-discharge curve, as it decreases the side crest efficiency (Figure IX-7). For $B_o/B_i = \infty$, the stage-discharge curve is not significantly modified compared with the model considering symmetric overhangs, even if the varied free surface levels traduce variations of the inlet key flow velocity.

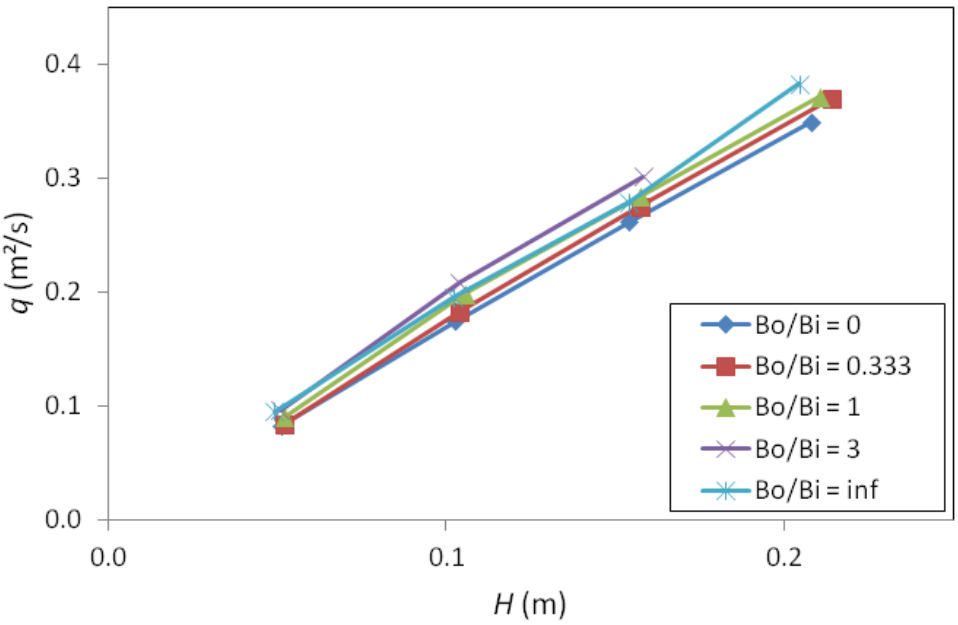

Figure IX-7 Stage-discharge curves of the models with hydraulic optimal PKW height

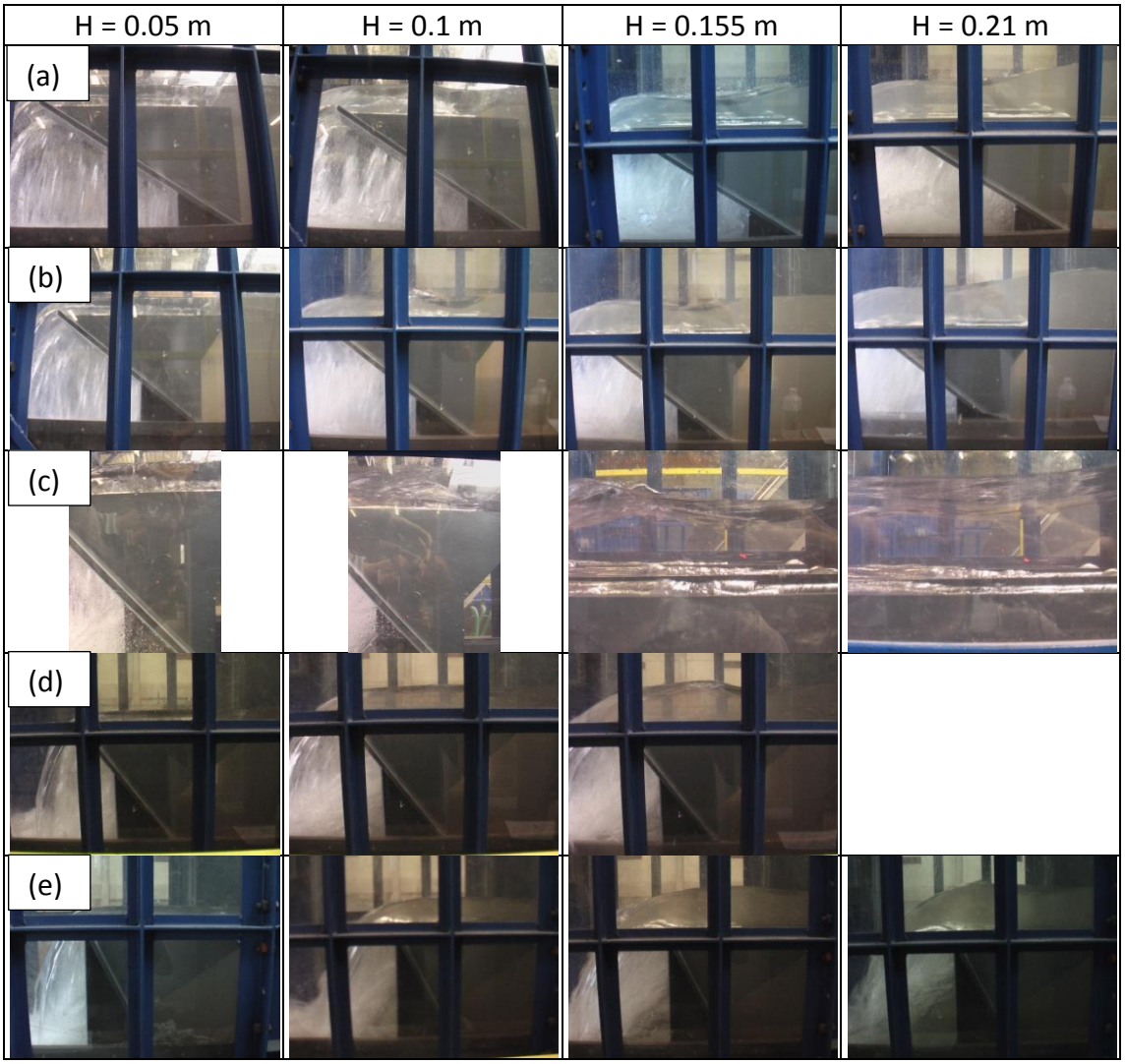

Figure IX-8 View of the inlet free surface variation with head for hydraulic optimal weir height: B_o/B_i = (a) – 0; (b) – 0.333; (c) – 1; (d) – 3; (e) – ∞

IX.3.2.2. Outlet key profile for hydraulic optimization of the PKW height

The observation of the free surface profiles along the outlet key (Figure IX-10) highlights supercritical flows whatever the overhangs position (Figure IX-9 – (a)). However, for $H \geq 0.1$ on the model with only upstream overhangs ($B_o/B_i = \infty$), the outlet slope is no more sufficient to ensure supercritical flows (Figure IX-9 – (b)). The outlet flow partially submerges the side crest, what decreases significantly the side crest discharge.

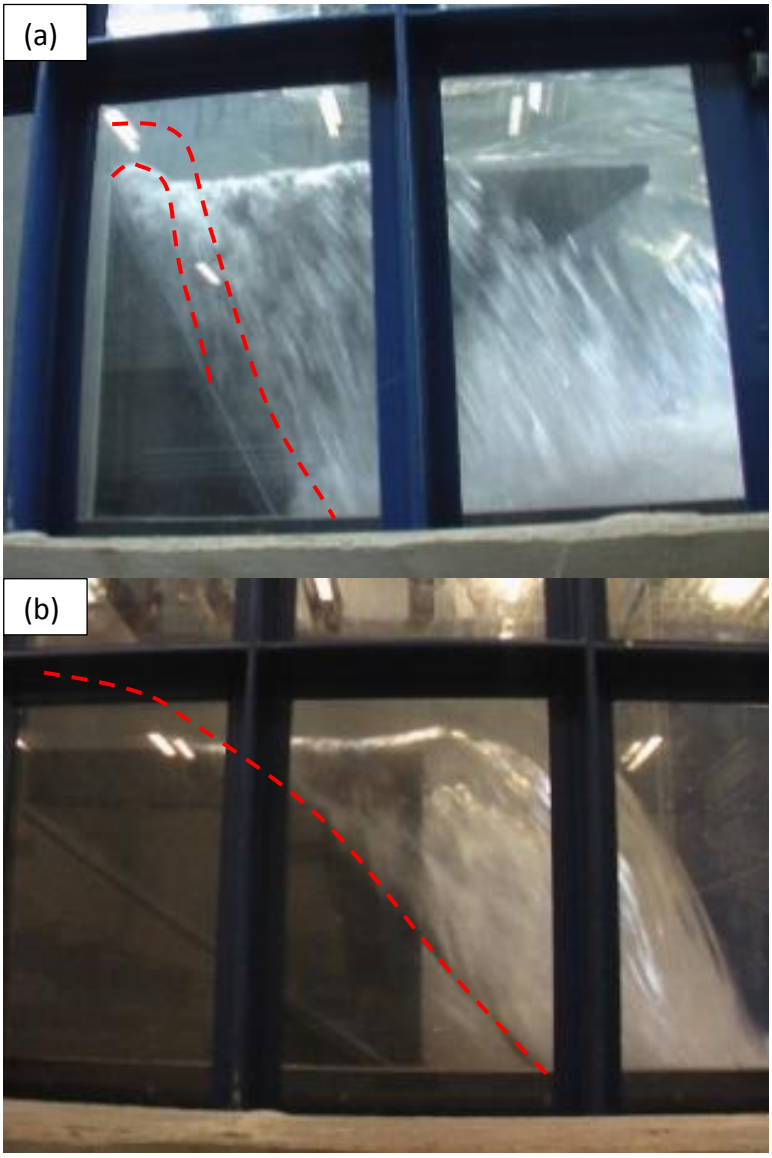

Figure IX-9 View of the outlet free surface variation for hydraulic optimal weir height and H = 0.155 m: B_o/B_i = (a) – 0; (b) – ∞

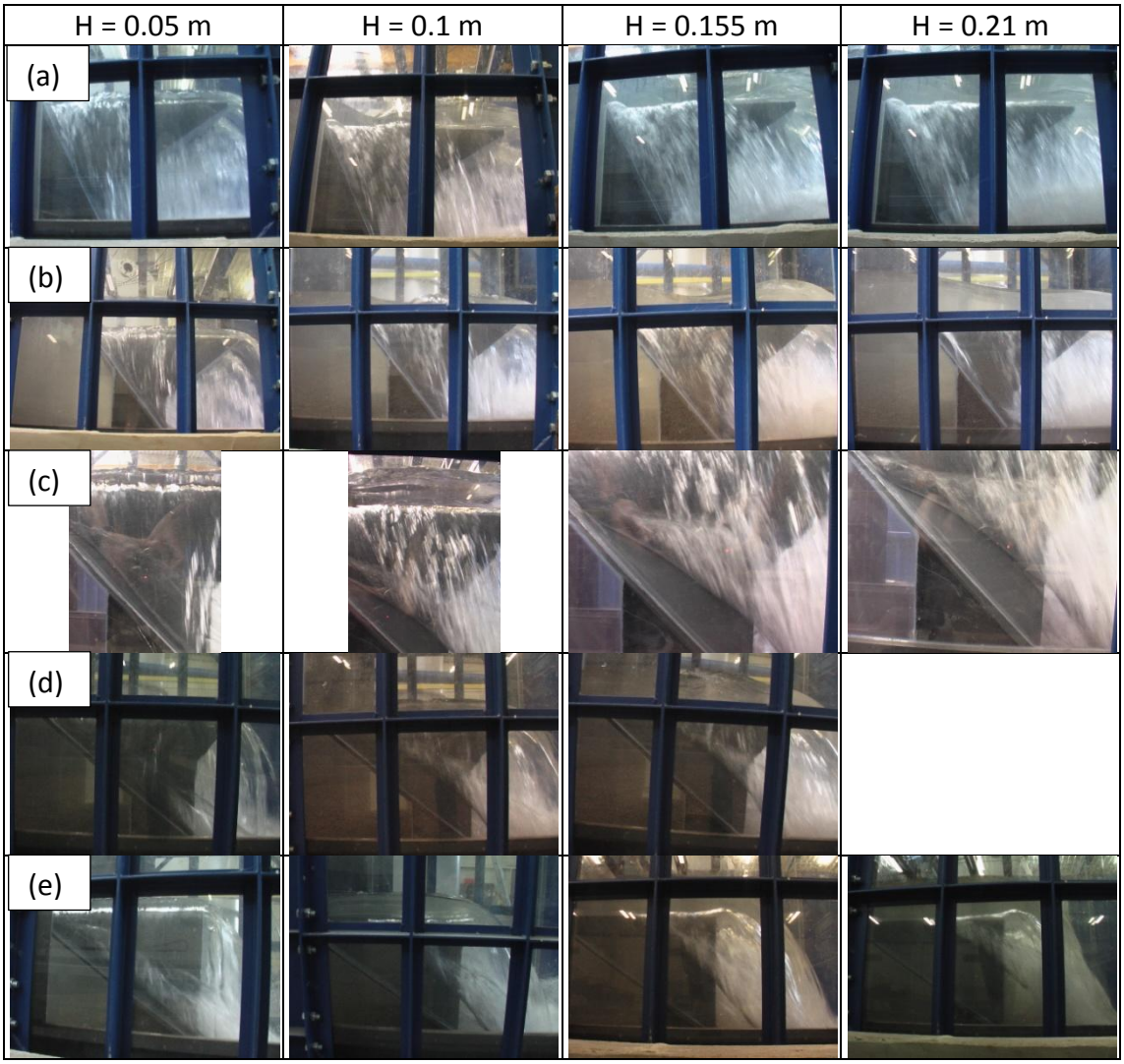

Figure IX-10 View of the outlet free surface variation with head for hydraulic optimal weir height: B_o/B_i = (a) – 0; (b) – 0.333; (c) –1; (d) – 3; (e) – ∞

This enables to explain the non-variation of the PKW efficiency in comparison with the symmetric model for this B_o/B_i value (Figure IX-7). The gain in efficiency obtained from the combined influence of velocity decrease and water height increase along the inlet key is counterbalanced by the loss in efficiency induced by the side crest submergence.

IX.3.2.3. Transverse profile for hydraulic optimization of the PKW height

Regarding the transverse free surface profiles (Figure IX-11), no influence of the overhangs position can be observed.

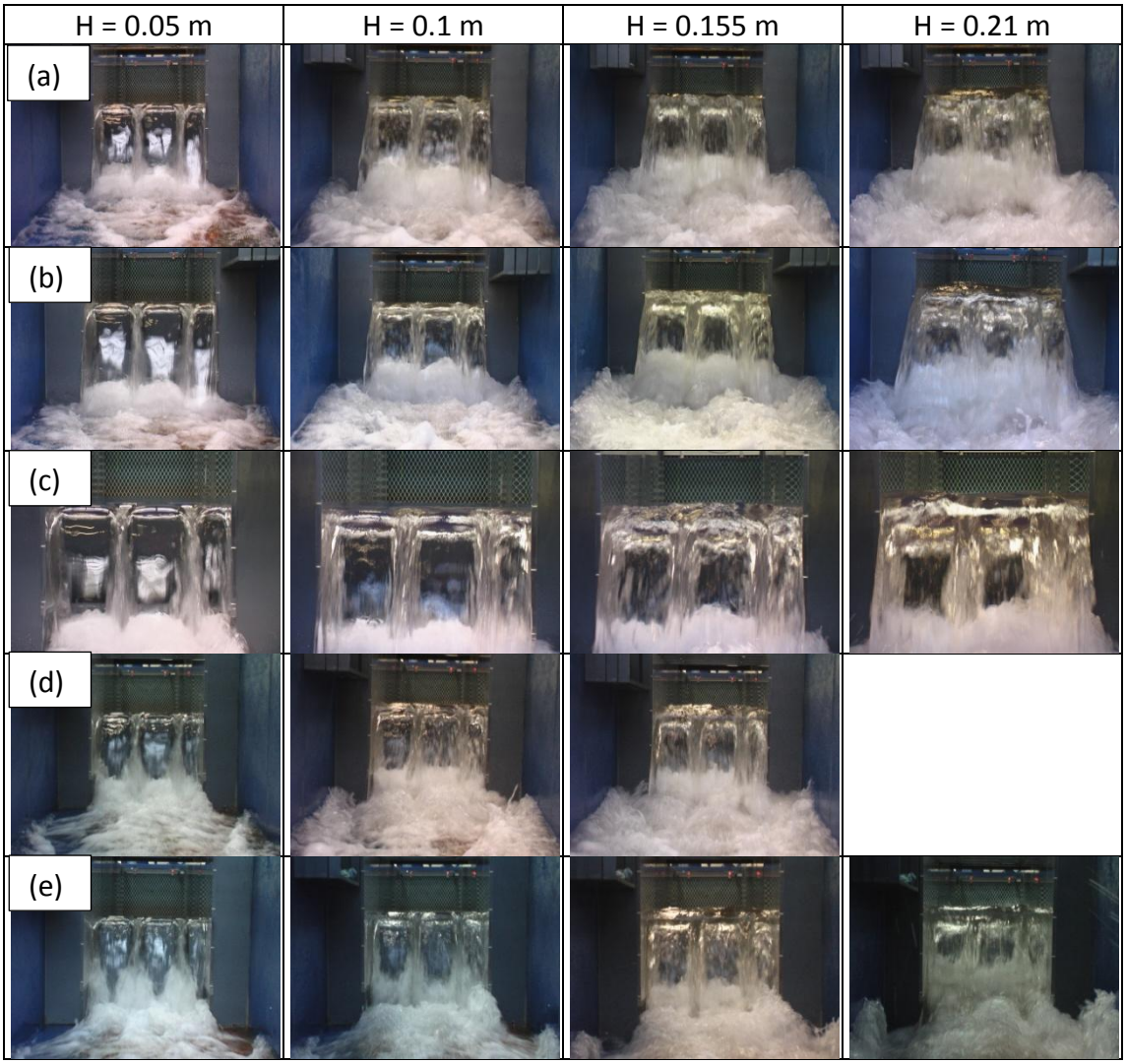

Figure IX-11 View of the transverse free surface variation with head for hydraulic optimal weir height: B_o/B_i = (a) – 0; (b) – 0.333; (c) –1; (d) – 3; (e) – ∞

IX.3.2.4. Inlet key profile for technico-economic optimization of the PKW height

Considering a technico-economic optimization of the weir height, a continuous decrease of the measured free surface level is observed from the upstream to the downstream of the inlet key (Figure IX-12). For B_o/B_i = 1, this decrease is quasi-constant along the key, traducing constant acceleration of the flow. For B_o/B_i > 1, the decrease is more important in the downstream part of the key, traducing more important flow acceleration near the downstream apex. For B_o/B_i < 1, on the contrary, the more important free surface decrease is observed at the inlet entrance, traducing a more important acceleration induced by the flow contraction. For high heads, this

decrease provides too important free surface slopes to allow a correct free surface measurement for lowest B_o/B_i ratios

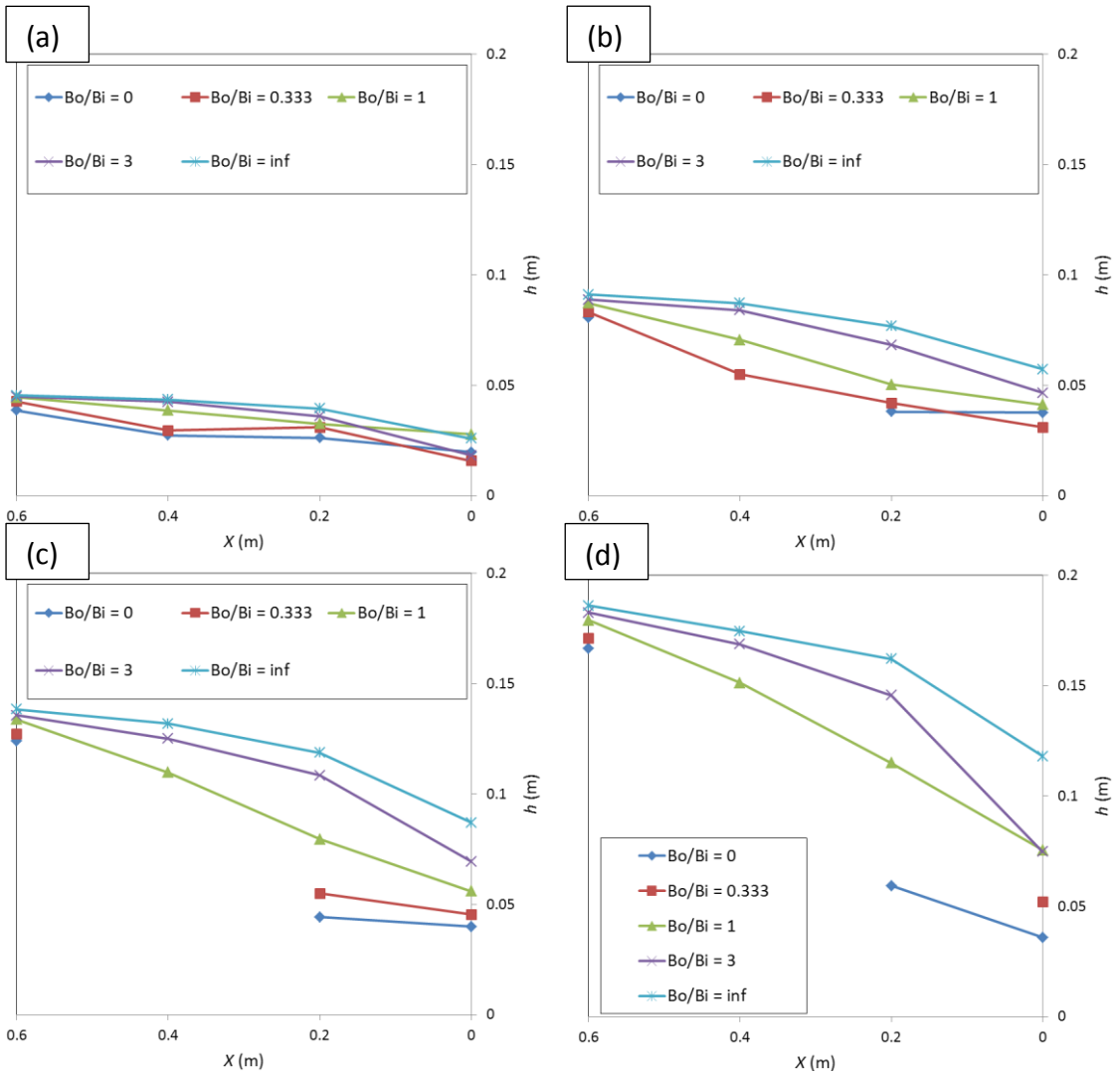

Figure IX-12 Free surface profiles in the middle of the inlet key for technico-economic optimal PKW height: (a) H = 0.05 m; (b) H = 0.1 m; (c) H = 0.155 m; (d) H = 0.21 m

The observation of the free surface profiles along the inlet key (Figure IX-15) confirms the measured flow characteristics. The free surface level decreases continuously from the inlet key entrance to its downstream apex (Figure IX-13). The slope of the free surface at inlet entrance is all the more important as the upstream overhangs length decreases. The slope of the free surface at the downstream apex is all the more important as the downstream overhangs length decreases.

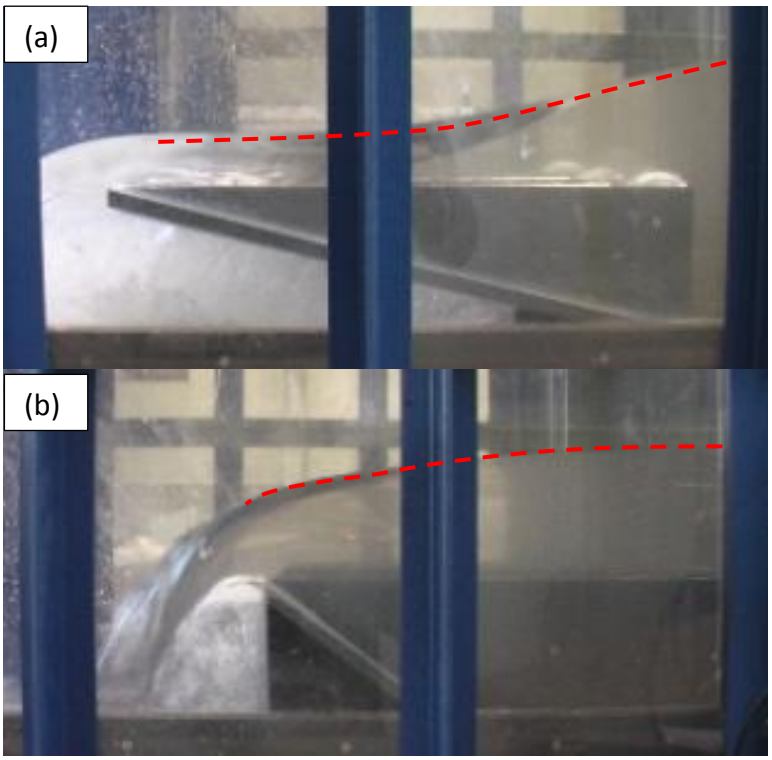

Figure IX-13 View of the inlet free surface variation for technico-economic optimal weir height and H = 0.155 m: B_o/B_i = (a) – 0; (b) – ∞

For $B_o/B_i < 1$, the higher longitudinal velocities and the corresponding lowering of the free surface level decrease the side crest efficiency and thus the PKW discharge (Figure IX-14). For $B_o/B_i > 1$, even if the free surface level increases for increasing B_o/B_i ratio, traducing lower inlet key velocities, the stage discharge curve is lowered. The flow velocity along the inlet key seems thus to have no influence on the side crest efficiency.

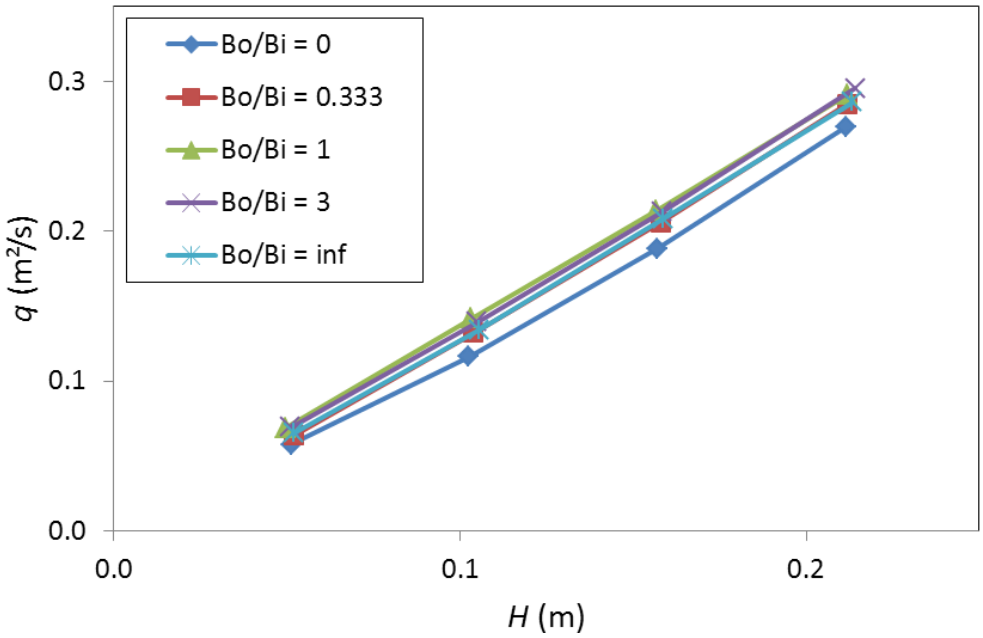

Figure IX-14 Stage-discharge curves of the models with technico-economic height

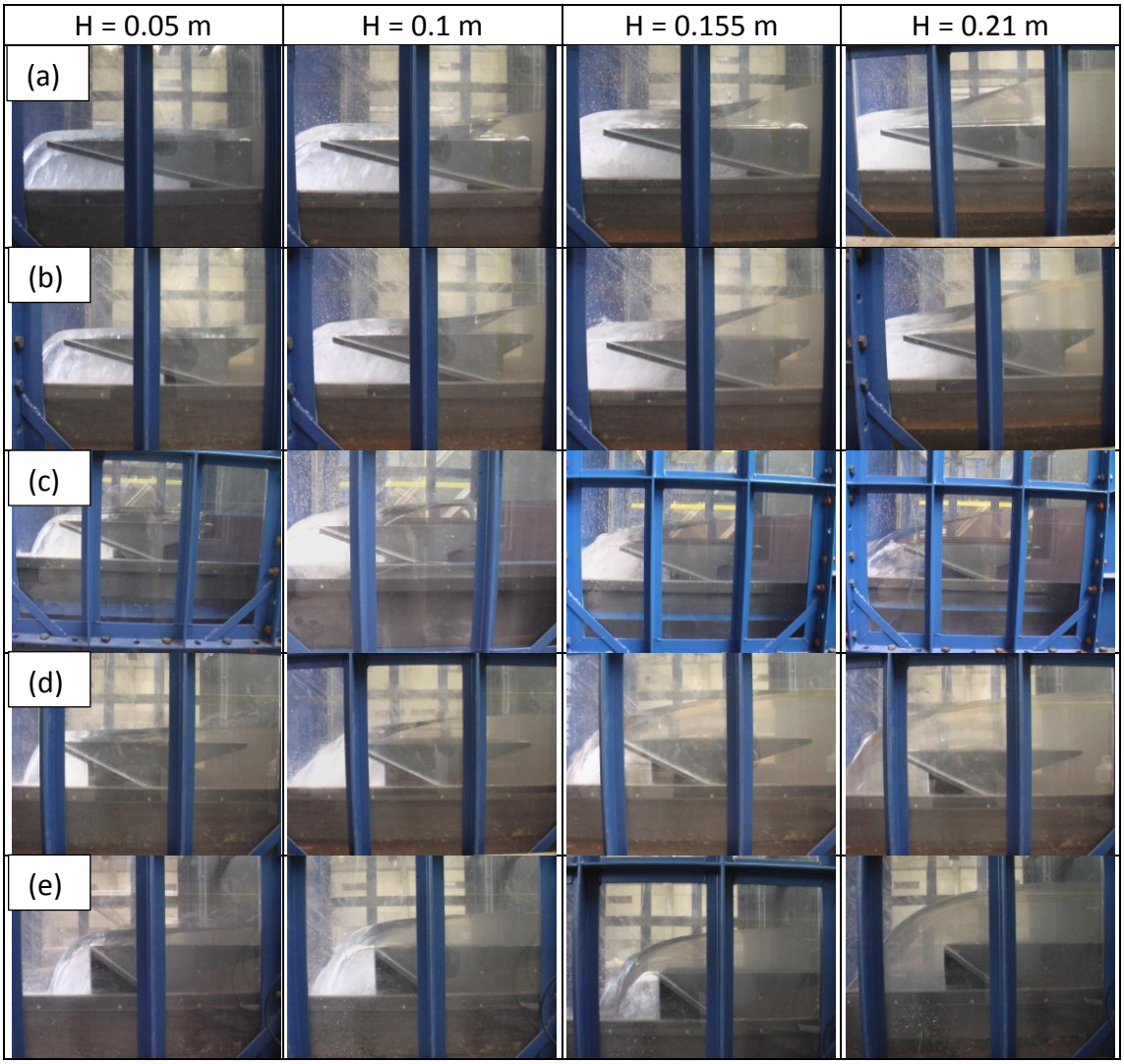

Figure IX-15 View of the inlet free surface variation with head for technico-economic optimal weir height: B_o/B_i = (a) – 0; (b) – 0.333; (c) –1; (d) – 3; (e) – ∞

IX.3.2.5. Outlet key profile for technico-economic optimization of the PKW height

Regarding the free surface profiles along the outlet key (Figure IX-17), subcritical flows have been observed on all tested models except for the lowest heads on models with longer downstream overhangs (Figure IX-16 – (a)). The subcritical outlet flow decreases the upstream crest efficiency. Furthermore, the free surface level rises over the crest on a non-negligible part of the side wall, what decreases the side crest efficiency on this part (Figure IX-16 – (b) and (c)).

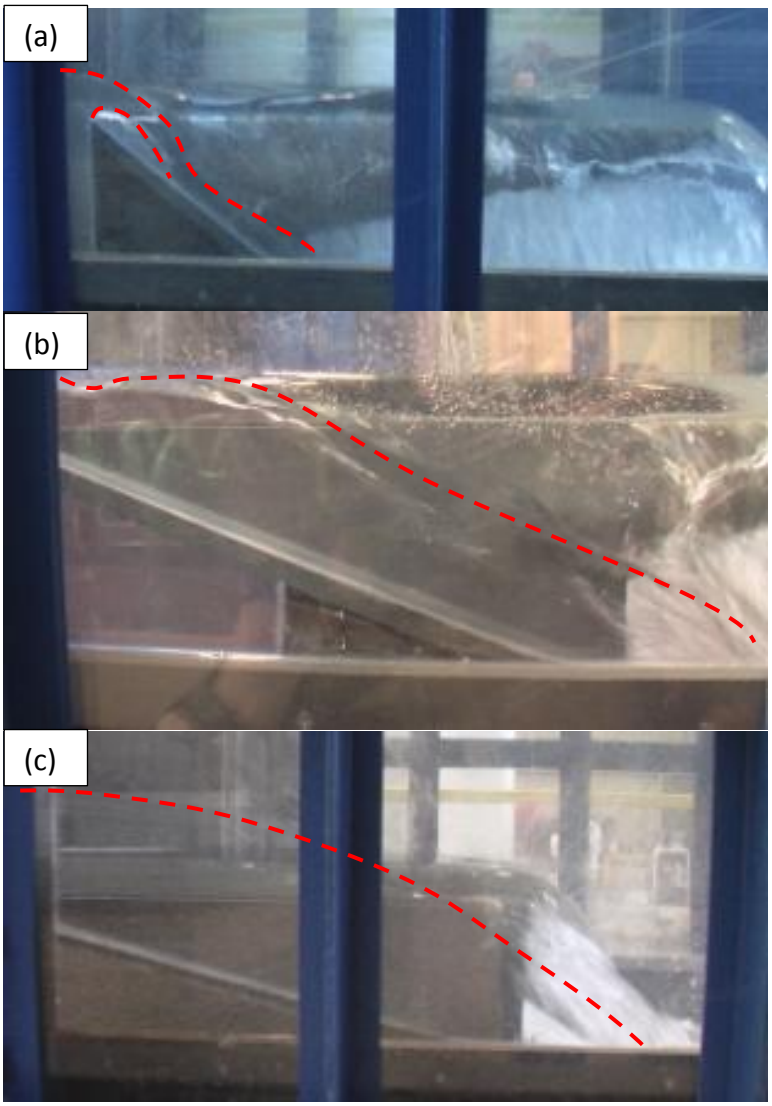

Figure IX-16 View of the outlet free surface variation for technico-economic optimal weir height and H = 0.05 m: B_o/B_i = (a) – 0; (b) – 1; (c) – ∞

As the submerged side crest length increases with decreasing outlet key slope, i.e. with increasing upstream overhangs length, the outlet key flow behaviour enables to explain the variation of the stage discharge curves for varied B_o/B_i ratios (Figure IX-14). For $B_o/B_i < 1$, the increase in side crest efficiency, observed with increasing B_o/B_i ratios, due to lower flow velocities and higher free surface levels along the inlet key stays more important than the decrease created by the partial submergence of the side crest by the outlet flow. The PKW discharge capacity increases with the B_o/B_i ratio. For B_o/B_i ratios increasing over 1, the length of submerged crest becomes of main importance and the PKW discharge capacity decreases.

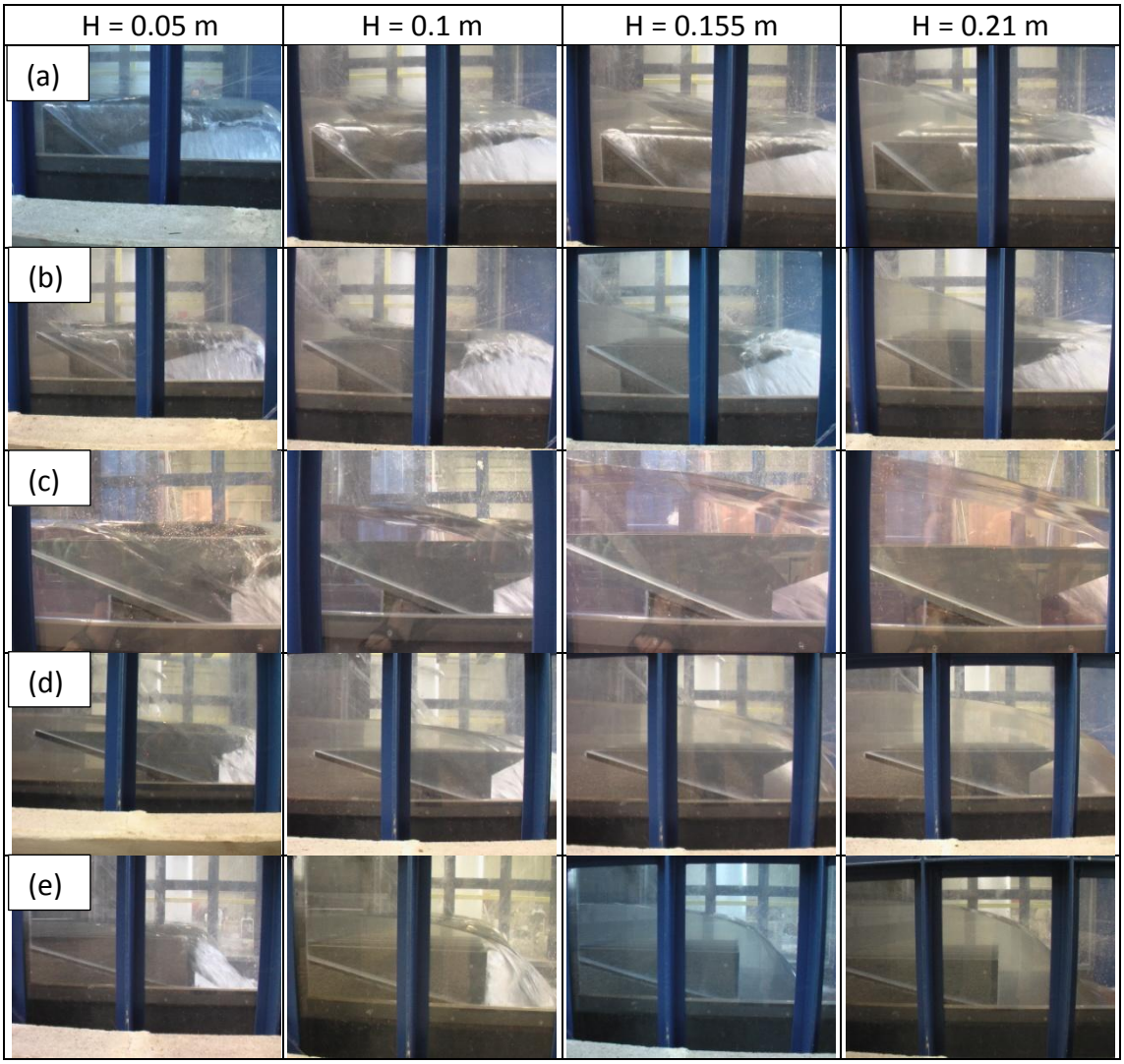

Figure IX-17 View of the outlet free surface variation with head for technico-economic optimal weir height: B_o/B_i = (a) – 0; (b) – 0.333; (c) – 1; (d) – 3; (e) – ∞

IX.3.2.6. Transverse profile for technico-economic optimization of the PKW height

The observation of the transverse free surface profiles (Figure IX-19) enables to highlight one more time the non-influence of the overhangs position on the interference zone between side nappes. However, the observation of transverse profiles allows highlighting the influence of the B_o/B_i ratio on the nappe aeration. Models with shorter downstream overhangs ($B_o/B_i \geq 1$) are no more aerated for high heads (Figure IX-18) and thus probably need artificial aerators.

Figure IX-18 No more air entrainment and leaping nappe on the model with technico-economic height optimization for H = 0.155 m and Bo/Bi = ∞

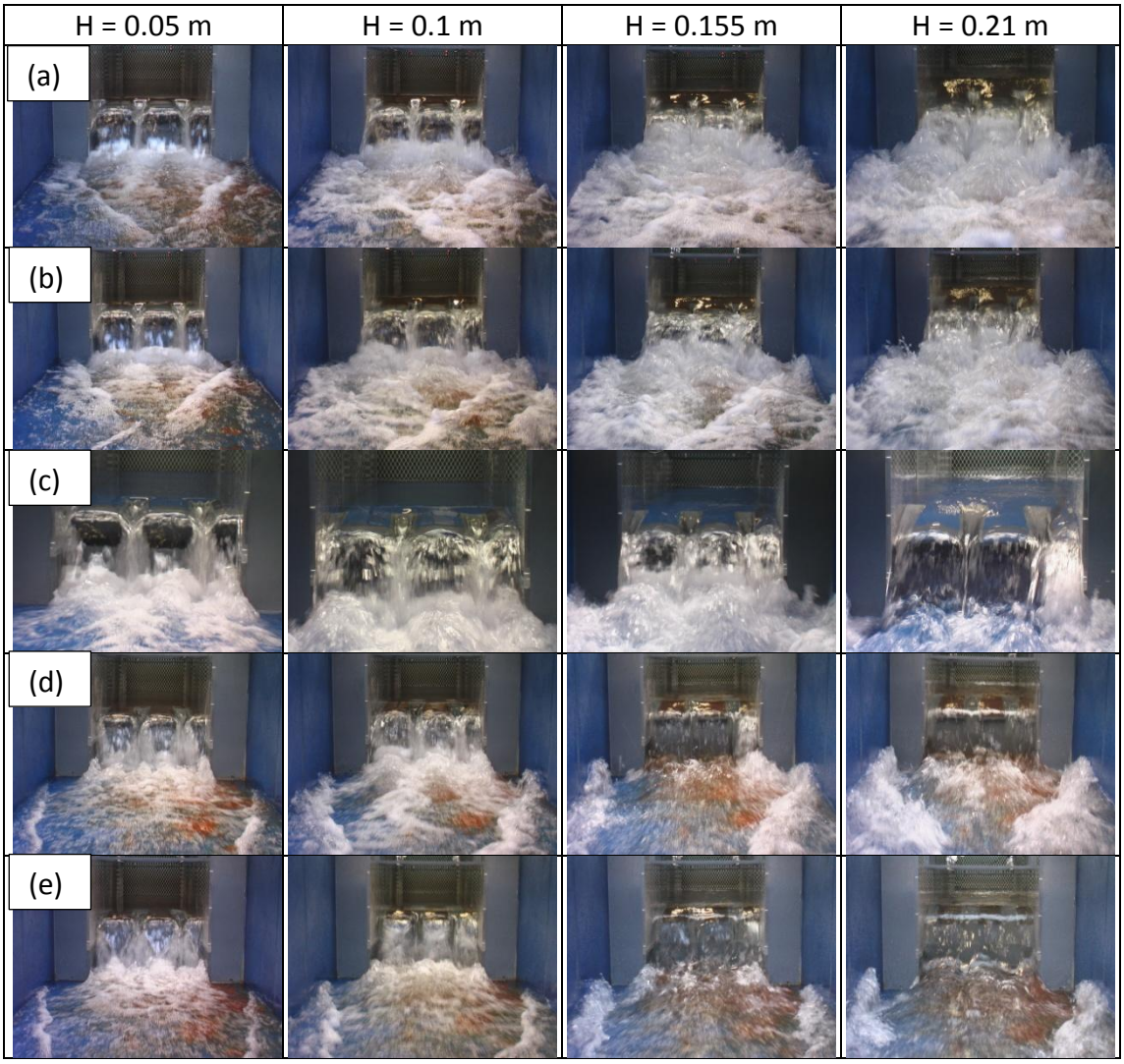

Figure IX-19 View of the transverse free surface variation with head for technico-economic optimal weir height: B_o/B_i = (a) – 0; (b) – 0.333; (c) –1; (d) – 3; (e) – ∞

IX.3.3. Analytical approach

Regarding the analytical formulation developed in VIII.4.3 the models with varying B_o/B_i ratios are poorly computed (Figure IX-20). This was expected from the comparison of the proposed analytical formulation with the Le Doucen [61] results (see VIII.4.3).

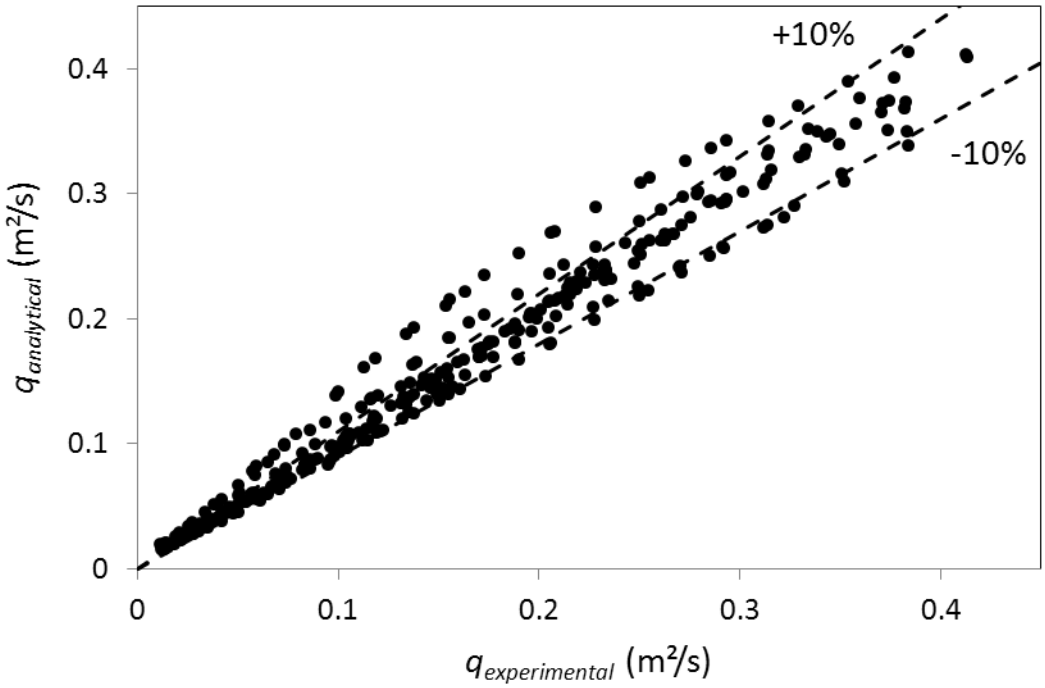

Figure IX-20 Comparison of the specific discharges computed by the analytical formulation proposed in VIII.4.3 and experimental results from models with varying B_o/B_i

The main cause may be due to the poor approach of the influence of the outlet key slope on the side crest submergence. The outlet key slope influence the definition of the two limits L_1 and L_2 characterizing the side crest submergence (Eqs. VIII-10 and VIII-11). However, in section VIII.4, only two outlet slopes were available to fit these limits. Applying a least square method to the results obtained on the 10 models with varying overhangs lengths, providing varying outlet slopes, the limits L_1 and L_2 are:

$$L_1 = -0.788 S_o^{-1.88} + 5 \qquad \text{IX-1}$$

$$L_2 = 0.236 S_o^{-1.94} + 5 \qquad \text{IX-2}$$

The comparison of the specific discharges computed applying this new definition of the limits L_1 and L_2 with the experimental discharges measured on the 10 tested models with varied overhangs lengths is shown on Figure IX-21. It highlights that the experimental results are approached with an accuracy of 10%, except for the model with only downstream overhangs and technico-economical optimized weir height. The loss in efficiency observed for low heads on this experimental model can be related to

the very low water depths observed on the downstream part of the inlet key, that are not sufficiently well represented by the proposed analytical approach.

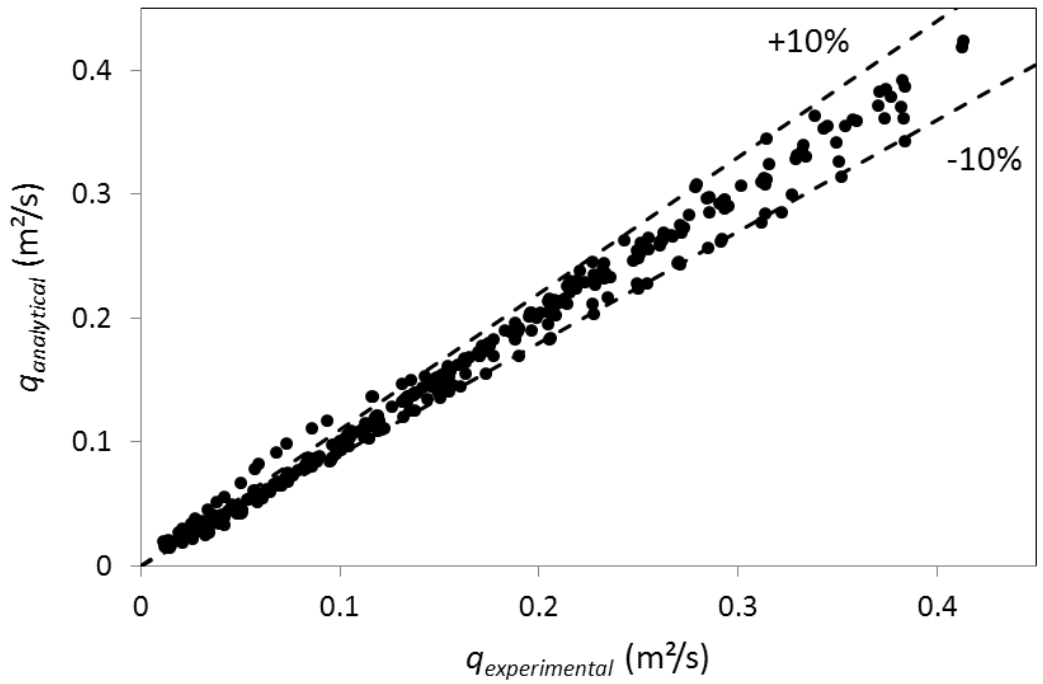

Figure IX-21 Comparison of the specific discharges computed by the corrected analytical formulation and experimental results from models with varying B_o/B_i

The proposed analytical formulation is one more time compared with the experimental results obtained by Le Doucen [61].

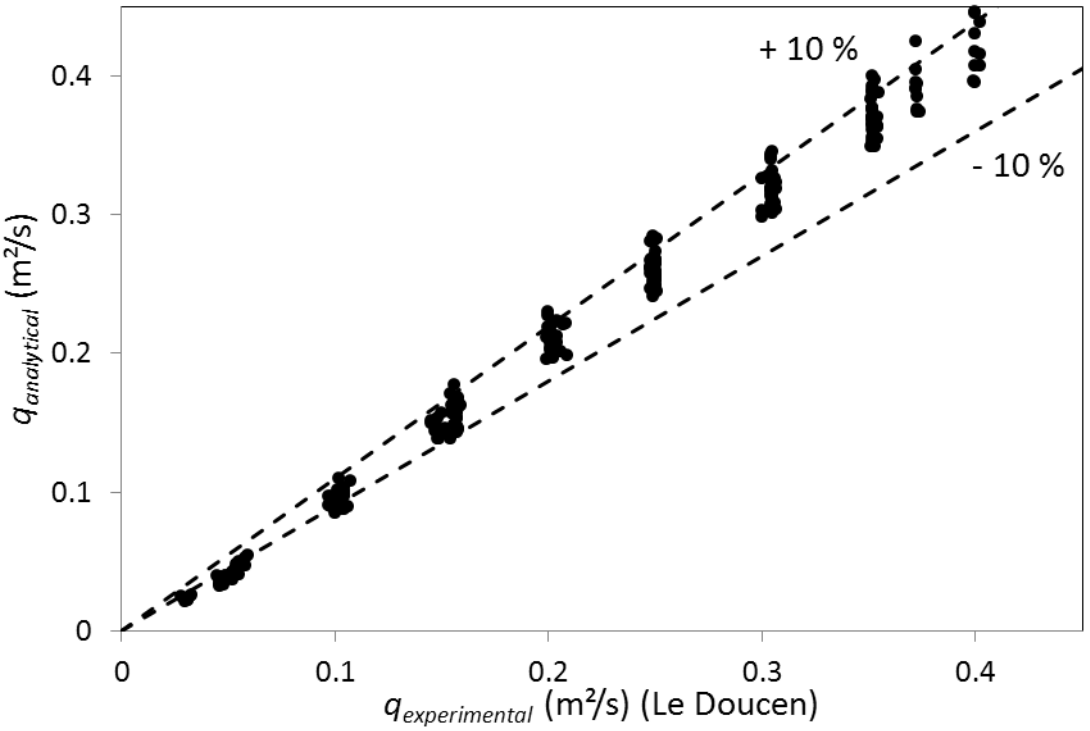

Figure IX-22 Comparison of the specific discharges computed by the final analytical formulation and experimental results of Le Doucen [61]

The comparison of the experimental results of Le Doucen, obtained for B_o/B_i = 1 and varied ratios L/W = 3 to 7, W_i/W_o = 0.5 to 2, and P_i/P_o = 0.72 to 1.4, with the final analytical formulation is shown on Figure IX-22. The accuracy of the analytical approach, compared with the results of Le Doucen, is around 10% for most of the tested geometries.

IX.3.4. Numerical approach

As for other studied parameters, the tested models with varied overhangs lengths have been modelled numerically using the enhanced version of Wolf1D-PKW (see XIV.2).

IX.3.4.1. Hydraulic optimization of the PKW height

Considering the hydraulic optimization of the weir height, the accuracy of the numerical model is 10% to predict the discharge capacity of a PKW geometry (Figure IX-23). However, whatever the B_o/B_i ratio, the PKW discharge capacity is systematically underestimated and the analytical formulation is more relevant regarding the comparison with experimental results.

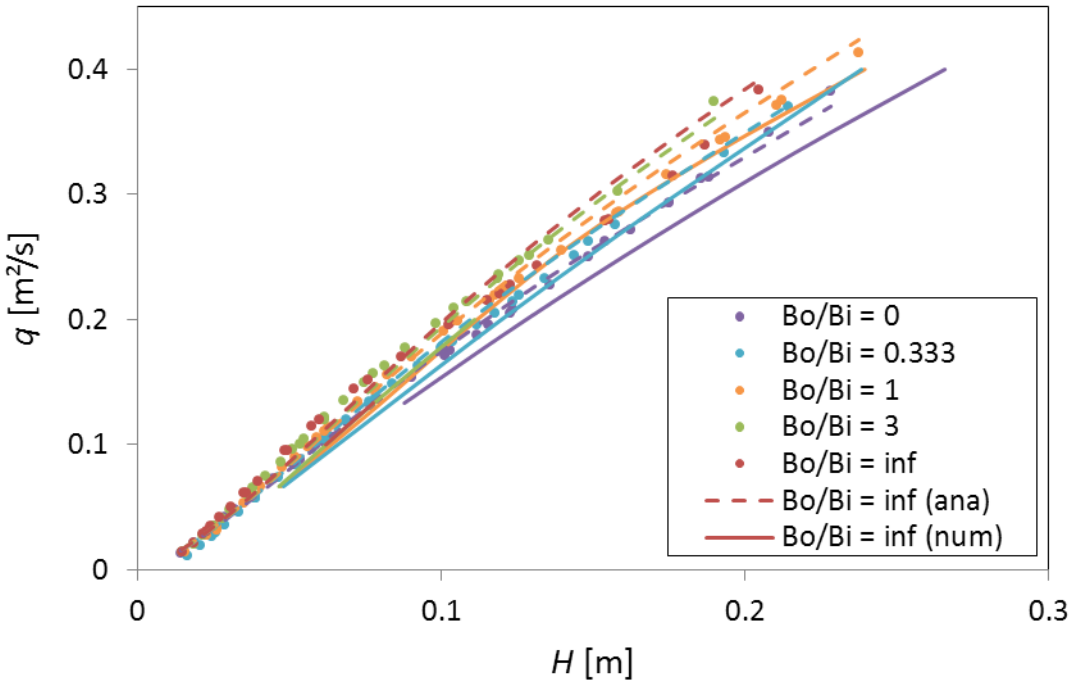

Figure IX-23 Comparison between stage discharge curves obtains from experimental, analytical and numerical approaches for hydraulic optimal weir height

The 1D numerical solver also gives information on the free surface profiles and on the position of the critical section along the inlet key.

IX.3.4.1.1. B_o/B_i = 1

Figure IX-24 and Table IX-2 show the comparison between the free surface profiles along the inlet and outlet keys computed with the enhanced version of Wolf1D-PKW for B_o/B_i = 1 and the experimental results.

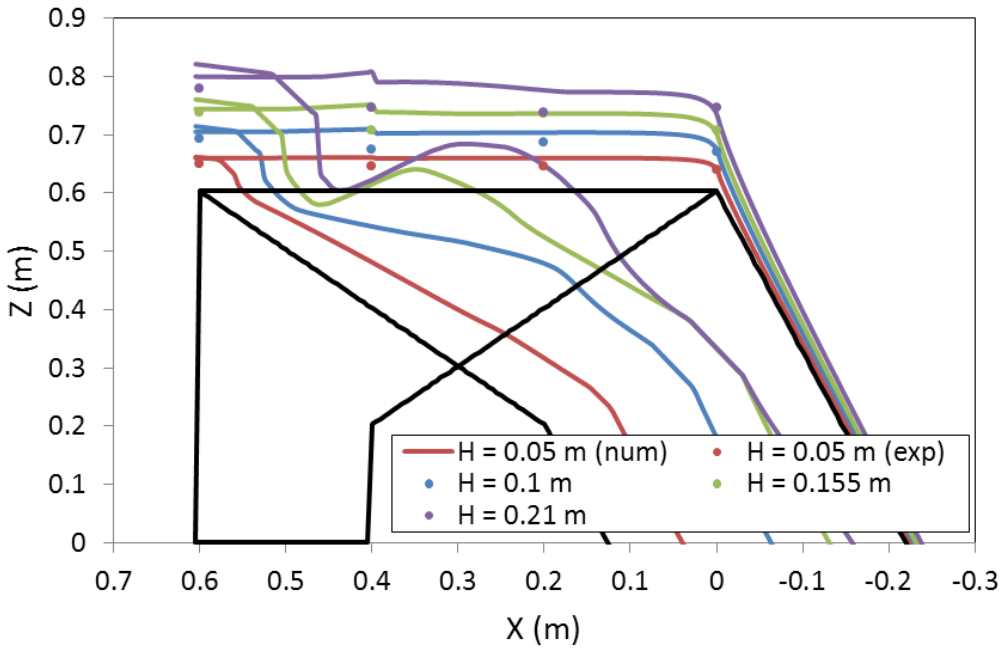

Figure IX-24 Comparison between measured free surface levels and profiles provided by Wolf1D-PKW for B_o/B_i = 1 and hydraulic optimal weir height

Table IX-2 – Comparison of experimental and numerical results for B_o/B_i = 1 and hydraulic optimal weir height

X (m)	*H* (m)	Δ*h*/*h* (%)	*X* (m)	*H* (m)	Δ*h*/*h* (%)
0.6	0.05	22.9	0.2	0.05	30.9
	0.1	13		0.1	18.7
	0.155	4.9		0.155	0.3
	0.21	10.9		0.21	27.9
0.4	0.05	31.3	0	0.05	3.5
	0.1	38.8		0.1	7.9
	0.155	30.9		0.155	3.8
	0.21	31.3		0.21	6.5

Regarding the inlet free surface profile, the upstream (*X* = 0.6 m) and downstream (*X* = 0 m) levels are in a better agreement with experimental results. However, the decrease observed in free surface level at the inlet entrance (*X* = 0.4 m) on the scale models is poorly represented by the numerical solver. That difference comes, one more time, from the bad consideration of the progressive lateral contraction by the flow solver.

Regarding the outlet free surface profile, the upstream part seems in agreement with the observations made on the scale model with a flow quickly passing by a critical depth. However, the hydraulic jump observed on the numerical results for highest heads is not observed on the scale model. This may come from the longitudinal transfer of the flow between inlet and outlet keys. Indeed, the solver considers well the side flow inclination in the calculation of the mass and momentum transfers

between the keys. However, the transfers are realized perpendicularly to the side crest. Practically, the transfer follows the side flow inclination that is non-negligible for high heads. That phenomenon decreases the discharges along the outlet key and delay the apparition of the hydraulic jump observed on the numerical model. This hydraulic jump, moving the free surface level over the side crest one, enables to explain the PKW loss in efficiency observed, for high heads, on numerical results compared with the experimental ones (Figure IX-23).

IX.3.4.1.2. $B_o/B_i = 0$

Figure IX-25 and Table IX-3 show the comparison of the free surface profiles along the inlet and outlet keys computed with Wolf1D-PKW for B_o/B_i = 0 and the experimental results.

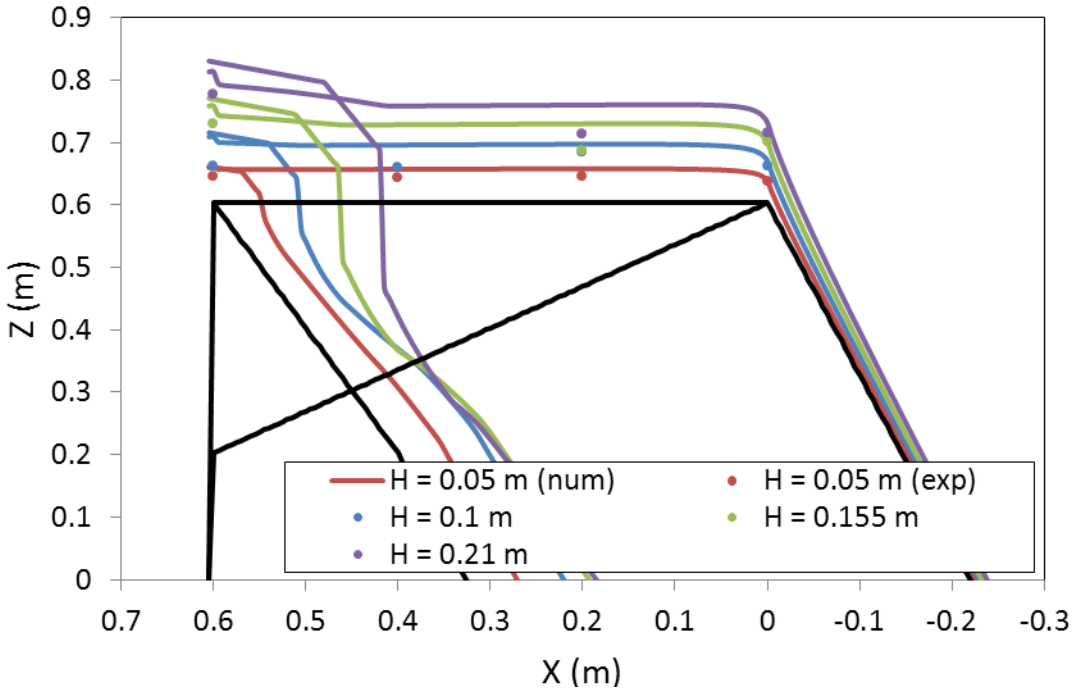

Figure IX-25 Comparison between measured free surface level and profiles provided by Wolf1D-PKW for B_o/B_i = 0 and hydraulic optimal weir height

Table IX-3 – Comparison of experimental and numerical results for B_o/B_i = 0 and hydraulic optimal weir height

X (m)	*H* (m)	Δ*h*/*h* (%)	*X* (m)	*H* (m)	Δ*h*/*h* (%)
0.6	0.05	28.5	0.2	0.05	29.6
	0.1	63.5		0.1	15.7
	0.155	12.3		0.155	50.8
	0.21	10.3		0.21	42.7
0.4	0.05	31.1	0	0.05	1.9
	0.1	61.1		0.1	12.7
	0.155	-		0.155	1
	0.21	-		0.21	13.9

Even if the lateral contraction at inlet key entrance is still poorly described, the comparison of inlet free surface profiles computed with the numerical solver and measured on the tested model are more similar at the key entrance (X = 0 m). This may be induced by the sharp flow contraction upstream the weir which limits the influence of the channel representation of the keys.

Regarding the outlet keys the profiles, no more hydraulic jump is observed on the numerical results. The outlet free surface remains under the crest level and the outlet flow has no influence on the side discharge. This enables to explain the better approach of experimental discharges for $B_o/B_i < 1$ (Figure IX-23).

IX.3.4.1.3. $B_o/B_i = 3$

Figure IX-26 and Table IX-4 show the comparison between the free surface profiles along the inlet and outlet keys computed with Wolf1D-PKW for B_o/B_i = 3 and the experimental results.

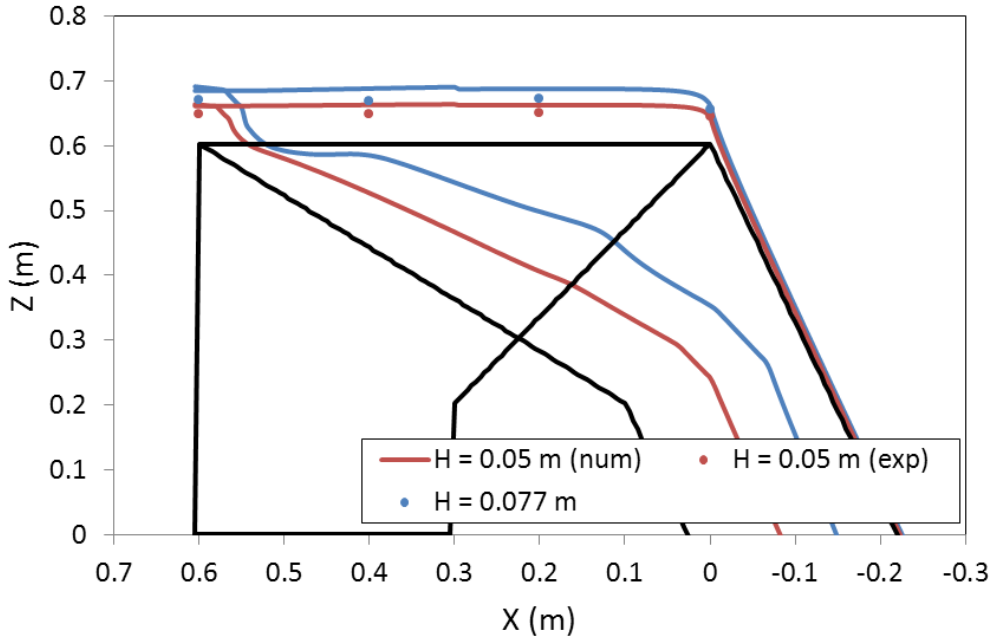

Figure IX-26 Comparison between measured free surface level and profiles provided by Wolf1D-PKW for B_o/B_i = 3 and hydraulic optimal weir height

Table IX-4 – Comparison of experimental and numerical results for B_o/B_i = 3 and hydraulic optimal weir height

X (m)	H (m)	$\Delta h/h$ (%)	X (m)	H (m)	$\Delta h/h$ (%)
0.6	0.05	25.1	0.2	0.05	24.5
	0.077	19.5		0.077	22.5
0.4	0.05	31.9	0	0.05	1.3
	0.077	29.7		0.077	13

This time only low heads have been computed. Indeed, for models with longer upstream overhangs, the solver doesn't more converge for high heads. This may be

induced by the influence of the consideration of mass exchange perpendicularly to the side wall. As seen on the model with symmetric overhangs (Figure IX-24), this simplification induced the apparition of a non-observed hydraulic jump along the outlet key. As the outlet slope decreases and the side crest discharge increases with increasing B_o/B_i, this phenomenon is amplified on models with longer upstream overhangs. The hydraulic jump influences the side crest working and makes unable the convergence of the solver.

IX.3.4.1.4. Control section in the inlet key

As the free surface profiles in the downstream part of the inlet key are not affected by the simplifications of the flow solver, whatever the upstream head or the overhangs lengths, the numerical results may help to the determination of the control section along the key. Figure IX-27 shows the variation of the distance B' between the downstream crest and the control section of the inlet key with head and overhangs lengths.

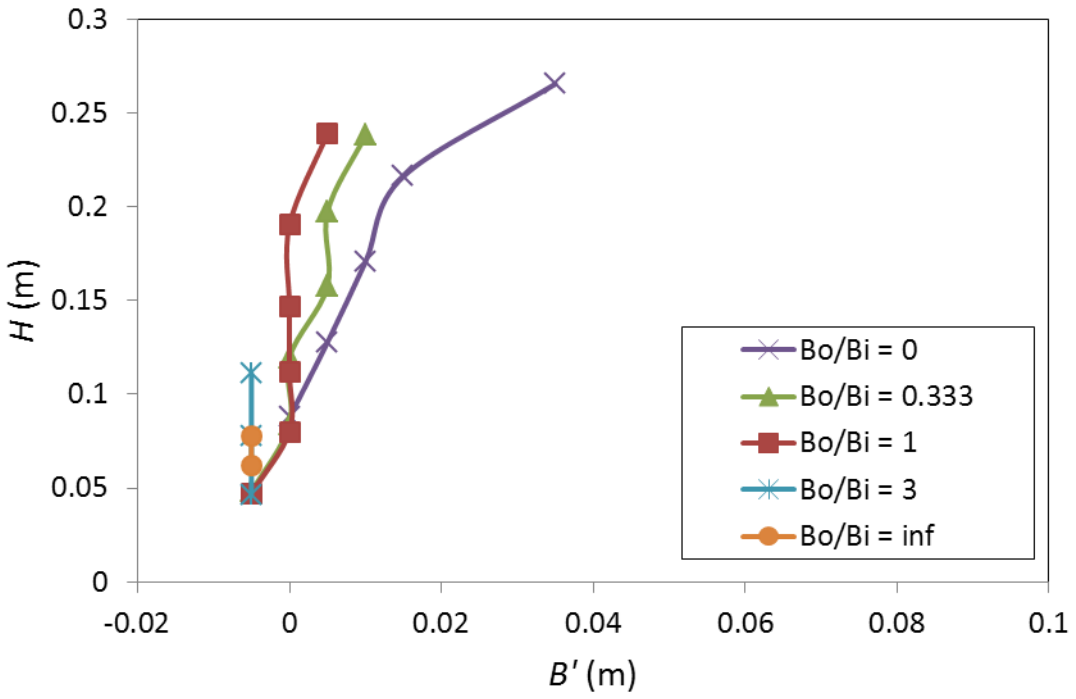

Figure IX-27 Variation of the inlet control section position with head and overhangs lengths for hydraulic optimal weir height

For $B_o/B_i > 1$, the control section of the inlet key stays on the downstream crest. Flow velocities in the inlet key are sufficiently small to avoid apparition of supercritical flows.

For $B_o/B_i < 1$, the control section of the inlet key moves upstream with increasing heads. Flow velocities along the inlet key become higher than the critical one due to the low water depths in the downstream part of the key, induced by smaller inlet slopes.

IX.3.4.2. Technico-economic optimization of the PKW height

Considering technico-economic optimization of the weir height, the accuracy of the numerical model becomes less relevant (Figure IX-28). The numerical results systematically under-estimates the experimental ones. The analytical results agree more with the experimental ones, except for the model with only downstream overhangs.

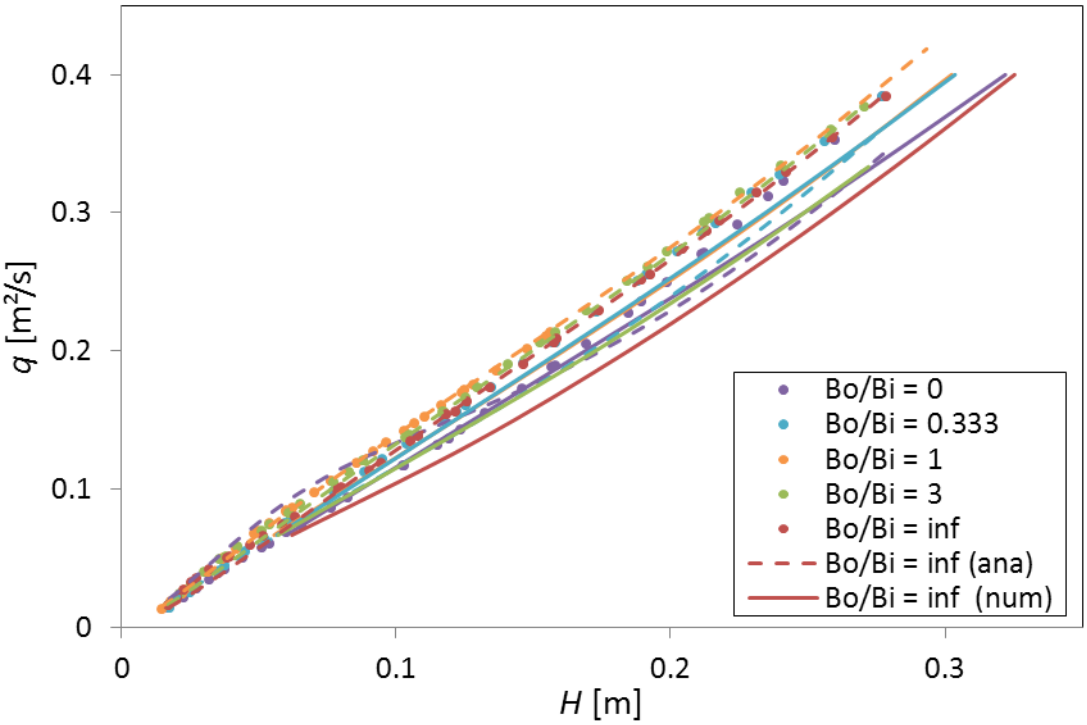

Figure IX-28 Comparison between the stage discharge curves obtains from experimental, analytical and numerical approaches for technico-economic optimal weir height

One more time, the interest of the 1D numerical solver is to give information on the free surface profiles and on the position of the critical section along the inlet key.

IX.3.4.2.1. $B_o/B_i = 1$

Figure IX-29 and Table IX-5 show the comparison between the free surface profiles along the inlet and outlet keys computed with the enhanced version of Wolf1D-PKW for $B_o/B_i = 1$ and the experimental results.

The inlet free surface profiles are this time closer from the experimental results at the inlet entrance (X = 0.4 m). The influence of the transversal flow contraction decreases and the one of the vertical contraction increases, as the weir height is decreased. As the flow solver computed well the vertical contraction, and not the lateral one, it is more efficient for low weir heights.

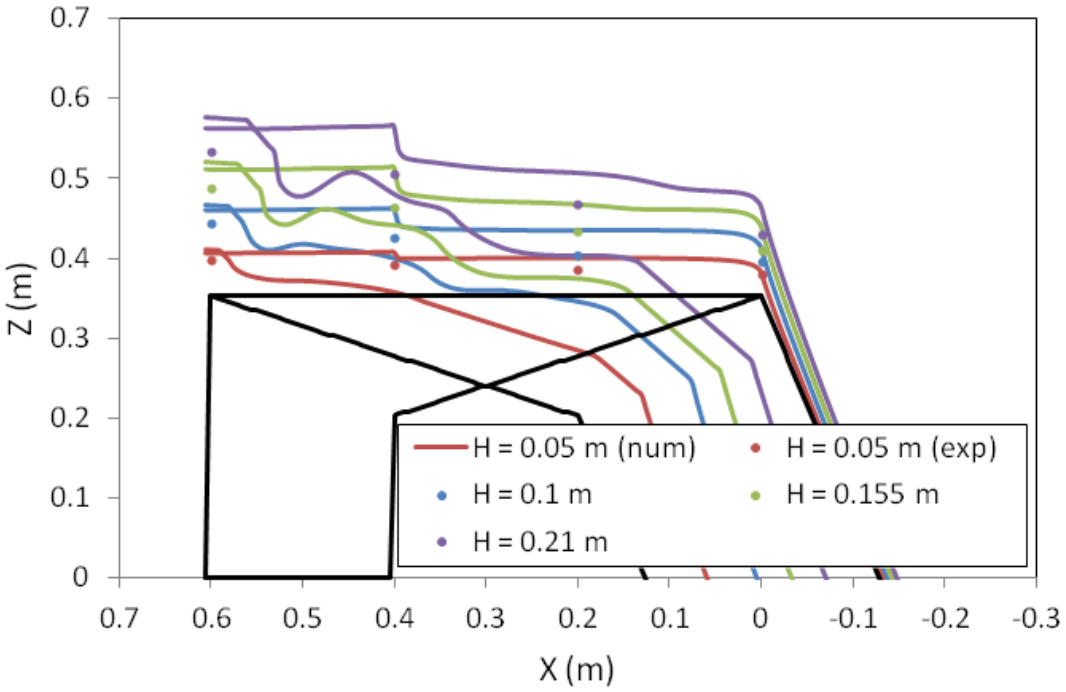

Figure IX-29 Comparison between the measured free surface levels and the profiles provided by Wolf1D-PKW for B_i/B_o = 1 and technico-economic optimal weir height

Table IX-5 – Comparison of experimental and numerical results for B_o/B_i = 1 and technico-economic optimal weir height

X (m)	*H* (m)	Δ*h*/*h* (%)	*X* (m)	*H* (m)	Δ*h*/*h* (%)
0.6	0.05	23.1	0.2	0.05	49
	0.1	18.5		0.1	56.7
	0.155	16.4		0.155	41.4
	0.21	15.3		0.21	32.5
0.4	0.05	29.5	0	0.05	11.8
	0.1	22.9		0.1	13
	0.155	18.3		0.155	18.7
	0.21	15.7		0.21	14.6

Regarding the outlet keys, the shape of the profiles are closer from the ones observed on the scale model than for the hydraulic optimal weir height. As the weir height decreases the transfer way between inlet and outlet keys decreases, and so the longitudinal transfer length. The assumption of a transfer perpendicular to the side wall becomes thus more accurate for low weirs.

IX.3.4.2.2. B_o/B_i = 0

Figure IX-30 and Table IX-6 show the comparison between the free surface profiles along the inlet and outlet keys computed with Wolf1D-PKW for B_o/B_i = 0 and the experimental results.

The sharp lateral contraction at the inlet key entrance (*X* = 0 m) is better approached, according to a more valuable channel representation of the key.

Regarding the outlet key profiles, the higher key slope enables a more quickly decrease of the free surface level, as observed on the experimental models.

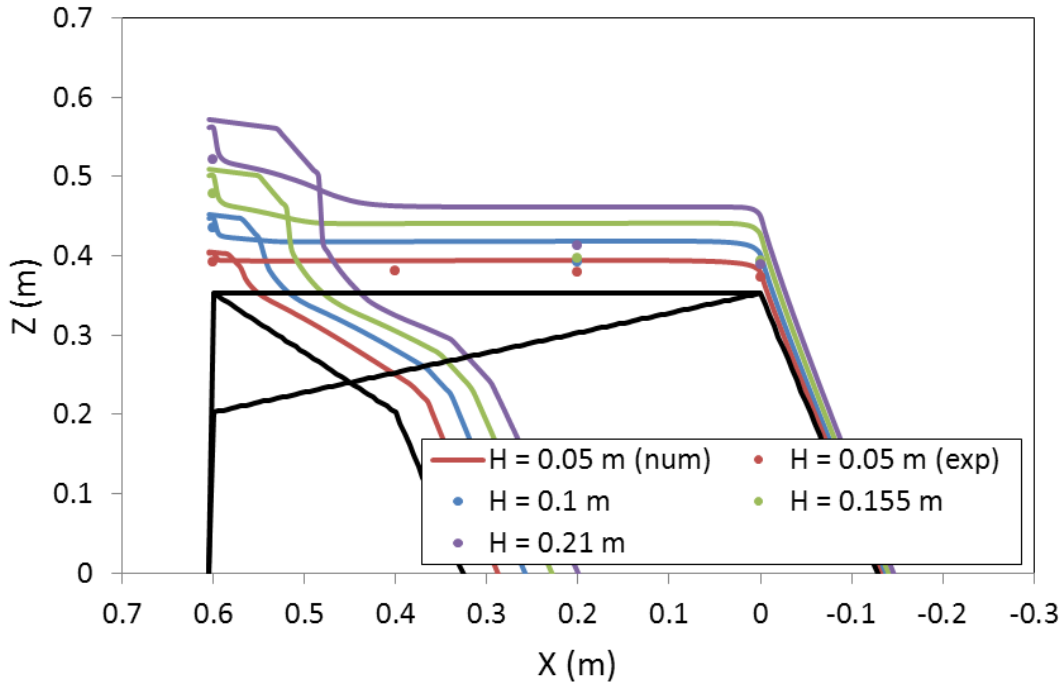

Figure IX-30 Comparison between measured free surface levels and profiles provided by Wolf1D-PKW for B_o/B_i = 0 and technico-economic optimal weir height

Table IX-6 – Comparison of experimental and numerical results for B_o/B_i = 0 and technico-economic optimal weir height

X (m)	*H* (m)	Δ*h*/*h* (%)	*X* (m)	*H* (m)	Δ*h*/*h* (%)
0.6	0.05	14.6	0.2	0.05	54.7
	0.1	10.3		0.1	68.3
	0.155	5.1		0.155	97.2
	0.21	6		0.21	82
0.4	0.05	46.7	0	0.05	32
	0.1	-		0.1	25.1
	0.155	-		0.155	26.6
	0.21	-		0.21	44.9

IX.3.4.2.3. B_o/B_i = 3

Figure IX-31 and Table IX-7 show the comparison between the free surface profiles along the inlet and outlet keys computed with Wolf1D-PKW for B_o/B_i = 3 and the experimental results.

The experimental results are approached with the same accuracy than on model with B_o/B_i = 1 along the inlet key.

Regarding the outlet keys profiles, decreasing the outlet slope enables slower decrease of the free surface level.

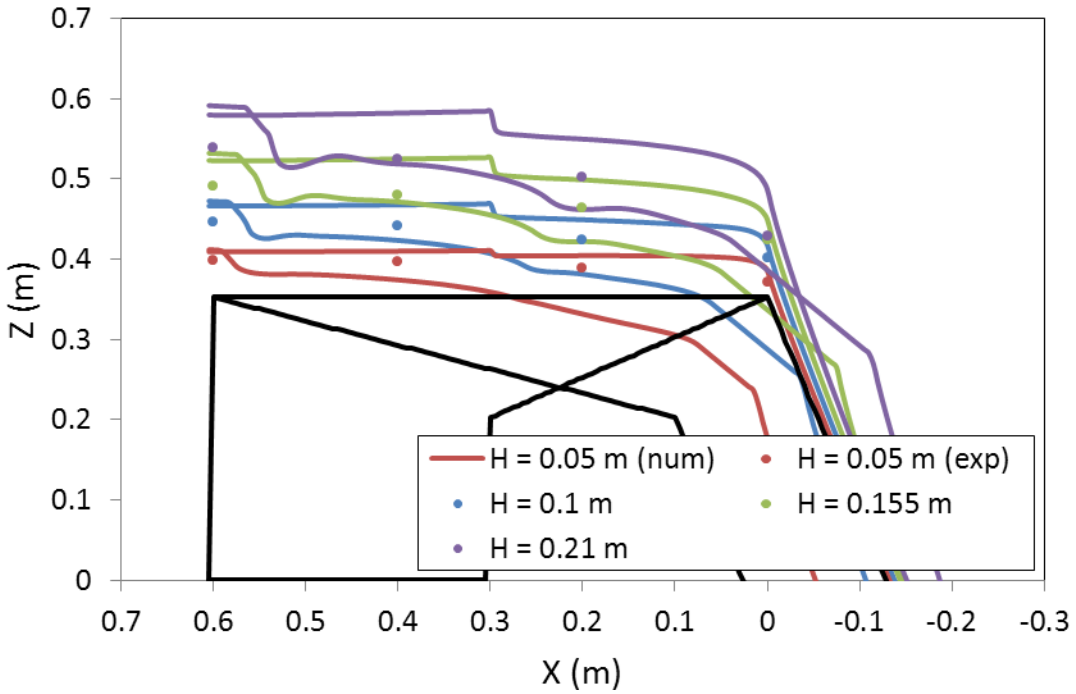

Figure IX-31 Comparison between measured free surface levels and profiles provided by Wolf1D-PKW for B_o/B_i = 3 and technico-economic optimal weir height

Table IX-7 – Comparison of experimental and numerical results for B_o/B_i = 3 and technico-economic optimal weir height

X (m)	*H* (m)	Δ*h*/*h* (%)	*X* (m)	*H* (m)	Δ*h*/*h* (%)
0.6	0.05	23.5	0.2	0.05	40.8
	0.1	21.9		0.1	34.7
	0.155	22.9		0.155	32
	0.21	21.4		0.21	32.5
0.4	0.05	32	0	0.05	33.6
	0.1	30.5		0.1	13
	0.155	34.8		0.155	9.3
	0.21	33.2		0.21	21.2

One more time, as for models with longer upstream overhangs, inducing lower outlet slopes, the discharge is mainly managed by the resilience capacity of the outlet key, a small increase of the free surface level may vary significantly the side crest discharge and thus the global weir efficiency. As the mass transfer is considered perpendicular to the side crest, a small increase of the free surface along the outlet key is provided by the solver. That decreases the efficient length of the side crest, what enables to explain the systematic underestimation of the discharge by the numerical approach (Figure IX-27).

IX.3.4.2.4. Control section in the inlet key

As the free surface profiles in the downstream part of the inlet key are not affected by the simplifications of the flow solver, whatever the upstream head or the overhangs lengths, the numerical results may help to the determination of the control

section along the key. Figure IX-32 shows the variation of the distance *B'* between the downstream crest and the control section of the inlet key with head and overhangs lengths.

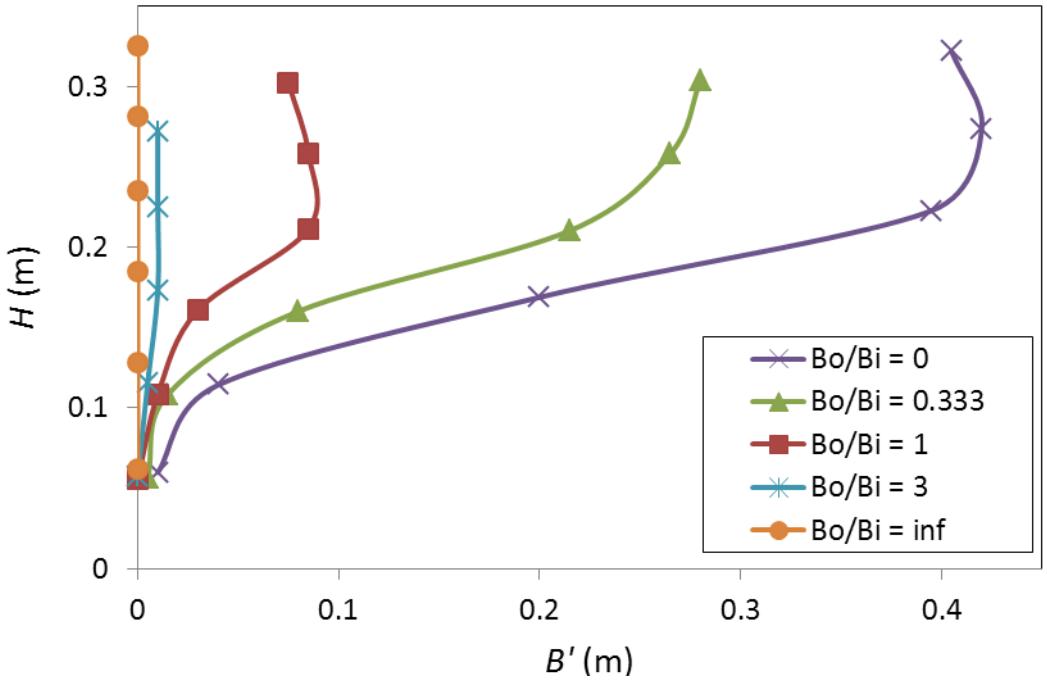

Figure IX-32 Variation of the inlet control section position with head and overhangs lengths for technico-economic optimal weir height

Moving the overhangs upstream enables to avoid critical section apparition whatever the low weir height.

For models with $B_o/B_i \leq 1$, the control section of the inlet key moves upstream to reach a maximum distance from the downstream crest for varying *H* values depending of the inlet slope. Then, for increasing heads, the control section moves downstream. Flow velocities along the inlet key become higher than the critical one due to the low water depths in the downstream part of the inlet key. However, for high heads, the submergence of the side crest by the outlet flow decreases the inlet key discharge and so the velocities, what moves the control section downstream. The position of the control section is all the more upstream as the B_o/B_i ratio decreases, decreasing the inlet slope.

IX.3.5. Design considerations

Until now, most of the PKW prototypes are close to the Type A PKW using symmetric up- and downstream overhangs for structural reasons (self-equilibrated structure, use of precast elements). Regarding pure hydraulics, Ouamane and Lempérière propose to use Type B PKW, using only upstream overhangs, to increase discharge capacities [94]. Regarding the above results, this last assumption is to correlate with the definition of the weir height.

For a low weir height configuration, which is the most used until now, the use of longer upstream overhangs decreases the outlet slope and so its resilience capacity. As, for this configuration, the side and upstream crests are mainly managed by the outlet capacity, there is no interest in using longer upstream overhangs. Furthermore, the use of downstream overhangs enhanced the downstream nappe aeration for high heads, avoiding the need in artificial aerators. Model type A are thus to encourage for low weir configurations.

For a high weir height configuration, which have to be encouraged when high level of hydraulic performance is researched, the use of longer upstream overhangs increases the inlet cross section which mainly manages the side crest efficiency. However, too long upstream overhangs induced one more time subcritical outlet flow that decreases the efficient length of the side crest. The hydraulic optimum is the one using the longest upstream overhangs able to avoid an outlet slope under the critical one.

IX.4. Conclusion

The study of the 10 models with varying overhangs lengths enables to conclude to an optimal B_o/B_i ratio near to 1 for a low weir height (P/W_u = 0.5) and to 3 for a high weir height (P/W_u = 1.33). For a PKW design based on pure hydraulic, a ratio of 3 is optimal. According to technico-economic interest, a symmetric configuration seems more relevant as it enables the use of precast elements.

The study of the free surface profiles enables to explain the hydraulic interest of a small increase of the upstream overhang length.

Considering the hydraulic optimal weir height (P/W_u = 1.33), for $B_o/B_i \leq 3$, the modification of the inlet cross section, modifying the inlet flow velocity, manages the side crest efficiency. A longer upstream overhang, providing a larger inlet cross section, increases the PKW discharge capacity. For $B_o/B_i = \infty$, the outlet flow becomes subcritical, as the outlet slope decreases. It submerged partially the side crest, what decreases significantly the side crest discharge.

The same behaviour is observed considering a technico-economic optimal weir height (P/W_u = 0.5). However, the main influence of the outlet key resilience is already observed for B_o/B_i = 3. This is due to the smaller weir height which induces a smaller outlet slope.

Models with low weir height (P/W_u = 0.5) and short downstream overhangs ($B_o/B_i \geq 1$) have also shown problems of aeration. For high heads, no more aeration is observed under the weir and the downstream nappe becomes leaping. Artificial aerators are thus needed to avoid the effect of the negative pressure and the nappe beating on the structure.

The exploitation of the Wolf1D-PKW solver enables to highlight the influence of the overhangs lengths on the position of the control section in the inlet key. For a high weir height (P/W_u = 1.33), the control section stays located on the downstream crest except for highest heads on the model without upstream overhang. For a low weir height (P/W_u = 0.5), the control section of the inlet key moves upstream to reach a maximum distance from the downstream crest for a H/P ratio approximately equals to 1.5. The maximum distance is all the longer as the downstream overhang length increases. For longer upstream overhang than downstream one, the control section stays at the downstream apex.

Finally, based on the experimental results, the analytical formulation of the discharge capacity of PKW has been, one more time, enhanced. It predicts all the experimental results with an accuracy of 10 %.

X. Validation

X.1. PKW of Escouloubre (France)

To validate the results of the experimental approach depicted in the previous chapters, the comparison is presented here between the observed discharges on the PKW of Escouloubre (France), the ones measured on a scale reproduction of the structure at the laboratory, the results of the numerical Wolf1D-PKW model and the analytical formulation.

X.1.1. Geometrical characteristics

The PKW of Escouloubre, operated by "*Electricité de France* (EDF)" is situated on the Aude River in the Pyrenees in the south of France. It is used as a spillway on the rest lake of the hydropower plant of Escouloubre and is currently used as a by-pass for the penstock of the hydropower plant of Nentilla. Its design discharge is about 13 m^3/s for a design head of 0.66 m.

The PKW is composed of a central inlet key, two outlet keys and, on both weir sides, two rectangular labyrinth inlet keys without overhang or bottom slope. The characteristics of the geometry are summarized in Table X-1 and Figure X-1. Figure X-2 shows up- and downstream views of the prototype PKW.

A 1:7 scale model has been used for the experimental approach (Figure X-3). The model has been placed in the experimental flume (see III.1) using the full flume width. Half the central inlet key and half the outlet key have also been modelled using the 1D numerical model Wolf1D-PKW (see XIV.2). Finally the proposed analytical formulation (see IX.3.3) has also been tested on the present model.

Table X-1 – Escouloubre PKW dimensions

	Prototype	Scale model	Numerical model
W	5.11 m	0.73 m	1.4 m
L	21.91 m	3.13 m	6.2 m
$P_i = P_o$	1.77 m	0.253 m	1.77 m
P_d	4.53 m	0.647 m	4.53 m
W_u	2.8 m	0.4 m	2.8 m
W_i	1.3 m	0.186 m	1.3 m
W_o	0.9 m	0.129 m	0.9 m
$T_s = T_i = T_o$	0.3 m	0.043 m	0.3 m
B	5.1 m	0.729 m	5.1 m
$B_i = B_o$	1.2 m	0.171 m	1.2 m

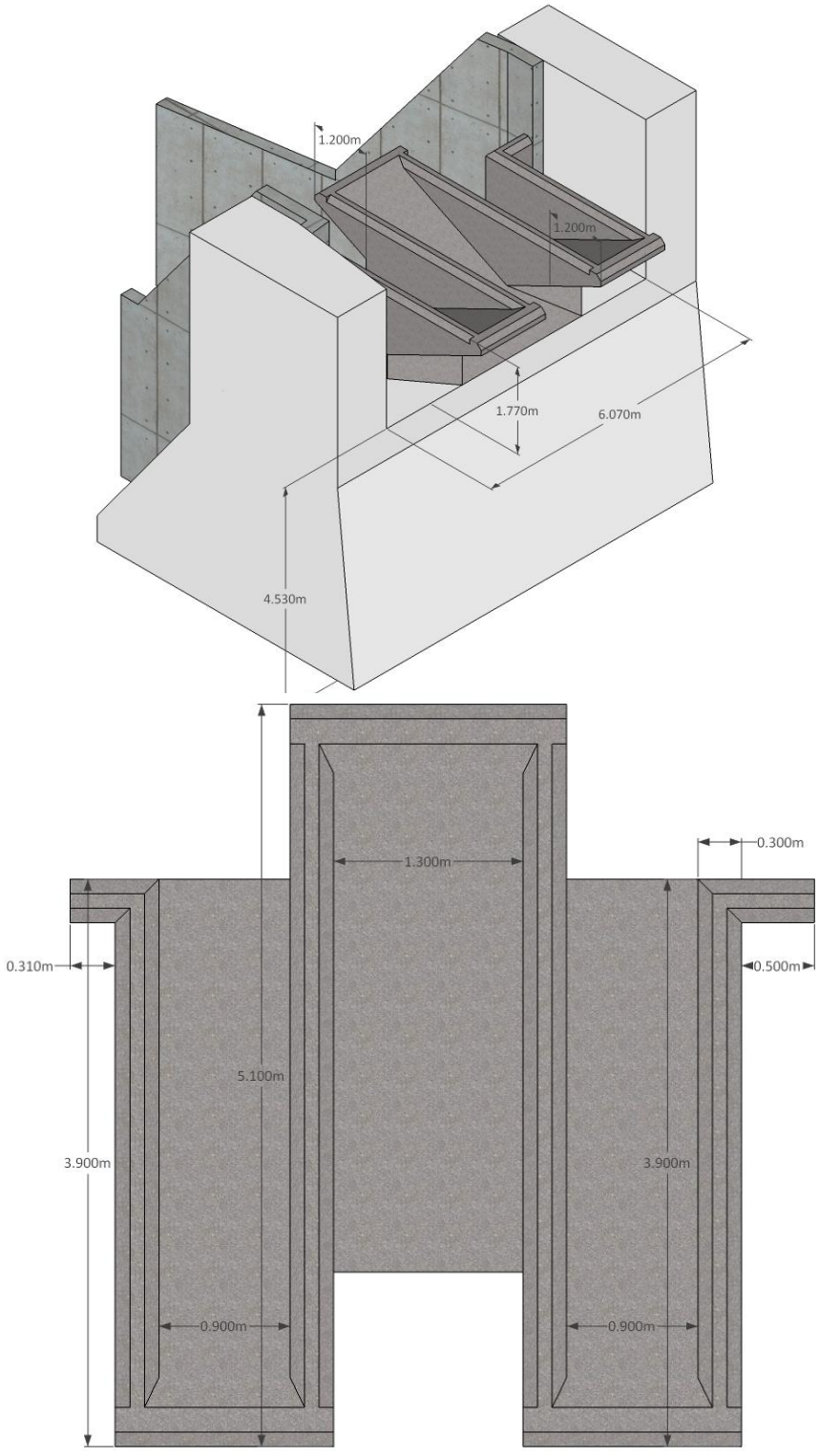

Figure X-1 Escouloubre prototype PKW layout

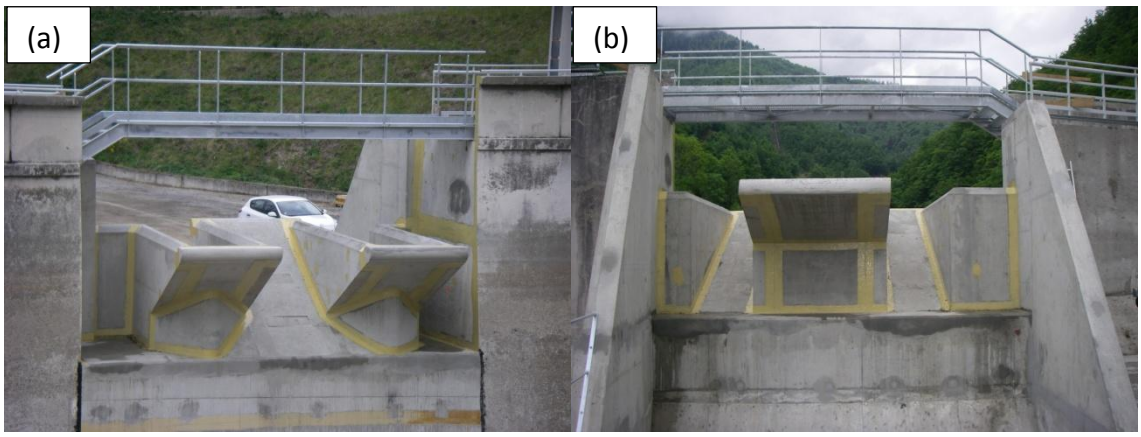

Figure X-2 Views of the prototype PKW of Escouloubre: (a) – upstream; (b) – downstream

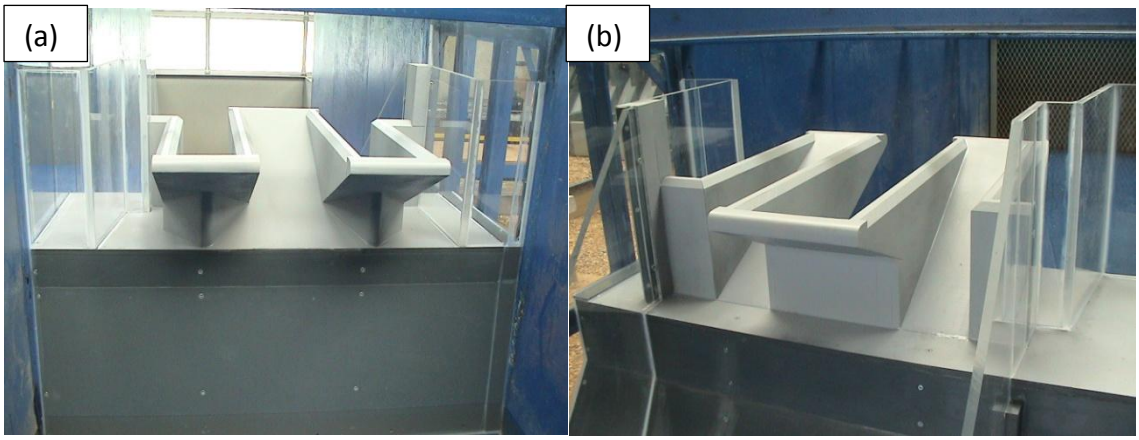

Figure X-3 Views of the scale model: (a) – upstream; (b) – downstream

X.1.2. Prototype model

As the model is located in between the Escouloubre and Nentilla power plants, tests on the discharge capacity have been done by closing the penstock of the Nentilla power plant and calibrating the upstream discharge through the one of Escouloubre power plant. Measurements of the reservoir level have been carried out for four constant discharges (Q = 1.2, 2.8, 5 and 10 m³/s). Figure X-7 shows the stage discharge curve calculated on the basis of these measurements on the prototype.

Figure X-4 to Figure X-6 show views of the prototype model under discharges of respectively 10, 5 and 1.2 m³/s. They highlight the good aeration of the nappe whatever the upstream head. They also highlight that the level of the interference zone between the side nappes rises with increasing heads. Finally regarding Figure X-4, the side walls downstream the weir seem under-designed as the flow begins to pass over these walls for a discharge of 10 m³/s, lower than the design discharge.

Figure X-4 Views of the prototype PKW for Q = 10 m³/s

Figure X-5 Views of the prototype PKW for Q = 5 m³/s

Figure X-6 Views of the prototype PKW for Q = 1.2 m³/s

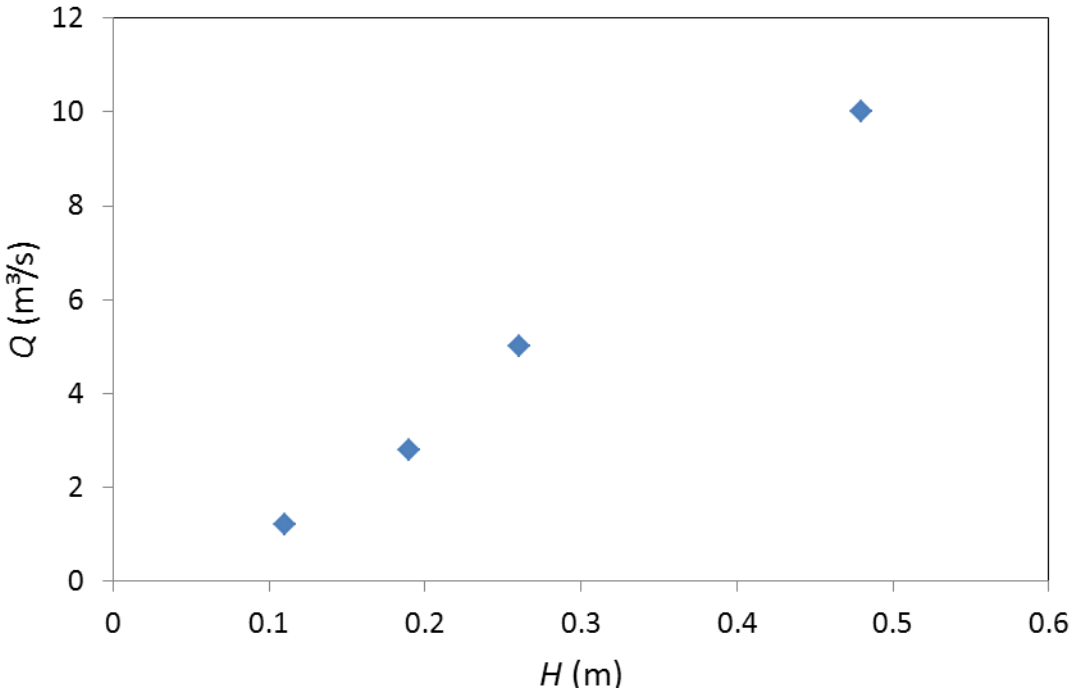

Figure X-7 Stage-discharge curve of the prototype PKW of Escouloubre

X.1.3. Physical model

Measurements of the upstream head have been performed for varied discharge on the physical model. The Figure X-11 shows the comparison of the stage discharges curves measured on the physical model and on the prototype.

The measurements on the scale model agree well with the ones performed on the prototype for high discharges ($Q \geq 5$ m³/s). The model confirms that the design discharge of 0.13 m³/s is released under an upstream head of 0.66 m, corresponding to the maximal reservoir elevation. However, for low discharges ($Q \leq 3$ m³/s), the scale model is more efficient than the prototype. For the corresponding heads, low water depths appear on the model and surface tension may influence the flow behaviour.

Figure X-8 to Figure X-10 show views of the physical model under discharges of respectively 77.1, 38.6 and 9.3 l/s corresponding to discharges of 10, 5 and 1.2 m³/s on the prototype. They highlight similar flow behaviour than the ones observed on the prototype for high discharges ($Q \geq 5$ m³/s - Figure X-4 and Figure X-5). As observed on the prototype, the downstream flow passes over the side walls of the scale model for a discharge corresponding to 10 m³/s. However, for the lowest discharge (Q = 1.2 m³/s), Figure X-10 shows depressed nappes all along the PKW crest when a good nappes aeration is observed on the prototype (Figure X-6). As a depressed nappe is more efficient than a springing one, it explains the variation in the observed discharge capacities on the scale model and on the prototype for low discharges. This highlights the limit of the scale model to fit the reality for too low heads.

Figure X-8 Views of the scale model for a discharge corresponding to Q = 10 m³/s

Figure X-9 Views of the scale model for a discharge corresponding to Q = 5 m³/s

Figure X-10 Views of the scale model for a discharge corresponding to Q = 1.2 m³/s

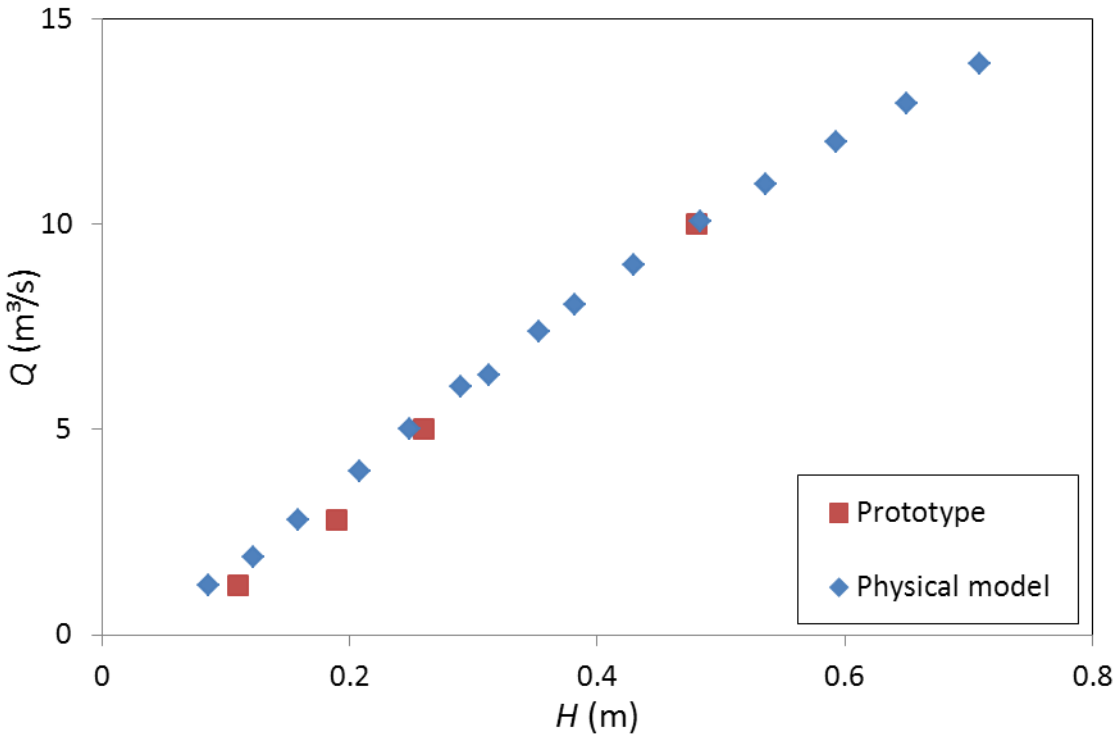

Figure X-11 Comparison of the stage-discharge curves of the physical model and the prototype

X.1.4. Analytical approach

To apply the analytical formulation developed in this research, the characteristics of the central inlet and outlet keys have been considered. The comparison between analytical results and prototype results in terms of specific discharges is shown on Figure X-12. It highlights an accuracy of the analytical approach of 10%.

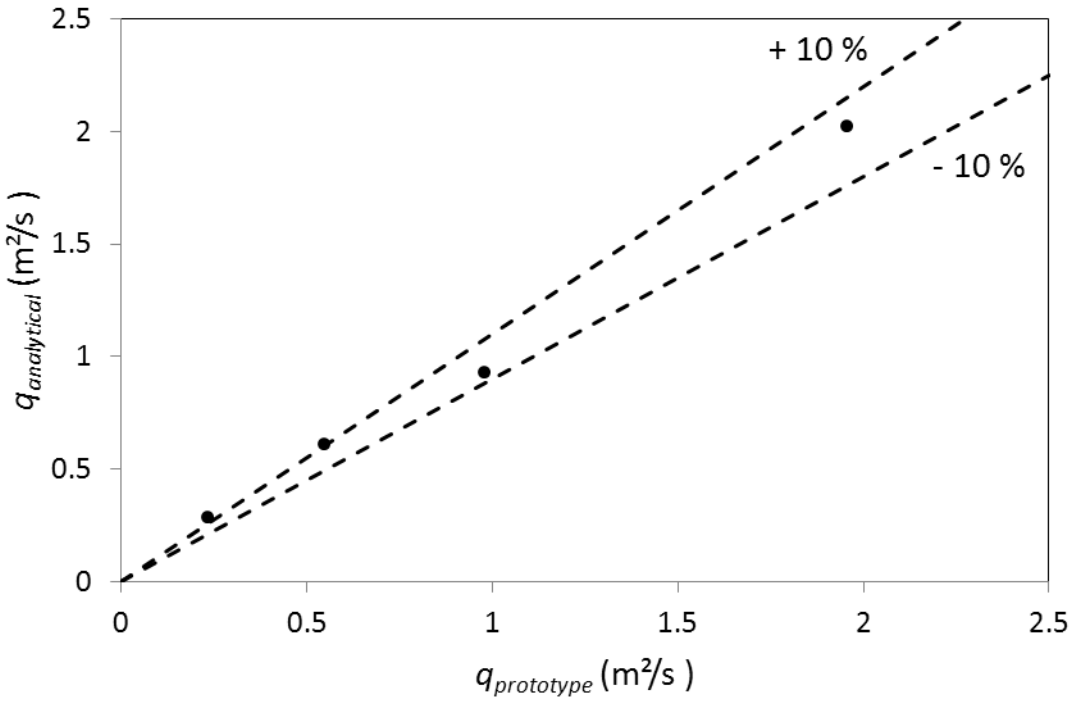

Figure X-12 Comparison between analytical and prototype specific discharges

The analytical formulation enables the drawing of a complete stage discharge curve (Figure X-13). It suggests that the design discharge could be evacuated under a head of 0.58 m largely under the design head, observed on the physical model. That may be due to the more important influence of the side effects on the discharge capacity for high discharges. Indeed, for $Q \geq 10$ m³/s, the flow contraction along the right and the left banks perturbs the flow over the side crests of the PKW (Figure X-14). This is not taken into account by the analytical formulation.

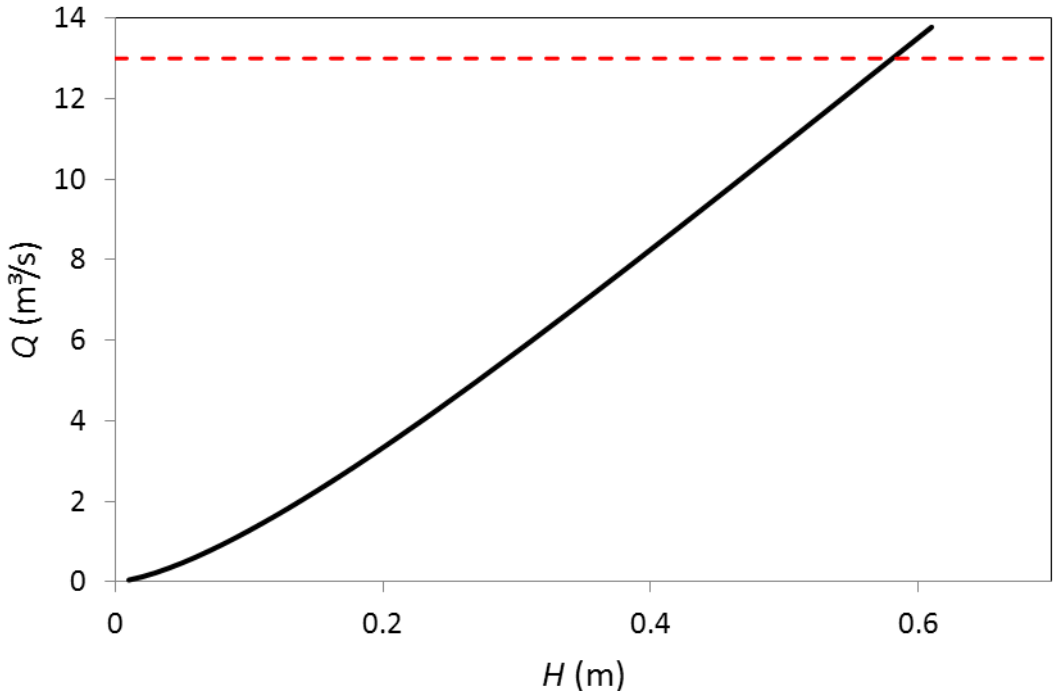

Figure X-13 Analytical stage-discharge curve of the PKW of Escouloubre

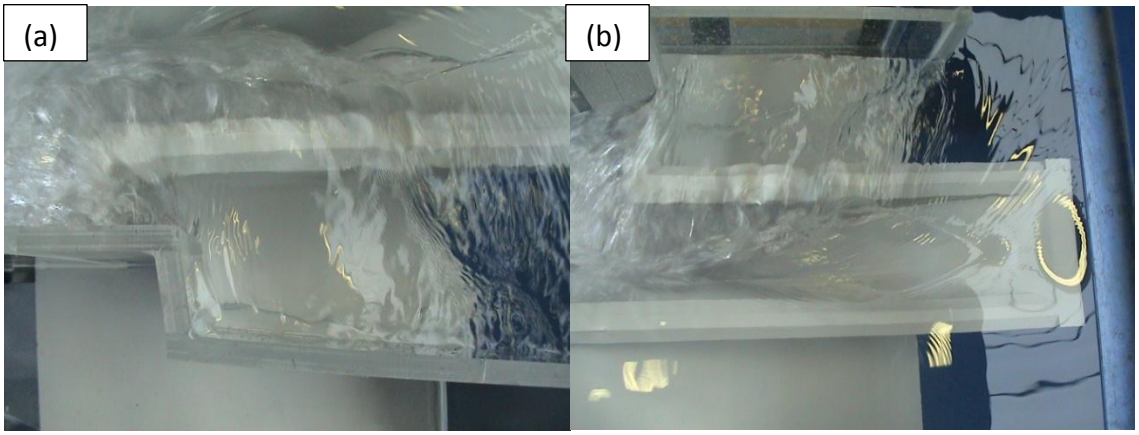

Figure X-14 Side effects observed on the physical model for a discharge corresponding to Q = 10 m³/s: (a) – left bank; (b) – right bank

X.1.5. Numerical approach

The PKW of Escouloubre has been modelled numerically using the enhanced version of Wolf1D-PKW (see XIV.2). Figure X-15 shows the comparison of the stage-discharge curve computed by the solver, for a half unit and extrapolated to the total

PKW width, and the measurements realized on the prototype model. Even if the solver gives results agreeing with in-situ measurements for high heads, it doesn't converge for very low heads, enabling no comparison with the prototype results.

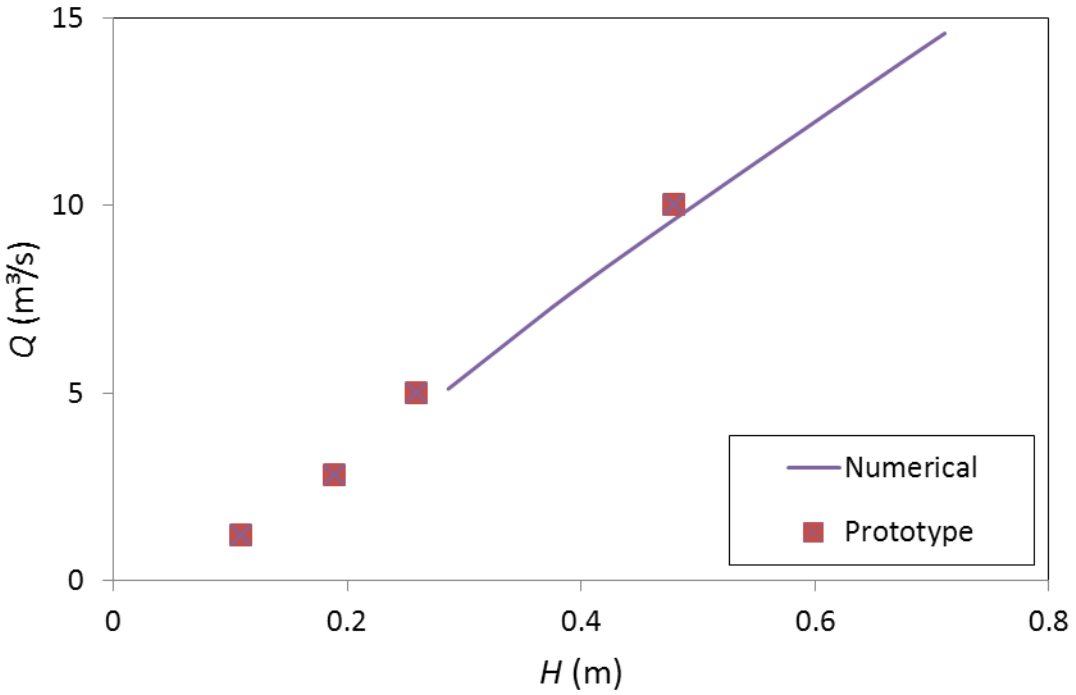

Figure X-15 Numerical stage-discharge curve of the PKW of Escouloubre

According to the numerical results, the design discharge of 13 m³/s is evacuated under an upstream head of 0.63 m, instead of 0.66 m measured on the physical model. One more time, the influence of the side effects, observed on the scale model (Figure X-14), is not taken into account by the numerical solver, what may explain this difference.

However, a main interest of the solver is to give more information about the free surface profiles and the position of the critical section along the inlet key without any measurements. Figure X-16 shows the free surface profiles for the discharges of 10 and 5 m³/s measured on the prototype PKW. As observed on the prototype, the outlet flow partially submerged the upstream part of the side wall, only for Q = 10 m³/s (Figure X-4).

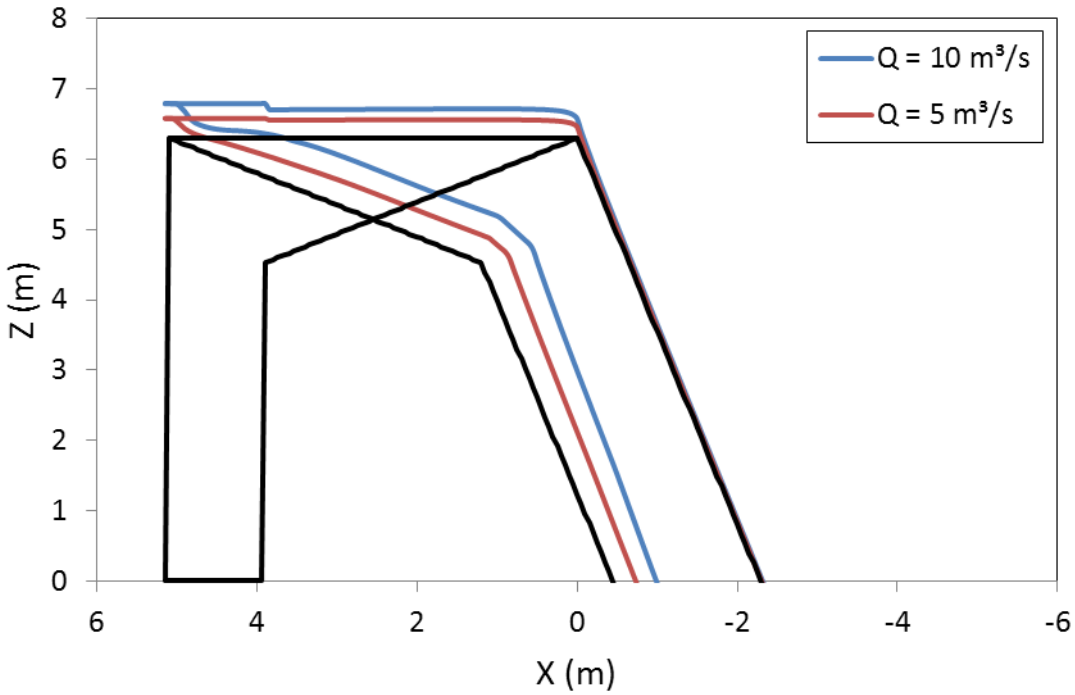

Figure X-16 Free surface profiles provided by Wolf1D-PKW

Regarding the variation of the position of the critical section along the inlet key for increasing discharges on the prototype structure (Figure X-17), the inlet cross section is properly calibrated to prevent apparition of a control section along the inlet key until discharges of 12 m³/s. For the design discharge the control section is situated only 0.05 m upstream of the downstream crest, corresponding to only 1% of the side wall length. So its influence remains negligible.

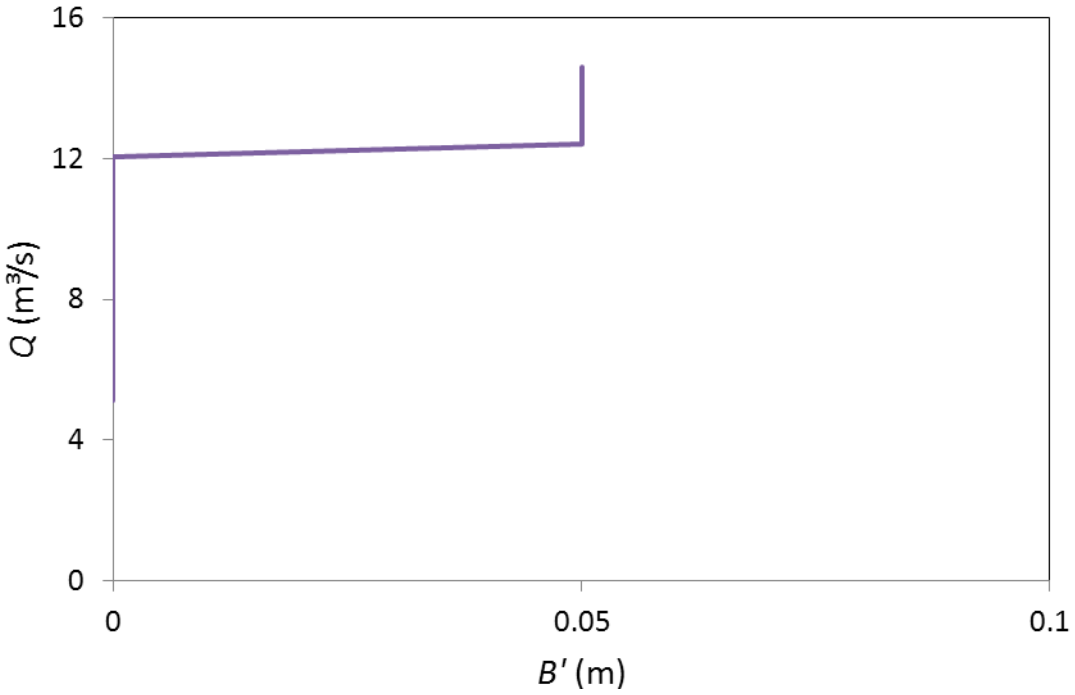

Figure X-17 Variation of the inlet control section position with global discharge on the Escouloubre PKW

X.1.6. Interests and limitations of the various approaches

The Figure X-18 shows the comparison of the stage-discharge curves provided by the physical, the analytical and the numerical approaches, and the measurements made on the prototype. Even if the three approaches are globally in agreement with the in-situ measurements, they all highlight advantages and limitations.

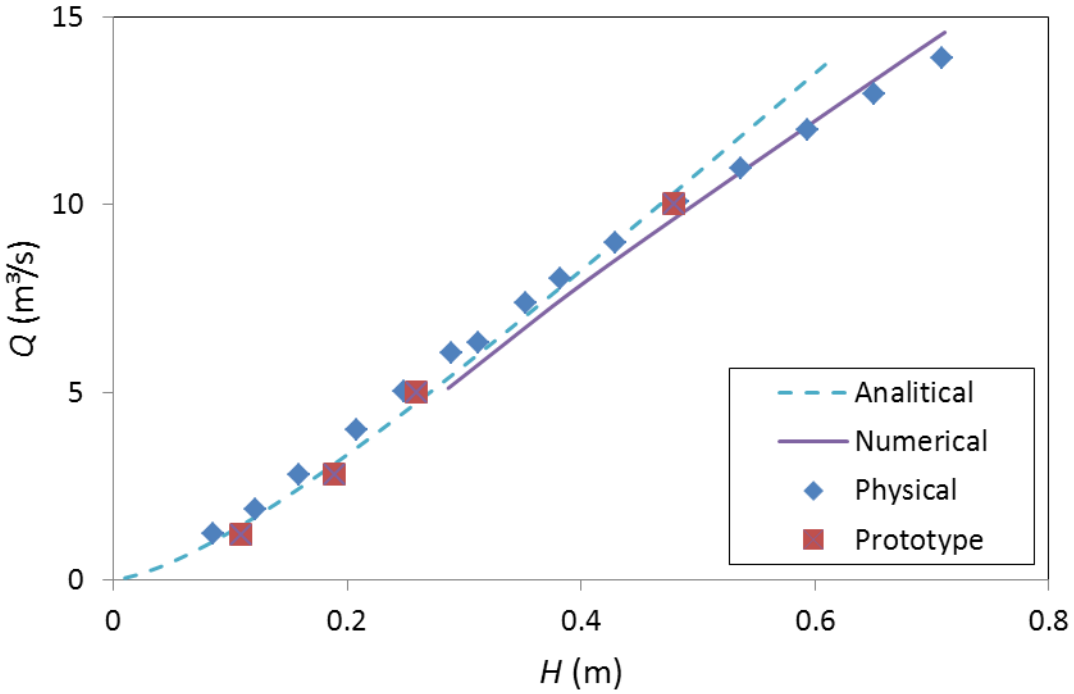

Figure X-18 Comparison of the stage-discharge curves provided by the various approaches

The physical approach seems to remain the best one as it enables the direct visualization of the flow. Furthermore, the side effects are represented as long as the modelled part of the reservoir is wide enough. It is thus a key tool for designers as well as to convince the project owner. However, a scale model is unable to represent the flows for too low discharges. Water depths under 0.03 m may induce surface tension effects.

The analytical formulation is the quickest method to be applied, and so the cheapest, to define the efficiency of a given geometry. However, it gives no information about the free surface shape and the flow repartition. This makes the design of the downstream structures more difficult. Furthermore, the side effects are not taken into account by the analytical formulation. If they become significant, the analytical approach is unsafe as it provides discharges higher than in the reality, as shown on the Escouloubre PKW.

The numerical solver shows limitation in the convergence for too small water depths. However, this approach remains cheaper than the physical one. One more time, the side effects are not taken into account by the solver. On Escouloubre, the

good agreement observed between the numerical and the physical results for high heads is not scientifically assessed. The side effects are compensated by the influence of the poor representation of the effective inlet key width along the upstream overhang. The main advantage of the numerical approach is to provide information about the flow repartition, the free surface profiles and the flow velocities along the structure without any measurements.

According to that, the analytical and numerical approaches are good tools for pre-design or for the enhancement of a well-known geometry. However, a scale model stays to be addressed as long as the designer has the feeling of dominating side effects of the final design or larger uncertainties of innovative geometries.

XI. Design of PKW

XI.1. Project approach

Regarding the results of this research, the definition of a single optimum design of PKW doesn't exist. Indeed, hydraulic, technical and economic interests induce high variations of the weir design depending on the project constraints and on the project engineer's point of view. The distinction between various approaches of the project may be done.

A first distinction may be done between new dam projects and rehabilitation projects. In rehabilitation projects, the costs of the demolition, as well as the dam unavailability during building, are generally of prime importance for the weir design. To respond to these constraints, P/W_u ratios near to 0.5 have to be preferred. Furthermore, existing structures are usually instrumented. The hydraulic optimization can therefore be realized on the basis of a confident hydraulic behaviour of the reservoir. Longer upstream overhangs (B_o/B_i near 3) and larger inlet widths (W_i/W_o between 1.2 and 1.5) have then to be favoured. On the other hand, for new dam projects, poor knowledge of the regional hydrologic context as well as a more easy incorporation of the weir in the dam structure favour designs based on the technical interests (P/W_u = 1.33, W_i/W_o = 1, B_o/B_i = 1).

A second distinction may be done on the financial interest, generally linked to the geographic localisation of the project. Projects in developing countries, such as in Africa, will give more importance to the simplicity of the design (W_i/W_o = 1, B_o/B_i = 1) to facilitate the use of precast elements for instance. Projects in industrialized countries will give more importance to the optimal design even if the gain in efficiency could reach only few percents. Longer upstream overhangs (B_o/B_i near 3) and larger inlet widths (W_i/W_o between 1.2 and 1.5) have then to be favoured.

Finally, the size of the project largely influences the PKW design. For projects with important discharges, generally encountered in Asia and Africa, and inducing a large number of PKW-units, the simplicity of the structure (W_i/W_o = 1, B_o/B_i = 1) should be favoured for an easier construction. For smaller projects with only a few number of PKW-units, the importance of improvement of the hydraulic behaviour becomes predominant. A higher weir height (P/W_u approaching 1.33), longer upstream overhangs (B_o/B_i near 3) and larger inlet widths (W_i/W_o between 1.2 and 1.5) have then to be favoured.

All these considerations must be kept in mind all along the design of a PKW. Hereafter, design advices based on the results presented in this research and on the distinctions between the various project approaches are given for the different stages of the design method proposed in section VI.2.

XI.2. Basis elements

The elements necessary to the design method are categorized in project and reference model elements. The project elements are the hydraulic and geometric specificities of the project (discharge, maximal head and available width) that are only managed by the local constraints. There is usually no flexibility on these constraints for the project engineer.

Regarding the reference model, a release capacity curve, issued from experimental tests, is necessary as well as the geometric characteristics of the tested model. From the studies realized in different laboratories around the world, the hydraulic performances of a large number of geometries are now available. As applying scale factors to the discharges observed on the experimental models stays more accurate than numerical and analytical approaches (see X.1.6), the method presented before (see VI.2) as to be favoured for PKW designs. However the numerical and the analytical approaches will be kept as a second tool for design optimization (see XI.4).

The importance of the choice of the reference model has been already demonstrated (see VI.2.6) and is the first stage of an efficient design. According to the analysis of the results obtained along this research, this choice may be realized more accurately.

For new dam projects, high weir geometries ($P/W_u \approx 1.33$) have to be preferred as they provide larger discharges (around 30% more efficient than low weir configurations) and can be incorporated in the dam structure. For rehabilitation projects, lower geometries ($P/W_u \approx 0.5$) seem to provide the best compromise between hydraulic and economic interests.

Regarding overhangs lengths, a model with symmetric overhangs has to be favoured for a general use. That makes the structure self-equilibrated, favours the use of precast elements, and provides a relevant hydraulic behaviour. However, for new dam projects in industrialized areas, the combination of a high weir geometry with longer upstream overhangs (B_o/B_i near 3) may improve the hydraulic design.

Finally regarding keys widths ratios, a W_i/W_o ratio of 1.25 has to be favoured for hydraulic reasons. However, for projects with a high number of PKW-units or for projects in developing countries, a W_i/W_o ratio of 1 seems to approach the best design combining economic, technic and hydraulic interests.

XI.3. Technico-economic optimization of the PKW design

After the scaling of the reference model for varied numbers of PKW-units (see VI.2.2) and the definition of the geometries enabling to verify the project constraints (see VI.2.3), a technico-economic optimization can be considered to choose the final design. At this stage of the design, the project approach (see XI.1) is the only one to influence the designer. The hydraulic optimization of the structure doesn't play a role anymore. It will be reintroduced in a new final stage of the method (see XI.5).

XI.4. Analytical formulation

During the research, an analytical formulation has been provided and enhanced according to the influence of the various parameters tested. The final proposed analytical formulation of the specific discharge of a PKW is:

$$q = q_u \frac{W_o}{W_u} + q_d \frac{W_i}{W_u} + q_s \frac{2B}{W_u} K_{W_o} \qquad \text{XI-1}$$

where the mean specific discharges on the downstream, the upstream and the side crests are respectively calculated by:

$$q_d = 0.445\left(1 + \frac{1}{1000H + 1.6}\right)\left(1 + 0.5\left(\frac{H}{H+P}\right)^2\right)\sqrt{2gH^3} \qquad \text{XI-2}$$

$$q_u = 0.374\left(1 + \frac{1}{1000H + 1.6}\right)\left(1 + 0.5\left(\frac{H}{H+P_T}\right)^2\right)\sqrt{2gH^3} \qquad \text{XI-3}$$

$$q_s = 0.41\left(1 + \frac{1}{833H + 1.6}\right)\left(1 + 0.5\left(\frac{0.833H}{0.833H + P_e}\right)^2\right) \left(\frac{P_e^{\alpha} + \beta}{0.833H + P_e{}^{\alpha} + \beta}\right) K_{W_i}\sqrt{2gH^3} \qquad \text{XI-4}$$

K_{Wo} is a coefficient taking into account the side crest length decrease induced by the outlet key flow and the side nappes interference. It is calculated by:

$$K_{W_o} = 1 \qquad \text{for } \frac{H}{W_o} \le L_1$$

$$K_{W_o} = \frac{2}{L_2 - L_1}^3 \left(\frac{H}{W_o}\right)^3 - \frac{3\ L_2 + L_1}{L_2 - L_1}^3 \left(\frac{H}{W_o}\right)^2 + \frac{6L_2L_1}{L_2 - L_1}^3 \left(\frac{H}{W_o}\right) + \frac{L_2^2\ L_2 - 3L_1}{L_2 - L_1}^3 \qquad \text{for } L_2 \ge \frac{H}{W_o} \ge L_1 \qquad \text{XI-5}$$

$$K_{W_o} = 0 \qquad \text{for } \frac{H}{W_o} \ge L_2$$

The limits L_1 and L_2 for the use of these formulations are respectively given by:

$$L_1 = -0.788 S_o^{-1.88} + 5 \qquad \text{XI-6}$$

$$L_2 = 0.236 S_o^{-1.94} + 5 \qquad \text{XI-7}$$

P_e is the mean weir height along the side wall, calculated by:

$$P_e = P_T \frac{B_o}{B} + \frac{P}{2}\left(1 - \frac{B_o}{B}\right) \qquad \text{XI-8}$$

α and β are parameters to characterized the influence of the inlet key slope on the side crest efficiency. They are calculated by:

$$\alpha = \frac{0.7}{S_i^2} - \frac{3.58}{S_i} + 7.55 \qquad \text{XI-9}$$

$$\beta = 0.029\, \mathrm{e}^{-\frac{1.446}{S_i}} \qquad \text{XI-10}$$

K_{Wi} is a coefficient taking into account the influence on the side crest efficiency of the modification of the inlet flow velocity induced by the inlet key width variation. It is given by:

$$K_{W_i} = 1 - \frac{\gamma}{\gamma + W_i^2} \qquad \text{XI-11}$$

where γ is calculated by:

$$\gamma = -0.0038 \frac{W_i}{W_o} + 0.0055 \qquad \text{XI-12}$$

The comparison of the final analytical formulation with the experimental results obtained on the 45 tested geometries is shown on Figure XI-1. It highlights an accuracy of 10% for most of the tested configurations.

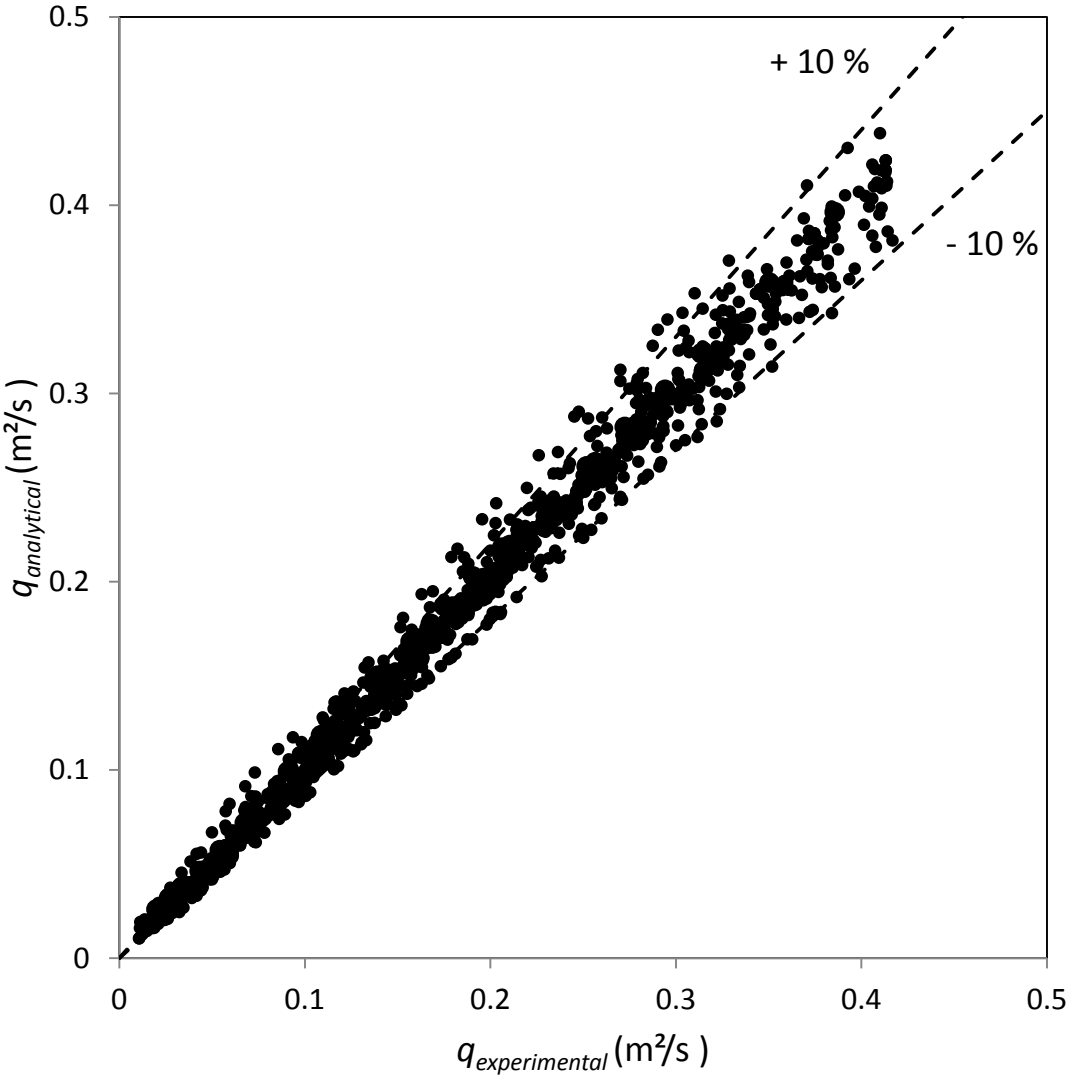

Figure XI-1 Comparison of the specific discharges computed by the final analytical formulation and all the experimental results

Even if this is less accurate than an experimental modelling, it provides a relevant tool to evaluate the influence of small variations of the geometric parameters around a well-known geometry.

XI.5. Final hydraulic optimization of the PKW design

A numerical flow solver dedicated to PKW has also been validated (see XIV.2). According to the accuracy of both numerical and analytical approaches, even if they are less accurate than an experimental modelling, they stay interesting tools to

improve a well-known geometry with small variations of the geometric parameters around their initial values.

A final hydraulic optimization may thus be realized around the pre-designed geometry using one or the two developed approaches. The free variables of the models can be set on the pre-designed stage-discharge curve defined after XI.3. Then the influence of low variations of the geometry can be studied on one or both models.

The use of the numerical solver and the analytical formulation enables thus the definition of original PKW designs, providing confident information on the stage-discharge curve as well as on the free surface profiles along the keys without representation on a scale model.

One more time, it is important to verify that the modifications of the pre-designed geometry don't interfere with the technico-economic interests of the project. Particularly, the influence of the W_i/W_o and B_o/B_i ratios has not to be studied if precast elements are favoured.

XII. Applications

XII.1. Introduction

Parallel to the experimental studies in idealized conditions, some real projects have also been studied on scale models by the Laboratory, showing interesting results. The study of these projects enables to highlight the importance to take into account the real project constraints in the design stage.

During the present research, two PKW prototypes have been studied for the Raviège Dam rehabilitation and for the new Ouldjet Mellègue Dam project.

XII.2. Design of a PKW for the Raviège dam rehabilitation [35, 38-41]

XII.2.1. Project overview

The first project studied is the one of the Raviège Dam. The Raviège Dam, operated by "*Electricité de France*" (EDF), is located on the Agout River, near the town of Toulouse, in South West of France. It is a concrete buttress 40 m high dam (Figure XII-1) built in 1957 for electricity production. The crest length is 227 m and the dam is composed of 13 plots. The hydropower plant is located at the dam toe, on the right side of the river.

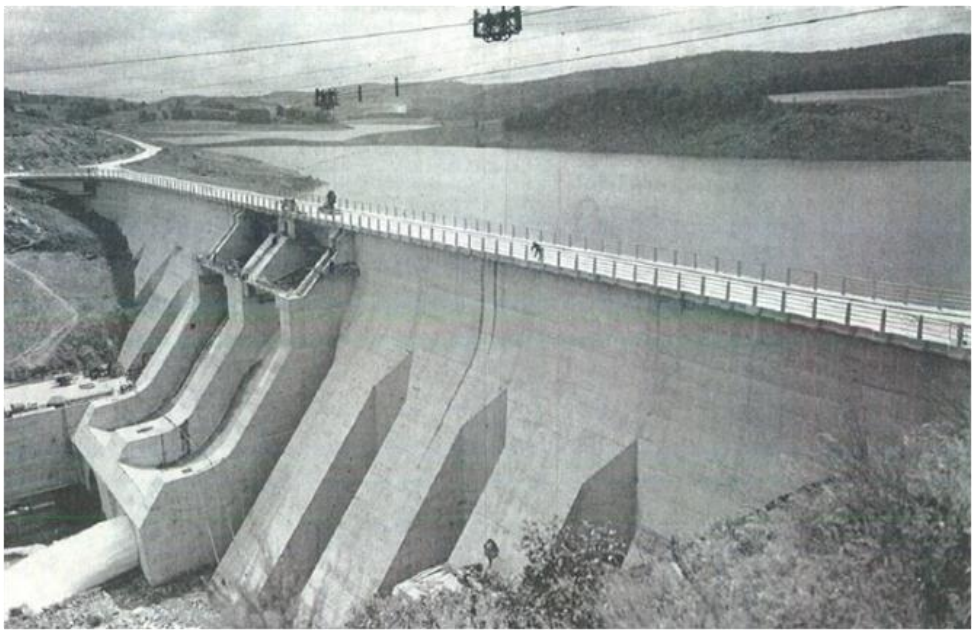

Figure XII-1 Raviège Dam at the end of the construction

The release capacity of the two existing gated spillways, located in the centre of the dam, is 1000 m³/s under the initial reservoir maximum water level. A recent update of the hydrology calculation of the dam catchment area revealed new extreme floods far more significant than the ones considered at the dam design stage. Indeed, the design flood peak discharge, calculating for a 1000 years occurrence, has been raised from 1000 m³/s to 1720 m³/s. The dam release capacity is thus not sufficient

regarding extreme floods and a project aiming at increasing the dam safety has been studied.

Most of the solutions to face safely the new extreme floods combined the use of the reservoir storage capacity and an additional spillway on top of the dam, on the left side of the existing gates. Following technico-economic studies including safety considerations, the new spillway has been designed as a free overflow one. A PKW and a fuse gate configuration have been studied, in particular using a 1:35 scale model of the dam built at the laboratory. Both solutions offer little maintenance, few operating issues and high reliability. Finally and because the cost assessments of both solutions were close, the dam owner decided to choose the PKW configuration.

XII.2.2. First PKW design

A first PKW solution has been validated to upgrade the discharge capacity of the dam. It has been pre-designed using the former presented method (see VI.2) based on the type B model of Hien et al. [46]. The PKW (Figure XII-2) consists in 8 full PKW-units and 4 modified half-units on both extremities and on both sides of a central pier. It extends thus on 3 plots of the existing dam. Upstream and downstream overhangs are respectively 4 and 3.24 m long, for a basis length of 6 m. The PKW length on the dam crest is 39.60 m, its height 4.67 m and it includes 1 m high parapet walls all over its crest. The inlet/outlet widths ratio is 1.5 and the upstream face of the outlet keys is profiled triangularly. The wall thickness is constant and equal to 0.35 m.

Figure XII-2 1:35 scale model of the first design for the Raviège PKW – Q = 24 l/s

The PKW crest level is equal to the normal reservoir level. For the maximum reservoir level, the head on the PKW is 2 m and the discharge 600 m³/s. The equivalent

discharge coefficient C_{dw} in this configuration is thus around 1.1. Lower is the head on the weir, more important is its release efficiency, with the highest values of C_{dw} exceeding 2. The influence of the PKW on flood attenuation is thus very positive. Indeed, during a flood, the very high release capacity of the PKW for low heads enables to keep intact the reservoir storage capacity before the peak flow. According to this first PKW geometry, the peak discharge is decreased from 1720 m³/s to 1450 m³/s for a 1000 years occurrence of the flood.

Regarding the results obtained on this first geometry, the global PKW width can be decreased as the flood discharge evacuated for the maximal reservoir level is largely over the design one. This enables to avoid the use of a pier in the middle of the weir and to limit the demolition of 2 plots of the existing dam, instead of 3 with the present geometry. According to these results and to the local safety rules, the maximal reservoir level has been raised of 0.4 m what enables to raise the crest level of the PKW by 1 m, increasing the normal reservoir level and so the storage capacity and the head for the hydropower plant.

XII.2.3. Final PKW design

The following paragraphs presents the optimal PKW solution designed to minimize the new spillway width on the dam crest while reducing the volume of the secondary structures to be build. This PKW includes the latest developments in PKW design such as non-constant thickness of the lateral walls and single outlet parapet walls. Considering that the existing gates will first operate, the new PKW will start to operate for major floods with return periods larger than 50 years.

The optimal PKW design for this project has been defined on the basis of the experience gained during the design and construction of EDF first four PKWs (Goulours Dam, St Marc Dam, l'Etroit Dam and Gloriettes Dam) [57, 58, 110] and following the study on hydraulic scale model of the first PKW solution.

The PKW (Figure XII-3) has a height of 4.22 m, a global width of 25.82 m and occupies the top of a little bit more than two blocks of the dam. Its crest is at the normal reservoir level. It counts for 5 inlet and 5 outlet keys framed by a specific inlet key on the right side and a specific outlet key on the left side (see XII.2.4). It uses non-symmetric overhangs, a 1 m high parapet wall on the outlets apex and a constant bottom slope of the inlets (no parapet wall, see XII.2.5). The side wall length is 13.24 m with 3.96 m long upstream overhangs and 3.45 m long downstream ones. The weir developed length is 176.6 m.

The side walls thickness varies from 0.35 to 0.25 m and decreases with the altitude in order to decrease the useless materials quantities and thus increase as much as possible the keys sections (see XII.2.6). At the crest level, the inlet keys width is 2.35 m and the outlet keys one is 1.60 m.

The outlet nose has a triangular shape. A concrete beam has been added upstream of the PKW to guarantee its stability by its own. Indeed, because the dam is affected by moderate concrete blowing pathology, the PKW will not be anchored to the existing dam to avoid potential stresses that could be generated by dam strain and displacements due to blowing effects.

According to this geometry the flood mitigation is about 350 m³/s. The discharge capacity of the final PKW is 300 m³/s under a head of 1.4 m, corresponding to the new maximal reservoir level. The gated spillway releases 1100 m³/s for this new maximal reservoir level.

Table XII-1 summarizes the main aspect ratios of the optimal Raviège Dam PKW.

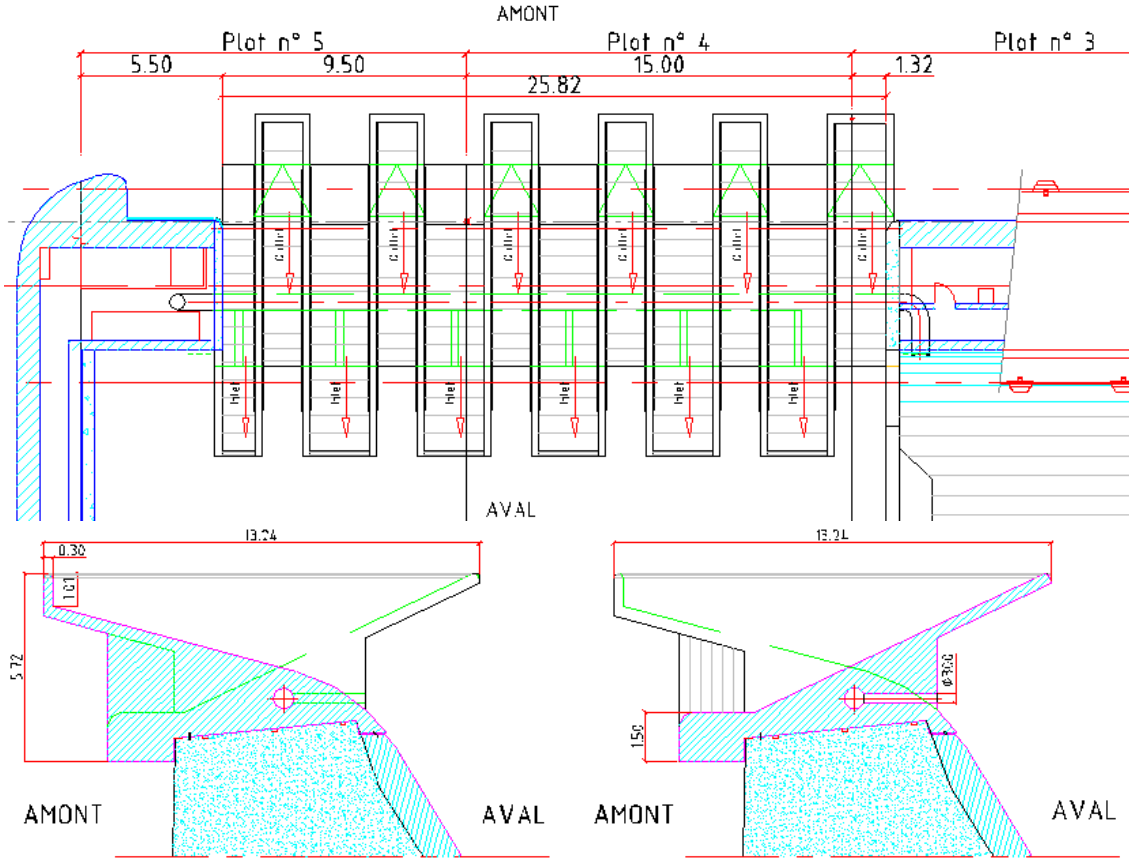

Figure XII-3 Plan view and typical sections of the PKW

Table XII-1 – Aspect ratios of the Raviège Dam PKW

L/W	6.97
W_i/W_o	1.47
P_i/W_u	1
P_i/P_d	0.139

XII.2.4. End keys

Right end key is a 1.30 m wide inlet key while left one is a 2.03 m wide outlet key (Figure XII-3). This choice is justified by the different constraints downstream. On the

right side of the spillway channel, the channel width is limited by the existing wall of the gated spillway, more than 5 m on the right of the PKW end. The lateral free overflow from an inlet induces thus no specific problem of channel apron or side wall to guide the water, while maximising the discharge capacity. On the left side of the spillway channel, the channel width and side wall height are conditioned by the flow from the weir. The use of an outlet key as end key enables to reduce the side wall height as the main flow is directed along the key axis at the key extremity (Figure XII-5).

XII.2.5. Parapet walls

Influence of parapet walls has been studied using or not a 1-m high parapet wall in the inlet key at constant weir height. As expected, a parapet wall on the inlet apex, keeping the key height constant, doesn't modify the discharge capacity of more than 5 % for the design head (Figure XII-4).

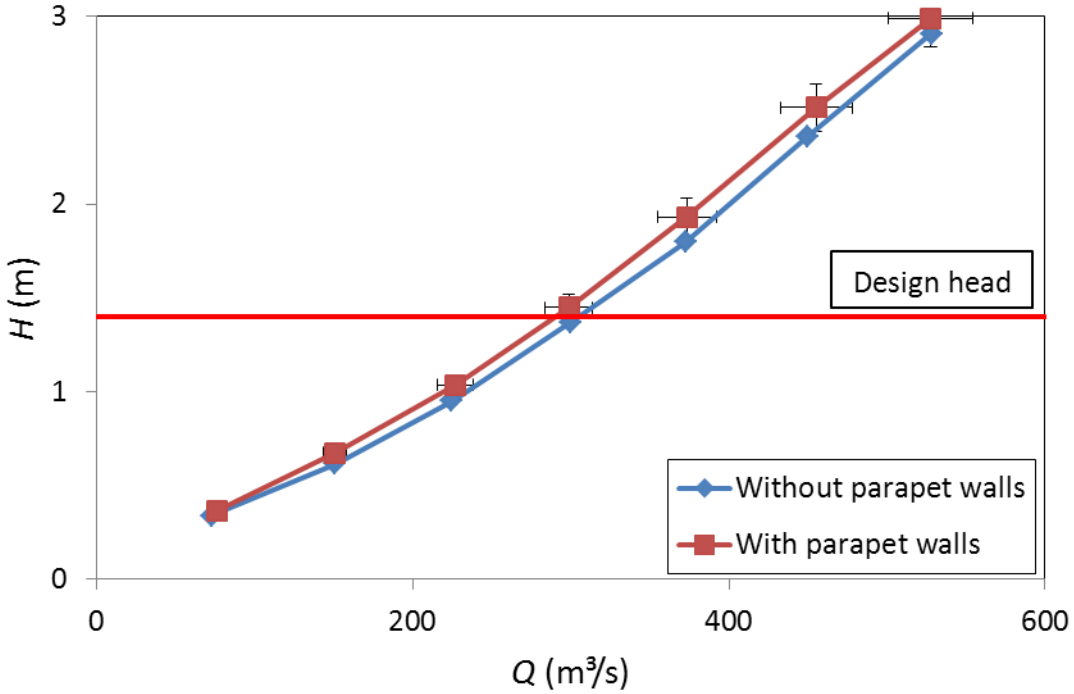

Figure XII-4 Stage discharge curves of the final PKW geometry with or without parapet walls along the inlet key

With parapet walls (Figure XII-5 – (b)), the jets from the inlet key apex are more spread for the same discharge than without the parapet (Figure XII-5 – (a)). This is because of the more important vertical component of the flow velocity on the crest in the presence of the vertical parapet, directing the jet upward to get over the obstacle. According to the negative effect of more spread jets increasing the size of the downstream side walls and to the limited difference observed on the discharge capacity, the final design has been performed without parapet walls along the inlet keys.

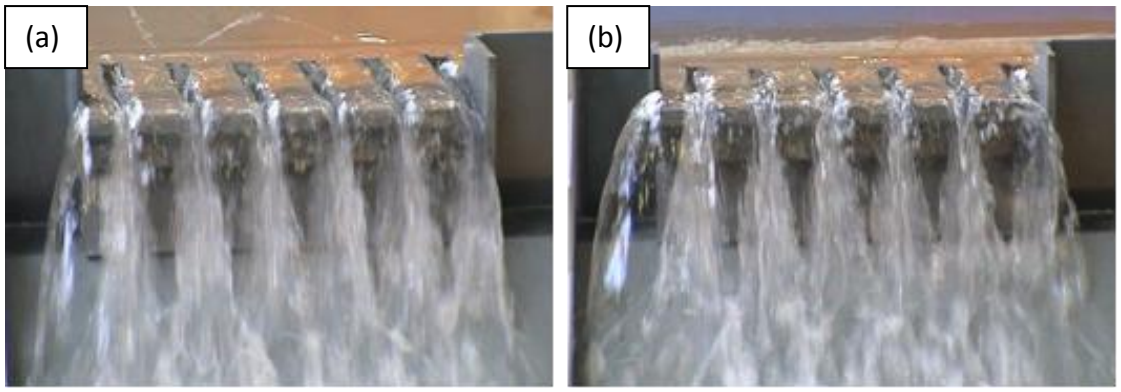

Figure XII-5 Variation of the flow features downstream of the weir without (a) and with (b) a 1-m high parapet wall on the inlet key apex

XII.2.6. Side walls thickness

The side walls thickness is a significant factor impacting the PKW discharge capacity, with potential loss in hydraulic efficiency larger than 15% (see V.2). Indeed, the side walls thickness represents a loss in the hydraulic effective section of both the inlet and outlet keys.

Using concrete to build the PKW, the best actual solution consists in having a variable thickness thinner at the top of the PKW than at the bottom, where more loads apply [110]. The EDF experience in construction on site of this type of wall, for instance at Les Gloriettes Dam, doesn't highlight particular difficulty or over-cost.

XII.2.7. Scale model

A hydraulic scale model has been used to determine the PKW features, to validate its integration within the existing structures and to design the downstream works. The scale model study has been realized considering the Froude similitude, with a 1:35 geometric scale factor. The model represented the whole dam structures, a 150 m long reach of the natural river downstream and a 230 x 210 m² area in the reservoir (Figure XII-6).

Experimental tests enable to determine the discharge capacity of the PKW (Figure XII-7) and show the very limited influence of the existing and projected spillways on their respective discharge capacities.

Despite the Raviège Dam PKW is subjected to non-negligible side effects due to its installation on an existing dam crest, it is interesting to compare its efficiency with the one of other weirs. Considering a Creager weir of same width on the dam crest, the Raviège Dam PKW is 3 times more efficient at the reservoir MWL (Figure XII-7). Regarding the results of Lempérière et al. [67] for the same type of PKW (type A) (Table XII-2), the Raviège Dam PKW is a little bit more effective in its pertinent range of head, i.e. lower than 1.5 m (reservoir level lower than MWL).

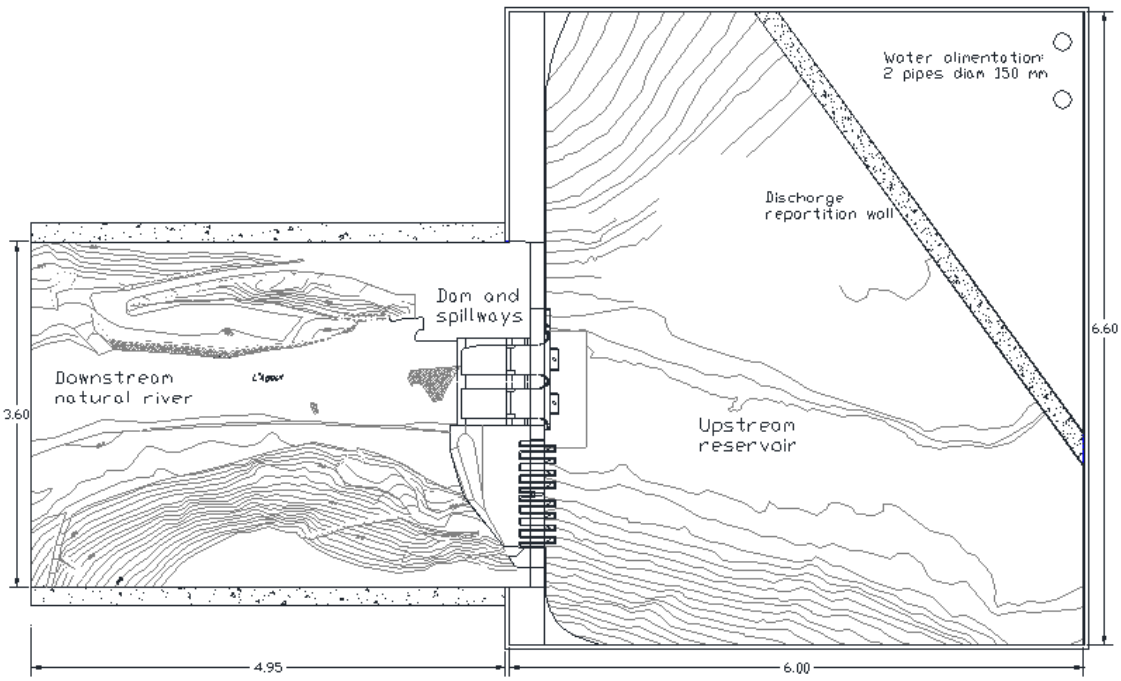

Figure XII-6 Plan view of the scale model – Dimensions in m

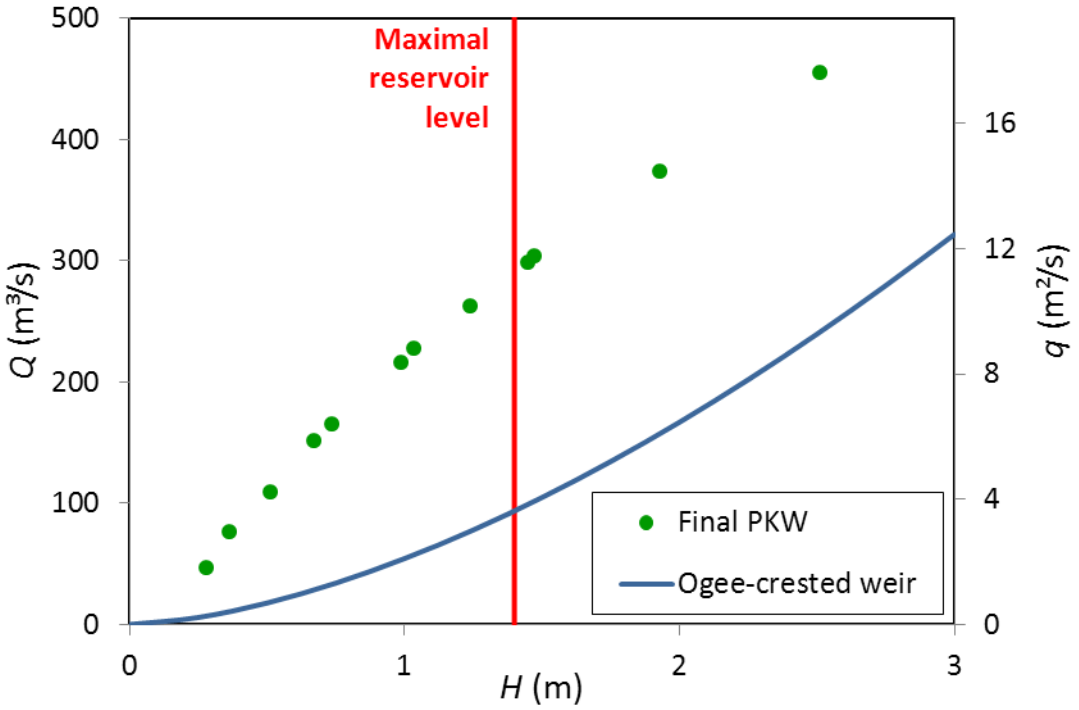

Figure XII-7 Head / discharge curve of the PKW and comparison with a Creager weir

Table XII-2 – Raviège dam PKW capacity compared with Lempérière et al. [67] model one

H (m)	Raviège Dam PKW	Lempérière et al. results
0.5	4.1 m²/s	3.5 m²/s
1	8.5 m²/s	8.2 m²/s
1.5	12 m²/s	12.5 m²/s
2	14.8 m²/s	15.6 m²/s

The final design of the flood control structures enables to maintain the normal reservoir level at its current elevation while releasing the updated design flood with a reservoir elevation 1.41 m above this normal level. In that case, peak discharge on the PKW is 300 m³/s and 1100 m³/s through the gates fully opened. The difference between the peak discharge entering the reservoir and the global peak discharge downstream of the dam is thus of about 350 m³/s for the design flood, corresponding to a peak attenuation of 18%.

A special care has been devoted to the study and design of the structures downstream of the PKW. Indeed, the new weir is located on the left side of the dam and the flow coming out of the weir has to be deviated to the right, towards the main river bed, to avoid damage to the left bank of the valley. The main difficulty of the design lies in the relative small energy of the flow coming out of the PKW combined to the reduced length of the spillway channel. This made hard the concentration of the flow and its deviation using a flip bucket or convergent walls.

The energy dissipation structure has been designed as a converging smooth channel with varied slopes and downstream deflectors. The final design consists in, from right to left: a 8.75 m wide sky jump, an intermediate inclined flat apron and a three sections side wall perpendicular to the spillway channel, reducing progressively its width (Figure XII-8 – (b)). This structure enables to concentrate the strongly aerated flows coming out of the PKW and to turn them towards the main river bed, on a place where the flow released through the gated spillways induces a thick water cushion (Figure XII-8 – (a)).

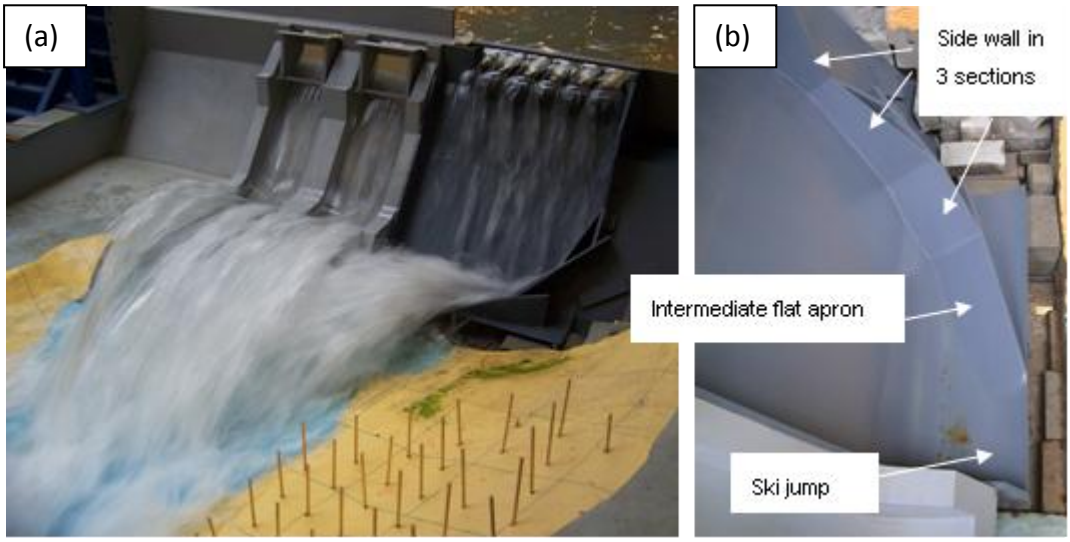

Figure XII-8 Peak discharge of the design flood on the scale model (a) and details of the downstream structure (b)

XII.2.8. Lessons learned from the study

This study highlights the importance for the PKW designer of the hydraulic optimization. The discharge capacity of the weir has been extensively studied through

the use of noses, of parapet walls only on some parts of the crest providing different outlet and inlet keys slopes, of non-symmetric keys widths and overhangs lengths. This comes from the nature of the project. Indeed, it consists in a rehabilitation project in a relatively well instrumented and industrialized area, motivating a more precise hydraulic investigation.

However, as the study consisted in a rehabilitation project, some structural considerations, inducing important economic consequences, imposed constraints to the hydraulic optimization of the PKW. The weir height was so limited by structural considerations. The second PKW configuration has finally been chosen as it extends only on 2 plots, instead of 3 for the first one, what induced important over-costs.

This study also revealed the importance of the design of the structure for the energy dissipation. Indeed, the PKW provides large specific discharges with relatively low energy level, as losses of energy are already provided by the varied interactions between jets downstream of the structure.

XII.3. Design of a PKW for the Ouldjet Mellègue project dam [35, 37, 39, 40]

XII.3.1. Project overview

Another study has been undertaken with "*Tractebel Engineering - Coyne et Bellier*" to design a PKW upstream of a stepped spillway. The Ouldjet Mellegue Project in Algeria concerns the building of a 50 m-high RCC dam equipped with a free surface spillway. The structure has to release a discharge up to 3500 m³/s, corresponding to a 10 000-years flood, under a head of 4.5 m, while the available length on the dam crest is limited to 100 m. The PKW is thus the only possible solution.

XII.3.2. PKW design

The PKW pre-design has been realized according to the former presented method (see VI.2) based on the models of Ouamane and Lempérière [94] and of Karelle [53].

Requested flood release capacities and dam site geometry constraints lead to design a non-symmetric PKW, made of 12 outlet and 11 inlet keys. The outlet keys width is 3.2 m and the inlet keys one is 4.4 or 5.4 m, one inlet key out of two having at the centre a 1 m wide pier (Figure XII-9). Side walls thickness is 0.4 m. The total width of the PKW on the dam crest is 97.8 m. The PKW height is 6.8 m, the length of the upstream overhang is 2.85 m and the one of the downstream overhang is 3.18 m. The length of the side walls is 16.2 m for a base length of the structure equal to 10.17 m. The bottom slope is 28.32° in the outlet keys and 27.7° in the inlet keys. Steps have been designed in the outlet keys, such as suggested by Leite Ribeiro et al. [63]. The outlet upstream face is not profiled and there is no parapet wall on the weir crest,

which is horizontal. A 1.8 m wide specific outlet key at each of the weir extremities enables to simplify the design of the side walls at the weir entrance and to limit the height of the lateral walls in the spillway channel. The developed length of the PKW is 451.1 m. Its main aspect ratios are summarized in Table XII-3.

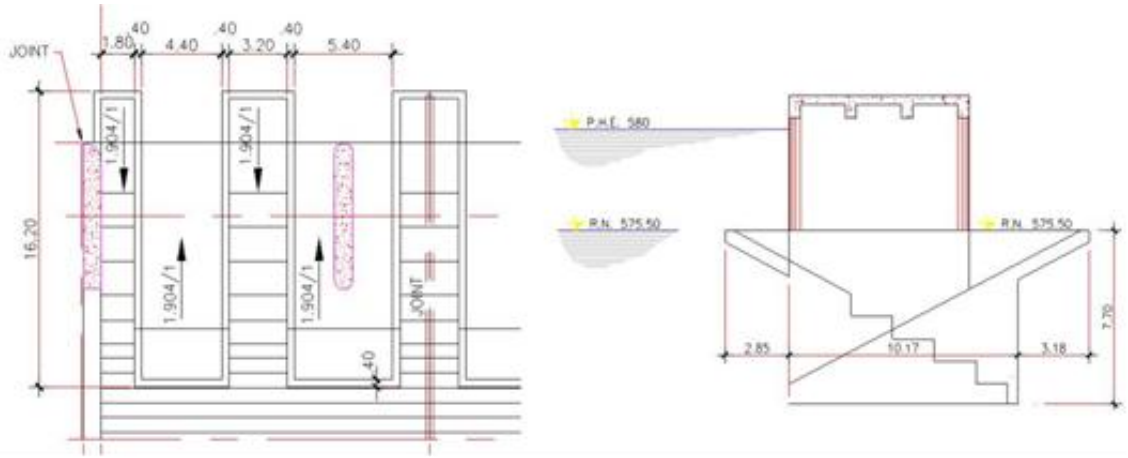

Figure XII-9 Partial plan view and typical cross section of the Ouldjet Mellegue PKW - Dimensions in m

Table XII-3 – Aspect ratios of the Ouldjet Mellegue PKW

L/W	4.61
W_i/W_o	1.37
P/W_u	0.81
P/P_d	0.176

Discharge coefficients related to the weir width on the dam crest ranging from 1.85 for an upstream head ratio *H/P* equal to 0.1 to 0.8 for an *H/P* ratio equal to 0.7 are provided by this geometry. The maximum discharge is 3330 m³/s under a 4.5 m head; the maximum specific discharge is 34 m²/s in the spillway.

XII.3.3. Energy dissipation

In this project, the PKW is projected upstream of a stepped spillway and a downstream stilling basin. Indeed, PKW geometric features create interacting flows and jets downstream and thus energy dissipation and air entrainment. These observations suggest that the use of a PKW to control the flow upstream of a stepped spillway may help in enhancing energy dissipation on the downstream channel. In order to verify this assumption and to validate the spillway project geometry, two scale models studies have been carried out.

An existing facility at the laboratory has been used to compare, in an idealized environment, the energy dissipation on a stepped spillway downstream of a PKW with the one which takes place on the same spillway equipped with a standard ogee-crested weir. This facility is made of a 2 m high and 0.494 m wide stepped spillway linked to an upstream reservoir and a 3 m long downstream horizontal channel (Figure

XII-10). The spillway slope is 52° with 3 cm high regular steps. Bank walls are made of steel, PVC or Plexiglas plates. An adjustable vertical gate is situated at the downstream extremity of the horizontal channel. The reservoir is supplied in water by a regulated pump connected to a pressurized pipes network.

Three different models of weir have been considered upstream of the stepped spillway. In a first time, tests have been done with a standard ogee-crested weir [27]. The global spillway height is 2.039 m in that case. In a second time, two varied layouts of a PKW have been placed on the top of the stepped spillway (Figure XII-11). The first one (PKW 1) represents 1.5 inlets and 1.5 outlets while the second one (PKW 2) is made of 2.5 inlets and 2.5 outlets. In both cases, the aspect ratios of the PKW are almost identical (Table XII-4). Only the scale of the models varies. PKW 2 dimensions are generally 1.6 times smaller than PKW 1 ones, except the global width which is kept constant to the experimental facility one, and the walls thickness which as to match the commercial dimensions of PVC plates. With PKW 1, the global spillway height is 2.258 m and it is 2.156 m with PKW 2. The scale factor of PKW 1 regarding the Ouldjet Mellegue Project prototype is 1/26. It is 1/42 for PKW 2.

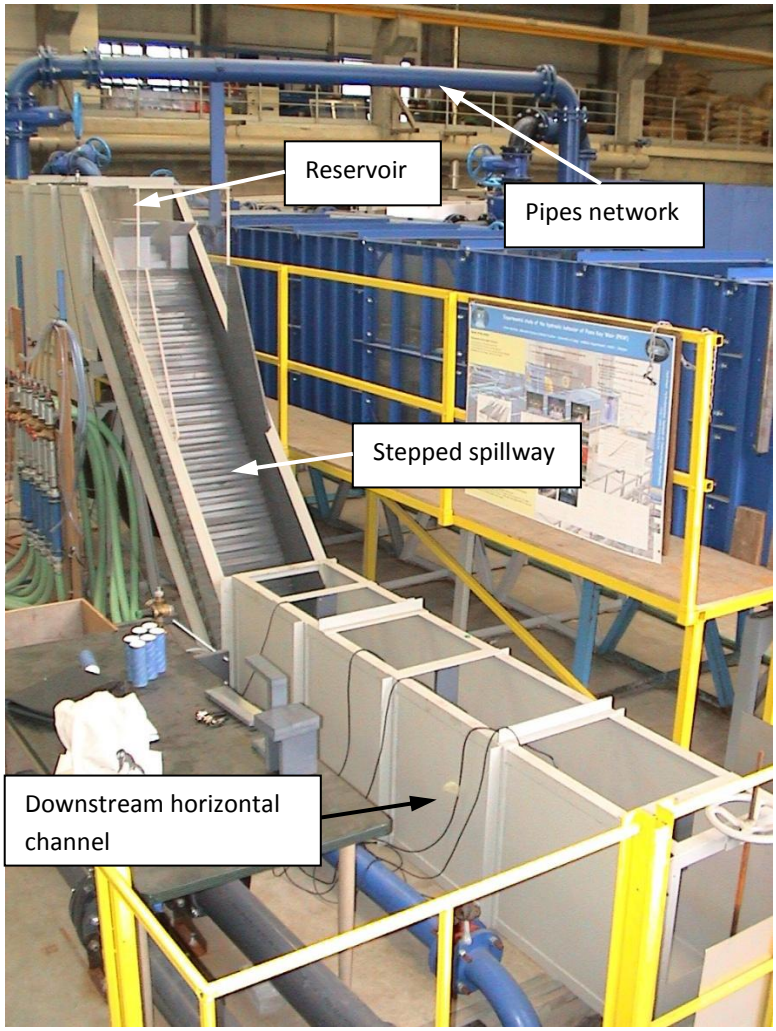

Figure XII-10 Global view of the experimental facility

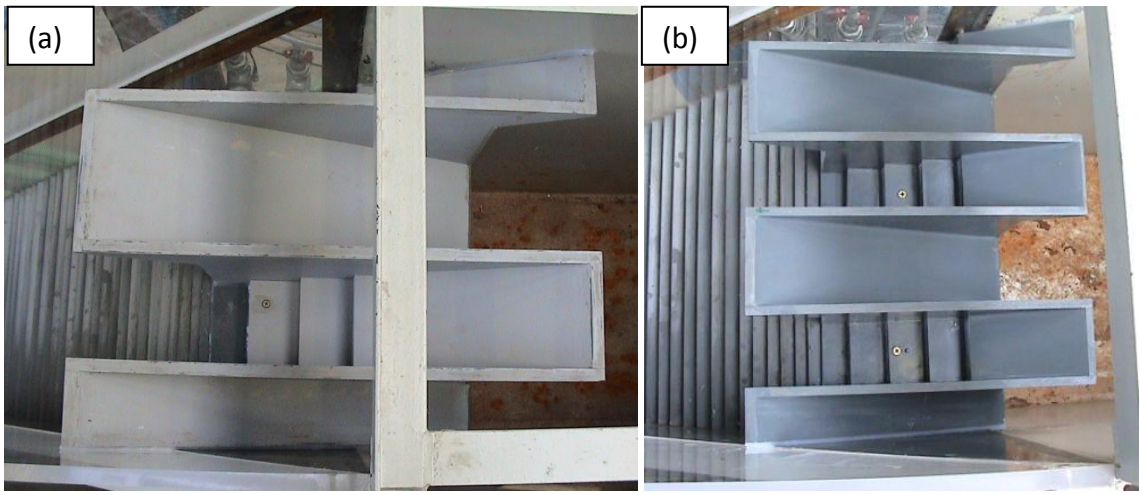

Figure XII-11 PKW 1 model (a) and PKW 2 one (b)

Table XII-4 – General dimensions and aspect ratios of PKW 1 and 2

	PKW1	PKW2
W_i (m)	0.169	0.098
W_o (m)	0.123	0.077
T_s (m)	0.015	0.01
P (m)	0.262	0.163
B (m)	0.623	0.388
B_o (m)	0.139	0.087
B_i (m)	0.11	0.068
W_i/W_o	1.37	1.27
P/W_u	0.81	0.84
$2T_s/L_u$	0.02	0.02
L/W	4.78	4.88

The tests consisted in computing, for several constant discharges, the energy dissipation on the weir and along the spillway. This has been done by comparison of the head in the reservoir H_{up} and the head at the spillway toe H_{dw} (Figure XII-12). For the first one, it can be easily calculated from the reservoir level measurements h_{up}. For the second one, because of air entrainment and flow velocity, it is difficult to measure accurately the flow depth directly at the spillway toe. An indirect method has thus been applied [104].

By means of regulating the gate downstream of the horizontal channel, a hydraulic jump has been created at the middle of the channel. The first conjugate depth (supercritical – upstream) has been calculated from the measured depth downstream of the jump, which is the second conjugate depth (subcritical) and is less varied and aerated.

The water depth has been measured by probes 4 and 5 (Figure XII-12) to define the second conjugate depth of the hydraulic jump and then calculate the first

conjugate depth, which has been considered to compute the residual flow energy at the dam toe. In addition, direct measurements of the water depth by probes 1 and 2 (Figure XII-12) enable to compute a rough direct evaluation of the residual energy downstream of the spillway. This shows a general overestimation of around 50% of the measured downstream water depth compared with the calculated one (Figure XII-13). This is in agreement with the observation of a strong aeration of the flow at the spillway toe.

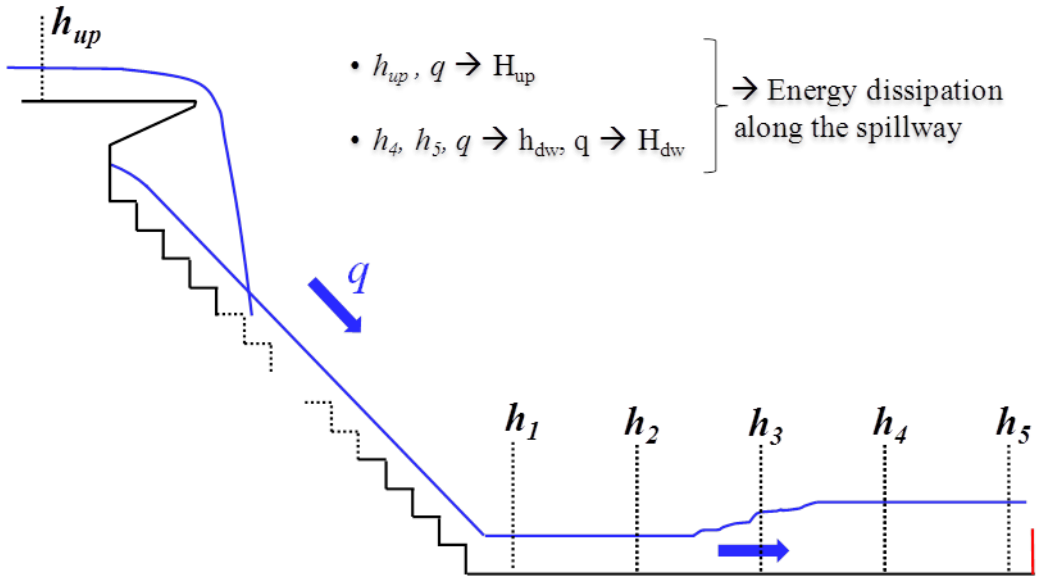

Figure XII-12 Sketch of the experimental facility and tests principle

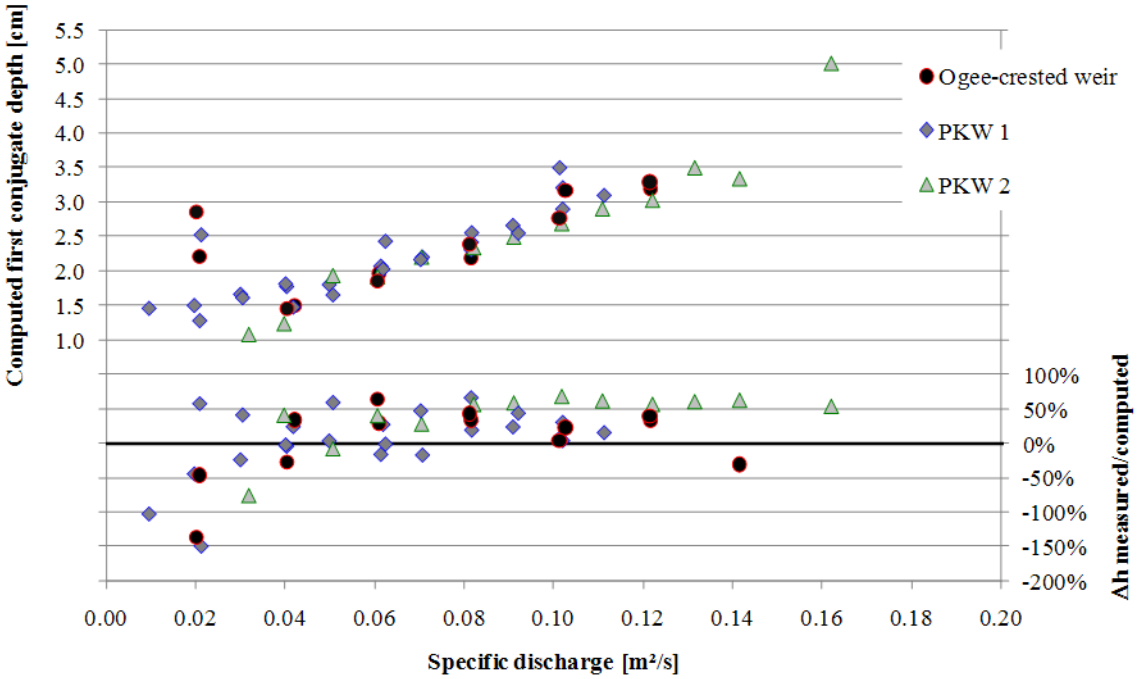

Figure XII-13 Computed first conjugate depths and relative difference in between measured depths at probes 1 and 2 and computed one as a function of the specific discharge in the spillway

The results of the tests carried out with the three weir configurations for discharges ranging from 0.01 to 0.08 m³/s are summarized on Figure XII-14 in the way used by Boes and Hager [14], where H_{dam} is the dam height and h_c the critical depth computed from the spillway and weir width.

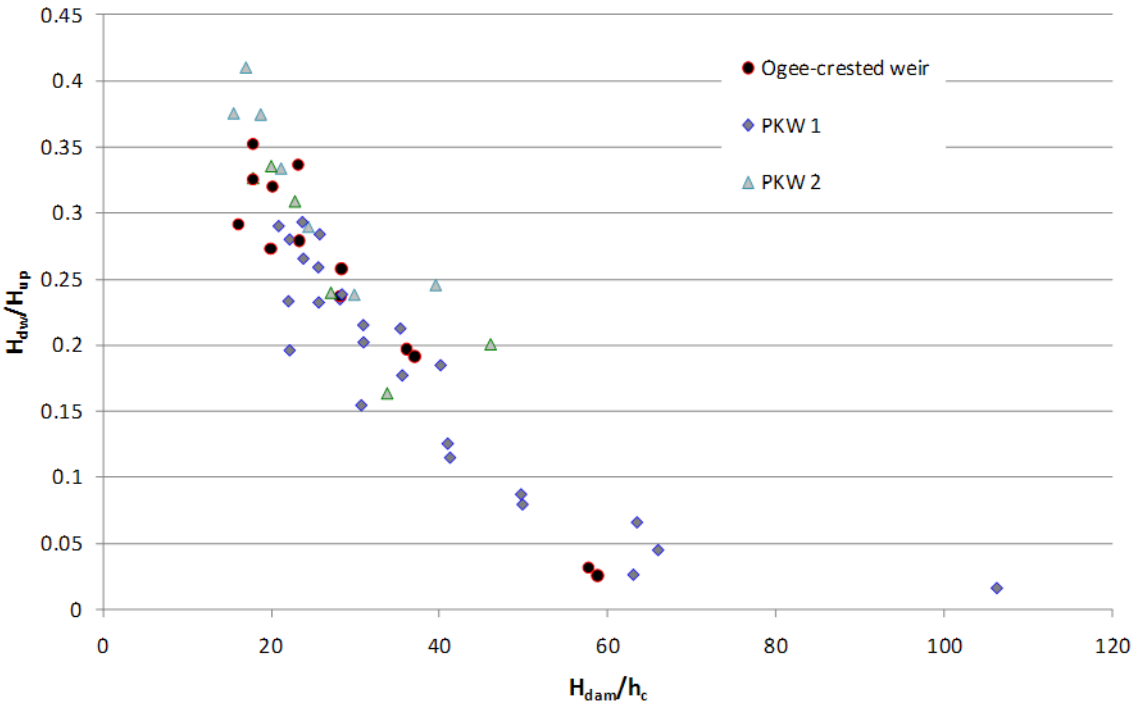

Figure XII-14 Relative downstream head ratio H_{dw}/H_{up} depending on relative spillway height H_{dam}/h_c

Regarding energy dissipation, no clear difference appears in between the tested configurations. This can be explained by the spillway length which is certainly sufficient to reach near uniform flow conditions at the spillway toe in the range of discharges considered. Indeed, according to Boes and Hager [14], for the spillway slope considered in this paper, the minimum relative dam height $H_{dam,u}/h_c$ to attain uniform flow is 20.5.

Despite additional tests with smaller spillway lengths are still under progress, for the same specific discharges in the spillway, important differences in the flow have been observed depending on the type of weir. With both PKW geometries, the flow is fully aerated at the beginning of the spillway, while it is not the case with the ogee-crested weir (Figure XII-15). These observations are consistent with the ones of Ho Ta Khanh et al. [47]. They suggest quicker effective energy dissipation downstream of a PKW than downstream of an ogee-crested weir, thanks to the rapid developing of skimming flow conditions.

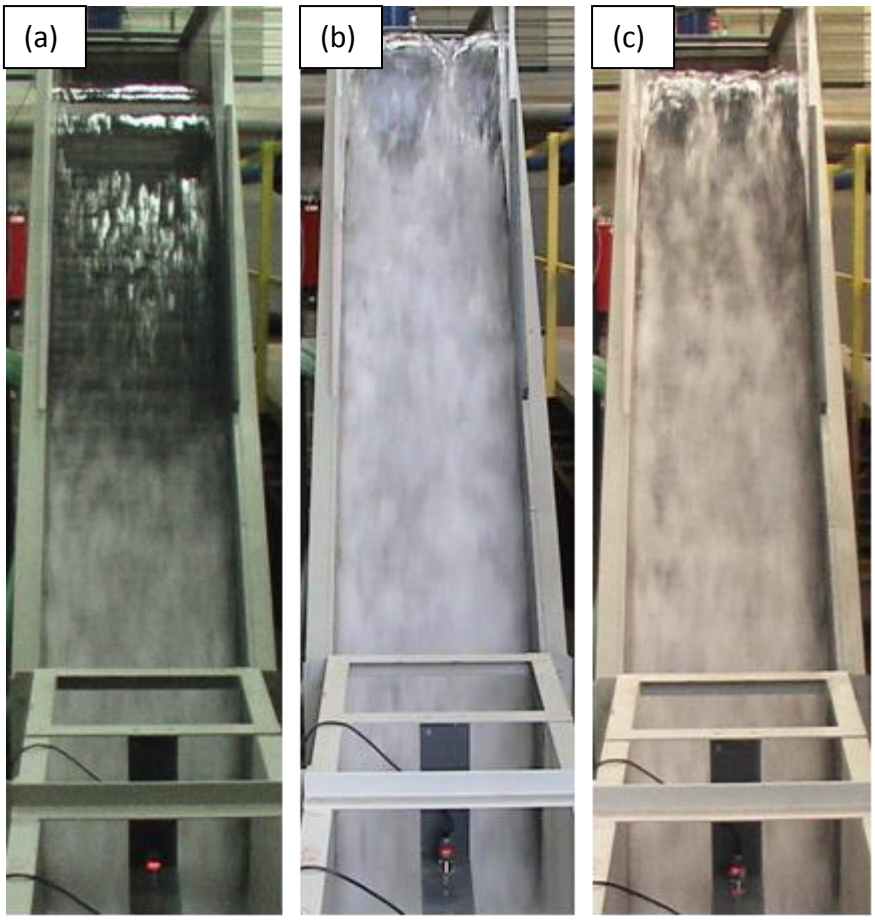

Figure XII-15 Aeration of the flow downstream of the ogee crested weir (a), PKW 1 (b) and PKW 2 (c) – Discharge of 0.05 m³/s

The aeration of the flow on the first steps of the spillway downstream of a PKW is underlined on the pictures of Figure XII-16 for rather high discharges. No air can be seen on the steps in the outlet, but air entrainment begins just downstream of the PKW toe, upstream of the impact point of the jet coming out from the inlet apex.

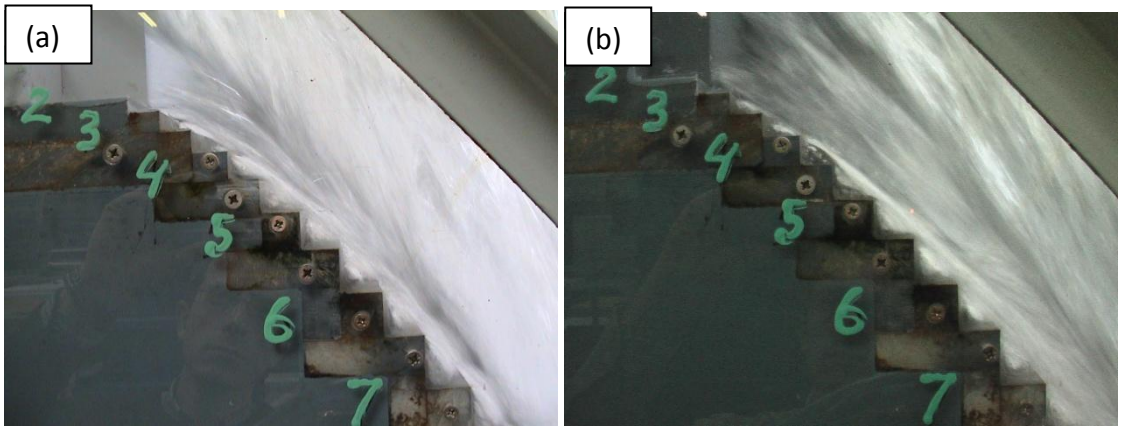

Figure XII-16 Aeration of the flow on the first steps – PKW 1, Q = 0.05 m³/s (q = 0.1 m²/s – (a)) and PKW 2, Q = 0.07 m³/s (q = 0.14 m²/s – (b))

XII.3.4. General hydraulic scale model

In a second time, a general scale model of the dam and spillway structures has been built using the Froude similarity and a 1:50 geometric scale factor (Figure XII-17). In addition to the weir, the spillway channel and the stilling basin, the scale model represented a 300 m long reach of the natural river downstream and a sufficient area of the reservoir to avoid an effect of the boundary conditions on the flow over the weir.

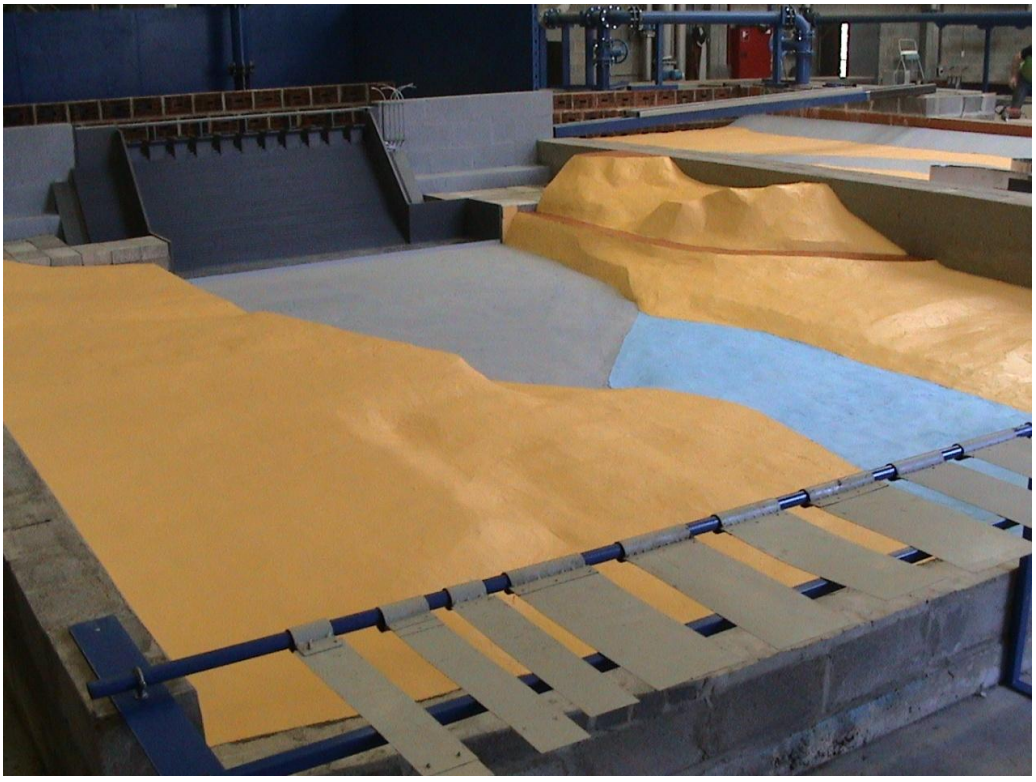

Figure XII-17 Downstream view of the general hydraulic scale model of the Ouldjet Méllegue Dam

The discharge injected in the reservoir is the upstream boundary condition. The water level in the reservoir is imposed by the PKW release capacity. The water level in the downstream reach is regulated using small steel strips (Figure XII-17) according to the river rating curve.

This general model enables to validate the general layout of the spillway, to determine the release capacity of the PKW, to optimize the design of the spillway channel and the stilling basin and to measure the characteristics of the flows released in the downstream natural river for discharges up to the 10 000 years flood.

The comparison of the stage-discharge curve measured on the scale model with the estimated one from the pre-design method (Figure XII-18) shows good agreement except for lowest heads for which the influence of the walls thickness has already been demonstrated (see V.2).

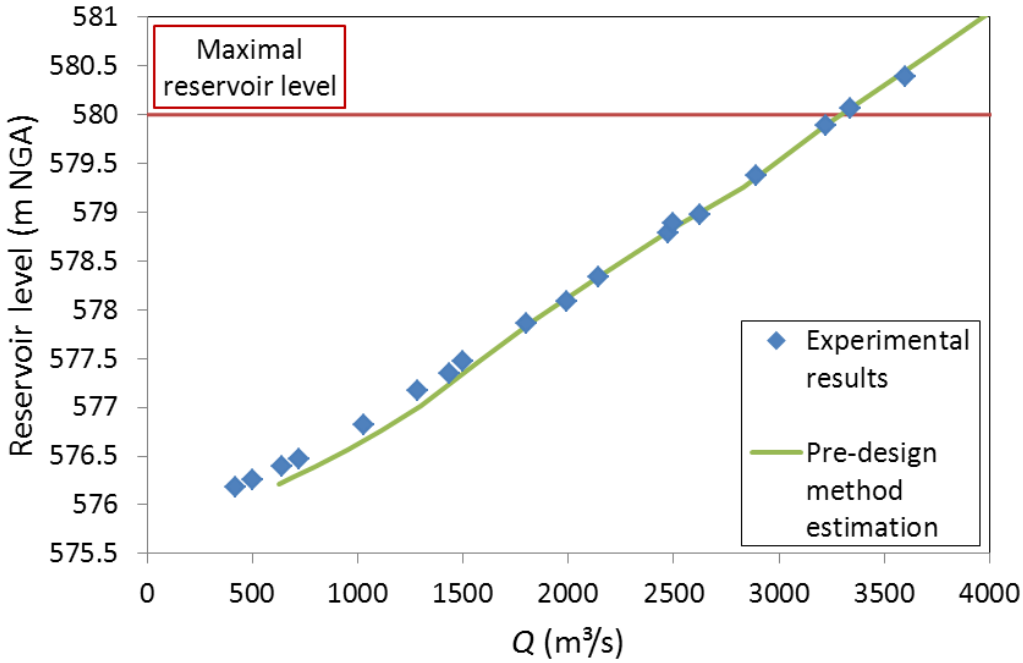

Figure XII-18 Comparison between experiments and estimated stage-discharge curve

The general scale model has also highlighted the presence of 2 hydraulic jumps at the dam toe (Figure XII-19). If the first one is situated as expected in the still in basin, it is no more the case for the second one that appears already for discharges of 1500 m³/s. That may induce erosion problems at dam toe.

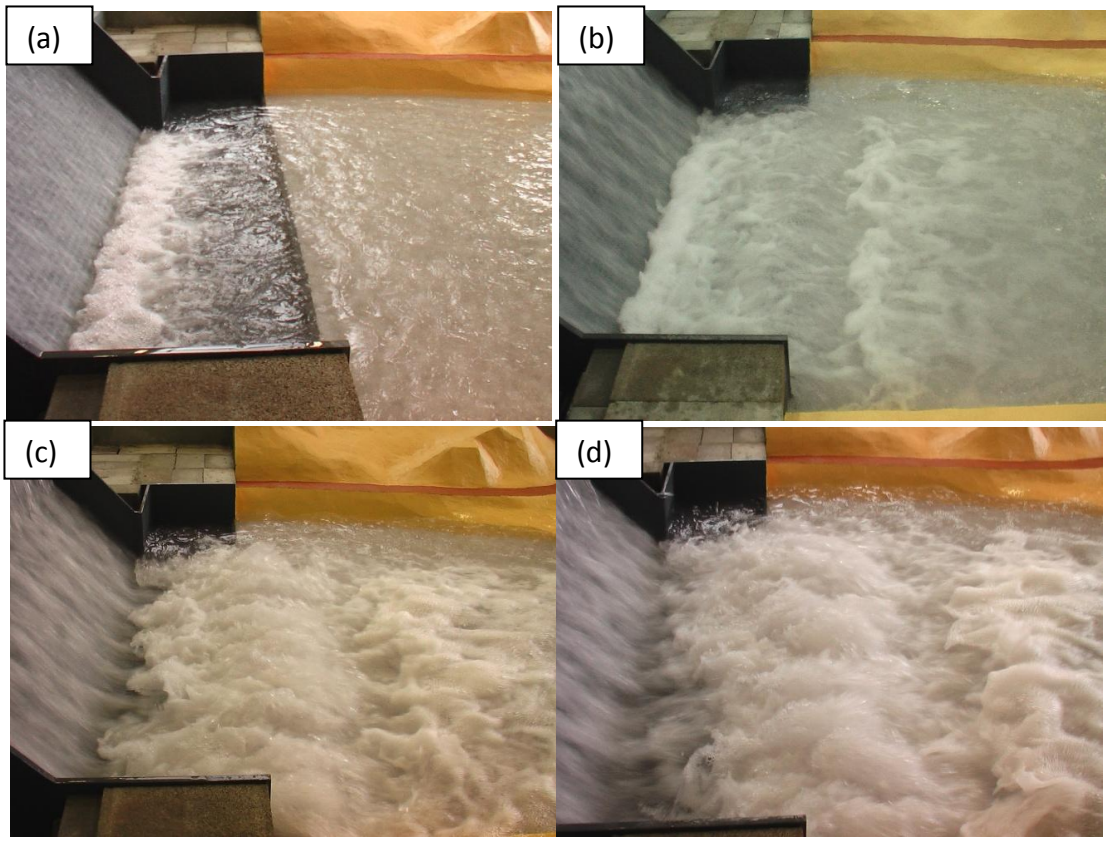

Figure XII-19 Position of the hydraulic jump at dam toe for discharges of 500 (a), 1500 (b), 2500 m³/s (c) and maximal reservoir level (d)

To reduce the second hydraulic jump, keeping the first one within the still in basin, the level of the entire still in basin has been decreased to avoid difference between the downstream wall crest and the topography levels (Figure XII-20).

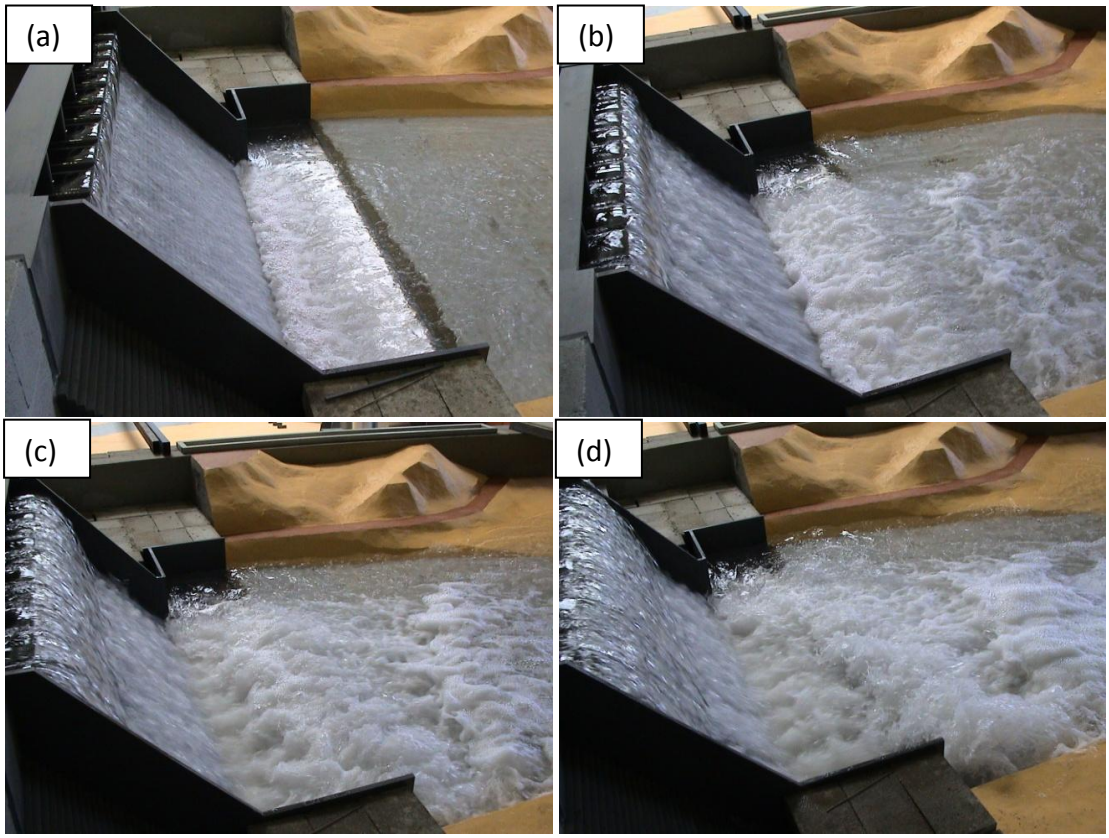

Figure XII-20 Decreased still in basin level - Position of the hydraulic jump at dam toe for discharges of 500 (a), 1500 (b), 2500 m³/s (c) and maximal reservoir level (d)

XII.3.5. Lessons learned from the study

As this project concerns a new dam situated in a poorly instrumented area, and as the hydraulic characteristics of the project involve a high number of PKW-units, the design has been largely managed by the research of the simplicity of the structure. Investigations on the hydraulic behaviour of the proposed design have thus been limited.

One more time, this study highlights the importance of the design of the structure for the energy dissipation. The study of common use of dissipative structures with PKW is a way that stays to study extensively in the future.

XIII. Conclusions

XIII.1. Interests and limitations of PKW use

The main objectives of the present research were to enhance the understanding of the flow over a PKW as well as to determine the influence of the main geometric parameters of the structure on its release capacity in order to provide efficient design tools. To achieve these goals, a large scale model has been firstly investigated. The model enabled the observation and the measurements of the flow characteristics all along the weir. In a second time, several scale models with variable geometries have been studied to highlight the influence of the main geometric parameters. The choice of the three studied parameters (the weir height, the keys widths and the overhangs lengths) has been realized on the basis of the results from the large scale model study.

According to the experience gained from the present research, the advantages of the PKW are confirmed and the physical fundament of the hydraulic efficiency can be explained. The PKW may release discharges until four times more important than ogee-crested weirs of same width. This is mainly due to the increase of the developed crest length. It also releases about 10% more important discharges than labyrinth weirs of same shape. This is mainly due to the use of upstream overhangs. Indeed, along the upstream overhangs, the larger cross section for the approaching flow decreases the flow velocities compared with labyrinth weirs. This increases the side crest efficiency, and thus the global weir discharge capacity, as the deviation of the flow is easier.

However, the results of this study also highlighted some limitations to the PKW interest. Indeed, for increasing upstream heads, the ratio of efficiency of the PKW, compared with a traditional ogee-crested weir, decreases. This is the result of various physical phenomena analysed in this work. The main cause of this loss in efficiency is the increase of the incoming flow velocity along the inlet key. Indeed, as this flow velocity increases, the side crest efficiency decreases, affecting significantly the PKW discharge capacity. Furthermore, the increase of the velocity along the inlet key may induce the apparition of a control section upstream of the inlet apex, reducing the effective crest length of the weir. Even if this phenomenon is of secondary importance, it may decrease up to 5% the maximal discharge capacity of the weir. Other phenomena of minor importance have been identified as affecting the PKW efficiency for increasing upstream heads. The consideration of the crest thickness and the lateral nappes interferences decrease the effective crest length in the range of 3%. Head losses at inlet key entrance also affect the upstream head of less than 3% on the studied models.

For very low heads, a limitation in efficiency has also been highlighted. It is only related to the crest shape. In order to limit the observed decrease in efficiency for low heads, rounded crests have to be preferred on prototypes designed for flow mitigation.

Finally, a main limitation of the weir efficiency may come from the outlet release capacity. As long as the outlet slope and width are not sufficient to ensure supercritical flows, the outlet free surface level grows for increasing discharges. If the free surface reaches the side crest elevation, the PKW efficiency significantly decreases. Furthermore, the interference of the nappes coming from opposite side crests may decrease the side weir efficiency for too narrow outlet keys. To prevent these undesirable effects of crest submergence and frontal nappes interaction, sufficiently sloped and wide outlet keys must be used for PKW design.

XIII.2. Advices for a better PKW design

As a result of this research, even if it appears that a unique optimal PKW design doesn't exist, keys tools are given to approach it with a confident accuracy. Furthermore, according to the experience gained from this study and to the definition of the project engineer interests, some rules should be followed.

From a hydraulic point of view, it is of prime importance to increase all the geometrical ratios that favour a larger inlet cross section, as it can be seen as the "*engine*" of the PKW. Increasing the inlet cross section decreases the flow velocity along to it, what increases the side crest efficiency, limits the apparition of a control section upstream the inlet apex and limits the head losses at inlet entrance. However, maxima have to be given to the increase of the related ratios if they affect the release capacity of the outlet key. Indeed, the outlet key can be seen as the "*brake*" of the PKW. Too small outlet widths and slopes elevate the free surface level over the side crest elevation and limit significantly the weir efficiency.

A PKW design associating a vertical aspect ratio P/W_u equal to 1.33, a keys widths ratio W_i/W_o equal to 1.25 and an overhangs lengths ratio B_o/B_i equal to 3 seems to be the hydraulic optimum for a developed length ratio L/W equal to 5.

However, the study highlights also the importance of the technico-economic criteria in the definition of an optimal PKW design. A high PKW (P/W_u = 1.33) is more effective from a hydraulic point of view and should thus be preferred for new dam projects. A low PKW ($P/W_u \approx 0.5$) should be preferred for rehabilitation projects. According to the economic interest of the use of precast elements in projects realized in developing countries, W_i/W_o and B_o/B_i ratios equal to 1 have to be selected for such projects. A B_o/B_i ratio equal to 1 has also to be used for low weir configurations ($P/W_u \approx 0.5$) as it provides then the hydraulic optimum.

Even if the design of a PKW stays based on the experimental knowledge of a reference geometry, the present research increases significantly the available data base and gives scientifically based rules for the choice of the reference geometry depending on the project characteristics. Furthermore, the exploitation of the experimental results obtained during this research enabled the definition of an

analytical formulation of the discharge capacity of the PKW depending on its geometrical characteristics. The accuracy of the formulation is 10%. The experimental results also helped to the development and to the enhancement of a numerical solver dedicated to PKW modelling. These two tools, validated on data gained in different laboratories, enable to refine an initial design without any physical modelling.

XIII.3. Perspectives

At the beginning of this research, the scientific knowledge on PKW hydraulics was near to zero. Even if the understanding of the flow over a PKW, the knowledge on the influence of the geometric parameters and the design rules for PKW have been largely enhanced, the study also revealed ways for further studies.

On a first hand, the importance of the structural and economic criteria has been highlighted to define an optimal PKW design. This gives the way for further researches. Indeed, until now, the consideration of the structural and economic consequences of a PKW design has been poorly approached. In order to improve that way, collaborations between hydraulic researchers, structural engineers and builders are inevitable. This is already initiated through the exchanges between the "*Ecole Polytechnique Fédérale de Lausanne*", "*Electricité de France*", "*Hydrocoop*" and the "*University of Liège*" that have enabled to initiate the combined hydraulic and technico-economic approaches of the PKW design through the present work and trough the latest prototype studies (Raviège, Malarce, Gage …).

On a second hand, the application of the PKW to prototype projects showed that a key issue is the study of the energy dissipation downstream of the weir. Even if the study of this topic has been initiated in several places, the development of a specific dissipation structure for PKW needs to be performed. According to the jets interactions and to the air entrainment observed along the structure, stepped spillways seem to be the best dissipative structures. Indeed, the PKW and the steeped spillway characteristics for energy dissipation are similar, decreasing the energy from the dam crest to its toe by interacting jets and limiting flow velocities. The combination of PKW with a smooth spillway ended by a ski jump remains less advantageous. This time, PKW and spillway working for energy dissipation are opposed. Indeed, the weir decreases the energy level by interacting jets when the ski jump needs of high level of energy to spread the incoming flow far from the dam toe. Furthermore, the key configuration induces a non-homogeneous flow repartition along the spillway width. Additional convergent structures are thus needed to reorient the flow along the spillway slope in order to increase and to homogenise the velocities before the ski jump.

Finally, the analytical formulation and the numerical model developed in this work could probably be enhanced. The consideration of compound cross sections for

the numerical solver should considerably improve the model results. Actually the main limitation of a more large use of the Wolf1D-PKW flow solver remains the bad representation of the flow velocities along the upstream overhangs, modifying consequently the representation of the head-discharge relation. The consideration of compound keys sections, instead of a channel representation, enables to solve this problem. The extension of the proposed analytical formulation to other L/W values seems to be also an interesting issue. In a first way, the comparison of the proposed formulation with experimental results obtained on models with a varying developed crest length is to performe.

XIV. Annexes

XIV.1. Effect of vertical inclination of sharp-crested weirs

XIV.1.1. Introduction

Even if the influence of approaching flow conditions on the release capacity of the usual free overflow structures has been well demonstrated [56], the influence of the upstream slope on the discharge capacity of a sharp-crested weir is still poorly described. This problem may be studied following two approaches: the first one considers a vertical sharp-crested weir progressively inclined downstream (Figure XIV-1 - (a)), when the second one considers a horizontal free overfall progressively inclined with an invert slope (Figure XIV-1 - (b)).

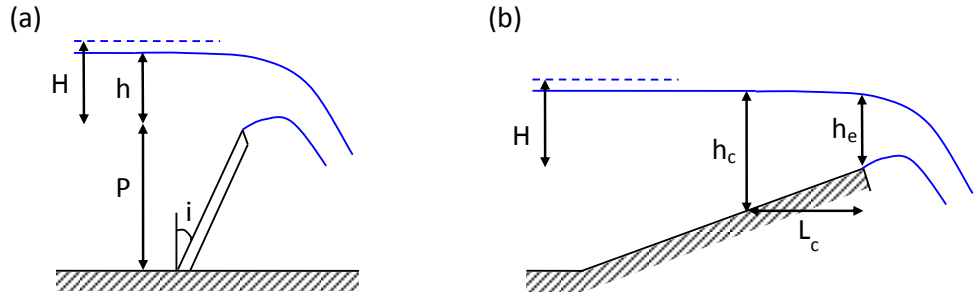

Figure XIV-1 Two approaches of the inclined weirs: (a) inclined sharp-crested weir, (b) inclined free overfall

XIV.1.1.1. Inclined sharp-crested weir

For vertical sharp-crested weirs, several authors propose formulations of the discharge coefficient C_{dL} depending on the ratio of the upstream energy head and the weir height H/P [54, 100, 106, 107]. The discharge could further be calculated from the Poleni equation (Eq. II-1).

The Swamee [106] formulation tends to the one of Kindsvater and Carter [54] for low values of H/P and to the experimental results of Rouse [102] when P tends to 0. However, Swamee gives a formulation of a discharge coefficient considering the upstream water height h instead of the energy head H (Figure XIV-1 – (a)) in Eq. II-1:

$$C_{dL}^{*} = 0.707\left[\left(\frac{14.14P}{8.15P+h}\right)^{10} + \left(\frac{h}{h+P}\right)^{15}\right]^{-0.1} \qquad \text{XIV-1}$$

$$q = C_{dL}^{*}\sqrt{2gh^{3}} \qquad \text{XIV-2}$$

Calculating the discharge using the Swamee formulation enables to define the energy head as a function of the weir height and the upstream water height:

$$\frac{H}{h}=1+0.5\frac{\left[\left(\frac{14.14}{8.15P+h/P}\right)^{10}+\left(\frac{h/P}{h/P+1}\right)^{15}\right]^{-0.2}}{\left(1+\frac{P}{h}\right)^{2}} \qquad \text{XIV-3}$$

the discharge coefficient related to the upstream head can be calculated by:

$$\frac{C_{dL}}{C_{dL}^{*}}=\left(\frac{H}{h}\right)^{-1.5} \qquad \text{XIV-4}$$

For a given energy head H and a given weir height P, Eq. XIV-4 enables to give the discharge coefficient C_{dL} by insertion of the water height h calculated by Eq. XIV-3 and of the Swamee discharge coefficient C_{dL}^{*} calculated by Eq. XIV-1. The curves of Figure XIV-2 represent this system of equations and enable to determine the specific discharge of a sharp-crested weir for given energy head and weir height.

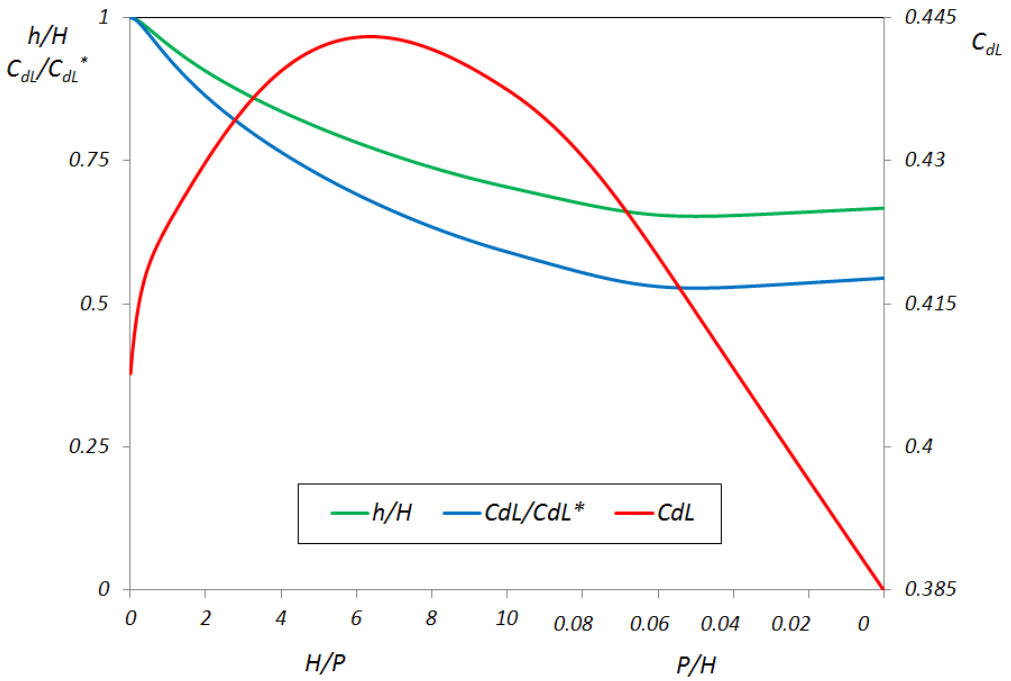

Figure XIV-2 Water/energy heads and discharge coefficients ratio for a general use of the Swamee formulation

To take into account the slope of a sharp-crested weir, Boussinesq [16] proposed a correction of the discharge coefficient:

$$K=1+0.3902\frac{i}{180} \qquad \text{XIV-5}$$

where i is the angle in degrees between the sloping weir and the vertical direction (Figure XIV-1 - (a)). Applying this coefficient K to the discharge coefficient C_{dL} issued

from the transformation of the Swamee formulation, different adimensional head/discharge curves are obtained depending on the weir inclination *i* (Figure XIV-3).

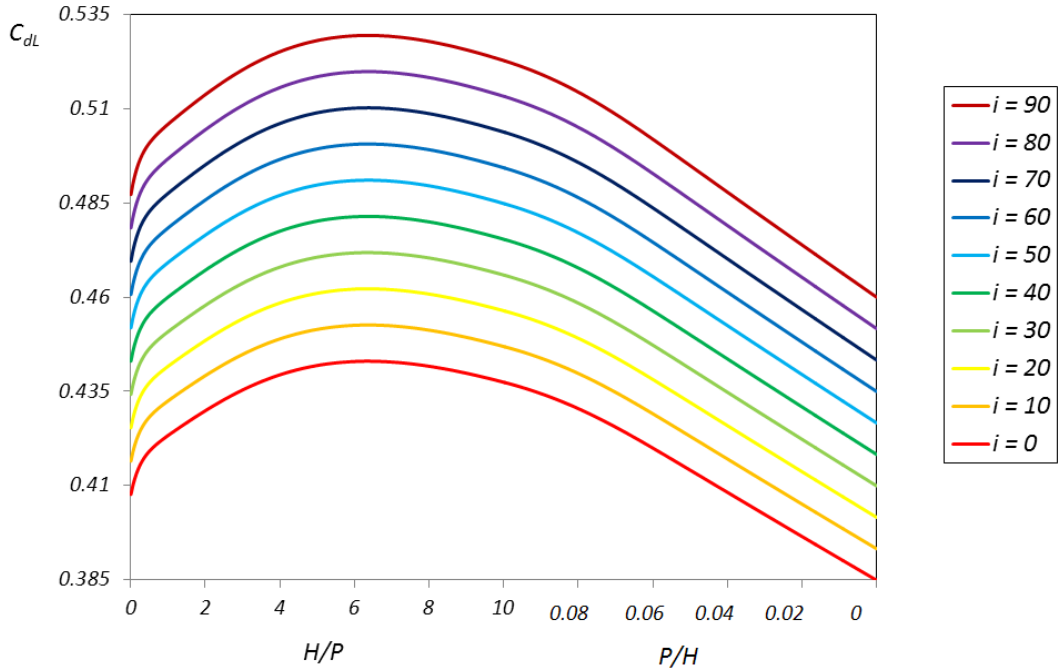

Figure XIV-3 Discharge coefficient curves for varied inclinations of sharp-crested weir

It is to be noticed that for *i* = 90° the sharp-crested weir becomes a horizontal free overfall for which the discharge coefficient is equal to 0.385, what is in contradiction with the results shown above. The same observation can be done for *P*/*H* values equal to 0. The application of the Boussinesq correction should thus be limited to a certain range of *i* and *H/P* values.

XIV.1.1.2. Inclined free overfall

For horizontal free overfall, the main goal of the researchers is to define a relation between the brink depth h_e and the critical depth h_c, which appears upstream of the free overfall (Figure XIV-1 – (b)). So that the discharge over a free overfall could be determined from measurement of the brink depth by:

$$q = \sqrt{g h_c^3} \qquad \text{XIV-6}$$

Several authors realized experiments to define the ratio between brink and critical depths h_e/h_c, depending on the channel slope and roughness [23, 43, 86, 99, 102]. For smooth bed, the formulation of the ratio h_e/h_c from Delleur et al. [23] seems to agree with the experimental results for the varied values of the ratio between the channel slope and the critical slope S_b/S_c:

$$3\frac{h_e}{h_c} = 2 + K_1\left(\frac{h_e}{h_c}\right)^3 \qquad \text{XIV-7}$$

$$\begin{cases} K_1 = 0.6 & S_b/S_c < -5 \\ K_1 = 0.3 + \sqrt{1 - \dfrac{S_b/S_c}{8}} & -5 < S_b/S_c < 1 \\ K_1 = 0.3 & 1 < S_b/S_c \end{cases} \qquad \text{XIV-8}$$

The solution of Eq. XIV-7 is:

$$\frac{h_e}{h_c} = \frac{2}{\sqrt{K_1}} \cos\left(\frac{1}{3}\text{acos}\ -\sqrt{K_1}\ + \frac{4\pi}{3}\right) \qquad \text{XIV-9}$$

To define an energy head/discharge relation for sloping overfalls, the position of the critical section from the crest L_c is still needed (Figure XIV-1 – (b)). Indeed, to evaluate the energy head from the critical depth, where a hydrostatic pressure repartition is observed, the difference between the bottom height and the overfall height is needed. For horizontal overfalls, this difference is equal to 0 and the energy head H is equal to $1.5h_c$. For sloping overfalls, the difference is equal to $L_c.S_b$ and the energy head H is equal to $1.5h_c$-$L_c.S_b$. Finally, the discharge coefficient of a sloping overfall can be calculated by:

$$C_{dL} = 0.707\left(1.5 - \frac{L_c S_b}{h_c}\right)^{-1.5} \qquad \text{XIV-10}$$

For an horizontal channel, Rouse [102] measured a L_c/h_c ratio equal to 3.8 when Rajaratnam and Muralidhar [99] measured L_c/h_c ratios between 2.24 and 2.94. Rajaratnam and Muralidhar [99] also measured L_c/h_c ratios between 5.66 and 6.23 for S_b = 0.0005 and between 1.52 and 1.75 for S_b = -0.0101. Assuming a continuous decrease of this ratio for more important values of the adverse slope, the critical section will be observed at the overfall point for S_b near -0.015. For higher slopes, generally used for PKW design, the overfall approach is no more valid as the critical section is placed downstream of the crest where the pressure repartition is no more hydrostatic.

XIV.1.2. Experimental set-up

In order to highlight the influence of the approaching bottom slope on the release capacity of the downstream crest of the PKW, five sharp-crested weir models with varied upstream bottom slopes (S_b = 0.27; 0.36; 0.47; 0.7; 1.19) have been studied. All the models have been placed in the experimental flume (see III.1) with a crest level P equal to 0.5 m over the bottom of the flume (Figure XIV-4).

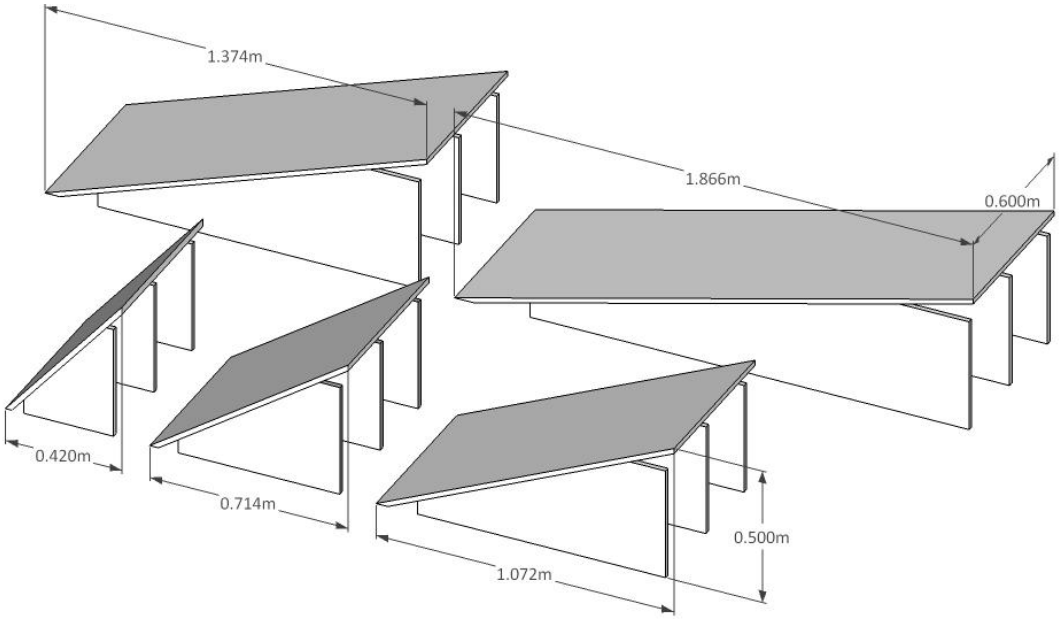

Figure XIV-4 Layout of the inclined sharp-crested weir models

XIV.1.3. Experimental results [77-79]

The Figure XIV-5 shows the variation of the specific discharge q with the upstream head H for the five tested models. The head/discharge curves of the five weirs are similar compared with the measurements accuracy. It seems thus that there is no effect of the variation of the bottom slope on the release capacity of the sharp-crested weir. However, the curves don't correspond with the SIA equation [107] results for sharp-crested weirs. The results show that the correction of Boussinesq is valuable for an angle i equal to 50°, corresponding to a slope S_b equal to 1.2 (Figure XIV-5). However, for lower slopes, the correction of Boussinesq is too important.

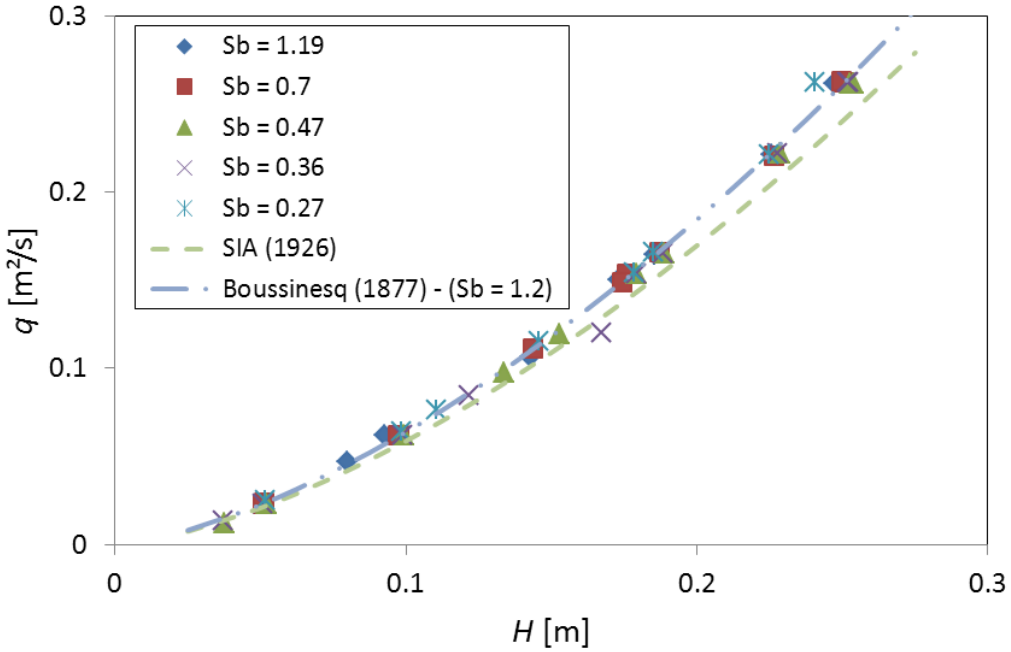

Figure XIV-5 Head/discharge curves of the inclined sharp-crested models and comparison with the SIA and the Boussinesq formulations

XIV.1.4. 2D-vertical numerical approach

To confirm the experimental results and to provide results for a larger range of bottom slopes, tests have also been conducted on a 2D vertical numerical flow solver. The Wolf2DV solver, developed at the University of Liège [26], has been used. This flow solver has already been validated on both pressurized and free surface flows applications [24, 25].

In a first time, the drawing of the free surface profiles computed by the solver for the studied sloping weir configurations (Figure XIV-6 to Figure XIV-10) enables to validate the 2D vertical numerical approach for the study of the influence of approaching slope on sharp-crested weir efficiency.

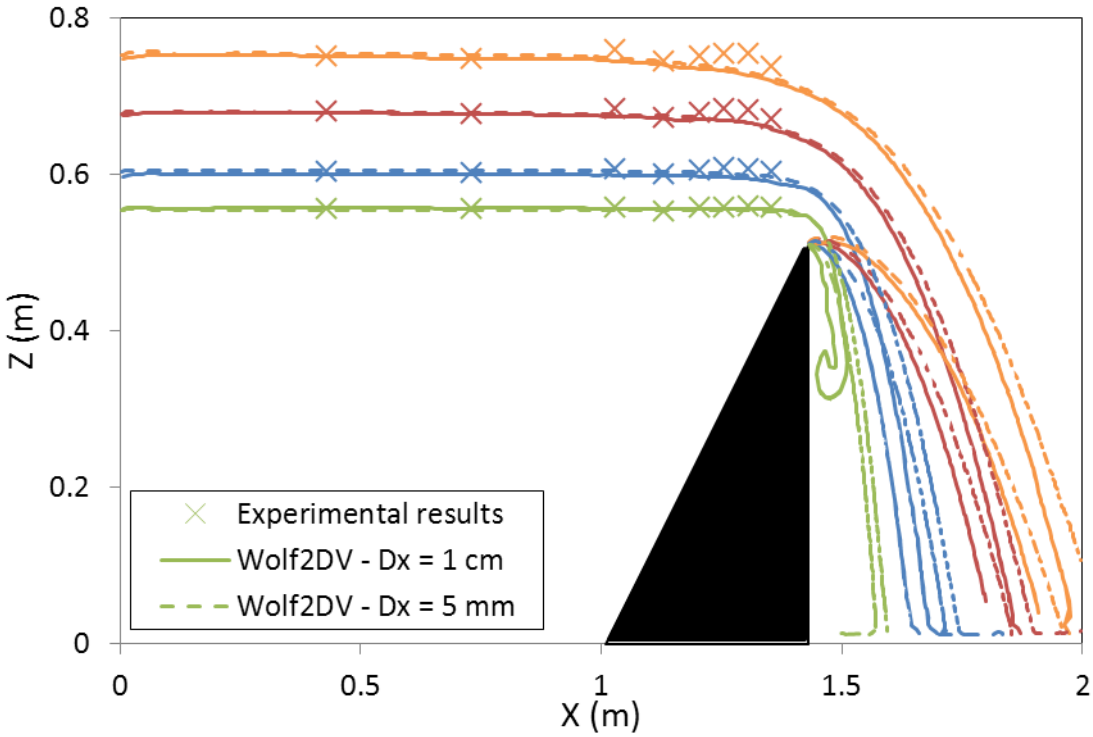

Figure XIV-6 Free surface profiles over a sharp crested weir considering an approaching slope S_b = 1.19

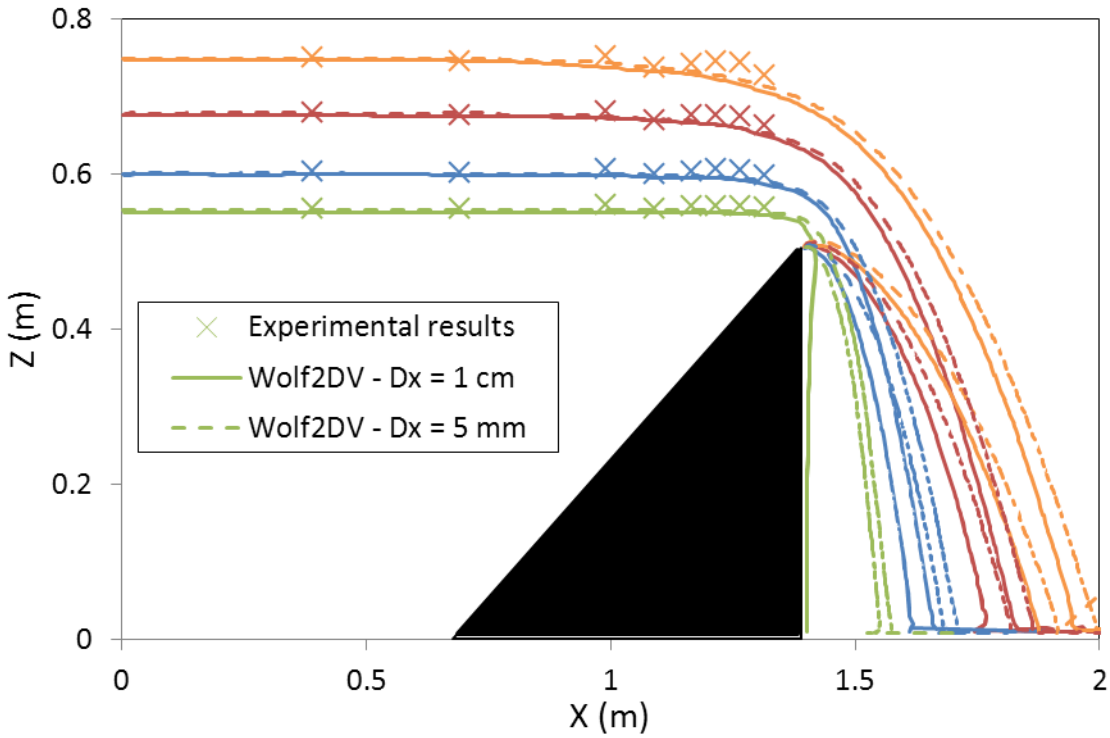

Figure XIV-7 Free surface profiles over a sharp crested weir considering an approaching slope S_b = 0.7

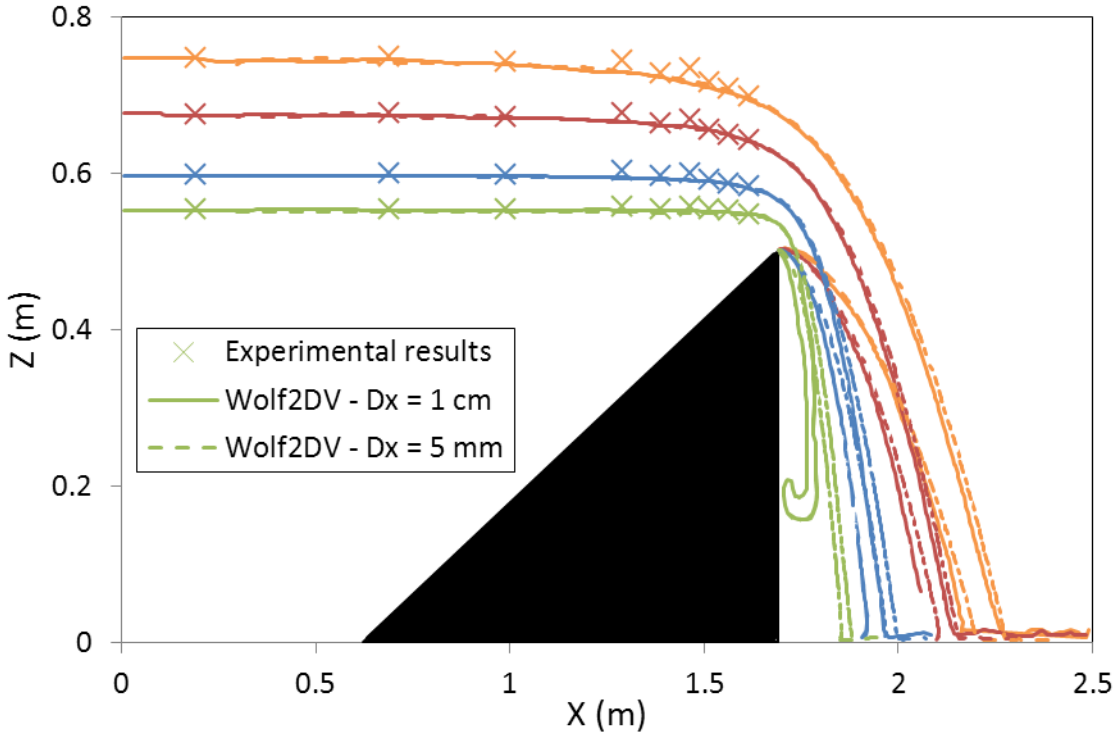

Figure XIV-8 Free surface profiles over a sharp crested weir considering an approaching slope S_b = 0.47

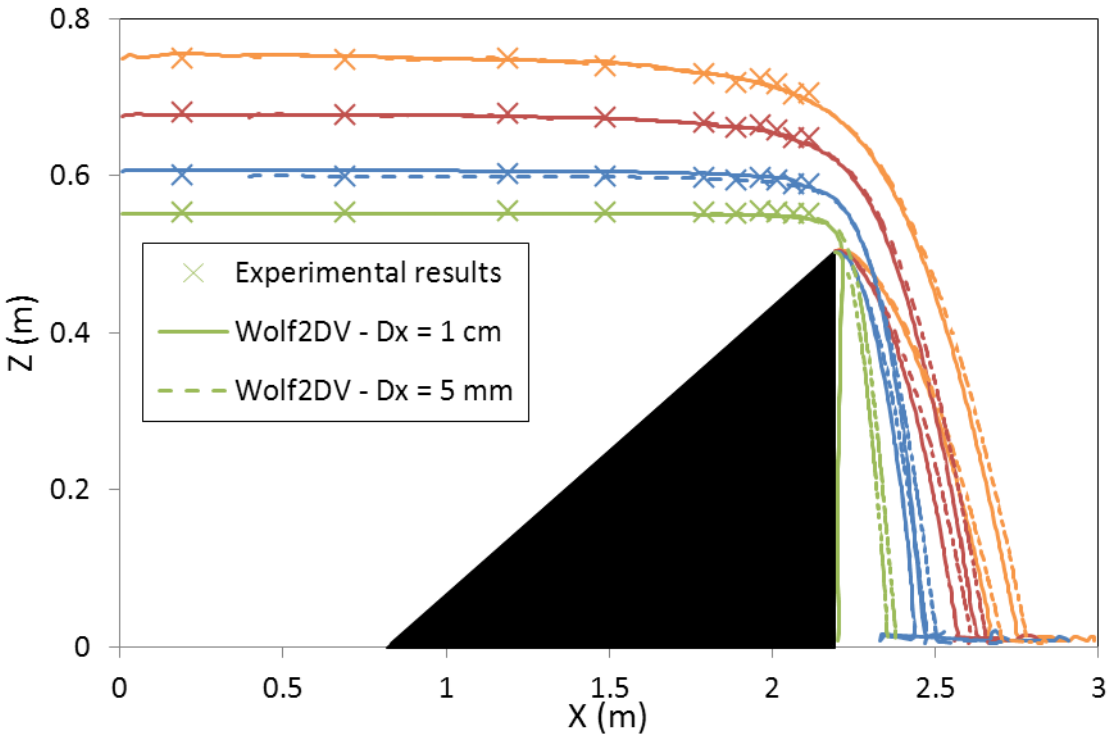

Figure XIV-9 Free surface profiles over a sharp crested weir considering an approaching slope S_b = 0.36

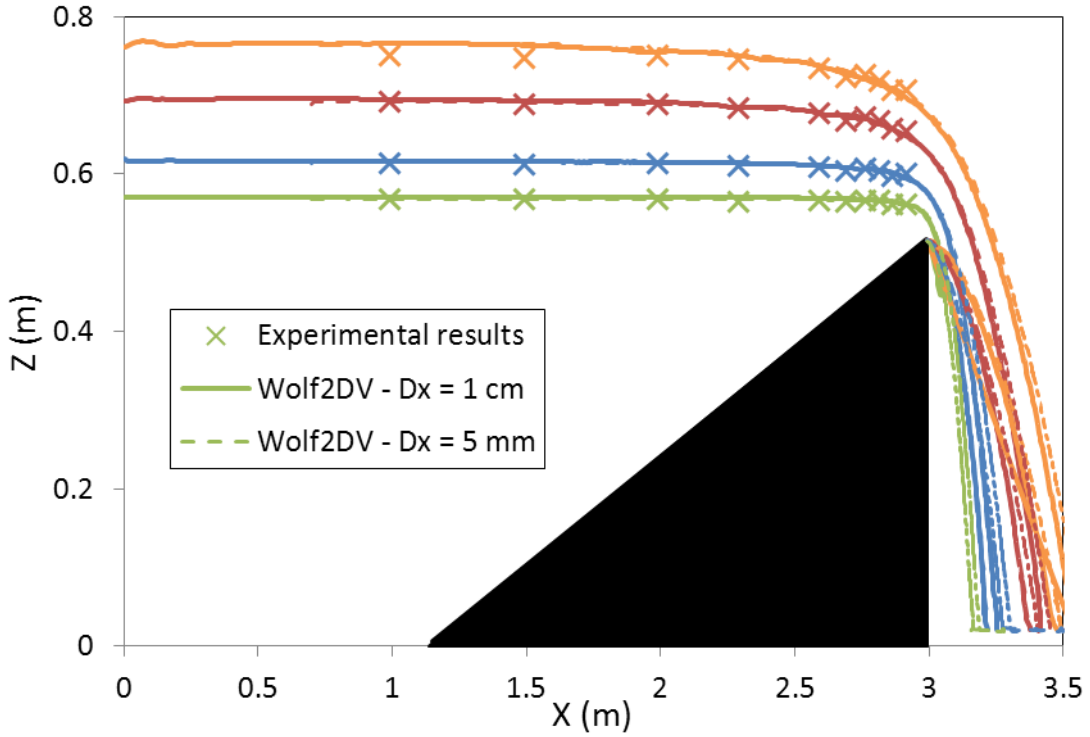

Figure XIV-10 Free surface profiles over a sharp crested weir considering an approaching slope S_b = 0.27

The numerical solver has then been used on a larger range of bottom slope to observe the variation of the sharp-crested weir performance for bottom slopes between 0.27 and vertical. The results highlight an optimal efficiency for bottom slope

near 1.2, whatever the specific discharge over the weir (Figure XIV-11). However, it also confirms low influence of the bottom slope variation between 0.3 and 4. The maximal loss in efficiency is then of 5% for the bottom slope equal to 0.3 compared with the one equal to 1.2.

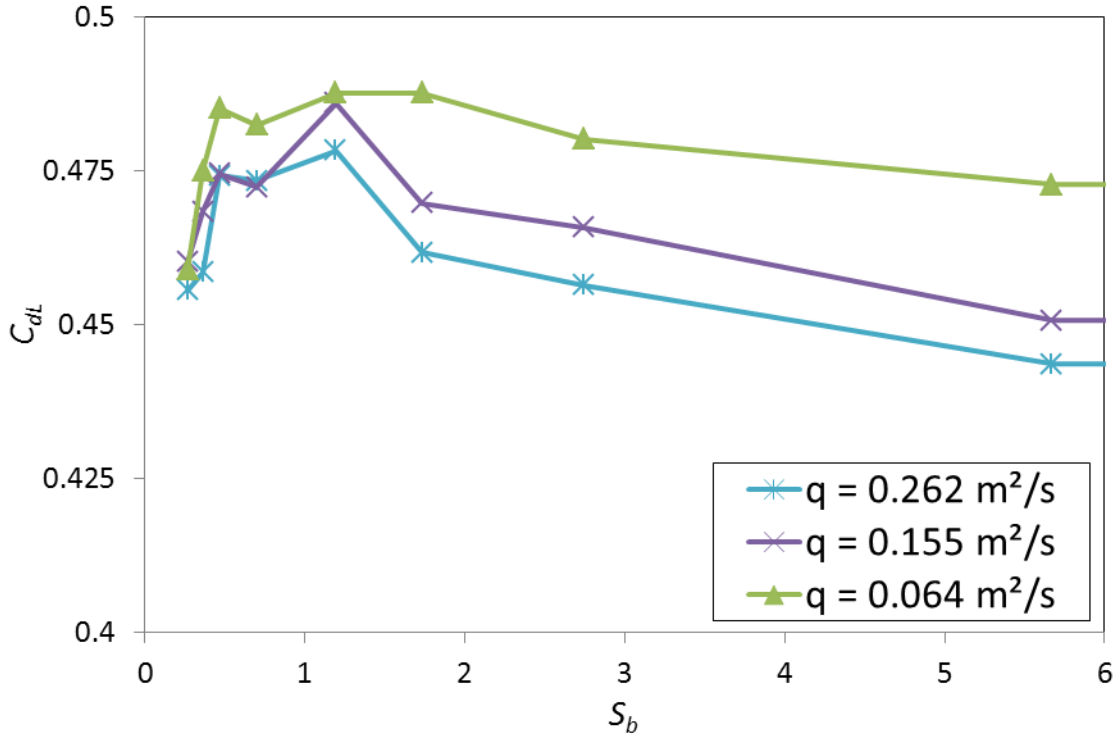

Figure XIV-11 Variation of the discharge coefficient computed by the Wolf2DV solver of a sharp-crested weir with the approaching bottom slope

XIV.1.5. Conclusion

For usual PKW geometries, with bottom slopes varying from 0.3 to 0.6 [65], there is a negligible effect of the inlet slope variation on the downstream crest capacity. Moreover, as the downstream crest length is close to 10% of the total developed one, the maximal variation in PKW efficiency, due to the influence of the variation of the inlet bottom slopes from 0.3 to 1.2 on the flow over the downstream crest, is 0.5%.

The discharge of the downstream part of the inlet crest could be calculated combining Eqs. II-2 and XIV-5 with i = 50°.

XIV.2. 1D numerical model for PKW

In order to couple experimental and numerical approach in the present research, a simplified numerical model of the flow over a PKW has been developed. The numerical model is based on a 1D modelling of the inlet and the outlet keys, taking into account the possible interaction between both flows by exchange of discharge and momentum along the side crest. The performance of the model, simple to apply and little time consuming, has been assessed through the comparison of the numerical results with experimental data.

XIV.2.1. Flow model [34, 36, 39]

The main goal of the numerical model is to help in identifying the most relevant geometric parameters of the PKW governing its discharge capacities and to assess their pertinent range of variation prior to undertaking experimental studies.

The numerical model considers the smallest hydraulic element of a PKW, made of a lateral wall, half an inlet and half an outlet key. The inlet and the outlet keys are modelled as parallel 1D channels, possibly interacting by exchange of mass and momentum along the side crest, and linked by an upstream reservoir (Figure XIV-12). To avoid the need for downstream boundary condition and considering that PKW usually works as a free weir, i.e. without influence of the tailwater level, the inlet and the outlet keys are both extended by independent steep slope channels, ensuring supercritical flow downstream of the simulation (Figure XIV-12).

According to experimental observations (see IV), the main flow direction in the outlet key follows the bottom slope. Consequently, the *x*-axis has been locally inclined in the numerical model. It is not the case in the inlet where the main flow direction is rather horizontal. The *x*-axis has thus been directed horizontally along the inlet key (Figure XIV-12).

The geometric parameters needed to set up the numerical model are the weir height P, the side crest length B, the up- and downstream overhangs lengths B_o and B_i and the inlet and outlet keys widths W_i and W_o. In the model, the inlet channel width is $W_i/2$ and the outlet channel one $W_o/2$.

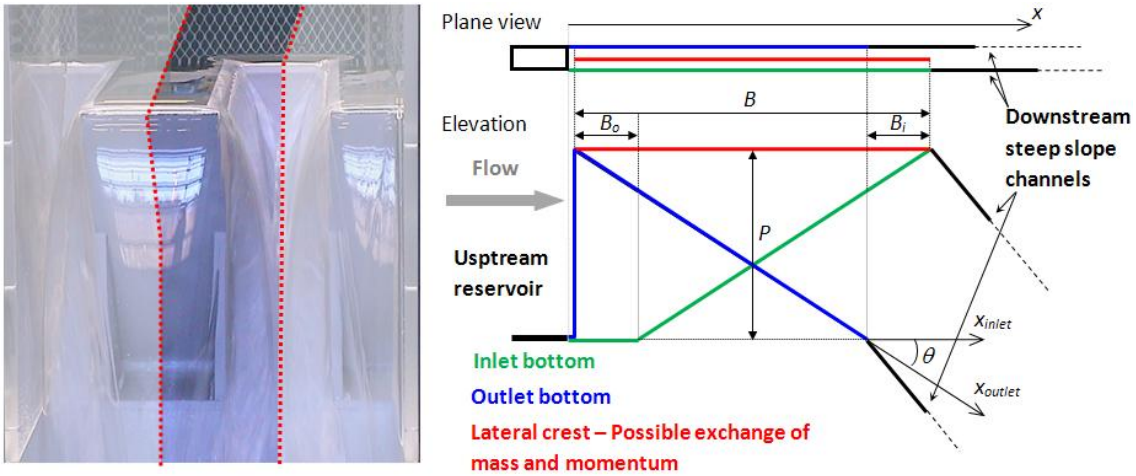

Figure XIV-12 Basic element of a PKW (left) and numerical model layout with main geometric parameters (right)

The flow model is based on the one-dimensional cross-section-averaged equations of mass and momentum conservation. In this standard 1D approach, it is basically assumed that velocities normal to the main flow direction are significantly smaller than those in this main flow direction. Consequently, the pressure field is

almost hydrostatic everywhere and the free surface is horizontal along the transverse direction.

The conservative form of the governing equations can be written as follows, using vector notations and assuming a rectangular cross-section of constant width:

$$\frac{\partial \mathbf{s}}{\partial t}+\frac{\partial \mathbf{f}}{\partial x}=\mathbf{S}_0-\mathbf{S}_f+\mathbf{S}_s \qquad \text{XIV-11}$$

where $\mathbf{s}=\begin{bmatrix}\Omega & Q\end{bmatrix}^T$ is the vector of the conservative unknowns. $\mathbf{f}$ represents the advective and pressure fluxes:

$$\mathbf{f}=\begin{bmatrix} Q \\ uQ+\frac{1}{2}g\cos\theta L h^2 \end{bmatrix} \qquad \text{XIV-12}$$

$\mathbf{S}_0$, $\mathbf{S}_f$ and $\mathbf{S}_s$ designate respectively the bottom slope, the friction terms and the lateral exchange terms:

$$\mathbf{S}_0=-g\cos\theta\Omega\begin{bmatrix}0 & \frac{\partial z_b}{\partial x}\end{bmatrix}^T+g\sin\theta\Omega\begin{bmatrix}0 & 1\end{bmatrix}^T \qquad \text{XIV-13}$$

$$\mathbf{S}_f=\begin{bmatrix}0 & \frac{\tau_{bx}}{\rho}\end{bmatrix}^T \qquad \text{XIV-14}$$

$$\mathbf{S}_s=\begin{bmatrix}q_s & \alpha u q_s\end{bmatrix}^T \qquad \text{XIV-15}$$

In Eqs. XIV-11 to XIV-15, t is the time, x the space coordinate, Ω the cross-section, Q the discharge, h the water depth, u the cross-section-averaged velocity, L the section width, z_b the bottom elevation, g the gravity acceleration, θ the inclination of x-axis, ρ the density of water, τ_{bx} the bottom shear stress, q_s the side crest unit discharge and α a coefficient, between 0 and 1, quantifying the change in momentum because of the lateral discharge.

The space discretization step in both channels is constant to take advantage of the lower computation time and the gain in accuracy provided by this type of regular grids. In addition, this enables a direct computation of the lateral exchanges mesh by mesh without interpolation of the flow variables.

Eq. XIV-11 is discretized in space with a finite volume scheme. This ensures a correct mass and momentum conservation, which is needed for handling properly discontinuous solutions such as moving hydraulic jumps. As a consequence, no

assumption is required regarding the smoothness of the solution. Reconstruction at cells interfaces is performed with a first order constant approach.

The fluxes **f** are computed by a Flux Vector Splitting (FVS) method, where the upwinding direction of each term of the fluxes is simply dictated by the sign of the flow velocity reconstructed at the cells interfaces [29, 32, 33]. It can be formally expressed as:

$$\mathbf{f}^{+} = \begin{bmatrix} Q & uQ^{\mathrm{T}} \end{bmatrix} \quad ; \quad \mathbf{f}^{-} = \begin{bmatrix} 0 & g\cos\theta L\dfrac{h^2}{2} \end{bmatrix}^{\mathrm{T}} \qquad \text{XIV-16}$$

where the exponents + and - refer to, respectively, an upstream and a downstream evaluation of the corresponding terms. A Von Neumann stability analysis has shown that this FVS ensures a stable spatial discretization of the terms $\partial\mathbf{f}/\partial x$ [28]. Besides low computation costs, this FVS has the advantages of being completely Froude independent and of facilitating the adequacy of discretization of the bottom slope term [29, 32].

The discretization of the topography gradients is always a challenging task when setting up a numerical flow solver based on the depth- or cross-section-averaged equations. The bed slope appears as a source term in the momentum equations. As a driving force of the flow, it has however to be discretized carefully, in particular regarding the treatment of the advective terms leading to the water movement, such as pressure and momentum.

The first step to assess topography gradients discretization is to analyse the situation of still water on an irregular bottom. In this case, momentum equation simplifies and there are only two remaining terms: the advective term of hydrostatic pressure variation and the topography gradient. In this case, according to the FVS characteristics, a suitable treatment of the topography gradient source term is a downstream discretization of the bottom slope and a mean evaluation of the corresponding water depths [31, 32]. For a cell *i* and considering a constant reconstruction of the variables, the bottom slope discretization writes:

$$-g\cos\theta\Omega\left.\frac{\partial z_b}{\partial x}\right|_i \rightarrow -g\cos\theta\frac{\Omega|_{i+1}+\Omega|_i}{2}\frac{z_b|_{i+1}-z_b|_i}{\Delta x} \qquad \text{XIV-17}$$

where subscript *i*+1 refers to the downstream cell along *x*-axis.

This approach fulfils the numerical compatibility conditions defined by Nujic [90] regarding the stability of water at rest. The formulation is suited to be used in both 1- and 2D models, along *x*- and *y*- axis [32]. Its very light expression benefits directly from the simplicity of the original spatial discretization scheme. Nevertheless, this

formulation constitutes only a first step towards an adequate form of the topography gradient as it is not entirely suited regarding water in movement over an irregular bed. The effect of kinetic terms is not taken into account and, consequently, poor evaluation of the flow energy evolution can occur when modelling flow, even stationary, over an irregular topography [31]. To overcome this problem on the upstream side of the outlet channel, i.e. where the topography gradient is locally the most important, the momentum equation has been locally replaced by the energy equation, using an approach depicted by Erpicum [31]. This technique has not been applied on the whole inlet and outlet lengths as it is not suited to compute correctly shocks such as hydraulic jumps [31], which can occur in the outlet.

The bottom friction is conventionally modelled with the Manning formula, where the Manning coefficient *n* characterizes the surface roughness and *R* is the hydraulic radius, specifically defined by Eq. XIV-19, where z_s is the lateral weir elevation, to take into account the reduced width of the inlet and the outlet keys.

$$\frac{\tau_{bx}}{\rho} = \frac{g n^2 \Omega u |u|}{R^{4/3}} \qquad \text{XIV-18}$$

$$R = \frac{\Omega}{L + \min\ h; z_s - z_b} \qquad \text{XIV-19}$$

Finally, the side crest unit discharge in the lateral exchange terms is computed on each point of the lateral weir depending on the head difference *ΔH* between the inlet and the outlet keys, without considering the kinetic terms along the inlet and outlet axis:

$$\Delta H = \max\ 0; z_{bi} + h_i - z_s\ - \max\ 0; z_{bo} + ho - z_s \qquad \text{XIV-20}$$

$$q_s = \mu \sqrt{2g|\Delta H|^3}\ \text{sgn}\ \Delta H \qquad \text{XIV-21}$$

$$q_{si} = -q_s \quad \text{and} \quad q_{so} = q_s \qquad \text{XIV-22}$$

where μ is the lateral weir discharge coefficient and subscripts *i* and *o* refer respectively to the inlet and the outlet channel.

The upstream reservoir is an important part of the numerical model as it distributes the discharge between the inlet and the outlet channel. It is also in the upstream reservoir that the value of the head on the PKW will be measured to define the release efficiency of the structure.

The upstream reservoir is modelled as two special twin 1D finite volumes, with distinct discharges Q_{Ro} and Q_{Ri} but a single cross-section value Ω_R, as depicted in Figure

XIV-13. The reservoir width is $W_i/2 + W_o/2$ and it is only one space step in length. All the source terms are neglected to compute the time evolution of the three reservoir variables. Eq. XIV-11 results merely in one mass balance equation:

$$\frac{d\Omega}{dt} + \frac{Q_{R/o} + Q_{R/i} - Q_{Up}}{\Delta x} = 0 \qquad \text{XIV-23}$$

and two momentum equations:

$$\frac{dQ_{Rj}}{dt} + \frac{u_{Rj}Q_{R/j} - \delta_j Q_{Up}^2 / \Omega_R}{\Delta x} + \frac{1}{2} g L_j \frac{h_{R/j}^2 - h_R^2}{\Delta x} = 0 \text{ with } j = i, o \qquad \text{XIV-24}$$

where the subscript *R* refers to the reservoir, *Ri* to the part of the reservoir upstream of the inlet key, *Ro* to the part of the reservoir upstream of the outlet key, *Up* to the upstream discharge boundary condition and *R/i* and *R/o* to the boundary between the reservoir cell and the first inlet and outlet cell respectively. δ_j is the ratio between the reservoir width and the inlet or the outlet width:

$$\delta_i = \frac{W_i}{W_i + W_o}; \delta_o = \frac{W_o}{W_i + W_o} = 1 - \delta_i \qquad \text{XIV-25}$$

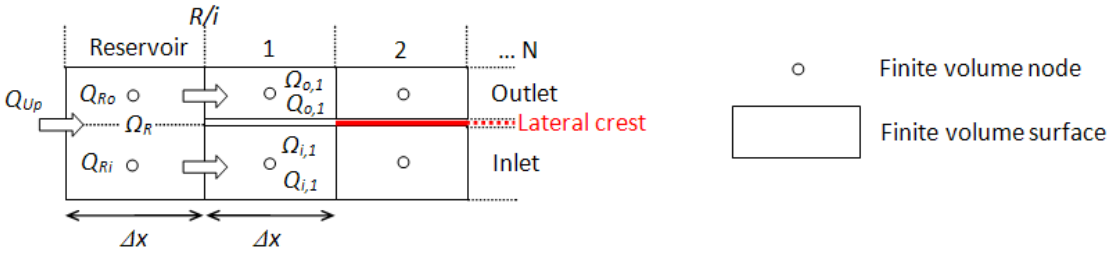

Figure XIV-13 Modelling of the upstream reservoir and links with the inlet and the outlet keys

The procedure to model the reservoir is very close to the ones developed by Erpicum and Dewals to link 1D and 2D models or to perform 2D multiblock – multimodel modelling [29, 32].

The value of the upstream discharge is the only value to be prescribed as a boundary condition. The steep slope of both channels in the downstream part of the model leads to supercritical flow and no outflow boundary condition is thus needed.

Since the model is applied to compute steady-state solutions, the time integration is performed by means of a 3-step first order accurate Runge-Kutta algorithm, providing adequate dissipation in time. For stability reasons, the time step is constrained by the Courant-Friedrichs-Levy condition based on gravity waves. A semi-implicit treatment of the friction term is used, without requiring additional computational costs.

Slight changes in the Runge-Kutta algorithm coefficients allow modifying its dissipation properties and make it suitable for accurate transient computations.

The solver has been written in Visual Basic using VB-Application in the software Microsoft Excel. With a typical space step of 5 mm to model standard experimental PKW 50 cm long and 10 cm wide, the computation of the flow over the structure takes less than 2 min on a desktop computer.

A convergence criteria has been defined on the basis of the discharge evolution in the reservoir (Q_{Ri}+Q_{Ro}) compared with the upstream discharge boundary condition. When the difference between both values is lower than a given tolerance during a fixed time, the computation is assumed to be converged.

XIV.2.2. Validations [34, 36]

To assess the model performance and accuracy, the numerical model results have first been compared with the experimental data measured on the 1:10 scale model of a PKW (see IV) and a number of various scale models of PK-Weir tested in different hydraulic laboratories (Laboratoire National d'Hydraulique et Environnement – EDF, Chatou, France; Hydraulic Department of Biskra University, Biskra, Algeria and Laboratoire d'Hydraulique des Constructions - ULg, Liege, Belgium). The main geometric parameters of the scale models are summarized in Table XIV-1. Some experimental tests have been realized using a support under the PK-Weir to simulate the weir position on a dam crest. This support affects the water height in the inlet key along the upstream overhang and thus the head/discharge curve. The support or dam height P_d has thus been considered for the numerical modelling. It has directly been accounted for in the inlet bathymetry.

Table XIV-1 – Geometric and numerical parameters of the scale models considered for comparison

Laboratory	Model	W_i (m)	W_o (m)	B_o (m)	B_i (m)	B (m)	P (m)	T_s (mm)	P_d (m)	μ	ϑ_o (°)	q (m²/s)
Chatou (2003)	1	.12	.08	.1	.1	.4	.2	2 (steel)	.3	.667	33.7	.01;.25
	2	.08	.12									
	3	.12	.08				.15				26.6	
	4	.10	.065									
Biskra (2006)		.09	.075	.103	.103	.412	.155	2 (steel)	0	.667	26.6	.01;.18
Liège (2008) [53]	1	.08	.10	.25	0	.5	.2	10 (PVC)	.2	.429	21.8	.01;.4
	2	.11	.07									
	3	.06	.12									
	4	.13	.05									
Liège (2009)		.18	.18	.185	.185	.63	.525	10 (PVC)	.2	.429	49.7	.01;.5

The numerical model has been built with a space step of 5 mm. The constant side crest discharge coefficient μ in Eq. XIV-21 is the one for thin (Chatou, Biskra) or thick

(Liège) crested weir. The Manning roughness coefficient *n* is 0.011 (PVC). α coefficient in Eq. XIV-15 is assumed to be equal to 1 (full exchange of momentum between the inlet and the outlet keys). The outlet axis inclination is given in Table XIV-1. The solver has been used to compute the flow over the PKW, and thus to compute the upstream head, for unit discharges ranging from 0.055 m³/s/m up to .0555 m³/s/m.

The numerical model has been used to compute the flow over the PK-Weir in the range of specific discharge, calculated with the width of the PK-Weir in the upstream reservoir, detailed in Table XIV-1. From these computations, the "numerical" head / discharge relations or the PK-Weir equivalent discharge coefficient [94] can be compared with the corresponding experimental data (Figure XIV-14 to Figure XIV-17).

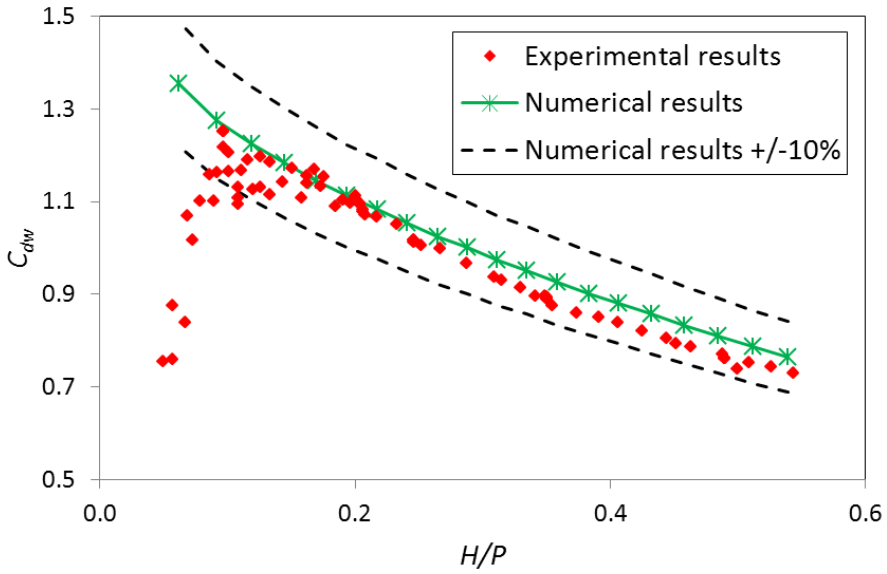

Figure XIV-14 Comparison of experimental and numerical results - Release capacity of the 1:10 scale model

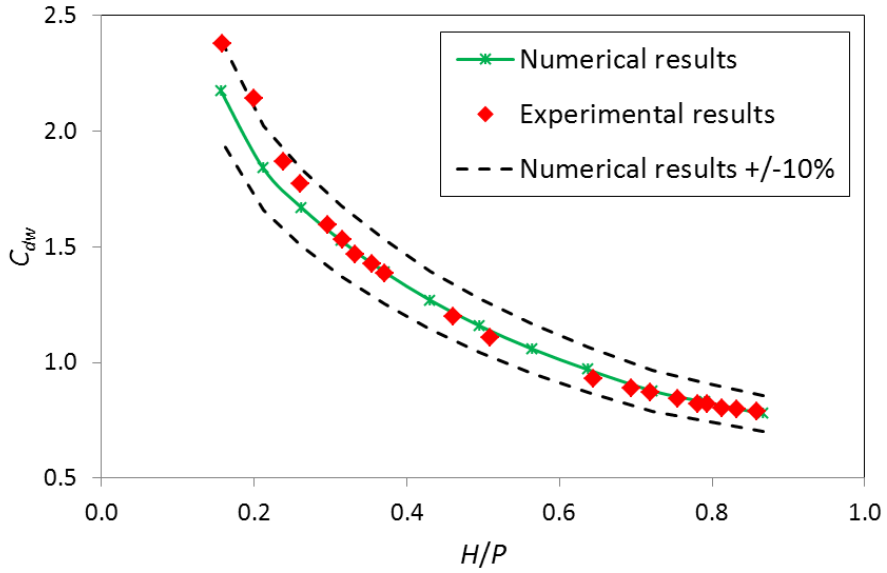

Figure XIV-15 Comparison of experimental and numerical results - Release capacity of the Biskra (2006) scale model

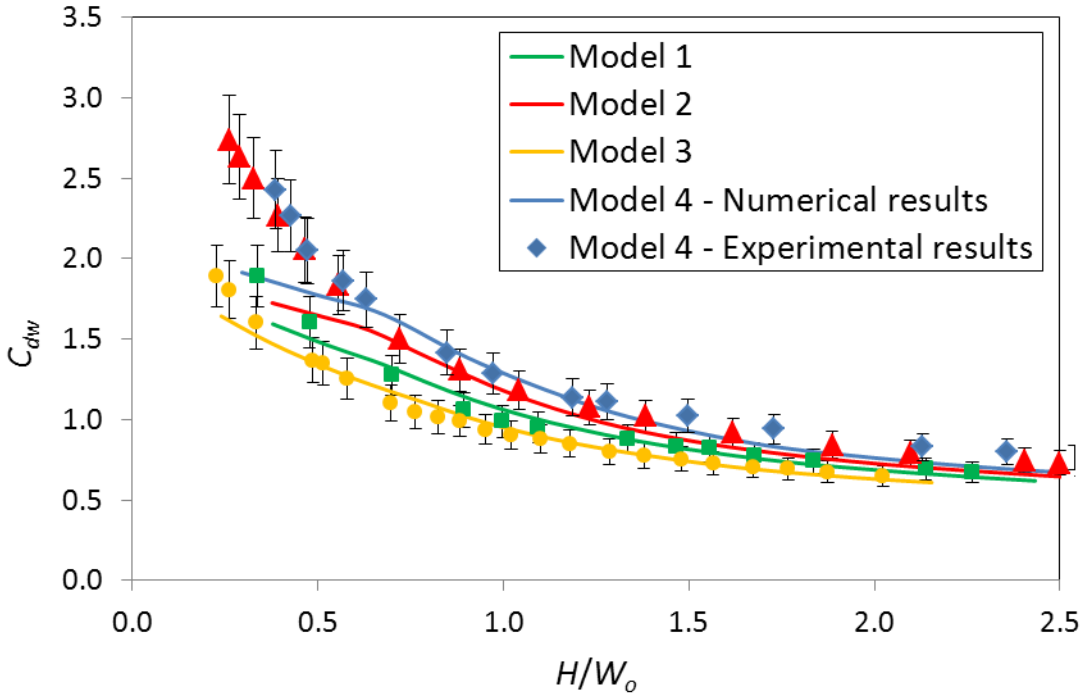

Figure XIV-16 Comparison of experimental and numerical results - Release capacity of the Liège (2008) models [53] (error bars = 10%)

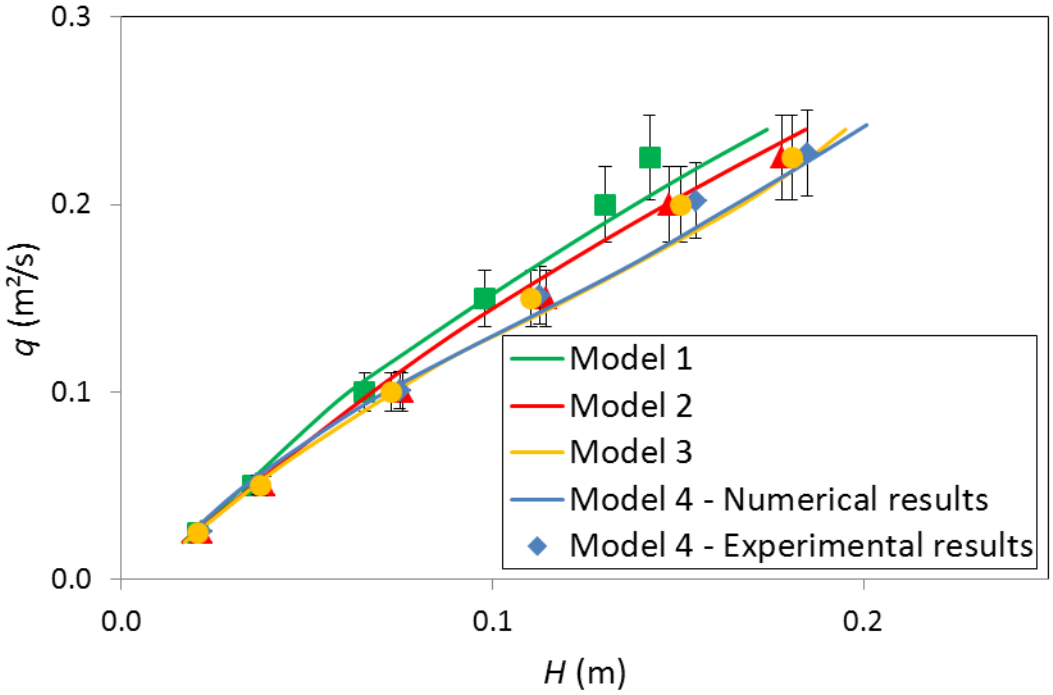

Figure XIV-17 Comparison of experimental and numerical results - Release capacity of the Chatou (2003) models (error bars = 10%)

The numerical results are generally in satisfactory agreement with the experimental ones, especially for moderate head ratios (Figure XIV-14 to Figure XIV-17). The numerical curves shape is close to the corresponding experimental ones. The numerical results are often around 10 percents of the experimental observations,

and very similar values are obtained with some geometries, such as Chatou 4, Biskra and Liege (2009).

For low head ratios and thick crest (Liege (2009), Figure XIV-14), the non-monotonous variation of the release capacity because of the weir thickness is not accounted for in the numerical model, and the numerical curve doesn't show the inflexion of the experimental data curve. For thin crest (Chatou 3 and Biskra for instance, Figure XIV-15 and Figure XIV-17), the numerical model assumptions seem in agreement with the real weir behaviour for decreasing head ratios (constant side crest discharge coefficient).

The numerical model convergence is limited for high head ratios, depending on the PKW geometry. When the water depth over the weir is high, the assumption of distinct flows in the inlet and the outlet keys is no more valid and no stable solution is reached by the solver.

Tests have been conducted with the Biskra model geometry to assess the influence of the discretization step and the α coefficient value in the momentum exchange terms (Figure XIV-18). A simulation has been performed with α equal to 1 in the inlet key (full loss of momentum) and 0 in the outlet key (no gain in momentum from the discharged water). When the free surface in the outlet key is under the side crest level, the numerical results are not affected by the α value in the outlet key. When the free surface level becomes higher, the weir efficiency decreases more when α is equal to 0 in the outlet key than when it is equal to 1. The comparison with the experimental results is better when α is equal to 1 in both the inlet and the outlet keys. This suggests an exchange of momentum between the two alveoli, at least for moderate and high heads, i.e. when the water level in the outlet key is higher than the side crest height on a significant length.

The results of the simulations with the Liège (2008) model geometry enable interesting observations. With the numerical model configuration depicted here before, the curves of Figure XIV-19 – A show the poor comparison with experimental data for models 2 and 4 with very small outlet key width compared with the width of the inlet key. Tests have been performed considering increased inlet and outlet keys widths, taking into account the thickness of the side crest (Figure XIV-19 - B). The width of half the inlet key is $(W_i+T_s)/2$ and the width of the half outlet key $(W_o+T_s)/2$. Calculations have also been done with a side crest discharge coefficient equal to 0.5 instead of 0.429, in order to increase the efficiency of the 1 cm thick side crest (Figure XIV-19 - C).

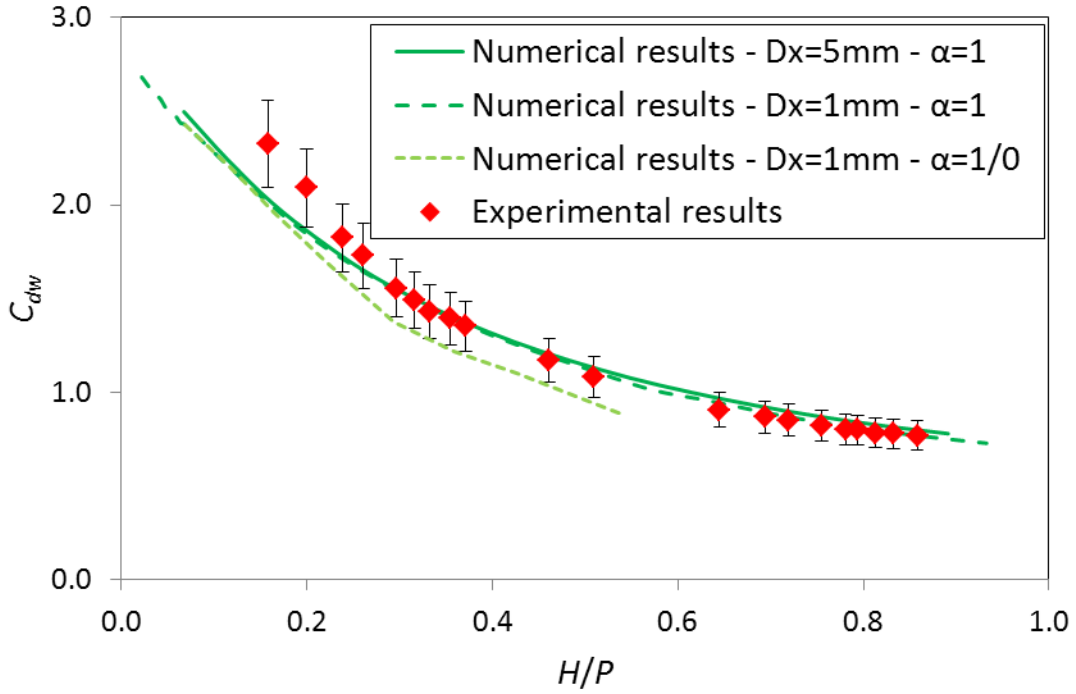

Figure XIV-18 Biskra (2006) model geometry – Effect of the space discretization step and α coefficient value on the numerical results (error bars = 10%)

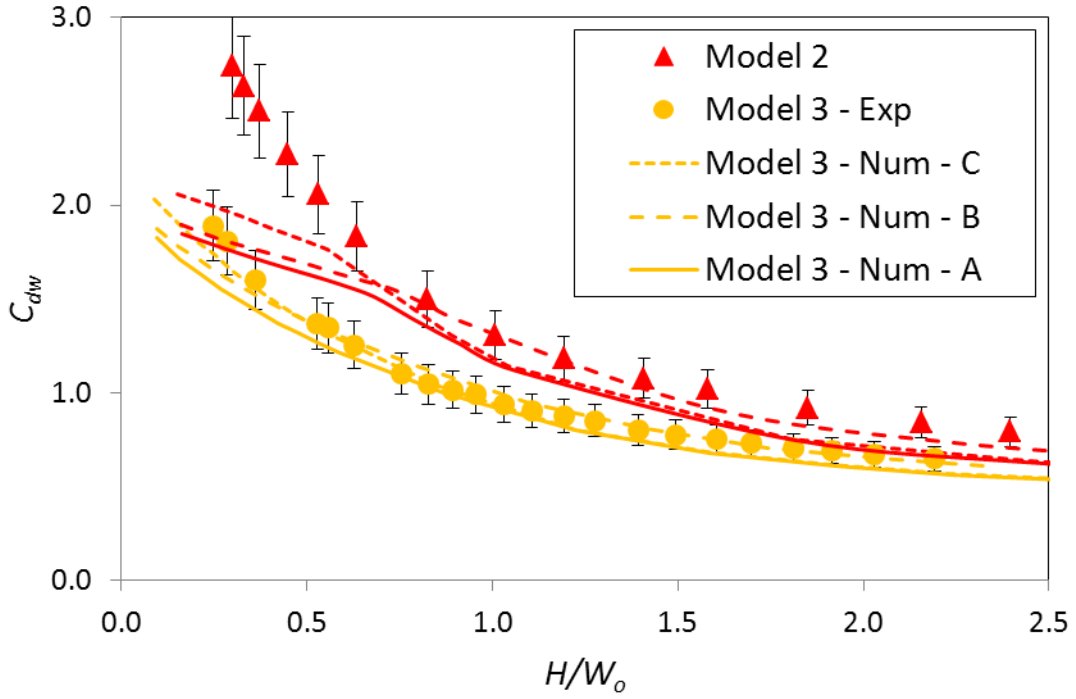

Figure XIV-19 Liège (2008) model geometry – A: inlet key width is $W_i/2$, outlet key width is $W_o/2$, μ=.429; B: inlet key width is $(W_i+T_s)/2$, outlet key width is $(W_o+T_s)/2$, μ=.429; C: inlet key width is $W_i/2$, outlet key width is $W_o/2$, μ=.5 (error bars = 10%)

With increased widths, the numerical results are closer to the experimental ones for all heads. With an increased side crest discharge coefficient, the numerical results are more satisfactory for lower heads, when only the inlet key flow governs the weir efficiency, and are unchanged for higher heads, when the weir is flooded (few

exchange of discharge between the inlet and the outlet keys). The inflexion point in the non-dimensional head/discharge curve of Figure XIV-19 for the Liège (2008) model 2 geometry (H/W_0=0.7) can be explained by an analysis of the free surface elevation curves along the outlet key (Figure XIV-20). When the discharge becomes higher than 0.05 m²/s, the water level in the outlet key gets quickly over the side crest level along a significant length, and thus strongly decreases the water exchange between the inlet and the outlet keys.

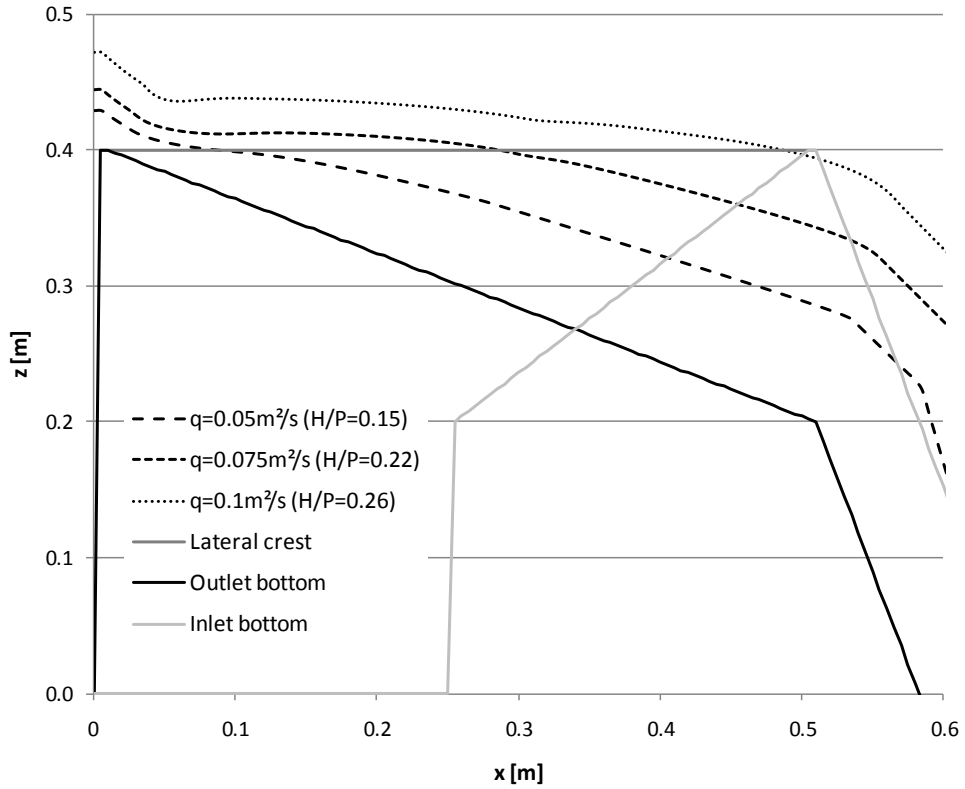

Figure XIV-20 Liège (2008) model 2 – Computed free surface levels along the outlet key

Regarding these first results, in a second step, the detailed numerical results have been carefully compared with the experimental measurements obtained along the present research in order to more precisely assess the solver relevance, and to help in improving the conceptual approach and the mathematical model. The influence of the model parameters such as μ and α has also been investigated.

XIV.2.3. Enhancements

Four parameters of the model may influence the final result of the simulation on a given PKW geometry: the size of the meshes, the width of the keys considered for the integration of the Navier-Stokes equations, the computation of the mass and momentum exchanges between the keys. The influence of the grid size has already been studied [36]. The influence of the inlet and outlet keys widths definition, and the μ and α coefficients are considered here. The influence of the three parameters has

been studied iteratively to avoid effects of parameters interference in the following conclusions.

Four PKW geometries have been studied to highlight the common influence of the parameters definition with geometrical specificities of the tested models. With W_u the width of a PKW-unit composed of an inlet key, two side walls and two halve outlet keys, the four tested models provide P/W_u ratios of 0.5 and 1.33 corresponding respectively to a technico-economic and an hydraulic optimal geometry (see VII) and W_i/W_o ratios of 0.796 and 1.5 corresponding with the limits of an attractive hydraulic efficiency (see VIII). The four models have been computed using the 1D-PKW model with 181 finites volumes for each key, considering 121 volumes along the side wall and 60 volumes to ensure a supercritical flow condition at the downstream end of the domain. The numerical model provides the stage-discharge curve for each geometry as well as free surface profiles along the keys.

A Strickler coefficient of $90 m^{1/3}/s$ has been used to characterize the bottom and side wall friction, corresponding with the PVC plates used in the experimental approach.

XIV.2.3.1. Mass exchange calculation

The numerical model uses Eq. XIV-21 to calculate the mass exchanges between the inlet and outlet keys. These exchanges correspond to the discharge passing over the lateral crest, working as a side weir. Hager [44] showed that the head to consider for calculation of the discharge over a side weir is equal to the difference between water height in the main channel and the crest level, without velocity term. To compute the lateral mass exchanges, only the μ coefficient of Eq. XIV-21 needs thus to be fixed.

A first approach is to consider the lateral crest as a perfect sharp-crested weir. The theoretical maximal value of the μ coefficient is then 0.667. However, traditional sharp-crested weirs provide μ coefficient near 0.43 [51]. The choice of these two values of the coefficient has been tested. However, discharge over a side weir doesn't exactly correspond to the discharge over a traditional sharp-crested weir. Indeed, the lateral discharge will be influenced by the longitudinal approach velocity, the outflow angle and the channel shape [44]. Two formulations for the μ coefficient computation have been tested for a better evaluation of the lateral discharge. The first one is the formulation proposed by Hager [44]:

$$\mu = 0.424c\left[\frac{1-W}{3-2y-W}\right]^{1/2} \qquad \text{XIV-26}$$

$$y = \frac{h}{H}; W = \frac{w}{H} \qquad \text{XIV-27}$$

where h is the water depth in the main channel (inlet key), H is the water head calculated as the sum of the water depth and the kinetic energy component in the main channel, w is the lateral weir height and c a coefficient traducing the influence of the crest shape. For a finite crest thickness T that is used on tested models, c is calculated as [44]:

$$c = 1 - \frac{2}{9\left(1 + \left(\frac{h-w}{T}\right)^4\right)} \qquad \text{XIV-28}$$

The second formulation studied is the one proposed by Oertel et al. [91]:

$$\mu = \frac{2}{3}\left[0.05\log\ 0.7\gamma\sqrt{Fr}\ + 0.35\right] \qquad \text{XIV-29}$$

$$\gamma = \ 1.44 - 2.4\sqrt{Fr} + Fr\ \frac{W_i^2}{B^2}; Fr = \frac{U}{\sqrt{gh}} \qquad \text{XIV-30}$$

where W_i is the main channel (inlet key) width, B is the lateral crest length, and U is the local velocity in the main channel.

After several iterations on the three parameters values to isolate the influence of the μ coefficient determination, the limits of lateral integration has been fixed at the key walls for high weirs (models 1 and 2) and at the center of the side walls for low weirs (models 3 and 4) (see XIV.2.3.3). The α coefficient is chosen equal to 1 in both inlet and outlet keys (see XIV.2.3.2).

Figure XIV-21 presents the comparison of the upstream heads versus specific discharge computed with the four ways to choose the value of the μ coefficient for the four geometries tested in the laboratory.

For small weir height (models 3 and 4) and high heads, the definition of the lateral discharge value doesn't influence the upstream head observed. That traduces the low influence of the lateral exchanges on the global efficiency of the PKW. Indeed, in these conditions of weir height and water head, the PKW is nearly fully submerged (Figure XIV-22) and the lateral discharge contributes to a very small part of the global discharge.

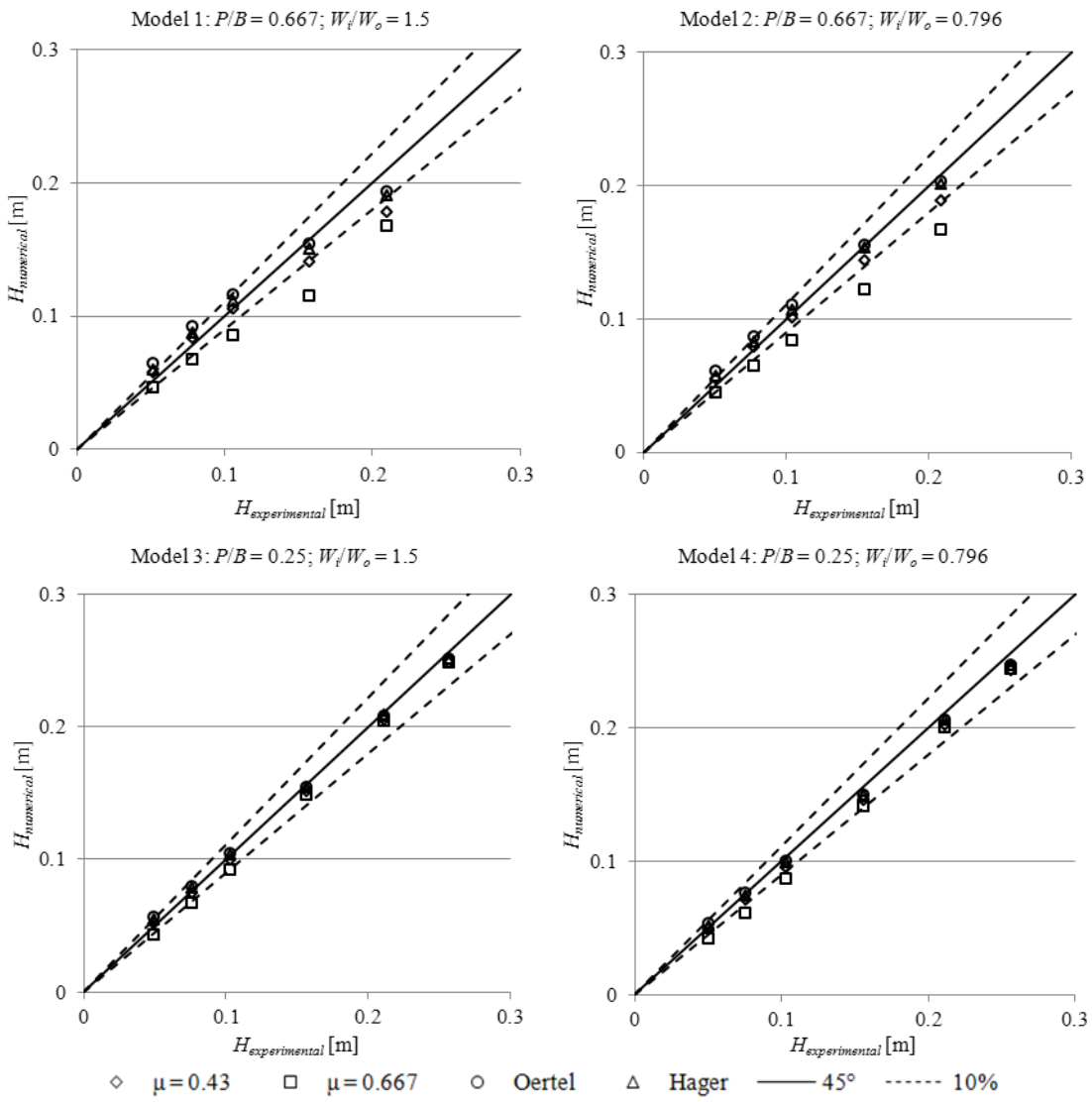

Figure XIV-21 Influence of the mass exchange calculation on the upstream head for given discharges

Figure XIV-22 PKW model 4 under a high upstream head (H = 0.256 cm)

For higher PKW height (models 1 and 2) and high heads, μ coefficient value of 0.667 or 0.43 underestimates the upstream head value until respectively 25% and 15%. The weir height induces outlet key slope sufficient to avoid the lateral crest

submersion. The high head provides non-negligible flow velocity along the inlet key. This influences mainly the lateral discharge, reducing the efficiency of the lateral crest. As the two formulations of Hager and Oertel take into account the influence of the approach flow conditions of the side weir, they provide better evaluation of the upstream head, in this case. The results of the two formulations are relatively closed and approach experimental results with a maximal error of 9% on the upstream head.

For low heads, as expected, a μ coefficient value of 0.667 underestimates systematically the upstream head. Indeed, the value of 0.667 is an idealized theoretical value and the experimental value of the μ coefficient is close to 0.43. As, for low heads, the velocity along the inlet key is negligible, the lateral discharge is close to the one of a sharp-crested weir and a μ coefficient value of 0.43 approaches the experimental upstream head with less than 6% error on the four tested models. The formulation of Hager provides upstream heads relatively close to the ones obtained fixing the μ coefficient to 0.43, keeping a maximal error of 9% on the experimental results. The formulation of Oertel is less relevant for low heads. Indeed, it systematically overestimates the upstream head until 17% for higher PKW height (models 1 and 2) and 5% for lower one (models 3 and 4).

Regarding the global results issued from the study of the four models, the mean relative error, calculated on the five upstream water heads studied on the four models, is equal to 6.0% and 14.8% fixing respectively the μ coefficient to 0.43 and 0.667, and to 5.2% and 6.9% using respectively the Hager and Oertel formulations. The maximal relative error is equal to 15.6% and 26.8% fixing respectively the μ coefficient to 0.43 and 0.667, and to 15.5% and 23.2% using respectively the Hager and Oertel formulations. There is practically no influence of the W_i/W_o ratio on the μ coefficient determination. Finally, even if the formulation of Hager is more CPU time consuming, it provides the better model results, a little bit better than the μ coefficient to 0.43. Moreover, the Hager formulation is based on the geometry of the weir and is thus more flexible. The Hager formulation has thus been chosen for a large use of the 1D PKW model. Fixing the μ coefficient to 0.43 will be conserved for particular conditions with a large set of data to compute, i.e. when the CPU time needs to be reduced.

XIV.2.3.2. Momentum exchange calculation

As there is a mass transfer from the inlet to the outlet keys, a momentum transfer has also to be considered. As presented here above, the momentum transfer is dependent of the angle between the lateral flow and the main channel flow directions. A α coefficient is thus introduced to quantify the exchange in momentum due to the lateral discharge. Four cases of α definition in both inlet and outlet keys have been studied.

The first case considers full momentum exchange from the inlet to the outlet key ($\alpha_i = \alpha_o = 1$). This should be the case if the lateral flow is parallel to the main flow in the

inlet and outlet keys, what is expected for very high water heads compared with the weir height. The second case considers no momentum exchange (α_i = α_o = 0). This should be the case if the lateral flow is orthogonal to the main flow in the inlet and outlet keys, what is expected for low water heads. The third case considers momentum extracted from the inlet key but not transferred to the outlet key (α_i = 1, α_o = 0). This could be the case if the lateral flow is parallel to the main flow in the inlet key and orthogonal to the main flow in the outlet key, what is expected for high water heads, inducing high longitudinal velocity along the main channel (inlet key) what reduces the lateral flow inclination [44], and high weir height, inducing a vertical falling of the lateral flow in the outlet one. Finally, a third case has been studied considering a α calculation depending on the lateral flow direction. From the lateral specific discharge q_l from Eq. XIV-21, the angle φ_i between the main flow direction in the inlet key and the lateral flow direction may be computed, considering that the lateral flow is horizontal over the inlet side wall (Figure XIV-23):

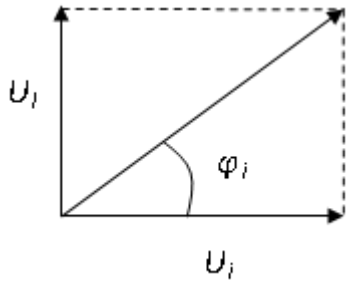

Figure XIV-23 Determination of the angle between the lateral flow and the inlet key directions

$$\tan\ \varphi_i = \frac{U_l}{U_i} \qquad \text{XIV-31}$$

where U_i is the velocity component along the inlet key and U_l is the lateral component of the flow velocity calculated based on the lateral discharge:

$$U_l = \frac{q_l}{Z_i - z_s} \qquad \text{XIV-32}$$

As the α_i coefficient is equal to 1 for a lateral flow parallel to the inlet key direction and to 0 for a lateral flow orthogonal to this direction, it may be calculated by:

$$\alpha_i = \cos\ \varphi_i \qquad \text{XIV-33}$$

For the outlet key, the lateral flow direction is no more horizontal. The variation of the free surface between the inlet and the outlet keys ΔZ must be considered as well as the outlet bottom slope S_o. Considering that the transition from the inlet free surface to the outlet one is realized from the lateral wall to the middle of the outlet

key, the angle φ_o between the main flow direction in the outlet key and the lateral flow direction is computed as (Figure XIV-24):

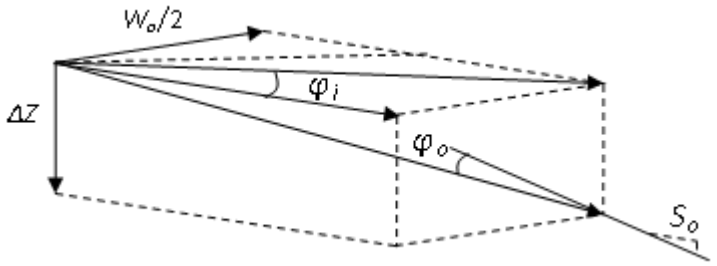

Figure XIV-24 Determination of the angle between the lateral flow and the outlet key directions

$$\tan\ \varphi_o\ = \tan\ \varphi_i\ \frac{\sqrt{1+S_o^2+\left(\frac{2\Delta Z}{W_o}-\frac{S_o}{\tan\ \varphi_i}\right)^2}}{1+\frac{2\Delta Z}{W_o}S_o \tan\ \varphi_i} \qquad \text{XIV-34}$$

As the α_o coefficient is equal to 1 for a lateral flow parallel to the outlet key direction and to 0 for lateral flow orthogonal to this direction, it may be calculated locally by:

$$\alpha_o = \cos\ \varphi_o \qquad \text{XIV-35}$$

After several iterations on the three parameters values to isolate the influence of the α coefficient determination, the limits of lateral integration has been fixed at the key walls for high weirs (models 1 and 2) and at the middle of the side walls for low weirs (models 3 and 4) (see XIV.2.3.3). The μ coefficient is computed by the Hager formulation (see XIV.2.3.1).

Figure XIV-25 presents the comparison of the upstream heads versus discharge computed with the three fixed values and the calculation based on geometrical considerations of the α_i and α_o coefficients for the four geometries tested in the laboratory.

For low heads, as expected, the fixed values of 0 for both α_i and α_o are in good agreement with the experimental results whatever the tested model. That means that the lateral flow for low heads is practically perpendicular to the main keys direction.

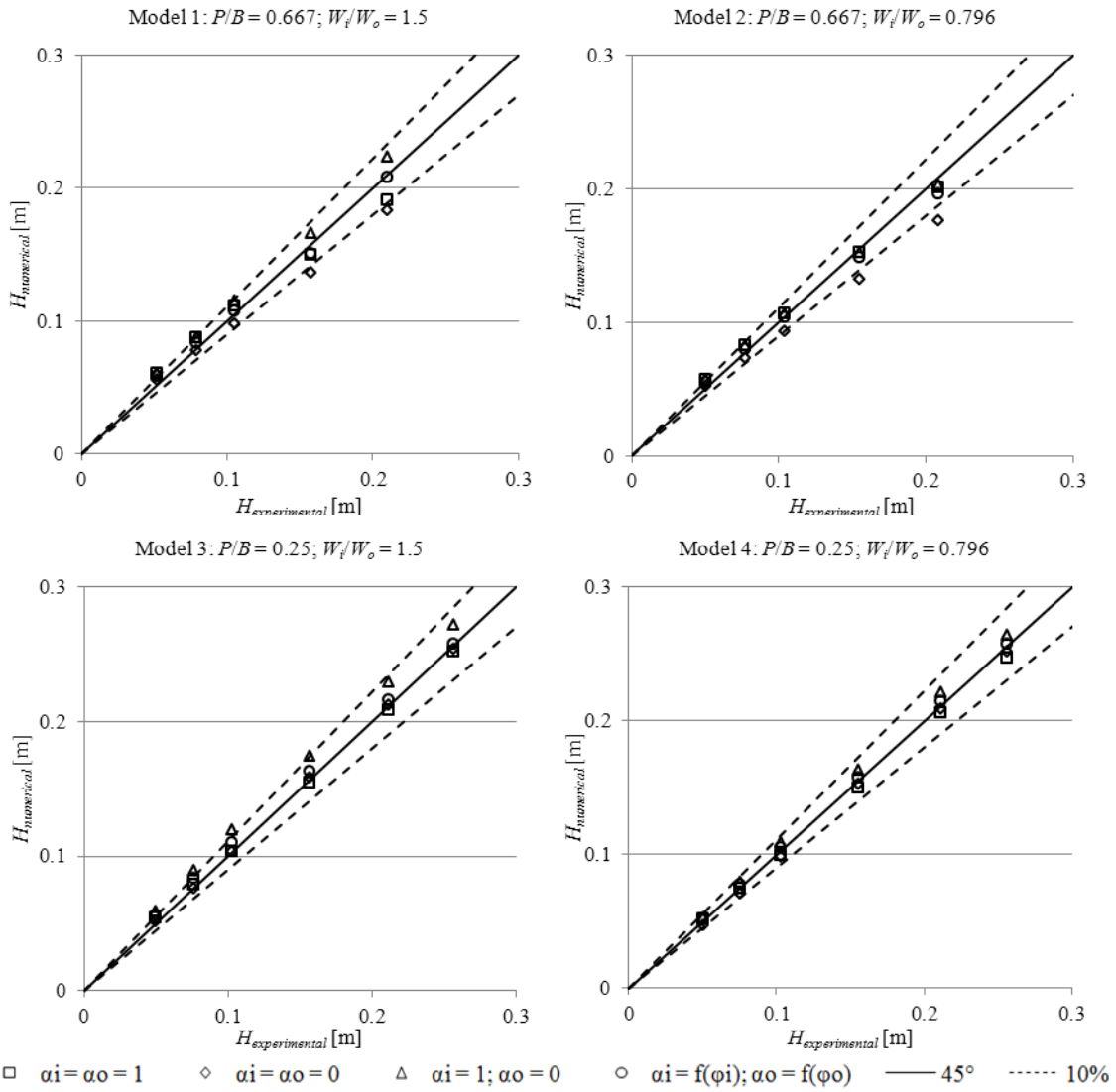

Figure XIV-25 Influence of the momentum exchange calculation on the upstream head for given discharges

For high heads and high weir height (models 1 and 2), the fixed values of 1 for α_i and 0 for α_o give a good approach of the experimental heads. Indeed, the high head provides non-negligible flow velocity along the inlet key what decreases the angle between the lateral flow and the main flow (along the inlet key) directions. However, the important weir height induces a high difference between free surfaces of the inlet and outlet keys. The lateral flow is thus falling vertically in the outlet main stream without momentum transfer.

For high heads and lower weir height (models 3 and 4), the difference between free surfaces of the inlet and outlet keys tends to be equal to 0. Almost the full momentum is thus transfered from the inlet to the outlet key. That is confirmed by the good agreement of the numerical heads, computed fixing both α_i and α_o values to 1, with the experimental heads on models 3 and 4.

Fixing the α_i and α_o values by the calculation of the lateral flow direction improves the global approach of the experimental results for high (models 1 and 2) as well as for low weir height (models 3 and 4). It enables tending to the best results obtained fixing the α_i and α_o values to 1 or 0 whatever the upstream water head.

Regarding the global results issued from the study of the four models, the mean relative error, calculated on the five common upstream water heads studied on the four models, is equal to 5.2%, 5.9% and 8.4% fixing respectively the α_i and α_o coefficients both to 1, both to 0, and respectively to 1 and 0. Fixing the α_i and α_o coefficients by calculation of the lateral flow direction, the mean relative error on the upstream water head is equal to 4.6%. The maximal relative error is equal to 15.5%, 15.3% and 18.1% fixing respectively the α_i and α_o coefficients both to 1, both to 0, and respectively to 1 and 0, and to 12.5% calculating their values based on the lateral flow direction. There is practically no influence of the W_i/W_o ratio on the α_i and α_o coefficients determination. Finally, even if the calculation of α_i and α_o is more CPU time consuming, the results obtained from this approach are closer from the ones obtained fixing the α_i and α_o values whatever the upstream head, and the calculation is only based on the geometry of the weir. From these last considerations, this approach should be applied for a large use of the 1D PKW model.

XIV.2.3.3. Keys widths definition

The 1D numerical model considers the Navier Stokes equations integrated over the transverse flow section, assuming a constant key width. If the vertical limits of integration are clearly defined by the bottom topography and the free surface elevation, the horizontal limits are not so clear. Indeed, two halve keys are computed but also a lateral wall which has a finite thickness. For the flow over the crest level, the limit of each key above the lateral weir thickness is not clearly defined.

A first approach could be to define the limits of integration in between the key walls, with $W_i/2$ and $W_o/2$ as keys widths, whatever the free surface level. This corresponds to a flow maintain in between these walls, what could be the case for low heads compared with the PKW height. In the following results this approach is identified as “In”.

A second approach is to define the limits of integration in the center of the lateral wall, i.e. considering $(W_i + T)/2$ and $(W_o + T)/2$ as keys widths, where T is the wall thickness. This could correspond to a free flow surface elevation largely over the lateral crest one, what is the case for very high heads compared with the PKW height. In the following results, this approach is identified as “Out”.

The influence of the limits of integration definition has been studied computing the μ coefficient by the Hager formulation (see XIV.2.3.1) and calculating the α coefficient as a function of the lateral flow direction (see XIV.2.3.2).

Figure XIV-26 presents the comparison of the upstream heads computed with the two key width definitions for given specific discharges on the four geometries tested in the laboratory.

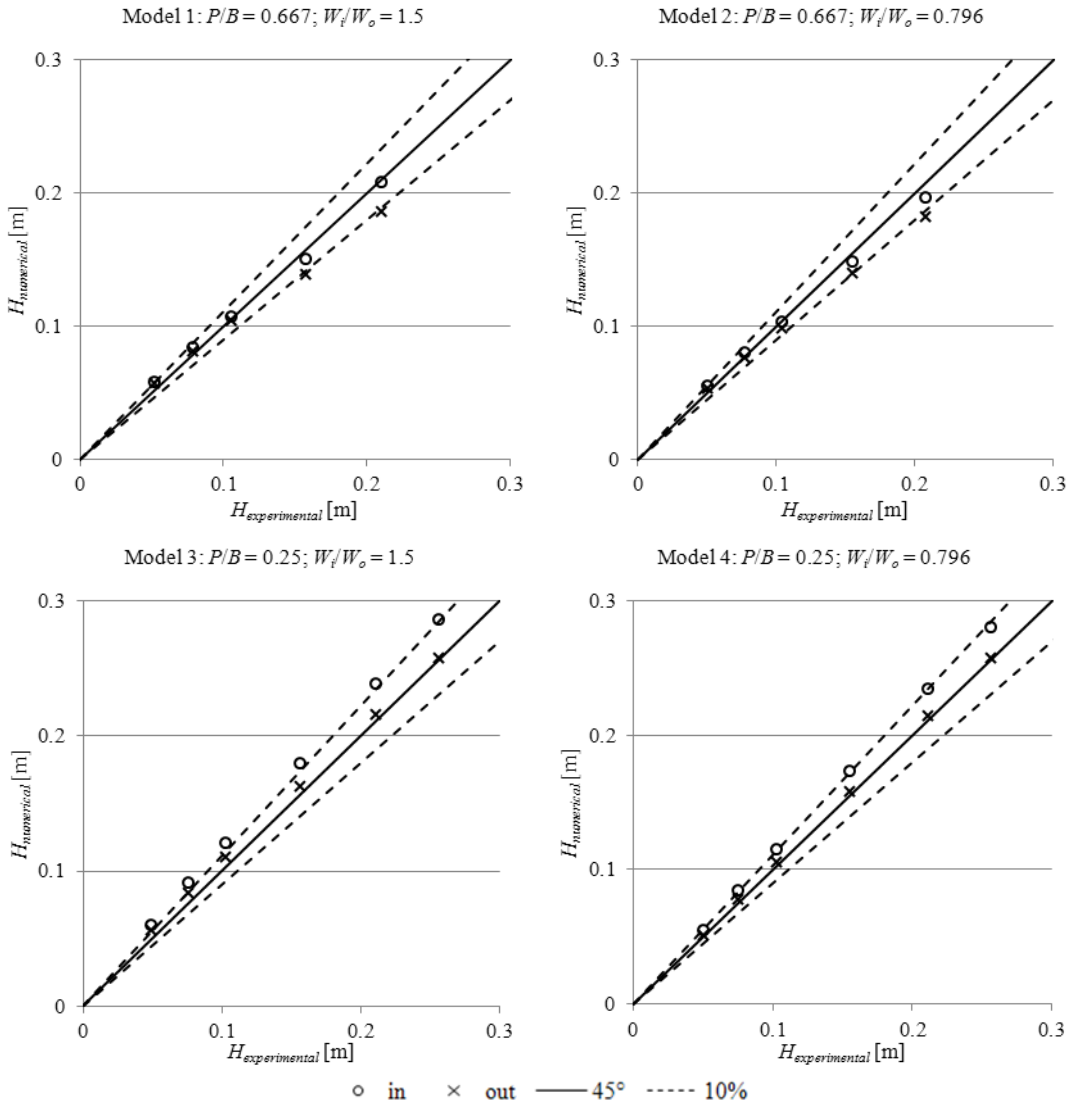

Figure XIV-26 Influence of the limits of integration definition on the upstream head for given discharges

For low heads and high weir height (models 1 and 2), both “In” and “Out” approaches provide results very close to the experimental results. In these conditions, the flow velocity along the inlet key stays negligible and has thus a limited influenced on the discharge calculation. However, with increasing heads, the “In” approach stays closer from the experimental results than the “Out” one, whatever the keys width ratio. That traduces the main importance of the PKW height *P* on the water head *H*. Indeed, even if *H* is multiplied until 4.5 from the lowest discharge, the *H*/*P* ratio stays under 0.55 and most of the cross section comes from the weir height rather than from the increasing water level.

For low weir height (models 3 and 4), the “Out” approach is closer from the experimental results whatever the upstream head. As expected, the lateral crest submergence has to be considered as it modifies significantly the computed flow velocities even for lowest heads. Most of the flow cross section is located above the weir crest elevation.

Regarding the global results issued from the study of the four models, the mean relative error on the upstream water head is equal to 9.1% with the “In” approach and to 5.7% with the “Out” approach. The maximal relative error is equal to 20.5% with the “In” approach and to 12.8% with the “Out” approach. However, regarding only high PKW models (models 1 and 2), the mean relative error on the upstream water head is equal to 5% and 7.3% respectively considering the “In” and the “Out” approaches. The respective maximal relative errors are equal to 12% and 12.8%. Regarding low PKW models (models 3 and 4), the mean relative error on the upstream water head is equal to 13.1% and 4.2% respectively considering the “In” and the “Out” approaches. The respective maximal relative errors are equal to 20.5% and 12.5%. From these considerations, the “In” approach has to be used for high PKW models. The “Out” approach should be conserved for low PKW applications. An approach considering compounded key sections should improve the limits of integration definition whatever the geometry. This approach is under study.

XIV.2.3.4. Conclusion

Based on the comparison of the upstream heads versus discharge computed by the numerical model with the ones measured on four experimental configurations of PKW, the use of the formulation developed by Hager for side weirs to calculate the mass exchange, combined with the calculation of the momentum exchange based on the determination of the lateral flow direction, enables to approach the experimental heads with a mean relative error of 4.6% and a maximal relative error of 12.5% on a large range of heads. Furthermore, combining these two approaches, the numerical model becomes only dependent of the PKW geometry without hydraulic variables to fix. However, the definition of the constant limits for the lateral integration of the Navier-Stokes equations in the inlet and outlet keys is not so clear. For high weir heights, the inlet and outlet keys widths have to be considered between the side walls of the keys. For low weir heights, the keys widths have to be considered between the middle of the lateral walls. The choice between the two approaches must be done based on the PKW geometry.

Further studies stay to realize to fix the method of determination of the limits of integration based on the ratio between the water height over the crest and the PKW height. An improvement of the numerical model scheme to consider compounded key sections might solve the problem of this determination.

XV. References

[1] (2001), http://www.dams.org/, The World Commission on Dams (Website).
[2] (2012), http://www.icold-cigb.org/, The International Comission On Large Dams (Website).
[3] (2012), http://www.gwsp.org/85.html, Global Water System Project (Website).
[4] (2012), http://www.vajont.net/, Comune di Longarone (Website).
[5] (2012), http://www.hydrocoop.org/, Hydrocoop (Website).
[6] Anderson R.M. (2011), *Piano Key Weir Head Discharge Relationships*, All Graduate Theses and Dissertations, Utah State University.
[7] Arthus-Bertrand Y. (2009), *Home*, EuropaCorp (Film).
[8] Arthus-Bertrand Y. (2012), *La soif du monde*, Hope Production (Film).
[9] Barcouda M., Cazaillet O., Cochet P., Jones B.A., Lacroix S., Laugier F., Odeyer C. and Vigny J.P. (2006), *Cost effective increase in storage and safety of most dams using fusegates or P. K. Weirs*, in proceedings of 22ème congrès des grands barrages, CIGB/ICOLD, Barcelona.
[10] Belaabed F. and Ouamane A. (2011), *Contribution to the study of the Piano Key Weirs submerged by the downstream level*, Labyrinth and piano key weirs-PKW 2011, CRC press, London, 89-95.
[11] Biener E. (1985), *Rehabilitation of old gravity dams*, in proceedings of 15th ICOLD congress, Lausanne, 21.
[12] Bieri M., Federspiel M., Boillat J., Houdant B. and Delorme F. (2009), *Spillway capacity upgrade of Gloriettes Dam: Environmental integration and energy dissipation*, in proceedings of HYDRO 2009, Lyon, France.
[13] Blanc P. and Lempérière F. (2001), *Labyrinth spillways have a promising future*, International Journal of Hydropower and Dams 8 (4), 129-131.
[14] Boes R.M. and Hager W.H. (2003), *Hydraulic design of stepped spillways*, Journal of Hydraulic Engineering 129 (9), 671-679.
[15] Borghei S., Jalili M. and Ghodsian M. (1999), *Discharge coefficient for sharp-crested side weir in subcritical flow*, Journal of Hydraulic Engineering 125, 1051.
[16] Boussinesq J. (1877), *Essai sur lar théorie des eaux courantes*, Mem. Présentés Acad. Sci 23, 46.
[17] Carlier M. (1972), *Ecoulement par les déversoirs*, Hydraulique générale et appliquée, Paris, France, 189-217.
[18] Carlier M. (1972), *Hydraulique générale et appliquée*, Eyrolles, Paris.
[19] CETMEF (2005), *Notice sur les déversoirs - Synthèse des lois d'écoulement au droit des seuils et déversoirs*, report, Compiegne, France, 1-89.

[20] Cicero G.-M., Guene C., Luck M., Pinchard T., Lochu A. and Brousse P.-H. (2010), *Experimental optimization of a Piano Key Weir to increase the spillway capacity of the Malarce dam*, in proceedings of 1st IAHR European Congress, Edinburgh, United Kingdom.
[21] Crookston B. and Tullis B. (2010), *Hydraulic performance of labyrinth weirs*, in proceedings of International Junior Researcher and Engineer Workshop on Hydraulic Structures, Edinburgh, UK.
[22] Das Singhal G. and Sharma N. (2011), *Rehabilitation of Sawara Kuddu Hydroelectric Project - Model studies of Piano Key Weir in India.*, Labyrinth and piano key weirs-PKW 2011, CRC Press, London, 241-250.
[23] Delleur J., Dooge J. and Gent K. (1956), *Influence of slope and roughness on the free overfall*, J. Hydraul. Div. 82 (4), 30–35.
[24] Detrembleur S., Archambeau P., Erpicum S., Dewals B. and Pirotton M. (2008), *An explicit projection method fpr solving incompressible Navier-Stokes equations*, in proceedings of 2nd International Junior Researcher and Engineer Workshop on Hydraulic Structures, Pisa, Italy.
[25] Detrembleur S., Dewals B.J., Erpicum S., Archambeau P. and Pirotton M. (2009), *A 2D vertical finite volume solver using a level set approach for simulating free surface incompressible flows*, European Journal of Mechanical and Environmental Engineering 2009 (3), 4-9.
[26] Detrembleur S. (2011), *Modèles d'écoulements incompressibles en plan vertical appliqués aux structures du génie civil*, PhD thesis, ArGEnCo department, University of Liège, Liège, Belgium.
[27] Dewals B.J., André S., Schleiss A. and Pirotton M. (2004), *Validation of a quasi-2D model for aerated flows over stepped spillways for mild and steep slopes*, in proceedings of Proc. 6th Int. Conf. of Hydroinformatics, Singapore.
[28] Dewals B.J. (2006), *Une approche unifiée pour la modélisation d'écoulements à surface libre, de leur effet érosif sur une structure et de leur interaction avec divers constituants*, PhD Thesis, University of Liege, Liège.
[29] Dewals B.J., Erpicum S., Archambeau P., Detrembleur S. and Pirotton M. (2006), *Depth-integrated flow modelling taking into account bottom curvature*, J. Hydraul. Res. 44 (6), 787-795.
[30] Dugué V., Hachem F., Boillat J.L., Nagel V., Roca J.P. and Laugier F. (2011), *PK Weir and flap gate spillway for the Gage II Dam*, Labyrinth and piano key weirs-PKW 2011, CRC Press, London, 35-42.
[31] Erpicum S. (2006), *Optimisation objective de paramètres en écoulements à surface libre sur maillage multibloc*, PhD thesis, University of Liege.
[32] Erpicum S., Dewals B.J., Archambeau P., Detrembleur S. and Pirotton M. (2009), *Detailed inundation modelling using high resolution DEMs*, Engineering Applications of Computational Fluid Mechanics, Accepted.
[33] Erpicum S., Dewals B.J., Archambeau P. and Pirotton M. (2009), *Dam-break flow computation based on an efficient flux-vector splitting*, Journal of Computational and Applied Mathematics In Press, Accepted Manuscript.

[34] Erpicum S., Machiels O., Archambeau P., Dewals B.J. and Pirotton M. (2010), *1D numerical approach to model the flow over a Piano Key Weir (PKW)*, in proceedings of SimHydro 2010, Nice, France.
[35] Erpicum S., Machiels O., Dewals B.J., Archambeau P. and Pirotton M. (2010), *Contribution to the study of Piano Key Weir hydraulics*, in proceedings of IECS2010, Graz, Austria.
[36] Erpicum S., Machiels O., Archambeau P., Dewals B. and Pirotton M. (2011), *1D numerical modeling of the flow over a Piano Key Weir*, Labyrinth and piano key weirs-PKW 2011, CRC Press, London, 151-158.
[37] Erpicum S., Machiels O., Archambeau P., Dewals B., Pirotton M. and Daux C. (2011), *Energy dissipation on a stepped spillway downstream of a Piano Key Weir - Experimental study*, Labyrinth and piano key weirs-PKW 2011, CRC Press, London, 105-112.
[38] Erpicum S., Nagel V. and Laugier F. (2011), *Piano Key Weir design study at Raviege dam*, Labyrinth and piano key weirs-PKW 2011, CRC Press, London, 43-50.
[39] Erpicum S., Machiels O., Archambeau P., Pirotton M. and Dewals B. (2012), *Hydraulic modelling of Piano Key Weirs: A composite approach*, in proceedings of Piano Key Weir for in-stream storage and dam safety (PKWISD-2012), New Delhi, India, 53-64.
[40] Erpicum S., Machiels O., Dewals B., Pirotton M. and Archambeau P. (2012), *Numerical and physical hydraulic modelling of Piano Key Weirs*, in proceedings of ASIA 2012 - 4th International Conference on Water Resources and Renewable Energy Development in Asia, Chiang Mai, Thailand.
[41] Erpicum S., Machiels O., Pirotton M., Nagel V. and Laugier F. (2012), *Piano Key Weir (PKW) solution to upgrade Raviège Dam spillway (France)*, in proceedings of 24th ICOLD congress, Kyoto, Japan.
[42] Falvey H. (2003), *Hydraulic design of labyrinth weirs*, Amer Society of Civil Engineers.
[43] Ferro V. (1992), *Flow measurement with rectangular free overfall*, Journal of Irrigation and Drainage Engineering 118 (6), 956-964.
[44] Hager W.H. (1987), *Lateral Outflow Over Side Weirs*, Journal of Hydraulic Engineering 113 (4), 491-504.
[45] Hervouet J.-M. and Petitjean A. (1999), *Malpasset dam-break revisited with two-dimensional computations*, Journal of Hydraulic Research 37 (6), 777-788.
[46] Hien T.C., Son H.T. and Khanh M.H.T. (2006), *Results of some piano keys weir hydraulic model tests in Vietnam*, in proceedings of 22nd ICOLD congress, CIGB/ICOLD, Barcelona, Spain.
[47] Ho Ta Khanh M., Hien T.C. and Hai N.T. (2011), *Main results of the P.K weir model tests in Vietnam (2004 to 2010)*, Labyrinth and piano key weirs-PKW 2011, CRC press, London, 191-198.

[48] Ho Ta Khanh M., Sy Quat D. and Xuan Thuy D. (2011), *P.K weirs under design and construction in Vietnam (2010)*, Labyrinth and piano key weirs-PKW 2011, CRC Press, London, 225-232.
[49] Ho Ta Khanh M., Hien T.C. and Quat D.S. (2012), *Research and development of P.K. Weirs in Vietnam since 2004*, in proceedings of Piano Key Weir for in-stream storage and dam safety (PKWISD-2012), New Delhi, India, 91-96.
[50] Idel'Cik I. (1969), *Memento des pertes de charge: coefficients de pertes de charge singulières et de pertes de charge par frottement*, Eyrolles.
[51] Johnson M.C. (2000), *Discharge coefficient analysis for flat-topped and sharp-crested weirs*, Irrigation science 19 (3), 133 - 137.
[52] Kandaswamy P.K. and Rouse H. (1957), *Characteristics of flow over terminal weirs and sills*, Journal of the Hydraulics Division of ASCE 83 (4), 1-13.
[53] Karelle Y. (2008), *Etude expérimentale du comportement hydraulique des déversoirs en touches de piano*, Master thesis, ArGEnCo, University of Liege, Liege, Belgium.
[54] Kindsvater C.E. and Carter R.W. (1957), *Discharge characteristics of thin plate weirs*, Journal of Hyd. Div. Proc. ASCE 83 (12), 1-36.
[55] Klopfenstein Jr R. (1998), *Air velocity and flow measurement using a Pitot tube*, ISA Transactions 37 (4), 257-263.
[56] Lakshmana Rao N.S. (1975), *Theory of weirs*, Advances in hydroscience, Academic Press, Urbana, Illinois, 309-406.
[57] Laugier F. (2007), *Design and construction of the first Piano Key Weir (PKW) spillway at the Goulours dam*, International Journal of Hydropower and Dams 14 (5), 94-101.
[58] Laugier F., Lochu A., Gille C., Leite Ribeiro M. and Boillat J.-L. (2009), *Design and construction of a labyrinth PKW spillway at Saint-Marc dam, France*, International Journal of Hydropower and Dams 16 (5), 100-107.
[59] Laugier F., Pralong J. and Blancher B. (2011), *Influence of structural thickness of sidewalls on PKW spillway discharge capacity*, in proceedings of Labyrinth and piano key weirs-PKW 2011, CRC Press, London, 159-165.
[60] Laugier F., Vermeulen J. and Pralong J. (2012), *Achievement of New Innovative Labyrinth Piano Key Weir Spillways (PKW)*, in proceedings of Piano Key Weir for in-stream storage and dam safety (PKWISD-2012), New Delhi, India, 25-42.
[61] Le Doucen O., Leite Ribeiro M., Boillat J.-L., Schleiss A. and Laugier F. (2009), *Etude paramétrique de la capacité des PK-Weirs*, in proceedings of Modèles physiques hydrauliques - outils indispensables du XXIe siècle, SHF, Lyon.
[62] Le Doucen O., Leite Ribeiro M., Boillat J.L. and Schleiss A. (2009), *Etude paramétrique de la capacité des PK-Weirs*, Lyon (unpublished work).
[63] Leite Ribeiro M., Albalat C., Boillat J.-L., Schleiss A.J. and Laugier F. (2007), *Rehabilitation of St-Marc dam. Experimental optimization of a piano key weir*, in proceedings of 32th IAHR Congress, Venice, Italy.

[64] Leite Ribeiro M., Boillat J., Kantoush S., Albalat C., Laugier F. and Lochu A. (2007), *Rehabilitation of St-Marc dam–Model studies for the spillways*, in proceedings of HYDRO 2007, Granada, Spain.
[65] Leite Ribeiro M., Bieri M., Boillat J.-L., Schleiss A.J., Delorme F. and Laugier F. (2009), *Hydraulic capacity improvement of existing spillways - Design of Piano Key Weirs*, in proceedings of 23rd congress of CIGB/ICOLD, Brasilia.
[66] Leite Ribeiro M., Boillat J.L. and Schleiss A.J. (2011), *Experimental parametric study for hydraulic design of PKWs*, Labyrinth and piano key weirs-PKW 2011, CRC press, London, 183-190.
[67] Lempérière F. and Ouamane A. (2003), *The piano keys weir: a new cost-effective solution for spillways*, International Journal of Hydropower and Dams 10 (5), 144-149.
[68] Lempérière F. (2009), *New Labyrinth weirs triple the spillways discharge - Data for an easy design of P.K.Weir*.
[69] Lempérière F., Vigny J.P. and Ouamane A. (2011), *General comments on Labyrinths and Piano Key Weirs: The past and present*, Labyrinth and piano key weirs-PKW 2011, CRC press, London, 17-24.
[70] Luck M., Lee E.-S., Mechitoua N., Violeau D., Laugier F., Blancher B. and Guyot G. (2009), *Modélisations physique et numérique 3D pour l'évaluation de la débitance et le design des évacuateurs de crue*, in proceedings of Modèles physiques hydrauliques - outils indispensables du XXIe siècle, SHF, Lyon.
[71] Machiels O., Erpicum S., Archambeau P., Dewals B.J. and Pirotton M. (2009), *Large scale experimental study of piano key weirs*, in proceedings of 33rd IAHR Congress, ASCE, Vancouver, Canada.
[72] Machiels O., Erpicum S., Archambeau P., Dewals B.J. and Pirotton M. (2009), *Analyse expérimentale du fonctionnement hydraulique des déversoirs en touches de piano*, in proceedings of Colloque CFBR-SHF: "Dimensionnement et fonctionnement des évacuateurs de crues", Paris, France.
[73] Machiels O., Erpicum S., Archambeau P., Dewals B. and Pirotton M. (2010), *Analyse expérimentale de l'influence des largeurs d'alvéoles sur la débitance des déversoirs en touches de piano*, La Houille Blanche (2), 22 - 28.
[74] Machiels O., Erpicum S., Archambeau P., Dewals B.J. and Pirotton M. (2010), *Experimental study of the hydraulic behavior of Piano Key Weirs*, in proceedings of IAHR-APD, Auckland, New Zeeland.
[75] Machiels O., Erpicum S., Archambeau P., Dewals B.J. and Pirotton M. (2010), *Piano Key Weirs, experimental study of an efficient solution for rehabilitation*, in proceedings of FRIAR, Wessex Institute of Technology, Milano, Italia, 95-106.
[76] Machiels O., Erpicum S., Archambeau P., Dewals B.J. and Pirotton M. (2010), *Hydraulic behaviour of Piano Key Weirs: Experimental approach*, in proceedings of 3rd International Junior Researcher and Engineer Workshop on Hydraulic Structures, IJREWHS'10, Edinburgh, United Kingdom.

[77] Machiels O., Erpicum S., Archambeau P., Dewals B. and Pirotton M. (2011), *Influence of the alveoli slopes on the discharge capacity of Piano Key weirs*, in proceedings of 34th IAHR congress, Brisbane, Australia.
[78] Machiels O., Erpicum S., Archambeau P., Dewals B. and Pirotton M. (2011), *Varying the alveoli slopes of Piano Key Weirs: Interests and limitations*, in proceedings of 6th International Conference on Dam Engineering, Lisbon, Portugal.
[79] Machiels O., Erpicum S., Archambeau P., Dewals B.J. and Pirotton M. (2011), *Influence of Piano Key Weir height on its discharge capacity*, Labyrinth and piano key weirs-PKW 2011, CRC Press, London, 59-66.
[80] Machiels O., Erpicum S., Archambeau P., Dewals B.J. and Pirotton M. (2011), *Piano Key Weir preliminary design method - Application to a new dam project*, Labyrinth and piano key weirs-PKW 2011, CRC Press, London, 199-206.
[81] Machiels O., Erpicum S., Dewals B., Archambeau P. and Pirotton M. (2011), *Experimental observation of flow characteristics over a Piano Key Weir*, Journal of hydraulic research 49 (3), 359-366.
[82] Machiels O., Erpicum S., Archambeau P., Dewals B. and Pirotton M. (2012), *On the Piano Key Weir hydraulics*, in proceedings of 2nd IAHR Europe Congress, Munich, Germany.
[83] Machiels O., Erpicum S., Archambeau P., Dewals B. and Pirotton M. (2012), *Influence of the relative alveoli widths on Piano Key Weirs efficiency for varied weir heights*, in proceedings of 24th ICOLD congress, Kyoto, Japan.
[84] Machiels O., Erpicum S., Archambeau P., Dewals B. and Pirotton M. (2012), *Influence of weir height and keys slope on PKW discharge*, in proceedings of 4th IAHR International Symposium on Hydraulic Structures, Porto, Portugal.
[85] Machiels O., Erpicum S., Pirotton M., Dewals B. and Archambeau P. (2012), *Experimental analysis of PKW hydraulic performance and geometric parameters optimum*, in proceedings of Piano Key Weir for in-stream storage and dam safety (PKWISD-2012), New Delhi, India, 97-114.
[86] Marchi E. (1993), *On the free overfall*, Journal of Hydraulic Research 31 (6), 777-790.
[87] Millet J.C., Chambon J., Soyer G. and Lefevre C. (1988), *Augmentation de la capacité des ouvrages d?évacuation de divers barrages*, in proceedings of 16ème congrès ICOLD, San Francisco, 1325.
[88] Muslu Y. (2001), *Numerical analysis for lateral weir flow*, Journal of Irrigation and Drainage Engineering 127, 246.
[89] Novak P., Moffat A.I.B., Nalluri C. and Narayanan R. (1990), *Hydraulic structures*, Unwin Hyman, London.
[90] Nujic M. (1995), *Efficient implementation of non-oscillatory schemes for the computation of free-surface flows*, J. Hydraul. Res. 33 (1), 101-111.
[91] Oertel M., Carvalho R.F. and Janssen R.H.A. (2011), *Flow over a rectangular side weir in an open channel and resulting discharge coefficients*,

in proceedings of 34th IAHR World Congress, Brisbane, Australia, 3675-3681.
[92] Ouamane A. (2006), *Hydraulic and costs data for various Labyrinth Weirs*, in proceedings of 22ème congrès des grands barrages, CIGB/ICOLD, Barcelona.
[93] Ouamane A. and Lempérière F. (2006), *Nouvelle conception de déversoir pour l'accroissement de la capacité des retenues des barrages*, in proceedings of Colloque international sur la protection et la préservation des ressources en eau, Bilda, Algérie.
[94] Ouamane A. and Lempérière F. (2006), *Design of a new economic shape of weir*, in proceedings of International Symposium on Dams in the Societies of the 21st Century, Barcelona, Spain, 463-470.
[95] Ouamane A. and Lempérière F. (2007), *Increase of the safety of dams. Rehabilitation of weirs*, in proceedings of ICOLD 75th annual meeting, St Petersburg.
[96] Pinchard T., Boutet J.M. and Cicero G.-M. (2011), *Spillway capacity upgrade at Malarce dam: Design of an additional Piano Key Weir spillway*, Labyrinth and piano key weirs-PKW 2011, CRC Press, London, 233-240.
[97] Pralong J., Montarros F., Blancher B. and Laugier F. (2011), *A sensitivity analysis of Piano Key Weirs geometrical parameters based on 3D numerical modeling*, Labyrinth and piano key weirs-PKW 2011, CRC Press, London, 133-139.
[98] Pralong J., Vermeulen J., Blancher B., Laugier F., Erpicum S., Machiels O., Pirotton M., Boillat J.-L., Leite Ribeiro M. and Schleiss A. (2011), *A naming convention for the Piano Key Weirs geometrical parameters*, Labyrinth and piano key weirs-PKW 2011, CRC Press, London, 271-278.
[99] Rajaratnam N. and Muralidhar D. (1968), *Characteristics of the rectangular free overfall*, Journal of Hydraulic Research 6 (3), 233-258.
[100] Ramamurthy A., Tim U. and Rao M. (1987), *Flow over sharp-crested plate weirs*, Journal of Irrigation and Drainage Engineering 113 (2), 163-172.
[101] Ranga Raju K.G., Prasad B. and Gupta S.K. (1979), *Side Weir in Rectangular Channel*, Journal of the Hydraulics Division of ASCE 105 (5), 547-554.
[102] Rouse H. (1936), *Discharge characteristics of the free overfall*, Civil Engineering 6 (4), 257-260.
[103] Sharma N. and Das Singhal G. (2012), *Physical modelling of Piano Key Weir for Sawra Kuddu Hydro Electric Project in India*, in proceedings of Piano Key Weir for in-stream storage and dam safety (PKWISD-2012), New Delhi, India, 123-132.
[104] Shvainshtein A.M. (1999), *Stepped spillways and energy dissipation*, Hydrotechnical construction 33 (5), 275-282.
[105] Sinniger R.O. and Hager W.H. (2004), *Constructions hydrauliques: écoulements stationnaires*, Presses Polytechniques et Universitaires Romandes, Lausanne.

[106] Swamee P.K. (1988), *Generalized Rectangular Weir Equations*, Journal of Hydraulic Engineering 114 (8), 945-949.
[107] Swiss Soc. Eng. Architects (1926), *Contribution à l'étude des méthodes de jaugeage*, report of Swiss Bur. of Water Res. Bulletin 18, Bern.
[108] Tullis B., Willmore C. and Wolfhope J. (2005), *Improving Performance of Low Head Labyrinth Weirs*, in proceedings, ASCE.
[109] Tullis J.P., Amanian N. and Waldron D. (1995), *Design of Labyrinth Spillways*, Journal of Hydraulic Engineering 121.
[110] Vermeulen J., Laugier F., Faramond L. and Gille C. (2011), *Lessons learnt from design and construction of EDF first Piano Key Weirs*, Labyrinth and piano key weirs-PKW 2011, CRC press, London, 215-224.